GEOLOGICAL SURVEY OF CANADA
OPEN FILE 7363

Geological framework, basin evolution, hydrocarbon system data and conceptual hydrocarbon plays for the Hudson Bay and Foxe basins, Canadian Arctic

D. Lavoie, N. Pinet, J. Dietrich, S. Zhang, K. Hu, E. Asselin, Z. Chen, R. Bertrand, J. Galloway, V. Decker, P. Budkewitsch, D. Armstrong, M. Nicolas, J. Reyes, B.P. Kohn, M.J. Duchesne, V. Brake, P. Keating, J. Craven and B. Roberts

2013

Natural Resources Canada | Ressources naturelles Canada

Canada

GEOLOGICAL SURVEY OF CANADA
OPEN FILE 7363

Geological framework, basin evolution, hydrocarbon system data and conceptual hydrocarbon plays for the Hudson Bay and Foxe basins, Canadian Arctic

D. Lavoie[1], N. Pinet[1], J. Dietrich[2], S. Zhang[3], K. Hu[2], E. Asselin[1], Z. Chen[2], R. Bertrand[4], J. Galloway[2], V. Decker[5], P. Budkewitsch[6], D. Armstong[7], M. Nicolas[8], J. Reyes[2], B.P. Kohn[9], M.J. Duchesne[1], V. Brake[1], P. Keating[10], J. Craven[10] and B. Roberts[10]

[1]Geological Survey of Canada, Quebec City, QC G1K 9A9
[2]Geological Survey of Canada, Calgary, AB T2L 2A7
[3]Canada-Nunavut Geoscience Centre, Iqaluit, NU X0A 0H0
[4]Institut National de la Recherche Scientifique – ETE, Quebec City, QC G1K 9A9
[5]Canadian Centre for Remote Sensing, Ottawa, ON K1A 0Y7
[6]Aboriginal Affairs and Northern Development Canada, Iqaluit, NU X0A 0H0
[7]Ontario Geological Survey, Sudbury, ON P3E 6B5
[8]Manitoba Geological Survey, Winnipeg, MN R2G 3P2
[9]Melbourne University, Melbourne, Victoria 3053, Australia
[10]Geological Survey of Canada, Ottawa, ON K1A 0E9

2013

doi:10.4095/293119

This publication is available for free download through GEOSCAN (http://geoscan.ess.nrcan.gc.ca/).

Recommended citation
Lavoie, D., Pinet, N., Dietrich, J., Zhang, S., Hu, K., Asselin, E., Chen, Z., Bertrand, R., Galloway, J., Decker, V., Budkewitsch, P., Armstrong, D., Nicolas, M., Reyes, J., Kohn, B.P., Duchesne, M.J., Brake, V., Keating, P., Craven, J., and Roberts, B., 2013. Geological framework, basin evolution, hydrocarbon system data and conceptual hydrocarbon plays for the Hudson Bay and Foxe basins, Canadian Arctic; Geological Survey of Canada, Open File 7363, 210 p. doi:10.4095/293119

Publications in this series have not been edited; they are released as submitted by the author.

Page

FIGURES

Page

TABLES

Page

ANNEX

SUMMARY

The Hudson Bay Platform covers ~820,000 km^2 and is the largest intracratonic basin in North America. The succession of the Hudson Platform consists mainly of Paleozoic strata, with a maximum preserved thickness of about 2500 m. The Paleozoic succession includes Ordovician to Devonian shallow marine carbonates, reefs and shales with locally thick Devonian evaporites. Paleozoic strata are unconformably overlain by erosional remnants of Jurassic, Cretaceous and mid-Cenozoic non-marine and marine strata. In a first phase of exploration (1973-1985), over 46,000 line-km of seismic reflection data were acquired and 5 offshore exploration wells drilled. Most of the seismic profiles and all of the exploration wells are located in a relatively small area in the central part of Hudson Bay.

Re-evaluation of the available seismic data indicates that syn-tectonic sedimentation occurred in Late Ordovician(?), Silurian and Early Devonian with significant depocentre migration with time. New biostratigraphic data, supported by the seismic evidence, indicate 3 major unconformities, with the most important ones at the Silurian-Devonian boundary and at the top of the Upper Devonian section.

New organic matter reflectance data (Rovit of 0.60 to 0.91%) indicate oil window conditions for the Ordovician – Silurian interval in parts of the Hudson Platform. Apatite fission track data indicate that analysed samples experienced significant annealing at temperatures > 60°C.

Available hydrocarbon system data are synthesized in 5 conventional petroleum plays, including recently recognized porous hydrothermal dolomites and reefs. Type I/II-S Upper Ordovician oil shales are recognized at several locations in the basin with TOC values up to 35% and thickness up to 15 metres. Lower Silurian shales may also have local hydrocarbon generation potential (TOC values up to 2%). New high-resolution bathymetric surveys in Hudson Bay led to the recognition of circular sea-floor depressions similar to fluid-escape pockmarks and preliminary interpretations of RADARSAT images suggest possible oil slicks at sea surface. Some direct hydrocarbon indicators are interpreted from the vintage seismic information. Taken together, these new hydrocarbon systems data suggest that large areas of the Hudson Platform are prospective for oil accumulations.

1. INTRODUCTION

1.1 Historical review and regional setting

The Hudson Platform represents the largest Phanerozoic sedimentary accumulation in Canada. It covers 820,000 km^2 (about 6% of the area of Canada), of which 2/3 is covered by water. The Hudson Platform encompasses parts of northeastern Manitoba, northern Ontario and Nunavut (Fig. 1). The Platform contains the large Hudson Bay Basin and the smaller satellite Moose River Basin to the south and the Hudson Strait and Foxe basins to the north. The Hudson Bay Basin is separated from the Moose River Basin by the Cape Henrietta Maria Arch whereas the Boothia-Bell Arch separates the Hudson Bay Basin from Foxe Basin (Sanford, 1987); the two arches are broad positive basement-involved structural elements for which the formation mechanism(s) is poorly understood. The Hudson Platform unconformably overlies and is encircled by Precambrian rocks. The basement includes metamorphic and igneous rocks of the PaleoProterozoic Trans-Hudson Orogen, a tectonic suture zone marking the contact between the Superior and Churchill cratons that underlie the southern and northern parts of the Hudson Platform, respectively (Eaton and Darbyshire, 2009).

The Hudson Bay Basin is the least studied intracratonic basin in North America; its surface area rivals that of other intracratonic basins (e.g., Michigan, Illinois, Williston basins, Fig. 1). The Hudson Bay Basin is characterized by the thinnest sedimentary succession and the shortest depositional history of the intracratonic basins of North America (Quinlan, 1987). This has been attributed to the stiff lithospheric root and high elastic thickness of the continental lithosphere beneath the basin, which may have existed since its formation (Kaminski and Jaupart, 2000). The Paleozoic succession of the Hudson Bay, Moose River and Hudson Strait basins consists of Middle-Upper Ordovician to Upper Devonian rocks with a maximum preserved thickness of about 2500 m in Hudson Bay. Older rocks are documented in the Foxe Basin, which is characterized by a Cambrian (?) to Silurian succession. Mesozoic (Cretaceous) to recently documented Cenozoic (pre-Pliocene) strata (Galloway et al., 2012) locally occur at the top of the succession in the Hudson Bay, Moose River and possibly Hudson Strait basins.

The Hudson Platform is the erosional remnant of a more extensive cratonic cover that probably had episodic connection during the Paleozoic (Sanford, 1987) and possibly Mesozoic (White et al., 2000) with platformal and basinal areas to the north (Arctic Platform) and south (St. Lawrence platform, Michigan and Williston basins).

Given its remote location and poor outcrops, Hudson Bay remains geologically one of the least studied sedimentary basin in Canada. The onshore extension of the Phanerozoic succession forms the Hudson Bay Lowlands and consists of a relatively thin succession of nearly flat-lying sedimentary rocks exposed in northeastern Manitoba, northern Ontario and northward, on Southampton, Coats and Mansel islands in Nunavut. Similarly, the Foxe Basin is a largely marine sedimentary basin with preserved onshore erosional margins expressed as

nearly flat-lying strata on Melville Peninsula and on Baffin Island.

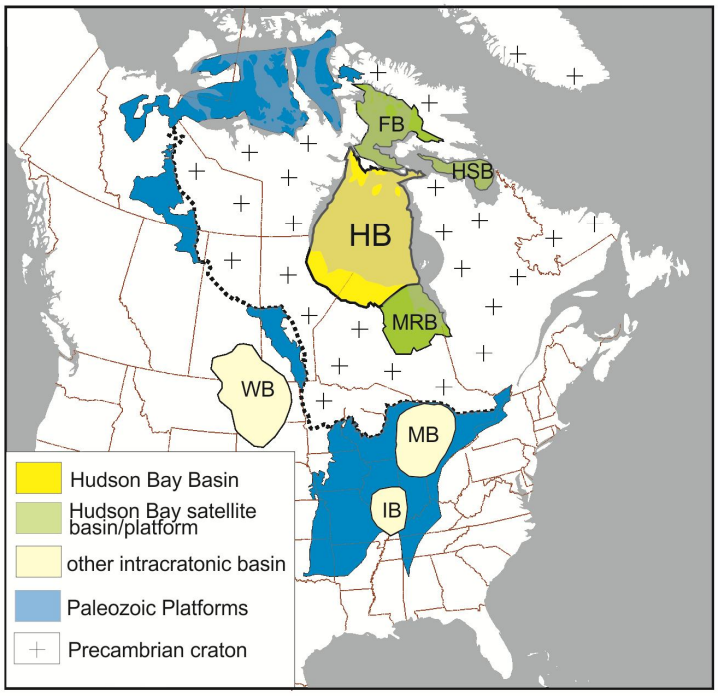

Figure 1: Simplified geological map showing the position of Paleozoic North American intracratonic basins and platforms. FB, Foxe Basin; HB, Hudson Bay Basin; HSB, Hudson Strait Basin; IB, Illinois Basin; MB, Michigan Basin; MRB, Moose River Basin; WB, Williston Basin.

Early explorers in the Hudson Bay area made episodic geological observations starting in the late 1880s (Bell, 1884, 1895), although it was only in the mid to late 1960s that regional-scale mapping was conducted by GSC officers along major rivers in Manitoba and Ontario (Nelson, 1964, Nelson and Johnson, 1966, Sanford et al., 1968, Sanford and Norris, 1973). Rocks of Ordovician, Silurian, Devonian, and Jurassic ages were mapped, although the geology is obscured by the very low relief, swampy muskeg terrain that covers the Hudson Bay Lowlands. Conversely, the first geological observations for Foxe Basin are those of Parry (1824, 1825) who recognized carbonates and collected fossils. The first significant regional coverage of the onshore extension of the Foxe Basin was part of a major GSC mapping operation (Trettin, 1975) and allowed the establishment of the Paleozoic stratigraphy by Lemon and Blackadar (1963).

1.2 First phase of hydrocarbon exploration

Hydrocarbon exploration and production successes in intracratonic basins to the south were the driving force behind the exploration activities that took place for both the onshore and

offshore domains of the Hudson Bay Basin.

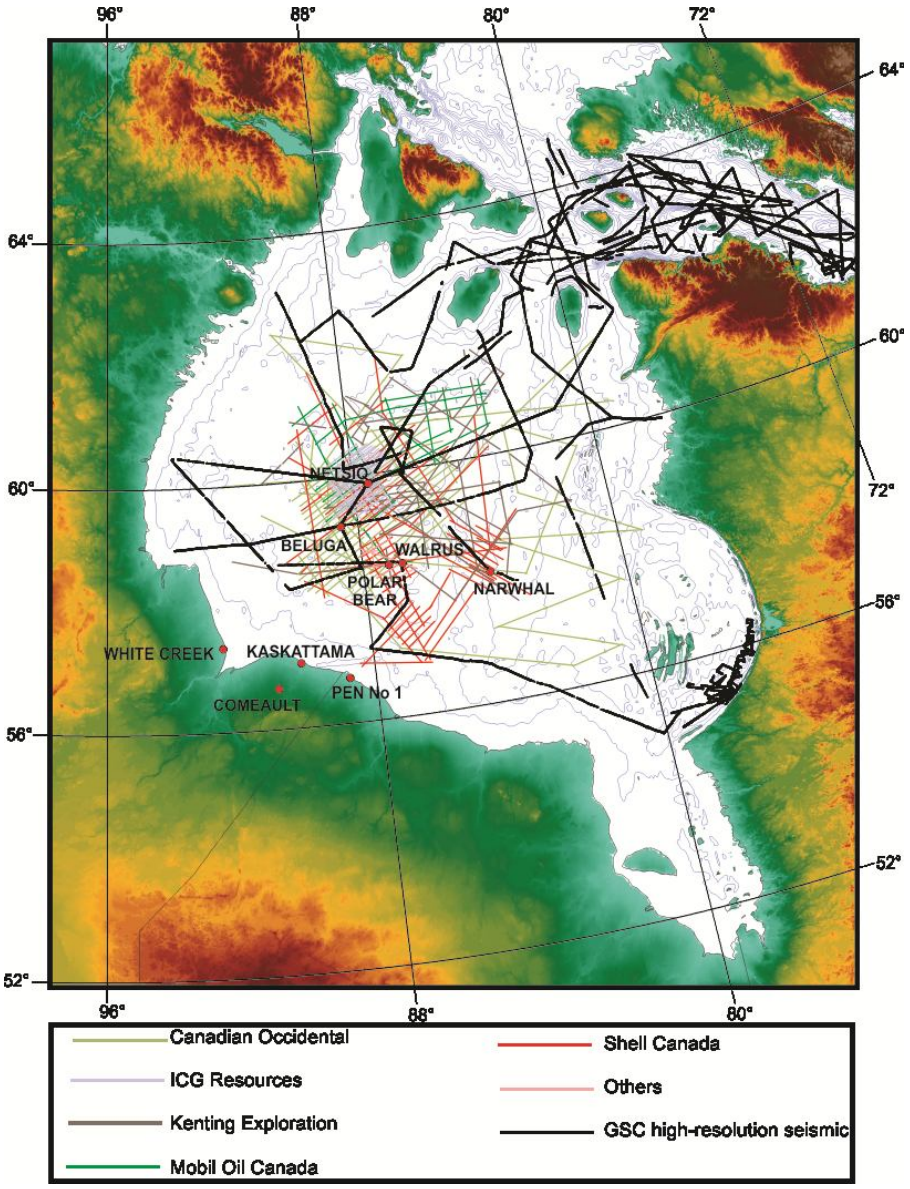

Figure 2: Physiographic setting of the Hudson Bay and surrounding areas. Main wells, seismic reflection lines collected by the industry during the period 1968-1983, and high-resolution seismic reflection lines collected by the Geological Survey of Canada are located

Onshore drilling started in 1964 (Manitoba) and in 1970, a total of 4 hydrocarbon exploration wells (3 in Manitoba and 1 in Ontario) were drilled; moreover, a significant number of base metal exploration and stratigraphic wells were also drilled. Given the nature of the terrain, no onshore seismic reflection data were acquired to help locate the hydrocarbon exploration wells. Industry offshore drilling started in 1969 shortly after a first marine seismic acquisition program showed that the sedimentary succession preserved in the central part of Hudson Bay is much thicker than its onshore counterpart. From late 1960s to 1990, the industry

and the Geological Survey of Canada acquired over 46,000 and 40,000 linear-km of deep and shallow seismic, respectively (Fig. 2). Industry seismic acquisition was largely concentrated in the central part of Hudson Bay and resulted in generally low quality seismic lines due acquisition problems. Based on the seismic information, the industry drilled 5 offshore wells between 1969 and 1985 (Fig. 2), three of them drilled near the "central high" (see below) and targeting fault-structural plays. No commercial discoveries were recorded from the onshore and offshore wells, although traces of oil and gas and bitumen-impregnated rocks were reported from all offshore wells. The lack of significant success resulted in the abandonment of the basin by the industry and the pessimistic conclusions that the succession was largely devoid of potential source rocks and too thin to be thermally mature (Tillement, 1975). Industry data (paper copies of seismic lines, digital well logs, cuttings and few cores) were all submitted to the National Energy Board for future use.

There has been no industry seismic reflection acquisition in the Foxe Basin; some limited GSC high resolution seismic was acquired in the adjacent Hudson Strait. Nonetheless, one exploration well (Rowley M-04 well) was drilled in 1971 on Rowley Island near the northern reach of the Foxe Basin. No hydrocarbon shows were reported from this well (Trettin, 1975).

In the late stage of the first phase of hydrocarbon exploration, a resource evaluation concluded that the Hudson Bay Basin has a resource potential of 818 MMbl (130×10^6 m^3) of recoverable oil and 3.2 Tcf (90×10^9 m^3) of recoverable gas (Procter et al., 1984). However, the geological data at that time was considered inadequate for a confident resource estimate. No resource evaluation is available for Foxe Basin.

2. GEOLOGICAL SETTING

2.1 General overview – Stratigraphy

A summary of the sedimentary succession is presented here, followed by a brief description of the stratigraphic units including the main lithological characteristics as well as the biostratigraphic data to support age assignment. Division of the sedimentary succession in formations and groups was first defined onshore in the southern part of the Hudson Platform and then extended to the entire platform (Figs 3 and 4). The link between the offshore and onshore stratigraphic units of Ontario and Manitoba is presented below. Nelson and Johnson (1966), Sanford (1987), Norris (1993), Hamblin (2008) and Zhang (2010) provide detailed overviews of the Paleozoic stratigraphy and links to North America Sequence framework. The stratigraphic framework for Foxe Basin is derived from the pioneer work of Lemon and Blackadar (1963) and from recent work by Zhang (2012, 2013) that resulted in a redefinition of some part of the succession (see below).

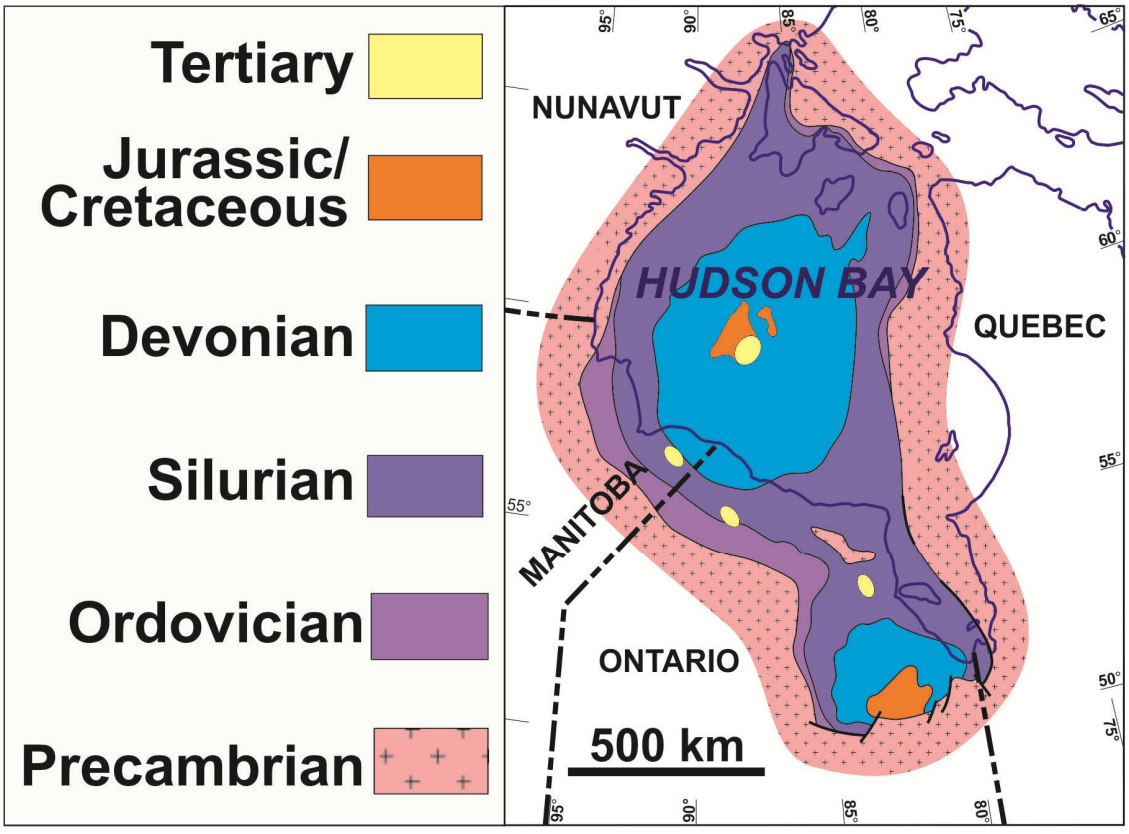

Figure 3: Simplified geological map of the Hudson Bay and Moose River basins, modified from Hamblin (2008) with the addition of Mesozoic and Cenozoic proven or potential patches.

2.1.1 Hudson Bay and Moose River basins – Summary.

The Paleozoic succession formed in shallow marine conditions and consists mainly of limestone, dolostone and evaporite, with minor amount of sandstone and shale (Sanford, 1987; Norris, 1993; Hu et al., 2011) (Figs. 4 and 5). Coarse-grained clastics are restricted to a thin interval at the base of the succession indicating that high topographic relief was absent around the basin during most of its formation. Backstripping, based on new paleontological data and well correlations, reveals an irregular subsidence history marked by several periods of exhumation (Pinet et al., 2013a).

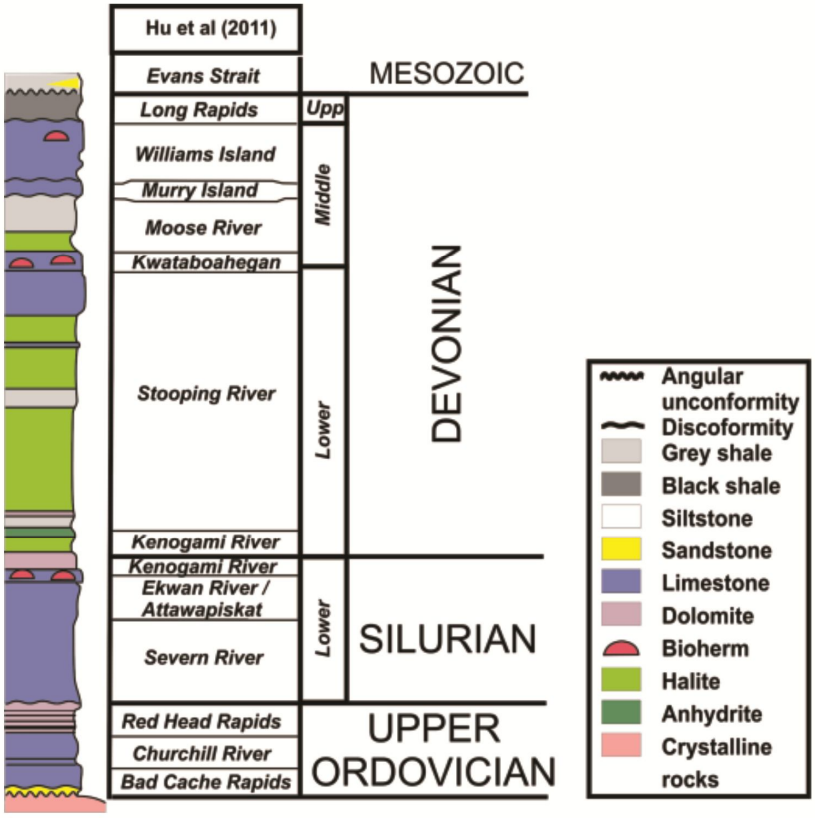

Figure 4: Schematic lithostratigraphic column of the Hudson Bay and Moose River basins

Upper Ordovician strata in the basin consist of a thin basal clastic unit and a carbonate-dominated succession that includes the Bad Cache Rapids Group, Churchill River Group and Red Head Rapids Formation (Zhang and Barnes, 2007). An unconformity likely controlled by a global end-Ordovician glacio-eustatic sea level fall marks the Ordovician-Silurian boundary. The lower Silurian succession (Suchy and Stearn, 1992) includes the carbonate-dominated Severn River, Ekwan River and lower Kenogami River formations, and locally developed metazoan reefs (Attawapiskat Formation).

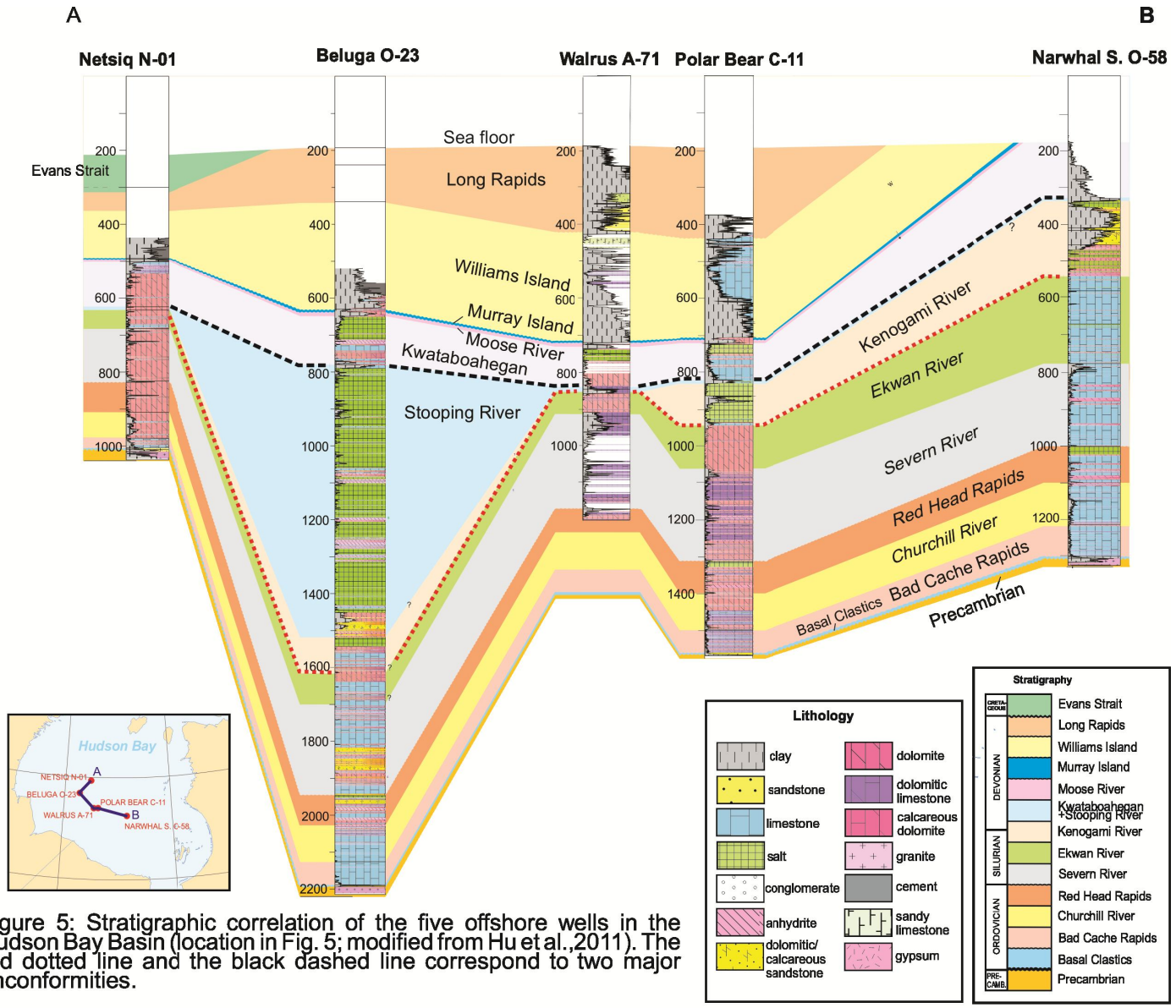

Figure 5: Stratigraphic correlation of the five offshore wells in the Hudson Bay Basin (location in Fig. 5; modified from Hu et al.,2011). The red dotted line and the black dashed line correspond to two major unconformities.

An unconformity within the Kenogami River Formation separates Lower Silurian and Devonian strata. Devonian strata in the Hudson Bay Basin are represented by a succession of Lower, Middle and Upper Devonian marine limestone and local reefs, evaporite and shale (Sanford and Norris, 1975; Thorpe, 1988) expressed in the Stooping River, Kwataboahegan, Moose River, Murray Island, Williams Island and Long Rapids formations. Several unconformities have been documented or interpreted within the Devonian succession (Sanford, 1987; Thorpe, 1988).

Pennsylvanian (Westphalian) strata in the Hudson Bay Basin were identified from biostratigraphic studies of the upper part of the Narwhal well (Tillement et al., 1976). Williams and Barss (1976) identified mixed assemblages of Westphalian, Cretaceous and Tertiary microfossils. Their definitive conclusion was that (in-situ) Pennsylvanian strata were not present.

The Paleozoic succession in the onshore and possibly in the offshore Hudson Bay Basin is locally overlain by thin, erosional remnants of Middle Jurassic, Lower Cretaceous and Cenozoic non-marine and marine sediments. In northern Ontario, an approximately 20 m thick succession of non-calcareous mudstones previously interpreted as Cretaceous is now considered as Miocene-Pliocene in age (Galloway et al., 2012: Gao et al., 2012). Most of the Hudson Bay Basin is blanketed by a thin section of Pleistocene glacial deposits and recent marine clays.

2.1.2 Foxe Basin – Summary

The first stratigraphic framework for the surroundings of the Foxe Basin was established at Admiralty Inlet, at the northwestern end of Baffin Island. Blackadar (1956) introduced the term Admiralty Group for the flat-lying Cambrian (?) – Lower Silurian carbonates and clastics on top of Precambrian. The group was initially composed of four units: the Gallery, Turner Cliffs, Ship Point, and Baillargé formations. Trettin (1969) restricted this group to the Gallery and Turner Cliffs formations, based of probable and proven disconformities below and above the Ship Point Formation; thus the Ship Point and Baillargé formations became independent units. The Ship Point Formation was defined originally as a dolomitic unit (~274 m) between the Turner Cliffs and Baillargé formations (Blackadar, 1956), and was redefined (Trettin, 1975) to include the original “member S3” of Trettin (1969), the sandstone-dominated upper part of the Turner Cliffs Formation. Thus, the sandstone unit was referred to as member A, and the original Ship Point Formation as member B (Trettin, 1975) of the redefined Ship Point Formation. Based on available biostratigraphic information, a *circa* 350 m thick Cambrian (?) – Middle Ordovician succession (Trettin, 1975) is present beneath the Upper Ordovician to Lower Silurian package in the Foxe Basin. This succession consists of two major sandstone-dominated units (Gallery Formation and member A of the Ship Point Formation) overlain by dolomite-dominated facies (redefined Turner Cliffs Formation and member B of the Ship Point Formation). These older-aged sediments are unknown in the Hudson Bay Basin

The Baillargé Formation (Trettin, 1969) unconformably overlies the Ship Point Formation in northern Baffin Island; the formation is Lower Ordovician to Lower Silurian in

age and consists of a lower dolostone-dominated unit and an upper limestone-dominated unit. In Foxe Basin, the Baillargé Formation is assigned to map-unit Ols and OScb, which are comparable to the combined Bad Cache Rapids and Churchill River groups, the Red Head Rapids, Severn River and Ekwan River formations (Trettin, 1975). The stratigraphic framework of the Upper Ordovician to Lower Silurian succession present on Melville Peninsula, as well as on the offshore islands and on southern Baffin Island was relatively similar to the one proposed for the Hudson Bay Basin, although some significant differences precluded the exact correlation and hence informal stratigraphic units were used for that time interval on the regional mapping (Trettin, 1975). It is currently unknown if younger than Early Silurian sediments were deposited in the Foxe Basin.

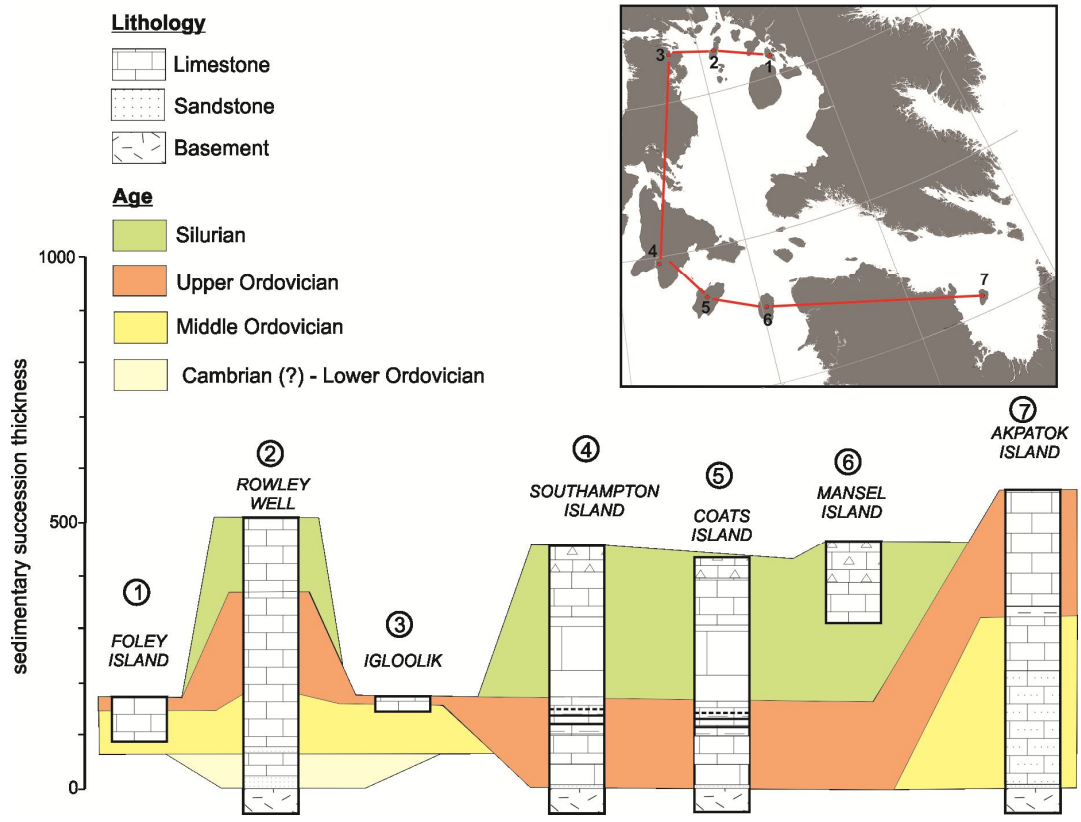

Figure 6: Stratigraphic columns of the preserved onshore sedimentary succession in the Foxe Basin and Hudson Strait areas.

2.1.3. Hudson Strait basins - Summary

Onshore, the Paleozoic succession surrounding the Hudson Strait is nearly flat-lying, and reaches a maximum thickness of 600 m (Fig. 6). Offshore, the Hudson Strait area comprises several fault-controlled sub-basins having a half graben geometry and sedimentary infill up to more than 2 km in the easternmost sub-basin.

The base of the succession formed in shallow marine conditions during Late Ordovician to Early Silurian time on Southampton and Coats islands and during Middle to Late Ordovician on Akpatok and Baffin islands. Nearby, on south Baffin Island, the succession comprises the Lower Ordovician Frobisher Bay Formation, the Upper Ordovician Amadjuak, Akpatok and Foster Bay formations, the overlying Lower Silurian strata are not formally defined (Zhang, 2012).

Offshore, an angular unconformity is documented at several locations in the hanging-wall of half grabens. Sanford and Grant (1999) tentatively ascribed a 'possibly Mesozoic age' to the strata above the unconformity.

2.2 Detailed stratigraphic account – Hudson Platform

2.2.1 Offshore Hudson Bay

The stratigraphy of the offshore domain of the Hudson Bay Basin was initially based on detailed well site interpretation of cuttings, sidewall cores and cores. Subsequent well logs, palynology and geochemical analyses and thin sections examination have completed the well site studies. All these reports for the five industry wells drilled in the Hudson Bay are available at the National Energy Board. Based on this information, complemented by interpretation of industry seismic and comprehensive fieldwork on the stratigraphically thin onshore extension of the Hudson Bay Platform and the thin but more complete succession in the Moose River Basin, Sanford and Grant (1998) presented the first holistic synthesis of the stratigraphy and structural framework of the Hudson Bay. Hamblin (2008) in his synthesis of the hydrocarbon systems elements for the Hudson Bay Platform presented the Sanford and Grant (1998) stratigraphic framework in the context of the North American Sequence stratigraphic framework of Sloss (1988). Zhang and Barnes (2007) carried out an extensive conodont biostratigraphic study of three offshore wells (Polar Bear C-11, Narwhal South O-58 and Walrus A-71) and three onshore wells (Penn Island #1, Comeault #1 and Kaskattama #1). Their work focussed on the Ordovician – Silurian part of the succession and offers the biostratigraphic framework used for this interval in this report; Zhang (2011a) reassessed some of the ages of the Upper Ordovician interval. Uyeno (1989) carried out complementary conodont study on some offshore wells. The biostratigraphy of the Devonian section was also addressed by S.N.P.A (1975) and Dolby (1986). As part of the Hudson Bay and Foxe basins project of the Geomapping for Energy and Minerals program, a detailed re-analysis of available offshore well logs was undertaken (Hu et al., 2011; Hu and Dietrich, 2012), as well as new palynological analyses (chitinozoans: Asselin, unp. results) of the better age constrained Ordovician-Silurian interval and the less constrained Devonian succession (Hu et al., 2011).

The well log cross-section (Fig.5) illustrates the major stratigraphic correlations between the five offshore wells drilled in the Hudson Bay Basin (Netsiq N-01, Beluga O-23, Walrus A-71, Polar Bear C-11 and Narwhal South O-58). Based on log interpretation and new biostratigraphic information on the Silurian-Devonian interval, the correlations differ from

previous work (Sanford and Grant, 1998). The five offshore wells penetrated Upper Ordovician to Devonian strata, unconformably overlying Precambrian granitic and metasedimentary (basement) rocks. One well (Netsiq N-01) encountered Cretaceous (?) strata, unconformably overlying the Paleozoic section. Three wells (Netsiq, Walrus and Polar Bear) were drilled on fault-block highs within the Central Hudson Bay Arch, with a thinner sedimentary package compared to the other two wells drilled off the Central Arch. The Walrus well terminated in the upper part of the Upper Ordovician carbonates; all others reached the Precambrian basement.

Ordovician

Upper Ordovician strata in the offshore domain of Hudson Bay consist of a thin basal clastic unit and a carbonate-dominated succession that includes from base to top, the Bad Cache Rapids Group, Churchill River Group and Red Head Rapids Formation.

- An undated and unnamed basal clastic unit is present in all wells drilled to Precambrian basement. This coarse sandstone to pebbly conglomerate is 4 to 6 m thick.
- The Edenian-Maysvillian Bad Cache Rapids Group (Nelson, 1963; Zhang, 2011a) consists of fossiliferous limestone and dolomitic limestone. This unit ranges from a minimum of 17 m (Netsiq well) to 86 m (Narwhal well).
- The early Richmondian Churchill River Group (Nelson, 1963; Zhang and Barnes, 2007; Zhang, 2011a) conformably overlies the Bad Cache Rapids Group. It is composed of dolostone, limestone and minor anhydrite with locally bituminous limestones. This unit ranges from a minimum of 70 m (Netsiq well) to 112 m (Narwhal well).
- The late Richmondian Red Head Rapids Formation (Nelson, 1963; Zhang and Barnes, 2007; Zhang, 2011a) consists of interbedded carbonates (mainly dolostone), shale and anhydrite with an overlying salt section (in the Beluga, Polar Bear and Narwhal wells). The lower Red Head Rapids Formation contains three oil shale intervals (Zhang, 2008). The formation thickness is between 83 m (Beluga well) and 100 m (Narwhal well).

Silurian

Lower Silurian strata in the offshore domain of the Hudson Bay are represented by the carbonate-dominated succession of the Severn River, Ekwan River, Attawapiskat and Kenogami River formations.

- The Llandoverian Severn River Formation (Sanford et al., 1968; Zhang and Barnes, 2007) is an assemblage of fine-grained fossiliferous limestone and dolostone that disconformably occurs over the Upper Ordovician Red Head Rapids Formation. Minor anhydrite and dolomitic sandstones also occurs. This formation ranges from 143 m (Netsiq well) to 256 m (Walrus well).
- The Llandoverian Ekwan River (Norris, 1986; Zhang and Barnes, 2007) and Attawapiskat (Wilson et al., 1941) formations have been lumped together in the well study because the distinctive element, the dominance of metazoan biostromes and

bioherms in the Attawapiskat Formation, could not be identified in well cuttings; moreover, the upper part of the Ekwan River Formation has been shown to be biostratigraphically-correlative with the Attawapiskat Formation. The combined units are dominated by dolostone beds in the Netsiq, Walrus and Polar Bear wells, fine-grained limestones are present in the Beluga and Narwhal wells. The combined Ekwan River and Attawapiskat formations reaches thickness of 50 m (Netsiq well) up to 157 m (Narwhal well).

- The Kenogami River Formation (Dyer, 1930) has been separated in two informal units, as new biostratigraphic data locate the Silurian-Devonian contact in that formation. The lower part of the formation (Llandovery) consists of limestone, dolostones and rare dolomitic sandstones. The Llandoverian interval of the Kenogami River Formation is not present in the high-standing fault blocks tested by the Netsiq and Walrus wells. Its total thickness ranges between 97 m (Beluga well) up to 150 m (Narwhal well).

Devonian

The Devonian succession consists of the upper Kenogami River, Stooping River, Kwataboahegan, Moose River, Murray Island, Williams Island and Long Rapids formations. This succession occurs over a significant unconformity that spans from the Llandoverian (Lower Silurian) to the Emsian (end Lower Devonian), a time interval of *circa* 20 Ma. Moreover, the recently acquired biostratigraphic data suggests the presence of other, less pronounced, time hiatuses in the succession, in particular at the base of the Murray Island and Williams Island formations.

- The Emsian – Givetian upper part of the Kenogami River Formation is dominated by evaporites. The succession has been identified in three wells (Beluga, Narwhal and Polar Bear) where it is 25, 70 and 114 m thick respectively.
- The Emsian - Givetian Stooping River Formation (Sanford et al., 1968) is characterized by major thickness and facies changes. A thick (738 m) succession of halite and minor carbonates occurs in the Beluga well, whereas in the other wells, the succession consists of shale and dolomitic limestones which is also developed at the top of the halite succession in the Beluga well. For the other wells, the thickness of formation is significantly thinner compared to that encountered in the Beluga well, ranging from 9 to 12 m in the Netsiq, Polar Bear and Walrus wells.
- The Emsian – Givetian Kwataboahegan Formation (Sanford et al, 1968) is characterized by a major facies change with the Narwhal well being dominated by shales with all other wells showing a succession of limestones and dolostones with minor shales. The formation thickness varies between 58 m (Beluga well) and 113 m (Narwhal well).
- The Givetian Moose River Formation (Wilson et al., 1941) consists of a succession of evaporites and shales with evaporites being replaced by carbonates in the Netsiq well. The formation thickness ranges from 26 m (Narwhal) to 84 m (Beluga

well).

- The Givetian Murray Island Formation (Sanford et al., 1968) is a thin unit (3 to 8 m) of highly variable percentage of shale, dolostone and evaporites.
- The Givetian-Frasnian Williams Island Formation (Kindle, 1924) consists of a lower shale unit, overlain by limestones and minor sandstones. The formation thickness varies from 128 m (Netsiq well) to 293 m (Walrus well).
- The Frasnian-Fammenian Long Rapids Formation (Sanford and Norris, 1975) is the youngest preserved Paleozoic unit. The formation has been intercepted in only two wells (224 m in Walrus well and 60 m in Polar Bear well) and the succession is dominated by shale.

Carboniferous ?

The presence of Westphalian (middle Pennsylvanian) strata was suggested by Tillement et al (1976) near the top of the Narwhal well, an assertion based on the occurrence of Carboniferous palynomorphs in fine-grained clastics. Williams and Barss (1976) re-examined the palynological assemblage of the upper part of the Narwhal well and suggested a contamination of the material either at the laboratory or from drilling pipes. The nearest clearly documented Pennsylvanian rocks are located in the center of the Michigan Basin, some 1500 km to the south and in the Williston basin at roughly the same distance to the southeast (Fig. 1).

Cretaceous ?

The Cretaceous ? Evans Strait Formation (Sanford and Grant, 1990) has been interpreted to by present at the top of the Netsiq well largely based on high-resolution seismic data. Although described as a clastic unit by Sanford and Grant (1998), there are no log or sample data available to determine the lithology of Cretaceous strata in the Netsiq well.

2.2.2 Ontario

Previous work and data sources in Ontario

The Hudson Platform of Ontario was mapped in 1967 during the GSC's Operation Winisk (Sanford et al. 1968). Norris and Sanford (1975) reported on Devonian stratigraphy of the Hudson Platform. Other significant stratigraphic reports and summaries include Savage and Van Tuyl (1919), Martinson (1952), Nelson (1963, 1964), Heywood and Sanford (1976), Cumming (1971, 1975), Norford (1964, 1971), Norford et al. (1989), Norris (1993), Zhang and Barnes (2007) and Hamblin (2008).

Maps of the Platform in northern Ontario were published by the Ontario Geological Survey (OGS 1991a, 1991b). Sanford and Grant (1998) published maps and cross sections of the Platform.

Hudson Bay Lowlands Subsurface Data

Subsurface data in the Hudson Bay Lowlands (HBL) of northern Ontario is very sparse

(Fig. 7). Most of our knowledge of the Paleozoic stratigraphy in the HBL comes from one deep well, Aquitaine Sogepet et al. Pen No. 1, that was cored and geophysically logged in 1969 near the shore of Hudson Bay and close to the Manitoba border. Top of bedrock was encountered at 41.80 m and coring of the bedrock commenced at a depth of 217.32 m. It was continuously cored down to the Precambrian basement, the top of which was intersected at a depth of 1021.33 m. This well is considered the reference well for the Paleozoic of northern Ontario. It was re-logged and re-sampled for this study (Fig. 8).

In 1971 Canadian Nickel Company Ltd. (later changed to INCO Ltd.) undertook an exploration program in the upper Winisk River area (Fig.7). Fourteen exploration holes were drilled and core from 2 of these, INCO # 49212 and #49204, are archived in the Ministry of Northern Development and Mines (MNDM) office in Timmins Ontario.

In 1978 and 1979, Prospection Ltd. drilled a number of mineral exploration holes west of the Sutton Inlier, approximately 35 km south-southeast of Peawanuck. Only short segments of core have been archived from 5 of these holes. They are stored at the Oil, Gas and Salt Resources Core Library in London, Ontario.

In 2001 Wallbridge Mining Ltd. cored a mineral exploration hole near the Severn River approximately 115 km southwest of Fort Severn (Fig.7). The core was left in the field and logged as part of this project (Armstrong, 2011).

Records of a few other mineral exploration drill holes in the HBL are known, but the locations of any resultant cores are unknown.

James Bay Lowlands Subsurface Data

Historical (~1929 to 1985) oil and gas exploration and mineral exploration centered on the Moose River Basin (MRB) in the southern James Bay Lowlands (JBL). In addition, during that period deep stratigraphic wells were drilled in the MRB by governments and the petroleum industry.

The recent discovery of diamonds, chromite and other mineral resources, has resulted in significantly more diamond drilling (i.e. coring), especially in the northwestern MRB. This has provided a large new data set, although typically without geophysical logs. Selected cores were logged and sampled in the field (Armstrong 2011). Some cores had been previously donated to the OGS and archived at facilities in Sudbury. Some of these were also logged for this project (Fig 7; Armstrong 2012).

Outcrops

Outcrops of Paleozoic bedrock are generally sparse in both the HBL and JBL (see Sanford et al. 1968). They typically occur along waterways and on the coast of Hudson Bay. Limited reconnaissance scale field work was carried out as part of this project during the summer of 2011 (Armstrong, 2011). Field work was helicopter supported and involved transects through previously mapped stratigraphy along selected rivers.

Three general areas were targeted for the first phase of this project (Fig. 7): 1) the Silurian section along the Severn River; 2) the upper Ordovician to Silurian sections along the

Attawapiskat, Muketei and Ekwan rivers; and 3) Upper Ordovician outliers in the upper Winisk River area.

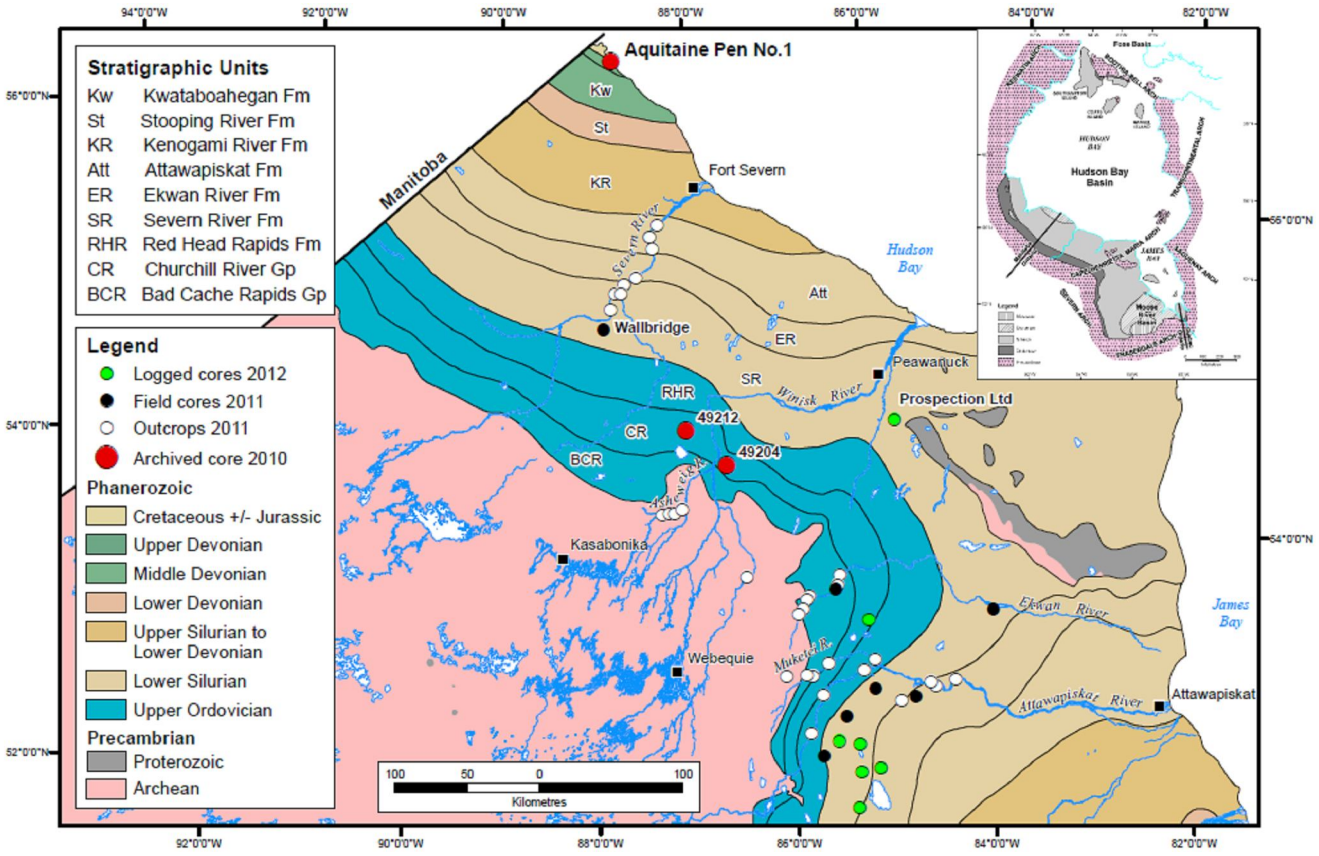

Figure 7: Geological map of the Hudson Bay Lowlands showing the location of wells cited in the text and outcrops studied in 2011.

Geologic Setting in Ontario

In northern Ontario, the southern Hudson Platform underlies the Hudson Bay and James Bay lowlands and is contiguous with the HBL in northeastern Manitoba.

The Platform in the HBL consists of Upper Ordovician to Middle (?) Devonian shallow marine carbonates with minor sandstones, mudstones and evaporites. Cretaceous marine sediments are interpreted to underlie the northernmost tip of Ontario, near the Manitoba border (Sanford and Grant 1990, 1998). As part of this project, Cenozoic sediments were discovered in an isolated outlier near the Winisk River (Galloway et al. 2011).

In the JBL, the Hudson Platform consists of a similar Paleozoic succession, but ranging up to Late Devonian in age, deposited in the Moose River Basin (MRB). Jurassic and Cretaceous non-marine sediments overlie the Paleozoic succession in the thickest part of the MRB, located in the southern JBL. Cenozoic age sediments were also described by Gao et al. (2012) in a sinkhole-like depression near the Victor diamond mine, approximately 100 km west of Attawapiskat.

The MRB and HBB are separated by an east-northeast trending basement high called the Cape Henrietta Maria Arch.

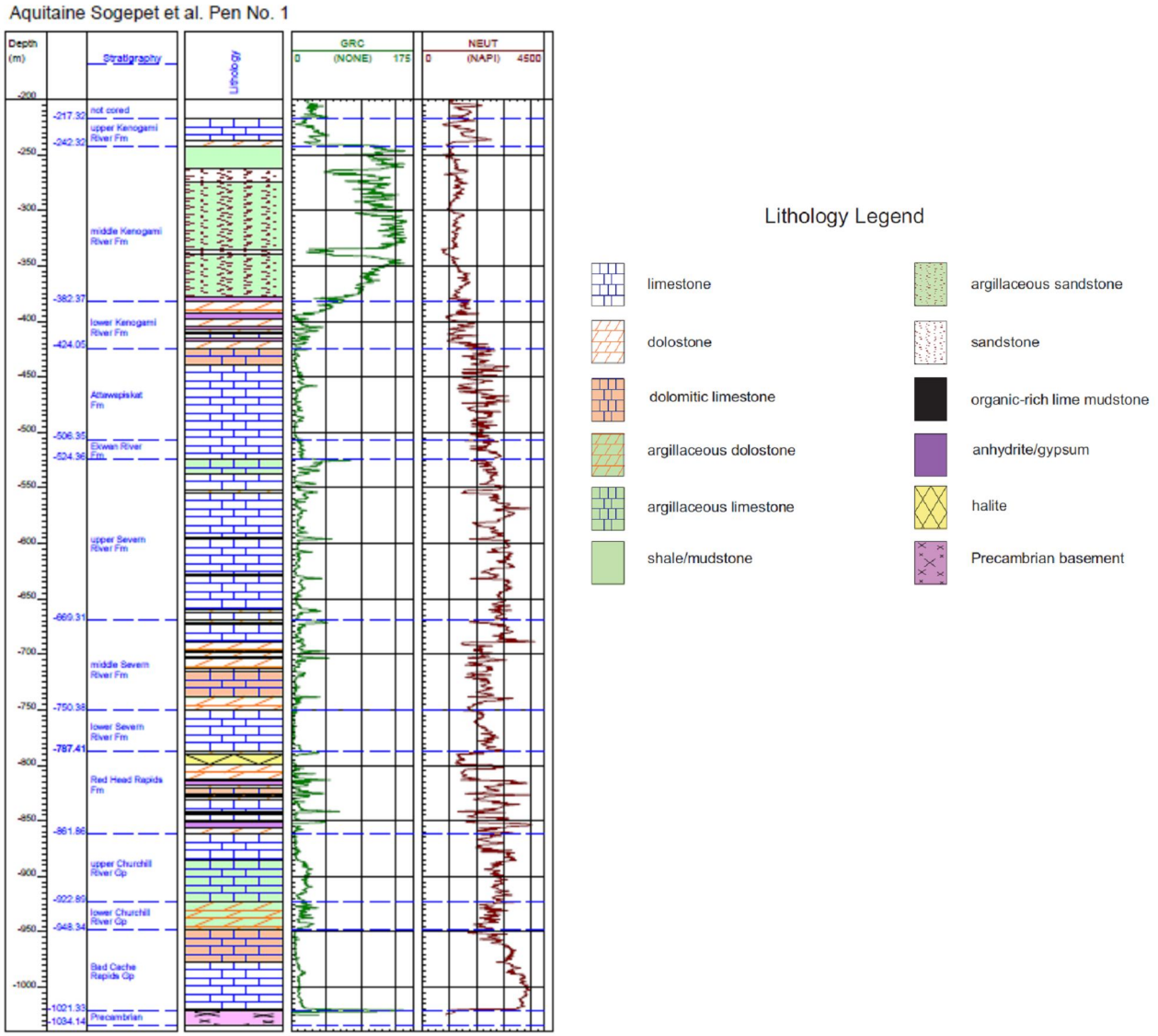

Figure 8: Stratigraphic column and well logs of the Aquitaine Sogepet et al. Pen No. 1 well.

Paleozoic

Upper Ordovician

The Upper Ordovician succession in northern Ontario records large-scale transgressive-regressive cycles, within which are locally well-developed metre- to decimetre scale evaporitic cycles. This succession consists of, in ascending order, the Bad Cache Rapids Group, Churchill River Group and Red Head Rapids Formation. Formational divisions of the Bad Cache Rapids and Churchill River groups as defined in northern Manitoba (e.g., Nelson 1963, 1964) have not previously been recognized in Ontario. Initially for this project, informal subdivisions were

constructed. Tentative correlations with the Manitoba stratigraphy are presented herein.

- ***Bad Cache Rapids Group***

The Bad Cache Rapids Group was proposed by Nelson (1963, 1964) for the Ordovician limestones and basal clastics that unconformably overlie the Precambrian basement in the Hudson Bay Lowlands in northern Manitoba. The entire Bad Cache Rapids Group in northern Ontario, as used in this study, is likely equivalent to the Portage Chute Formation of the Bad Cache Rapids Group in Manitoba.

The lower Bad Cache Rapids Group is a thin siliciclastic dominated, basal transgressive unit. It is characterized by basal white to green-grey, quartz-rich, argillaceous, calcareous sandstone to sandy shales, that grade upwards into moderately fossiliferous, sandy limestones with blue-rimmed burrows, locally abundant pyrite and blue-rimmed hard grounds. The lower Bad Cache Rapids is typically 2 to 3 m thick in the HBL and is up to 6.5 m thick in the MRB.

The upper Bad Cache Rapids Group consists of a relatively monotonous succession dominated by bioturbated, semi-nodular, burrow-mottled, fossiliferous limestones. Petrographic evidence (Desrochers, pers. comm. 2012) indicates continued transgression through the upper Bad Cache Rapids Group. This evidence includes the upward transition from restricted circulation marine fauna such as ostracods, gastropods and trilobites to more open circulation fauna including crinoids and brachiopods. Dasycladacean calcareous algae are common in the upper Bad Cache Rapids Group (Desrochers, pers. comm. 2012), indicating shallow (<10m) water depth. In the HBL, the upper part of this unit is typically dolomitic and contains evaporite minerals. In the MRB most of upper Bad Cache Rapids Group was dolomitized.

In the HBL the thickness of the upper Bad Cache Rapids Group ranges from about 70 m in Pen No 1 and approximately 80 m in the Wallbridge core to only about 10 m in the upper Winisk River area. In the northern MRB it ranges up to 30 m thick. Locally, especially in the northern MRB, the upper Bad Cache Rapids Group contains thin sandy dolostone beds. These are thought to represent periodic sea level lowstands, which would have exposed nearby paleotopographic highs.

Limestones and dolostones of the Bad Cache Rapids Group outcrop along many rivers flowing from the Precambrian Shield into the HBL and JBL (Sanford et al. 1968; Cumming 1975). The thin basal sandstones are seldom exposed.

- ***Boas River Formation***

The “Boas River Shale” was named after an outcrop along the Boas River on Southampton Island on the northern rim of the Hudson Bay Basin (Heywood and Sanford, 1976). This assignation has been modified since (Zhang, 2008). This poorly exposed outcrop consists of up to 2 m of dark brown to black, organic-rich lime mudstones containing graptolites, the trilobite *Pseudogygites* and calcareous concretions (Heywood and Sanford 1976). These “shales” were termed Boas River Formation by Sanford and Grant (1990), who also reported its occurrence in drill cores from the HBL in northern Ontario. Conodont biostratigraphic analysis of samples from these cores and the Southampton Island occurrence (McCracken 1990; McCracken and Nowlan 1989) indicates the Boas River Formation is middle Maysvillian in age and approximately equivalent to the Collingwood Member (Lindsay

Formation) of southern Ontario. However, most recent studies based on the extensive field mapping and sampling on Southampton Island and southern Baffin Island (Zhang, 2008, 2011a, 2012) indicated that more than one Upper Ordovician shale stratigraphic interval is developed in the basin.

The northern Ontario occurrences of the Boas River Formation in 2 mineral exploration cores from the upper Winisk River area (Sanford and Grant, 1990) have been confirmed (Armstrong and Lavoie 2010a, 2010b). An outcrop of this formation was discovered on the Asheweig River, 40 to 55 km to the southwest and south of the core locations (Armstrong 2011). One of these cores, INCO #49212, intersected 9.5 m of the Boas River Formation in apparent conformable (interbedded) contact with limestones of both the underlying Bad Cache Rapids Group and overlying Churchill River Group. The Asheweig River outcrop exposes almost 4 m of laminated dark brown grading upward into thin-bedded, non-laminated light grey-brown lime mudstones that are in turn sharply overlain by thin-bedded crinoidal grainstones and packstones. The crinoidal limestone may represent the basal beds of the overlying Churchill River Group.

St. Jean (2012) undertook a petrographic study of the Boas River Formation occurrences in Ontario. The organic-rich laminated facies exhibits grading and its fossil content is almost exclusively ostracods. Together, these suggest deposition as distal tempestites in an outer shelf or ramp setting with restricted anoxic to dysoxic waters.

The Boas River Formation has not been identified elsewhere in core or outcrop in northern Ontario or Manitoba (Nicolas and Lavoie, 2012), although data points are very sparse, especially in the HBL. Sanford and Grant (1998) interpreted the Boas River as a regionally distributed unit in northern Ontario, however to date only the only known occurrences are the 2 Winisk River area cores and Asheweig River outcrop.

- ***Churchill River Group***

Based on outcrops along rivers in northern Manitoba Nelson (1963, 1964) proposed the term Churchill River Group for Ordovician limestones that overlie the Bad Cache Rapids Group and underlie the Red Head Rapids Formation. In northern Ontario the Churchill River Group was informally divided for this project into a lower and upper unit.

The lower Churchill River Group is characterized by non-fossiliferous, tan dolomudstones with thin green shale beds and desiccation features (e.g., mudcracks), anhydrite nodules or beds and gypsum-filled fractures.

The lower Churchill River Group is approximately 25 m thick in Pen No 1 and is estimated to be of similar thickness in the Wallbridge core (unsure due to missing core). Approximately 20 m of a similar lithofacies occurs in INCO #49212, however it occurs above 4.5 m of bioclastic limestone that in turn overlies the Boas River Formation (see Figure 39.5 in Armstrong and Lavoie 2010a). This implies that the Boas River may be a unit within the upper Bad Cache Rapids Group, rather than separating the Bad Cache Rapids from the Churchill River Group.

In northern Ontario, the lower Churchill River Group appears to be equivalent to the Surprise Creek Formation of the Bad Cache Rapids Group of northern Manitoba (*see* Figure 2

in Le Fèvre et al. 1976). The Boas River Formation may then be a lateral facies equivalent of the Surprise Creek Formation.

The upper Churchill River Group consists of sparsely to moderately fossiliferous, bioturbated, semi-nodular, sometimes burrow-mottled limestone. Fauna is dominantly shelly, including brachiopods and gastropods, with locally abundant crinoids. The lower half of this unit is grey to green and argillaceous and the uppermost few metres are dolomitic and appear to be gradational with the overlying Red Head Rapids Formation. These informal subdivisions are indicated in the gamma ray log for Pen No. 1 (note the higher gamma ray response of the lower unit) and likely correspond to the Caution Creek and Chasm Creek formations of northern Manitoba (Nelson 1963, 1964).

The upper Churchill River Group is approximately 60 m thick in Pen No. 1. It is estimated to be 45 m thick in the Wallbridge core and 26 m thick in INCO #49212, where it subcrops beneath Quaternary drift. This unit thins to less than 5 m in the northern MRB and then appears to pinch out to the south. Where it is absent the Red Head Rapids Formation directly overlies the lower Churchill River Group. These units are difficult to distinguish because of their similar lithologic characteristics.

The Churchill River Group is not well exposed in northern Ontario (see Sanford et al. 1968). Outcrops of the lower Churchill River Group (mudcracked dolostones) occur on the upper Ekwan River (Armstrong and Lavoie 2012).

Jin et al. (1997) recognized distinct Maysvillian and Richmondian brachiopod assemblage zones respectively, for the Bad Cache Rapids and Churchill River Group. Based on these they determined that the Bad Cache Rapids Group did not extend into the Moose River Basin. Lithostratigraphic mapping for this project seems to contradict this interpretation. New conodont and chitinozoan samples will be analyzed to resolve this issue.

- ***Red Head Rapids Formation***

The youngest Ordovician unit in northern Ontario is the Red Head Rapids Formation. It is characterized by evaporitic cycles typically consisting of burrow-mottled, fossiliferous limestones that grade upwards into non-fossiliferous, locally laminated, tan dolosiltites and dolomudstones, that in turn become anhydrite-beading, tan dolomudstones, then anhydrite or halite beds and finally capped by grey to green argillaceous dolosiltites.

These strata were originally included in the Port Nelson Formation as defined by Savage and Van Tuyl (1919). As originally defined (Savage and Van Tuyl 1919), the Port Nelson Formation at its type section on the Nelson River in Manitoba, included blocks that contained the Silurian brachiopod *Virgiana* (Savage 1918) and thus the formation was considered Silurian. It was later determined (Nelson 1964) that these blocks were in fact boulders and not part of the outcrop which was later determined to by Ordovician (Norford et al. 1998). Some workers (e.g. Norford 1971; Norford et al 1998) advocated use of the term Port Nelson Formation. Nelson (1963, 1964) introduced the term Red Head Rapids Formation based on outcrops on the Churchill River. The later term is used more commonly (e.g. Cumming 1971; 1975; Heywood and Sanford 1976; Sanford and Grant 1990, 1998; Norris 1993). It is for these reasons that the term Red Head Rapids Formation is used in this report.

In Ontario halite beds only occur near the top of the Red Head Rapids Formation and only in Pen No. 1. In the northern MRB the burrow-mottled or fossiliferous marine limestone components of the Red Head Rapids cycles are virtually absent. Mudstones are more significant in the MRB and thin sandstones occur locally. Red coloured mudstones are especially abundant near but not at the top of this unit. They occur through the MRB and in the Prospection Ltd. cores located immediately northwest of the Sutton Inlier (Proterozoic sediments and mafic sills) on the northwest flank of the Cape Henrietta Maria Arch. The red mud is thought to originate from the weathering of exposed Precambrian iron formation during this sea level lowstand.

The Red Head Rapids Formation is poorly exposed in the Hudson Platform of northern Ontario. One outcrop of this unit, consisting of thin-bedded, mud-cracked, argillaceous dolostone, occurs on the Attawapiskat River, just above where it meets the Muketei River (Armstrong 2012).

The Red Head Rapids Formation is approximately 74 m thick in Pen No. 1 and is estimated to be approximately 38 m in the Wallbridge core. In the northern MRB it ranges from 50 to 16 m thick, thinning towards the southwest.

Recent conodont biostratigraphic analysis (A.D. McCracken, pers. comm. February 15, 2013) indicates that the uppermost Red Head Rapids Formation, as described here for the northern Moose River Basin, contains "Silurian-aspect" conodonts such as *Ozarkadina oldhamensis*. This implies that the upper part of the Red Head Rapids Formation may be Hirnantian (uppermost Ordovician) in age. Further work is required to confirm this and positively identify the Ordovician-Silurian boundary in northern Ontario.

Silurian

The Lower Silurian Seven River Formation is dominated by poorly developed evaporitic cycles. Biostromal and biohermal limestones of the Llandovery Ekwan River and Attawapiskat formations disconformably overlie the Seven River Formation and are disconformably(?) overlain by evaporite-bearing dolomudstones, red mudstones and brecciated dolostone, traditionally assigned to the Wenlock to Lower Devonian Kenogami River Formation (e.g. Norris 1993) with little biostratigraphic control. Biostratigraphic evidence from offshore wells suggests these latter strata are mainly Middle Devonian (Hu et al. 2011).

- ***Severn River Formation***

The oldest Silurian strata in the Hudson Platform are shallow marine carbonates of the Severn River Formation. Proposed by Savage and Van Tuyl (1919) based on a series of outcrops along the Severn River, south of the mouth of the Fawn River, the Severn River Formation was later expanded (Sanford et al. 1968) to include outcrops up to 10 km downstream of the Fawn River. Sanford et al (1968) also included the underlying Nelson River Formation of Savage and Van Tuyl (1919) and the upper member of Red Head Rapids Formation of Nelson (1963, 1964). Subsequently, Sanford and Norris (1973) removed Ordovician strata (Red Head Rapids), so that the Severn River Formation is now defined as Silurian limestones unconformably overlying the Ordovician Red Head Rapids Formation and

disconformably overlain by limestones of the Ekwan River Formation (Heywood and Sanford 1976).

The Severn River Formation is characterized by tan coloured, burrow-mottled, bio-wackestones to bio-packstones that are punctuated by thin green argillaceous dolosiltites. Dolostones and anhydrite occur in evaporitic cycles that are best developed in the middle of the formation. The resulting informal 3-fold division consists of a middle evaporitic unit over- and underlain by more fossiliferous units. These units may correlate with the 3 conodont ecozones of Le Fèvre et al. (1976) for the Severn River Formation.

The lowest unit of the Severn River Formation consists of approximately 37 m (in Pen No. 1) of, in ascending order, almost chalky dolomudstone grading rapidly up into 'ribbon' limestone to dolomitic lime mudstone, and then to fossiliferous, burrow-mottled bio-wackestones and brachiopod-rich packstones that consist almost exclusively of the brachiopod *Virgiana decussata* (Jin et al. 1997).

No exposure of the lower part of the Severn River Formation was found on the Severn River. An outcrop of *Virgiana*-bearing limestone was discovered in the northern Moose River Basin, on the Muketei River approximately 4.5 km from where it meets the Attawapiskat River. The lower unit (i.e. *Virgiana* beds) also occurs in all of the drill cores from the northwest Moose River Basin that were collared at that level or higher.

The middle unit of the Severn River Formation is approximately 81 m thick in Pen No. 1. In the subsurface it consists of cycles of burrow-mottled, fossiliferous, bio-intraclastic and peloidal, wackestones, packstones and grainstones, overlain by anhydrite-bearing dolomudstones and capped by light green argillaceous dolosiltites. Outcrops of the middle unit occur along the Severn River, south of the Fawn River. These outcrops contain abundant small stromatolitic mounds and beds, thin tabular dolomudstones, intraclastic rip-up beds and moulds after evaporite minerals and/or rip-up clasts.

The upper unit of the Severn River Formation consists of up to 145 m (in Pen No. 1) of burrow-mottled, sparsely to moderately fossiliferous, bio-wackestone, with thin bio- and/or intraclastic pack-grainstone beds, local 'ribbon' limestones and laminated lime mudstones. There are also some thin argillaceous intervals and by thin light green argillaceous dolosiltite layers. Although possibly cyclic like the middle unit, cycles in the upper unit do not appear to be as clearly developed and there is no evidence of significant evaporites.

Outcrops of the upper Severn River Formation occur on the lower Fawn River and on the Severn River near and below where it joins the Fawn River. These outcrops consist of thin- to medium-bedded, semi-nodular, burrow-mottled bioclastic wackestones and packstones with local thin grainstones. Crinoidal material is common. Other fossils include small tabulate corals and stromatoporoids, locally abundant brachiopods and gastropods. Two of these outcrops, located approximately 3 km north of the Fawn River, appear to be structurally disturbed, with broad low angle anticlinal dips and a minor offset fault.

The upper disconformable contact of the Severn River Formation with the overlying Ekwan River Formation was observed in outcrops on the Severn River (~11 km north of the Fawn River) and on the Attawapiskat River (~35 km east of the Missisa River). The uppermost

section of the Severn River Formation on the Severn River consists of a recessive, yellow-tan weathering, greenish coloured dolosiltite and dolomudstone beds, containing vuggy to cavernous porosity that may be karstic in origin. These dolomitic beds sharply overlie nodular, burrow-mottled, fossiliferous limestones more typical of the upper Severn River Formation.

On the Attawapiskat River, the uppermost Severn River Formation consists of burrow-mottled bio-wackestones with thin bio- and intraclastic pack- to grainstones. Semi-nodular, burrow-mottled, skeletal packstones and then very fossiliferous biostromal beds of the Ekwan River Formation disconformably overlie the Seven River Formation.

- ***Ekwan River Formation***

The term Ekwan River limestones was proposed by Savage and Van Tuyl (1919) for outcrops of fossiliferous limestones along the Ekwan River underlying coral reefs of the Attawapiskat Formation. The Ekwan River Formation is characterized by well-bedded, fossiliferous, biostromal limestones (Norris 1993) with locally abundant chert nodules (Sanford et al. 1968). It is variously interpreted to overlie the Severn River Formation conformably (Norris 1993; Jin et al. 1993) or disconformably (Suchy 1992; Suchy and Stearn 1992). Preliminary results of this study favour the latter interpretation. It is conformably overlain by biohermal limestones of the Attawapiskat Formation and where the Attawapiskat is absent (e.g. southern Moose River Basin) it is directly overlain by the Kenogami River Formation (Norris 1993). The upper part of the Ekwan River Formation is considered to be coeval with the lower part of the Attawapiskat Formation (Norris 1993).

The lower part of the Ekwan River Formation is well exposed in cliffs along the Attawapiskat River, approximately 35 km east of the Missisa River. There, over 8 m of stromatoporoid and coral biostromal limestone (rudstone) and semi-nodular, burrow-mottled, skeletal packstone disconformably overlie approximately 2 m of the Severn River Formation. The lowermost, very fossiliferous and bioclastic beds of the Ekwan River Formation are also exposed on the Severn River approximately 11 km north of the Fawn River, where they disconformably overlie dolostones of the Severn River Formation.

In this study, the Ekwan River Formation was observed in only one well, Pen No. 1. In that core this unit is not as fossiliferous as observed in outcrops, consisting mainly of skeletal, semi-nodular packstones. Its basal contact was placed at a sharp and possibly disconformable contact at the top of an argillaceous limestone. This corresponds with a sharp increase in gamma ray response (Fig. 8). Its upper conformable contact with the biohermal boundstones of Attawapiskat Formation is marked by a slight decrease in gamma ray response. The Ekwan River Formation is approximately 18 m thick in Pen No. 1.

- ***Attawapiskat Formation***

Savage and Van Tuyl (1919) proposed the term Attawapiskat coral reefs for outcrops of coral and stromatoporoid bearing limestones along the Ekwan and Severn rivers. Reefs of this formation on the Attawapiskat River were initially described by Bell (1887). More recent studies of the Attawapiskat Formation reefs and their fauna include Chow and Stearn (1988), Suchy (1992), Suchy and Stearn (1992, 1993) and Jin et al. (1993).

As part of the present study, outcrops of the Attawapiskat Formation on the Severn

River were examined and the formation was logged in the Pen No. 1 core. This formation is approximately 82 m thick in Pen No. 1, where it consists of 2 coral-stromatoporoid boundstones separated and overlain by crinoidal to skeletal packstones and grainstones as well as megalodont bivalve and gastropod-bearing wackestones. Very porous "*Nuia*" (Suchy 1992) grainstones occur towards the top of the formation. In Pen No 1, glauconite occurs near the top of the formation suggesting a disconformable contact with the overlying evaporitic dolostones Kenogami River Formation. A conformable upper contact with the Kenogami River Formation has been reported by Norford (1971) and Jin et al. (1993).

The Attawapiskat Formation is well exposed in outcrops along the Severn River, from about 45 to 60 km south of its mouth. The most spectacular outcrops, located approximately 55 km from the mouth, expose very thick-bedded, biohermal lenses and associated bioclastic and draping beds. At the southern end of this outcrop belt a large outcrop mapped as Attawapiskat Formation Sanford et al. (1968). This outcrop consists of thin-bedded, fossiliferous limestone containing small (1 to 2 m across by <0.5 m high) biostromal lenses with large chain corals, crinoids, gastropods and the brachiopod *Trimerella*. This outcrop may be lower Ekwan River Formation.

The stratigraphically highest outcrop of the Attawapiskat Formation on the Severn River (~ 45 km from mouth of river) consists of a number of low domal or exhumed domal outcrops of thin to thick, tabular bedded, sparsely to very fossiliferous limestone and dolostones which are draped over underlying reefs.

- ***Kenogami River Formation***

The Kenogami River Formation was proposed by Dyer (1929) for outcrops of red and green shale and dolostone on the Kenogami and other rivers in the Moose River Basin. This formation is divided into 3 informal lithostratigraphic members (Sanford et al. 1968): a lower member consisting of interbedded dolostone and gypsum or anhydrite; a middle member consisting of gypsiferous red and green mudstone, siltstone and sandstone and minor dolostone; and an upper member consisting of oolitic and brecciated dolostone. The lower member is considered to be Upper Silurian (Sanford et al. 1968) due to its apparent conformable relationship with the underlying Attawapiskat Formation; however, biostratigraphic evidence is lacking. Lower Devonian (Gedinnian and Siegenian) spores are reported for the upper member in the Moose River Basin (McGregor et al. 1970; McGregor and Camfield 1976). The Silurian-Devonian boundary is likely somewhere in the middle member.

In Pen No. 1, approximately 207 m of the Kenogami River Formation was cored, representing all 3 members. An additional overlying 6.5 m of the upper member was identified in logs for this well (from files at the Ontario Oil Gas and Salt Resources Library, London, Ontario) giving a total thickness of 213.5 m. In the Moose River Basin this formation is up to 250 m thick (Sanford 1987).

A recent re-appraisal of available biostratigraphic data and new chitinozoan and conodont biostratigraphic data (Hu et al. 2011) indicates that much of the approximately 800 m that had been assigned to the Kenogami River Formation (e.g. Sanford 1987) in offshore wells in Hudson Bay is late Early Devonian (Emsian) in age and therefore is equivalent with the

overlying Stooping River Formation. Hu et al. (2011) reassigned these offshore strata to the Stooping River Formation (Fig. 5). New biostratigraphic data are being sought for the onshore occurrences of the Kenogami River Formation.

Outcrops and cores containing the Kenogami River Formation in the Moose River Basin have not yet been examined for this project.

Devonian

A Lower, Middle and Upper Devonian succession of shallow marine carbonates, evaporites and shales and minor marginal marine to continental siliciclastics is preserved in the Moose River Basin in the southern James Bay Lowlands. Lower to Middle Devonian strata are also reported from the upper (un-cored) part of the Pen No. 1 well in the extreme northwest of Ontario. Reports on and reviews of these Devonian strata include those by Sanford et al. (1968), Sanford and Norris (1973, 1975), Stoakes (1978), Sanford (1987), Telford (1988), Bezys and Risk (1990), Johnson et al. (1992) and Norris (1993). Biostratigraphic reports include those by McGregor et al. (1970), McGregor and Camfield (1976), Uyeno and Bultynck (1993), Levman and von Bitter (2002) and Klapper et al. (2004).

The generalized Devonian lithostratigraphy of the Moose River Basin consists of, in ascending order:

- gypsiferous red and green mudstones to sandstones of the middle Kenogami River Formation (discussed above);
- oolitic and brecciated dolostones of the upper Kenogami River Formation (discussed above);
- fossiliferous, cherty limestones and dolostones of the Lower Devonian Stooping River Formation;
- arkosic siliciclastics of the Lower Devonian Sextant Formation that are restricted to the southern margin of the basin and are considered equivalent to parts of the Stooping River Formation and possibly the upper Kenogami River Formation (Telford 1988);
- coral and stromatoporoid dominated biostromal limestones of the Lower to Middle Devonian Kwataboahegan Formation;
- gypsum beds and associated thin carbonates and shales of the Middle Devonian Moose River Formation;
- fossiliferous limestones and dolostones of the Middle Devonian Murray Island Formation, the base of which is commonly brecciated;
- interbedded shales and fossiliferous limestones of the Middle Devonian Williams Island Formation;
- black and grey shales and minor limestones of the Upper Devonian Long Rapids Formation.

Devonian strata were not examined in Ontario during this part of the project, with the exception of the Kenogami River Formation in Pen No. 1. They will be the subjects of future work.

Mesozoic - Jurassic

- ***Mistuskwia Beds***

Unconsolidated mud and sand of Middle Jurassic age are known from limited subsurface data in the Moose River Basin (Telford et al. 1975; Norris 1977; Telford and Verma 1982; Telford et al. 1991). Called the Mistuskwia Beds (Telford and Verma 1982), these have been interpreted as deltaic (Hamblin *in* Telford and Verma, 1982) to lacustrine (Telford and Long 1986). These beds unconformably overlie Paleozoic rocks and are unconformably overlain by either Cretaceous or Quaternary sediments.

Cretaceous

- ***Mattagami Formation***

The Mattagami Formation (Keele 1920; Dyer 1928) consists of unconsolidated varicoloured and kaolinitic clays, silica sands, and lignite. It is exposed in outcrops on the Mattagami, Missinaibi, and Abitibi rivers and associated tributaries. It is very well exposed along Adam Creek, a diversionary channel for hydroelectric dams in the Smokey Falls area. Due to its potential lignite and industrial mineral resources, this unit has been the subject of outcrop and drilling studies since the 1930s (e.g. Dyer and Crozier 1933; Norris et al. 1976; Telford and Verma 1982; Try et al. 1984; Telford and Long 1986; Telford et al. 1991). The Mattagami Formation unconformably overlies Precambrian to Devonian strata in the Moose River Basin and locally disconformably overlies the Jurassic Mistuskwia Beds.

Palynological studies have determined the Mattagami Formation to be Middle to Late Albian (Early Cretaceous) in age (Norris in Telford and Verma 1982). Sedimentological studies suggest it was deposited in a large anastomosing fluvial system (Try et al. 1984)

- ***Evans Strait Formation***

Cretaceous sands and clays identified in boreholes and offshore seismic surveys in Hudson Bay (Grant and Sanford 1988) have been assigned to the Evans Strait Formation (Sanford and Grant 1990). These deposits have been interpreted to occur in the extreme northwestern corner of Ontario, near the Manitoba border (Ontario Geological Survey 1991; Sanford and Grant 1998).

Cenozoic

- ***Un-named Units***

Two occurrences of Cenozoic sediments have been recently discovered in northern Ontario. Approximately 16.5 m of lacustrine clays and silts of possible Miocene age were discovered overlying Ordovician limestones in a mineral industry core drilled near the Winisk River (Galloway et al. 2011). Approximately 265 km to the southeast, near the Victor Diamond Mine, 170 m of lacustrine sands and peat and glacial till of Pliocene age were discovered in a large depression in the Paleozoic bedrock (Gao et al. 2012).

2.2.3 Manitoba

Introduction

The onshore stratigraphy of the Hudson Bay Lowland in northeastern Manitoba was first constructed from mapping shoreline outcrops along the coast of Hudson Bay and inland

along river valleys; variably thick Quaternary glacial and lacustrine sediments cover most of the Paleozoic rocks. Drilling and full coring of three exploratory oil wells provided key subsurface information. These wells are Sogepet Aquitaine Kaskattama Prov. No. 1, Houston Oils et al Comeault Prov. No.1 and Merland et al. Whitebear Creek Prov. Additional stratigraphic information was also available from stratigraphic test holes drilled by the Manitoba Geological Survey, mineral exploration boreholes, and geotechnical holes, the latter from along the Nelson River near Manitoba Hydro hydroelectric dam sites.

The Manitoba section consists of Ordovician, Silurian and Devonian sedimentary strata (Figs. 9 and 10) that overlap the Precambrian crystalline basement from the southwest edge of the basin and form a basin-ward thickening wedge to the northeast. The strata have a general northeast dip with the formation contacts striking northwest-southeast onshore; the actual spatial extension of the rock units results from erosion of a more extensive sedimentary succession that once extended over the Canadian Shield.

Ordovician **-** The Ordovician section consists of the lowermost Bad Cache Rapids Group, the middle Churchill River Group and the uppermost Red Head Rapids/Port Nelson Formation, and is dominated by carbonate rocks with evaporitic and argillaceous beds near the top of the section. This succession represents cycles of normal marine carbonate deposition with cyclic episodes of restricted evaporitic deposition.

- ***Bad Cache Rapids Group***

The Bad Cache Rapids Group is present in the Kaskattama Prov. No. 1 core, Comeault Prov. No. 1 core, Pennycutaway No. 2 core, Kennco No. 5 core, and four Arctic Star cores (ADD-5-1, ADD-6-1, ADD-9-1, and ADD-16-1). This group is dominated by a carbonate succession with minor evaporitic cycles. The lower unit of the group (Portage Chute Formation) consists of limestone and sandstone and is overlain by the Surprise Creek Formation dominated by dolostone and anhydrite. This group is present throughout the northeast Manitoba, with the exception of in the vicinity of the town of Churchill, where islands of Precambrian-aged Churchill Quartzite were exposed above sea level during the Caradocian, thus restricting sedimentary deposition of the Bad Cache Rapids Formation.

- *Portage Chute Formation*

The Portage Chute Formation is divided into two members. At the base, member 1 is a light brown-yellow to olive-green grey, fine-grained, poorly consolidated quartz-rich argillaceous calcitic sandstone and dark grey fissile shale that forms a thin veneer over the underlying Precambrian crystalline basement rocks. Quartz sand is commonly fine-grained, angular and poorly sorted, with occasional coarse grains scattered throughout. Sandstone is faintly laminated in places, but is more commonly massive to burrow mottled with *Planolites* and *Chondrites* burrows. Fine-grained pyrite is common either disseminated or as clusters in the sandstone, occasionally pyrite lines small vugs, and can be occasionally manganiferous. Porosity is moderate, dominantly intergranular with subordinate small vugs and pinpoint. Bituminous residue is common along fracture surfaces. The member becomes limier upwards, as a result the contact is gradational as the limy sandstone of the member 1 grades into the siliciclastic limestone of member 2. Member 1 correlates to the Winnipeg Formation in the

Williston Basin in southwestern Manitoba. This member represents the initial flooding event of the basin.

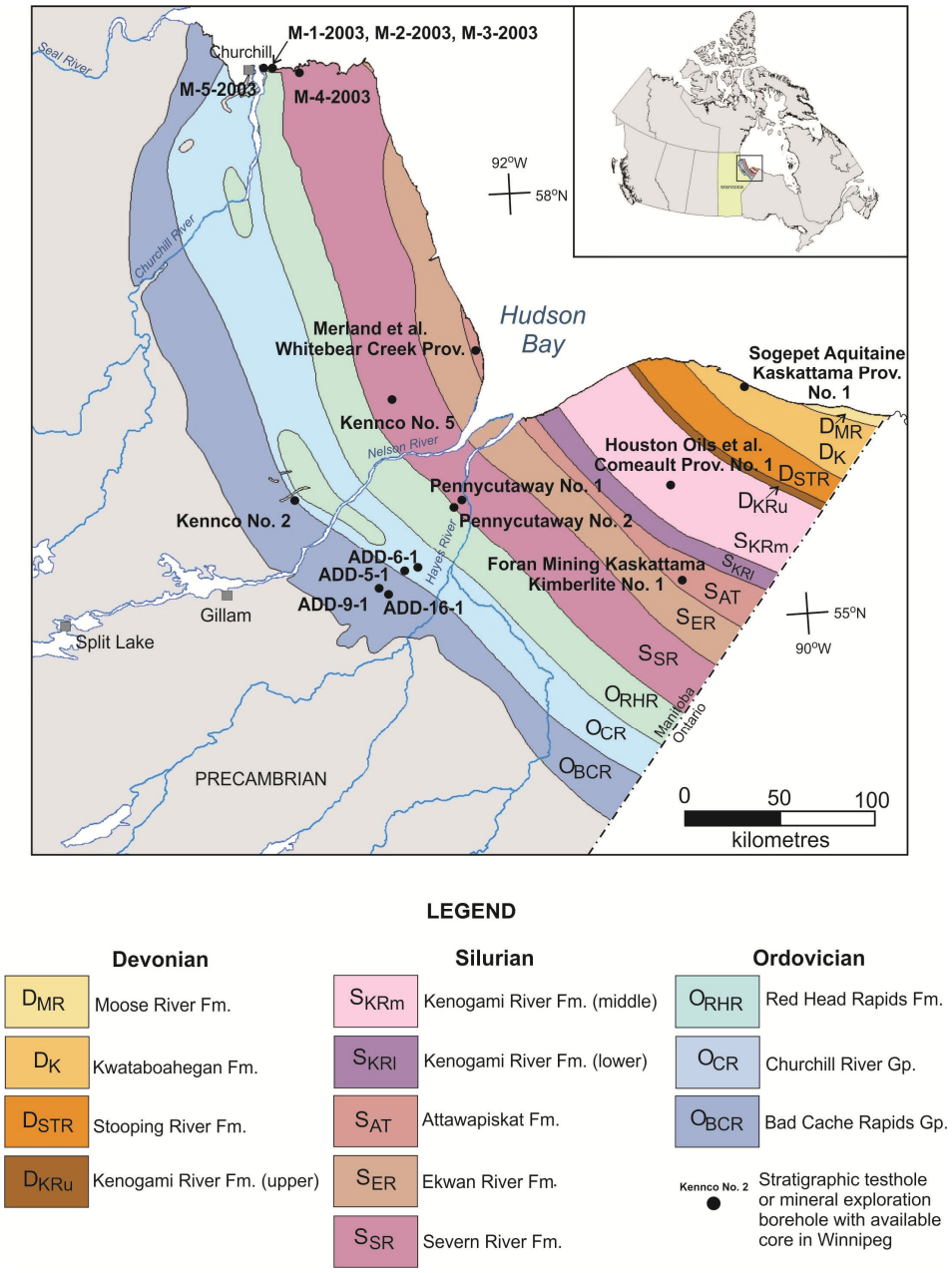

Figure 9: Geological map of the Hudson Bay Lowlands in northeastern Manitoba with the location of the provincial stratigraphic, mineral and hydrocarbon exploration wells.

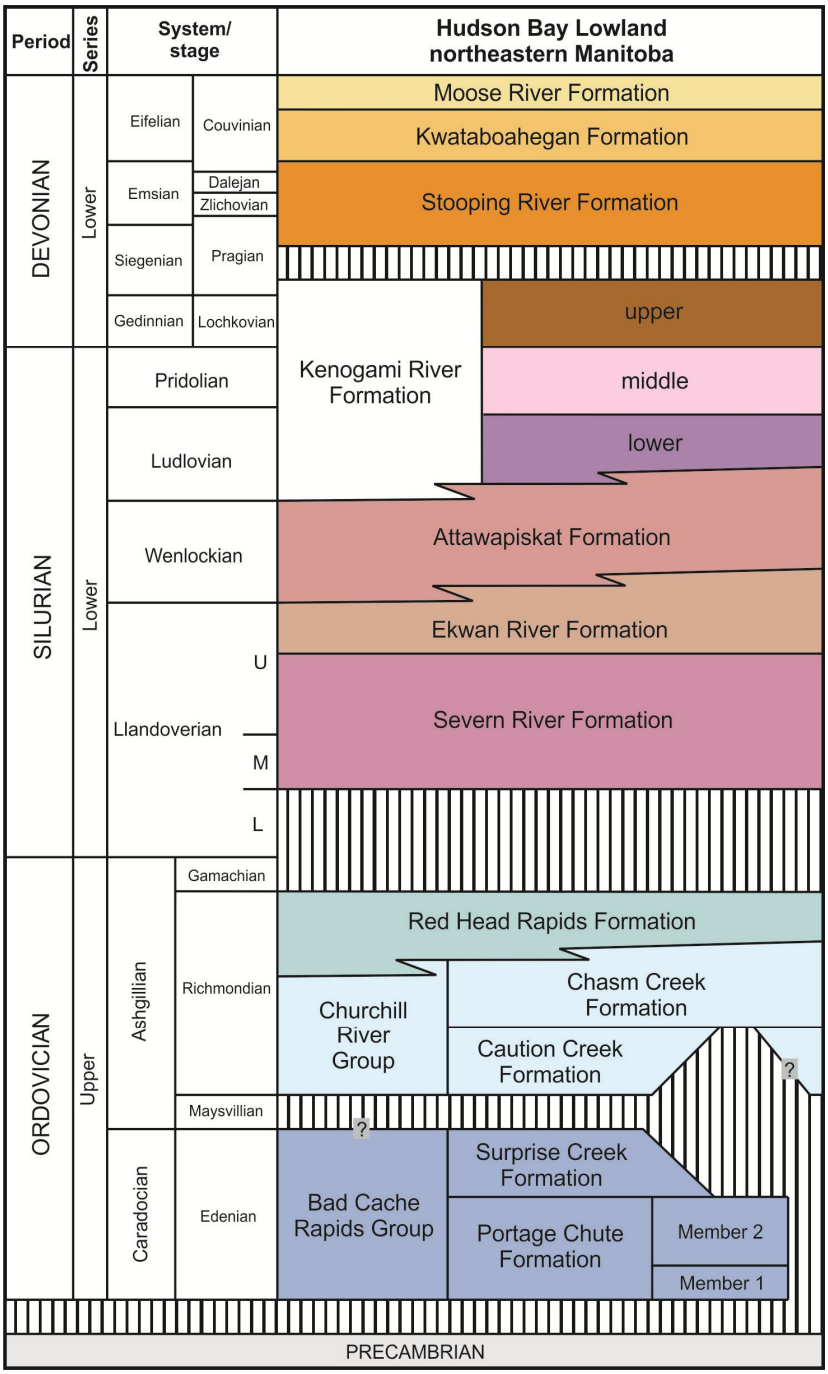

Figure 10: Stratigraphy of the Hudson Bay platform in Manitoba. Modified from Nicolas and Lavoie (2010).

Member 2 consists of light brown argillaceous wackestone near the base grading gradually to a medium brown mudstone-wackestone up section. Basal beds have floating medium to coarse quartz grains, whereas upper beds have chalky white to grey chert nodules throughout. This member is bioclastic throughout and has occasional thin crinoid-rich beds, and commonly mottled with *Thalassinoides* and *Chondrites* burrows; fossil fragments include

crinoids, corals, cephalopods, gastropods, brachiopods, trilobites and ostracods. Where bioclastic beds are less abundant, there is an increase in brown argillaceous content, both as stringers and within the limy matrix, with blue-grey anhydrite nodules in places. The porosity of this member is tight to moderate, and occurs mostly as pinpoint, intercrystalline and vuggy porosity. Bituminous residue occasionally occurs along open vertical fractures and infilling pore spaces near the base of member 2. The mottled appearance is characteristic of this member, and is similar to and correlates with the lower part of the Red River Formation in the Williston Basin. The upper contact to the Surprise Creek Formation is gradational over a short distance and easily picked in core when there is a change from calcareous (Portage Chute) below to dominantly dolomitic (Surprise Creek) above. On a geophysical log this contact is best picked where the gamma ray reading increases significantly up-section (due the increase in argillaceous content), above the low gamma ray reading of the Portage Chute Formation limestone. This member represents further flooding of the basin grading to a normal marine environment.

- *Surprise Creek Formation*

The Surprise Creek Formation is a light brown, massive to laminated, occasionally mottled, dolomitic mudstone to light brown to grey-green, platy argillaceous dolostone, with dark grey anhydrite interbeds and nodules. Dark brown, paper-thin shale laminae occur in places, often breaking up the core. Rock Eval™ 6 analyses of these shale laminae have returned TOC values up to 1.35 wt. % in the Selco Pennycutaway No. 2 core (Nicolas and Lavoie, 2012b). Dark grey to black wisps and stringers commonly occur around mottles and occasional nodules. Cyclic anhydrite beds occur through the formation; these cycles are similar to those seen further up section in the Red Head Rapids Formation but are less well defined. This formation is generally tight, and has poor pinpoint and intercrystalline porosity. Dolostone grades to slightly burrow mottled towards basal contact; this formational contact is characterized by a change from dolomitic above and calcareous below. The Surprise Creek represents a period of shallowing in the basin leading to a more restricted evaporitic environment. This formation correlates with the upper part of the Red River Formation in the Williston Basin.

- ***Churchill River Group***

The Churchill River Group can be seen in the Kaskattama Prov. No. 1 core, Comeault Prov. No. 1 core, and part of the Whitebear Creek Prov. core, Pennycutaway No. 2 core, Kennco No. 5 core, the five stratigraphic cores drilled by the Manitoba Geological Survey in the Churchill area (M-1-03, M-2-03, M-3-03, M-4-03, M-5-03), and the Arctic Star ADD-6-1 core. The Churchill River Group is divided in two formations: the lower Caution Creek Formation and the upper Chasm Creek Formation. The distinction between the two units is subtle in core, and best picked on geophysical logs. This group consists dominantly of mottled to nodular dolomitic mudstone to wackestone with occasional dark brown argillaceous laminae and stringers, and represents a return to normal marine deposition. The porosity in this group is generally poor and is dominantly pinpoint to intercrystalline with rare small vugs. Except in the vicinity of the town of Churchill where it directly overlies the Precambrian rocks, this group sits directly on the Bad Cache Rapids Group. The Churchill River Group correlates to the Stony

Mountain Formation in the Williston Basin.

- *Caution Creek Formation*

The Caution Creek Formation consists of light to medium grey-brown burrow-mottled dolomitic wackestone to packstone, with common *Thalassinoides* and *Trypanites* (Duncan, 2012) burrows. The amount of bioclastic fragments (brachiopods, corals, crinoids, nautiloid cephalopods, and trilobites) generally increase with depth. Nodules in upper beds are commonly light brown, massive and have a chalky appearance. Lower wackestone to packstone beds have black specks of organic detritus throughout.

The contact between the Caution Creek and Chasm Creek formations is gradational and subtle in core. It can be best located by a slight change in argillaceous content and a change from dominantly grey in the Caution Creek to more brown in the Chasm Creek. On a gamma-ray log, the contact is placed where the log character changes from a slightly higher gamma ray reading (more argillaceous limestone) in the Caution Creek to a slightly lower gamma ray reading (cleaner limestone) in the Chasm Creek.

- *Chasm Creek Formation*

The Chasm Creek Formation consists of upper and lower units of light to medium brown dolomitic mudstone with occasional *Thalassinoides* and *Chondrite* burrows and white, grey and brown chert nodules. Locally, mudstone grades to wackestone where thin bioclastic beds occur, with the sparse but similar fossil assemblages as those seen in the underlying Caution Creek Formation. The largest trilobite in the world, *Isotelus rex*, was discovered near the top of the Churchill River Group section (Rudkin et al., 2003) along the Hudson Bay shoreline. The upper contact to the Red Head Rapids/Port Nelson Formation is sharp, and is marked by a change from a normal marine mottled dolomitic mudstone to a laminated mudstone representative of a more restricted environment.

Duncan (2012) studied the interval from the uppermost Caution Creek Formation to the lowermost Severn River Formation. In the Caution Creek, the open subtidal lithofacies association is represented by skeletal to burrow mottled (dolo) wackestone; the intertidal association is represented by nodular to burrow mottled dolomudstone; and the supratidal association is represented by a thin bed of massive to laminated dolomudstone.

- ***Red Head Rapids/Port Nelson Formation***

The strata overlying the Churchill River Group have been referred to as the Port Nelson Formation (Savage, 1918; Savage and Van Tuyl, 1919; Nelson and Johnson, 1966; Johnson and Nelson, 1969; Norford, 1971; Norford et al., 1998) and the Red Head Rapids Formation (Nelson, 1963, 1964; LeFèvre et al., 1976; Sanford and Grant, 1990; Norris, 1993; Sanford and Grant, 1993). These formational assignments were made from isolated outcrops where their stratigraphic relationships and their faunal assemblages were poorly known (Norford et al., 1998). Norford et al. (1998) argue that the proper assignment should be Port Nelson Formation not only by historical precedent and stratigraphic procedure, but also on the basis of new biostratigraphic data, which confirms that it is Late Ordovician and not Silurian in age. Despite Norford et al.'s (1998) arguments, some researchers use the term Red Head Rapids Formation that can lead to some confusion in the literature. Whether following historical precedent or the

popular usage for this formation naming, it seems accepted that the two formational names represent the same Late Ordovician Richmondian (or younger) strata.

Wong (2011) divided the Red Head Rapids/Port Nelson Formation into six lithofacies that are grouped into three lithofacies associations. The open subtidal association includes: lithofacies A – greyish-green dolomudstone; lithofacies B – skeletal wackestone; and lithofacies C – mottled-nodular lime mudstone. The saline peritidal association includes: lithofacies D – massive-laminated dolomudstone; and lithofacies E – interlaminated dolomudstone, anhydrite and halite. The saline mud flat association consists of lithofacies F – anhydrite. Wong (2011) identified four meter-scale, shallowing- and brining-upward carbonate-evaporite cycles in the three studied cores. Duncan (2012) identified a few sparse fossils within the skeletal wackestone beds including fragments of corals (solitary and colonial), bryozoans, echinoderms; trace fossils are present and include *Trypanites*, *Thalassinoides* and *Chondrites*. Duncan (2012) also identified a chitinous fossil that resembles a rare primitive chitinous prawn-like burrower; further study of this unusual fossil is needed to verify its taxonomy.

The Red Head Rapids/Port Nelson Formation can be seen in the Kaskattama Prov. No. 1 core, Comeault Prov. No. 1 core, and Whitebear Creek Prov. core and four of the stratigraphic cores drilled by the Manitoba Geological Survey in the Churchill area (M-1-03, M-2-03, M-3-03, M-4-03). In these wells, this formation consists of interbedded light brown to grey-green dolostone and dark grey anhydrite, with dark brown, occasionally organic, argillaceous to shaly stringers and laminae throughout, and occasional gypsum beds or crystal-rich layers (often seen as lath-like molds within a dolostone). Anhydrite is dark grey with medium grey mottling, occasionally nodular, and locally displays chicken wire textures. The formation consists of cycles consisting of: (1) light brown massive to faintly laminated dolostone at the base with anhydrite nodules whose concentrations increase upward until it grades to (2) thick laminated to mottled dark grey anhydrite beds with medium to brown dolostone matrix and laminae, it then sharply transits to (3) green-grey finely bedded dolostone at the top. The thick anhydritic/evaporitic cycles may or may not be present, depending on paleogeographic position in the basin. In the Kaskattama No. 1 core, there are six well-defined evaporitic cycles, in the Comeault No. 1 core there are four evaporitic cycles, while in the Whitebear Creek core there are four short cycles, with anhydrite beds absent. Evaporitic environment in the Whitebear Creek core is shown by evaporite lath molds, at times making the core rubbly. Upper contact to Severn River Formation is sharp and erosional. Millimeter-scale organic argillaceous mudstone or shale stringers and laminae have been identified as oil shale with TOC values as high as 8.44 wt. % in the Whitebear Creek Prov. core (Nicolas and Lavoie, 2012b). This formation represents a depositional change from normal marine in the Churchill River Group to restricted and evaporitic conditions. This formation correlates to the Stonewall Formation of the Williston Basin.

Silurian **-** The Silurian section consists of a carbonate succession with diverse bioconstructions. This whole section correlates to the Interlake Group in the Williston Basin, with more accurate formation-scale correlations being difficult.

- ***Severn River Formation***

The Severn River Formation can be seen in the Kaskattama Prov. No. 1 core, Comeault Prov. No. 1 core, Whitebear Creek Prov. core, and Kennco No.5 core. It consists of a thick package of light brown to dark grey interbedded nodular, laminated and burrow mottled mudstone to wackestone, with occasional bioclastic packstone interbeds. The beds are mostly calcareous but laminated beds tend to be more dolomitic. Porosity is variable, ranging from poor in nodular mudstone beds, to excellent in bioclastic beds. Hairline vertical fractures are present; some are infilled with mudstone whereas open fractures are lined with dark brown to black bituminous residue. Intraformational breccia beds occur uncommonly throughout the formation but are more common in the lower half. Anhydrite content increases with depth. Anhydrite is grey to blue-grey and occurs as nodules, thin beds and locally display chicken wire texture, it is commonly associated with blue-grey mottled argillaceous mudstone; occasional euhedral lath-shaped crystal molds occur in patches in mudstone. Medium to dark brown argillaceous stringers and laminae are common, some fluorescing under ultraviolet light, suggesting the presence of oil and/or oil shale (Nicolas et al., 2012); Hand-picked fragments with TOC values up to 1.79 wt. % are present in the Whitebear Creek Prov. core (Nicolas and Lavoie, 2012b). *Virgiana decussata* brachiopods are characteristic of the basal beds.

- ***Ekwan River Formation***

The Ekwan River Formation can be seen the Kaskattama Prov. No. 1 core, Comeault Prov. No. 1 core, Whitebear Creek Prov. core and the Kaskattama Kimberlite No.1 core. This formation is dominated by medium brown wackestone-packstone with some grey-brown, occasionally dolomitic, mottling. Basal contact with the Severn River Formation is sharp and erosional in places, while the upper contact with the Attawapiskat Formation is gradational. The upper portion of this formation has strong lithofacies similarities with the Attawapiskat Formation, and is bioclastic and peloidal limestone, mottled to faintly bedded with occasional brown argillaceous stringers; fossils include stromatoporoids, crinoids, ostracods, brachiopods, bivalves and colonial and solitary corals.

Pietrus (2013) divided the Ekwan River into seven lithofacies grouped into three lithofacies associations. The subtidal lithofacies association consists of five lithofacies: lithofacies A – skeletal floatstone to rudstone; lithofacies B – skeletal mudstone to wackestone; lithofacies C – intraclast floatstone; and lithofacies D – peloidal wackestone. The intertidal lithofacies association consists of two lithofacies: lithofacies E – laminated dolostone; and lithofacies F – laminated lime mudstone. The seventh lithofacies of Pietrus (2013) was a supratidal lithofacies association consisting of lithofacies G – nodular anhydrite, but it is now interpreted that this lithofacies belongs to the Severn River Formation. These three lithofacies associations are interpreted to represent the marine platform interior of a rimmed-shelf setting.

- ***Attawapiskat Formation***

The Attawapiskat Formation in Manitoba can be seen in the Kaskattama Prov. No. 1 core, Comeault Prov. No. 1 core, Whitebear Creek Prov. core and Kaskattama Kimberlite No.1 core. This formation overlies and likely interfingers with the Ekwan River Formation. Reefoid beds are generally considered to belong to the Attawapiskat Formation, but picking a contact is very challenging, especially in core.

The Attawapiskat Formation is dominated by light brown to tan reefoid to peloidal and oolitic limestone with local dark grey mottling and is occasionally slightly dolomitized. Porosity ranges from poor pinpoint and intercrystalline, to excellent where moldic and fenestral porosity dominates. Some pores are filled with silt and others are partly lined with euhedral dolomite crystals. Stromatoporoid beds are commonly interbedded with fossiliferous, bioclastic grainstone beds. Fossils include corals (including solitary rugose corals, *Favosites*, *Halysites* and *Heliosites*), stromatoporoids, brachiopods, bivalves, ostracods, crinoids, echinoderm fragments, and trilobite fragments (Ramdoyal, 2012).

Ramdoyal (2012) divided the Attawapiskat into ten lithofacies grouped into three lithofacies associations. The subtidal association (inner shelf) consists of: lithofacies A – mottled to nodular wackestones; lithofacies B - stromatoporoid-coral framestones (patch reefs); lithofacies C – stromatoporoid-coral rudstones (reef flank beds); lithofacies D – peloidal intraclastic wackestone and grainstones; lithofacies E – skeletal mudstone to wackestone; lithofacies F – peloidal intraclastic bindstones; lithofacies G – interbedded skeletal wackestone and intraclastic rudstones; and lithofacies H – graded oolitic grainstones and wackestones. The intertidal (tidal flat) association comprises of lithofacies I – laminated skeletal mudstones to wackestone, and the supratidal (tidal flat) association comprises of lithofacies J – laminated dolostones.

- ***Kenogami River Formation***

The Kenogami River Formation in Manitoba is only seen in the Kaskattama Prov. No. 1 core (Nicolas, 2011). This formation is divided into three members: lower, middle and upper Kenogami River members, with the middle member being the thickest and most distinct.

The lower Kenogami River member consists of a light to medium brown laminated, slightly wavy bedded dolomitic mudstone to light grey-green argillaceous dolomitic mudstone, with occasional grey-green argillaceous to shaly partings. Evaporite beds occur near the top and decrease in thickness with depth, they consist of grey to white anhydrite with gypsum nodules that are surrounded by dark brown argillaceous partings and laminae. Occasional disseminated very fine-grained pyrite is present, and sepiolite has been reported. Porosity is low and occurs as pinpoint and intergranular. The upper contact is not preserved in core.

The middle Kenogami River member consists of rusty red-brown and grey-green dolomitic silty shale to shaly siltstone and evaporite. Siltstone is mottled in places, laminated to wavy bedded with occasional ripple marks and cross-laminations. Soft sediment deformation is common, with evidence of bioturbation and burrowing. There are possible syneresis cracks. Thin (2-10 mm), white anhydrite and gypsum beds are common, with the beds increasingly evaporitic with depth. Near the base of the middle member, the anhydrite beds are pink and thicker. The member has occasional anhydrite- and gypsum-healed vertical fractures with poor pinpoint porosity, but has moderate intergranular porosity further up section. The upper contact is not preserved in core, but given the distinct colour difference between the middle and upper members, the contact is probably relatively sharp.

The upper Kenogami River member is a light brown to tan mudstone, mostly massive with some mottling and occasional laminations. In the Kaskattama No. 1 core, this unit is highly

fractured with poor pinpoint and intergranular porosity.

Although not time equivalent, the middle member resembles the Devonian Torquay Formation of the Three Forks Group (Nicolas, 2012) in the Williston Basin in southwestern Manitoba. The Ashern Formation of the Williston Basin, which marks the base of Devonian sedimentary deposition (McCabe, 1971; Martiniuk, 1992; Nicolas and Barchyn, 2008), is very close in age, and has some lithological similarities to both the upper and middle members, with the major differences being the Kenogami River Formation is significantly thicker than the Ashern Formation (Nicolas and Barchyn, 2008; Nicolas, 2011).

Devonian

- ***Stooping River, Kwataboahegan and Moose River formations***

Overlying the Kenogami River Formation, in ascending order, are the Stooping River, Kwataboahegan and Moose River formations. The latter formation does not outcrop and has not been cut by a well. Devonian-aged formations in Manitoba are only seen in the Kaskattama Prov. No. 1 core. The Kaskattama core begins in the interpreted Kwataboahegan Formation, but poor core recovery makes this difficult to confirm. The underlying Stooping River Formation also has very poor core recovery. As a result, lithological characterization of these formations is difficult. Nicolas (2011) interpreted the upper cored portion (which starts at a vertical depth of 20 m) to be the Stooping River Formation, with the uncored uppermost portion containing the Kwataboahegan and Stooping River formation contact.

The recovered core, although highly fragmental, can be separated up into a lower calcareous and an upper dolomitic units. The lower unit is a dark grey argillaceous mudstone with common conglomeratic zones and erosional textures; sub-angular to subrounded coarse-grained light brown argillaceous mudstone fragments occasionally float within a dark brown to dark grey argillaceous mudstone matrix. The upper unit is a light brown to tan dolostone with occasional argillaceous shaly intervals including some grey-green angular fragments within a light brown mudstone matrix.

2.2.4 Southampton Island

Paleozoic rocks on Southampton Island are exposed in the southern and western parts of the island, as well as a small isolated block on the eastern margin of the island (Cape Donovan area, Fig.11). The succession includes the Upper Ordovician Bad Cache Rapids and Churchill River groups and Red Head Rapids Formation and Lower Silurian Severn River, Ekwan River and Attawapiskat formations (Fig. 12).

Upper Ordovician

The lithostratigraphic nomenclature of the Ordovician succession on Southampton Island is similar to that identified in the offshore Hudson Bay wells.

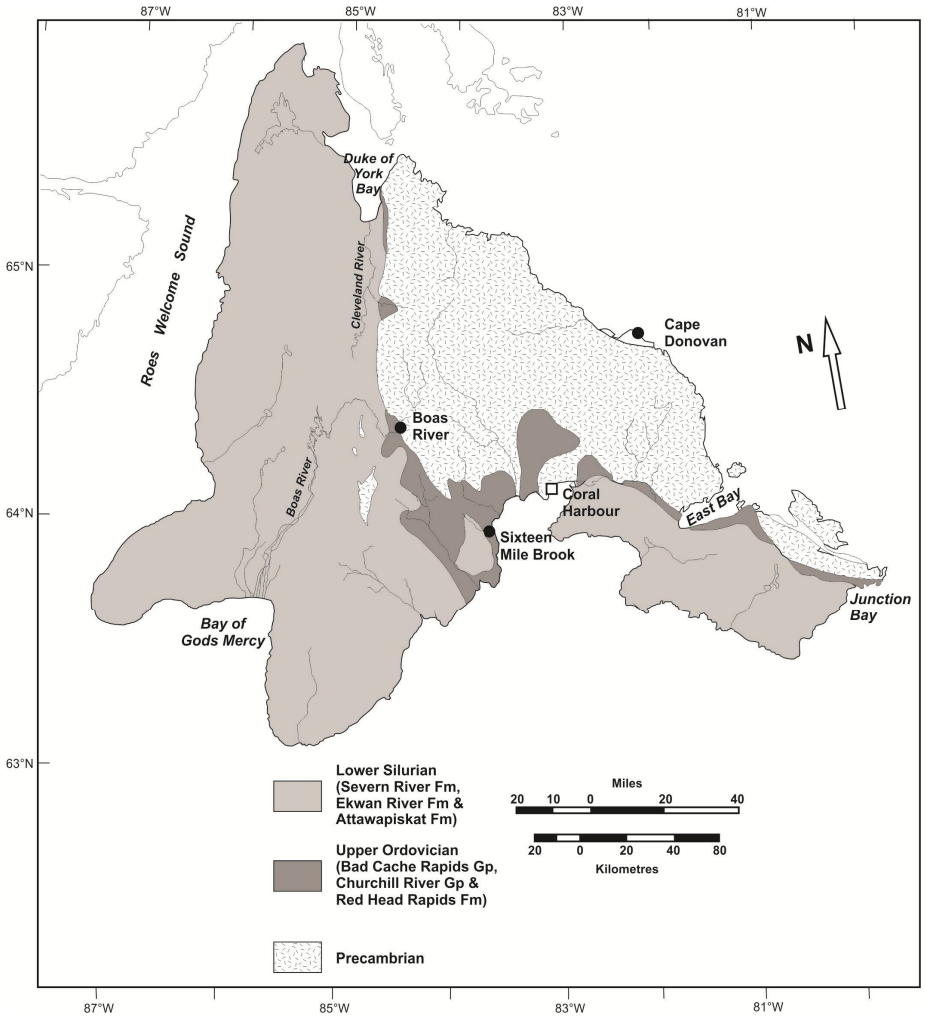

Figure 11: Simplified geological map of Southampton Island, adapted from Zhang (2008).

- The Edenian – Maysvillian Bad Cache Rapids Group unconformably overlies the Precambrian basement. It includes two different lithological units, a thin basal clastic interval (~ 2 m) and a dark grey or brownish grey fossiliferous limestone. The total thickness of the group, measured in a complete section on Southampton Island, is about 65 m (Zhang, 2011a).
- The early Richmondian Churchill River Group lies on top of the Bad Cache Rapids Group. It is composed of greenish grey or greyish brown argillaceous bioclastic limestone. The contact between the Bad Cache Rapids and Churchill River groups was interpreted either as a disconformity or the stratigraphic position of the "Boas River shale" as suggested by Sanford (in Heywood and Sanford, 1976). However the contact was demonstrated as conformable and no "Boas River shale" has been identified between the two units (Zhang, 2008). No complete section of the entire Churchill River Group was found; the exact thickness of the group is unknown on Southampton Island.

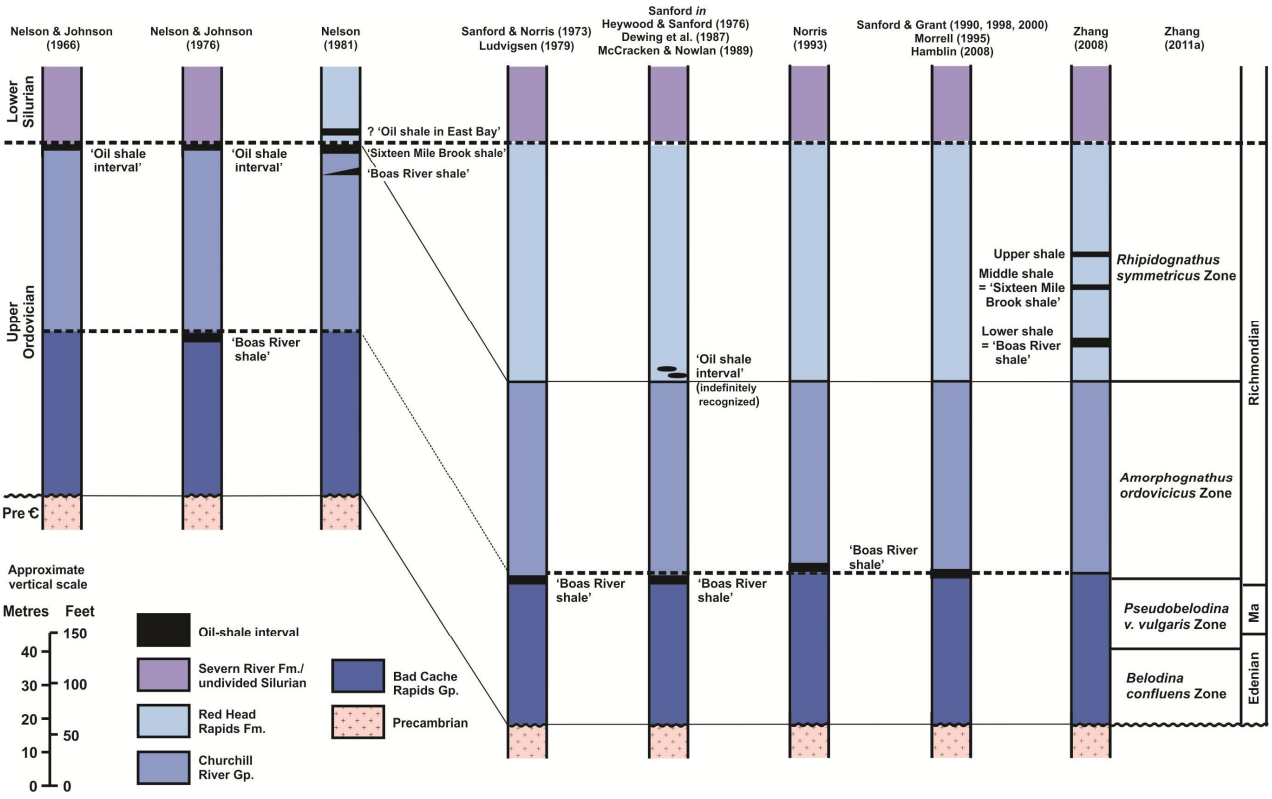

Fig. 12: Evolution of the stratigraphic framework on Southampton Island with a focus on stratigraphic interpretation of Upper Ordovician oil shales. From Zhang and Lavoie (2013).

- The late Richmondian Red Head Rapids Formation conformably overlies the Churchill River Group, and is disconformably overlain by the Lower Silurian Severn River Formation. The formation is divided into four units by Zhang (2008): unit 1 (29 m), thin-layered and laminated argillaceous dolomitic limestone interbedded with three oil shale intervals; unit 2 (10–15 m), massive breccia dolostone/limestone interpreted as related to hydrothermal fluid circulation; unit 3 (>10 m), thick, massive biostromal dolostone and dolomitic limestone; and unit 4 (thickness uncertain), thin-bedded dolomitic limestone with bioherms The three oil shale intervals in unit 1, discovered in Cape Donovan on Southampton Island, were informally named lower (>1 m thick), middle (0.4 m thick) and upper (0.5 m thick) oil shale intervals. The “Boas River shale” (Sanford in Heywood and Sanford, 1976) and “Sixteen Mile Brook shale” (Nelson and Johnson, 1966) were correlated to the lower and middle oil shale intervals (Zhang, 2008, 2011a).

Lower Silurian

The lithostratigraphic nomenclature of the Silurian succession on Southampton Island is similar to the one identified in the Hudson Bay offshore wells, although the Ekwan River and Attawapiskat formations can be separated given the possibility to map out the bioconstruction

facies of the Attawapiskat Formation.

- The Llandoverian Severn River Formation disconformably overlies the Upper Ordovician Red Head Rapids; it consists primarily of light to medium brown microcrystalline limestone and dolostone. No complete section of the formation is known on Southampton Island and its true thickness is unknown, but was estimated to be about 150 m (Sanford in Heywood and Sanford, 1976).
- The Llandoverian Ekwan River Formation is divided into three lithological units: unit 1 formed by algal limestone; unit 2 made up of massive limestone; unit 3 that consists of crinoidal limestones and dolostone. No complete section of the formation is known on the island and its thickness has been evaluated to be about 90 m (Sanford in Heywood and Sanford, 1976).
- The Llandoverian Attawapiskat Formation is a reef-bearing carbonate unit characterized by algal and stromatoporoid bioherms. It was originally interpreted to overlie the Ekwan River Formation and be the youngest Paleozoic unit on the island (Sanford in Heywood and Sanford, 1976); detailed facies and biostratigraphic information show that the Attawapiskat Formation is a lateral equivalent facies of the upper Ekwan River Formation (Zhang and Barnes, 2007). A thickness of over 50 m was estimated for the Attawapiskat Formation (Sanford in Heywood and Sanford, 1976).

2.3 Detailed stratigraphic account – Foxe Basin and Hudson Strait

Paleozoic rocks in Foxe Basin and Hudson Strait are exposed on southern Baffin Island and on Melville Peninsula (Zhang, 2012, 2013), and are preserved in the offshore areas of Foxe Basin and Hudson Strait (Sanford and Grant, 1990; 1998; Pinet et al., 2013b). They were described on Akpatok Island and from Akpatok L-26 well (Workum et al., 1976) in Ungava Bay.

2.3.1 Foxe Basin

In Foxe Basin, the stratigraphic succession consists of the Cambrian (?) Gallery and Turner Cliff formations, the upper Lower Ordovician Ship Point Formation and Upper Ordovician Frobisher Bay, Amadjuak, Akpatok and Forster Bay formations, the new biostratigraphic framework is discussed in Zhang (2013). The lower Paleozoic succession is capped by a Lower Silurian unit informally assigned to the Severn River Formation (Sanford and Grant, 1990).

Cambrian (?)

The assumed Cambrian (no biostratigraphic data) rocks are primarily exposed at the northern end of the Foxe Basin and in the Rowley well.

- The Cambrian (?) Gallery Formation (Lemon and Blackadar, 1963) unconformably overlies Precambrian gneiss in the Rowley M-04 well (Trettin, 1975). The formation is about 30 m thick and is dominated by fine-grained to pebbly sandstones that are commonly porous and friable.
- The Cambrian (?) Turner Cliff Formation (Lemon and Blackadar, 1963, Trettin, 1975) conformably (?) overlies the Gallery Formation; in the Rowley M-04 well, the formation is about 45 m thick and consists of various dolostone facies indicative of a general tidal flat environment. A significant unconformity is interpreted to occur at the top of the Turner Cliff Formation (Trettin, 1975).

Ordovician

Upper Lower Ordovician and Upper Ordovician rocks are widely distributed in the basin; regional stratigraphic observations indicate that these units are thinner in a northwesterly direction.

- The upper Lower Ordovician Ship Point Formation (Lemon and Blackadar, 1963) is only present in the northern reach of the Foxe Basin. On Melville Peninsula and in the Rowley M-04 well (Trettin, 1975), the Ship Point Formation is composed of sandstones and dolostones with a thickness of about 80 m.
- The Upper Ordovician Frobisher Bay Formation (Sanford and Grant, 2000) consists of grey to light brown, thin-to medium-bedded limestone and dolomitic limestone; the 10-15 m thick Froshisher Bay Formation unconformably and disconformably overlies the Precambrian basement on southern Baffin Island and the Ship Point Formation on Melville Peninsula, respectively.
- The Upper Ordovician Amadjuak Formation (Sanford and Grant, 2000) thins from 70 m on southern Baffin Island to a thickness of about 40 m on Melville Peninsula (Zhang, 2012, 2013); the Amadjuak Formation consists mainly of grey-brown shaly limestone, argillaceous limestones and nodular limestone beds. A 2 m thick organic-rich black shale outcrop is visible in the lower Amadjuak Formation on southern Baffin Island (Zhang, 2012, Fig. 13). This shale unit was previously interpreted to occur between the Amadjuak and Akpatok formations (Sanford and Grant, 1998, 2000), this shale unit was not recognized farther northeast on Melville Peninsula (Zhang, 2013).
- The Upper Ordovician Akpatok Formation (Sanford and Grant, 1990) is seen only at a single outcrop on southern Baffin Island, where about 9 m of light grey argillaceous limestone were assigned to that formation (Sanford and Grant, 2000; Zhang, 2012).
- The Upper Ordovician Forster Bay Formation (Sanford and Grant, 2000) occurs in a poorly exposed area on southern Baffin Island and was interpreted to reach a thickness of 45 m or more. In her recent survey, Zhang (2012) did not find outcrops of Forster Bay Formation, instead, brown argillaceous dolostone rubble are found scattered in the area assumed to be underlain by the Forster Bay Formation. The

brown argillaceous dolostone rubbles at these localities on southern Baffin Island are similar to the rock in the laminated beds of unit 1, Red Head Rapids Formation on Southampton Island (Zhang 2008). Based on her work on Melville Peninsula, Zhang (2013) estimated that the total thickness of both Akpatok and Forster Bay formations is about 50 m.

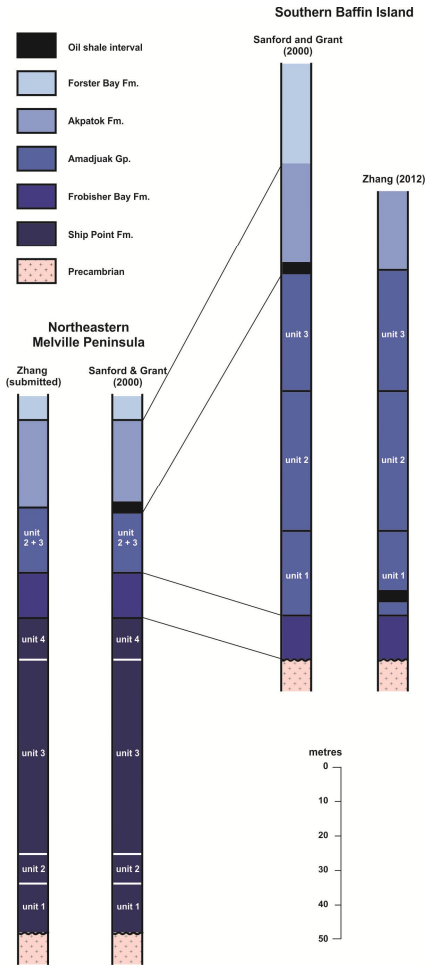

Figure 13: Correlation at the formation level of the Ordovician stratigraphy on southern Baffin Island and northeastern Melville Peninsula; the two distinct stratigraphic interpretations for the oil shale on southern Baffin Island are shown, note that Zhang (2013) did not recognize oil shale on Melville Peninsula.

Silurian

Lower Silurian strata are present in the central part of Foxe Basin. These are the youngest preserved onshore rocks

- Unnamed Lower Silurian carbonate strata are only preserved in the on some island in Foxe Basin and offshore area with a thickness of about 150 m in the Rowley M-04 well (Trettin, 1975), they were also identified as carbonate xenoliths containing Early Silurian conodonts, discovered in kimberlite pipes on Hall Peninsula, southern Baffin Island (Zhang and Pell, 2013). These carbonates consist of fine-grained, locally dolomitized, lime mudstone and wackestone. They can host a

significant biota of brachiopods (including *Virgiana decussata*) and crinoids.

2.3.2 Hudson Strait

The stratigraphic record of Hudson Strait is based on mapping of Akpatok Island in Ungava Bay and description of the Akpatok L-26 well drilled on the island (Workum et al, 1976; Sanford and Grant 1990). The stratigraphy was extended offshore based on seismic data by Sanford and Grant (1990) and Pinet et al. (2013b).

Ordovician

Middle and Upper Ordovician carbonate rocks were described by Workum et al. (1976) and Sanford and Grant (1990). The carbonates overlie a thin (8 m) veneer of undated arkosic sandstones unconformably overlying the Precambrian basement.

- Middle Ordovician (Whiterockian) strata originally known as the Ship Point Formation consist predominantly of lime mudstone, sometimes dolomitized with subordinate beds of dolostone, sandstone and shales. Workum et al. (1976) interpreted that this mixed carbonate and clastic interval has a thickness of 180 metres. Sanford and Grant (1990) introduced the Ungava Bay Formation for that succession.
- Upper Ordovician carbonates consist of diverse limestone textures (lime mudstone to packstone / grainstone) with minor shales. These were assigned to the upper Bad Cache Rapid and Churchill groups by Workum et al. (1976). Sanford and Grant (1990) used the stratigraphic framework of nearby south Baffin Island and indentified the Frobisher Bay (26.3 m) and Amadjuak (146 m) formations. Sanford and Grant (1990) identified 5 m of brown bituminous limestones that overlie the Amadjuak Formation; these were assigned to the Boas River Formation. Finally, they introduced the Akpatok Formation for a succession of at least 240 m of lithofacies-diverse, thin-bedded limestones (lime mudstone, wackestone and packstone) for which they assumed a Late Ordovician age.

Cretaceous

Based on seismic profiling and proposed correlation with the Hudson Bay Basin, Sanford and Grant (1990) suggested the presence of over 1000 m of Cretaceous sediments (interpreted sandstone and shale) assigned to the Evans Strait Formation, unconformably overlying the Lower Paleozoic succession. Pinet et al. (2013b) interpretation of the seismic data indicates the presence of up to 2000 m of post-Ordovician sedimentary strata.

2.4 Structural and tectonic framework

2.4.1 Hudson Bay Basin

Hudson Bay Basin appears to have a relatively simple geometry in seismic data, characterized by a lower sedimentary package cut by high-angle faults, overlain by a saucer-shape, essentially undeformed upper sedimentary package. Normal (or transtensional) faults imaged in seismic reflection profiles indicate that the basin was, at least partly, extensional during the deposition of the older sedimentary package. However, the depocenter location underwent significant changes during the Paleozoic and variable exhumation values required by new maturation data (see below) indicate that several mechanisms influenced the subsidence/exhumation history of the basin. In particular, the influence of far-field events and dynamic topography transmitted by large-scale mantle flow in the continental interior (creating long-wavelength tilting and unconformities) is suspected but not yet proven.

Onshore, the Paleozoic succession surrounding the Hudson Bay is nearly flat lying and faults documented in the field are characterized by small (< 10 m) displacement, except on the northern edge of the basin (northern fault array, Jefferson and Hamilton, 1987; Pinet et al., 2013a).

Offshore, a detailed knowledge of the geometry of the Hudson Bay Basin is hampered by the low quality of old vintage seismic data. The main structural feature is a NNW trending composite central high (central high of Roksandic, 1987; Mid Bay ridge of Thorpe, 1988; Central Hudson Bay Arch of Sanford and Grant, 1990) that consists of numerous high angle faults and fault blocks and adjacent subbasins (see further in the hydrocarbon play section). The central high is oriented nearly perpendicular to Precambrian basement structural trends (Eaton and Darbyshire, 2009) and extends for a minimum length of 500 km. Based on cross-cutting relationships of seismic reflections and variations in thickness of sedimentary packages on both sides of the high-angle faults, it is proposed that the faults were possibly active in Late Ordovician time and certainly active in Early Silurian and Early Devonian time. The physical-timing relationship of this central high with the Late Silurian – Early Devonian Boothia Uplift to the north (Thorsteinsson and Uyeno, 1980) is likely but cannot be prove unequivocally.

Another major structural feature is a WNW-trending fault array that forms the northern boundary of the basin and separates the Hudson Bay Basin from the Foxe Basin (Sanford and Grant, 1990, 1998). This fault array parallels the Hudson Strait that connects the Hudson Bay to the Atlantic Ocean and limits structurally controlled, imbricated basins characterized by preserved sedimentary successions that are much thicker (~2 km) than those preserved on adjacent islands (<0.6 km). The fault array, part of the Bell Arch, may have been tectonically active during the Cretaceous or even later (Pinet et al., 2013b).

2.4.2 Foxe Basin

Historically, the lower Paleozoic succession of the Foxe Basin was included in the

Arctic Platform (Douglas, 1970) and hence not directly linked with the Hudson Basin to the south. Christie (1972) introduced the term Foxe Basin for a tectonic succession of isolated areas with lower Paleozoic sediments between south Baffin Island to northwest Baffin Island including the islands in marine Foxe Basin (*sensu stricto*) and the northeast corner of Melville Peninsula. From regional mapping of these areas, the lower Paleozoic strata are found in fault-bounded structural depressions including grabens and half-grabens developed in Precambrian crystalline rocks of the Churchill craton. Trettin (1975) used the term "Foxe-Baffin structural depression" to encompasses the entire succession of more or less isolated structural basins filled by lower Paleozoic succession. The age of the faulting leading to the formation of grabens and half-grabens is poorly constrained and was interpreted to be post-Lower Silurian (Trettin, 1975).

The history of development of the Foxe Basin is largely unknown and its relationship with the tectonic mechanism active in the formation of the Hudson Bay Basin is speculative.

2.5 Basin evolution

As noted by Allen and Armitage (2012), the basin fill of intracratonic basins is commonly composed of several megasequences, some of which may be associated with entirely different mechanisms of formation.

Hamblin (2008) attempted a first regional synthesis of the classical North American Sequence framework (Sloss, 1988) for the Hudson Bay Basin. New biostratigraphic ages and a reinterpretation of the stratigraphy provide a new geological framework for the Hudson Bay Basin (Hu et al., 2011). Based on subsidence analysis and seismic interpretation, the Hudson Bay Basin succession is divided into several sequences (Pinet et al, 2013a).

2.5.1 Sequence 1 (Upper Ordovician)

The oldest Paleozoic rocks of the Hudson Bay Basin were deposited in shallow marine waters possibly connected with the St. Lawrence and Arctic platforms or in a restricted extensional basin characterized by numerous small faults. In either case, submarine relief was subdued and sedimentary thickness quite uniform. This sequence consists of a relatively thin (< 6 m) layer of basal clastics overlain predominantly by limestone, dolomitic limestone, dolostone and evaporites in the Bad Cache Rapids, Churchill River and Red Head Rapids formations (Fig. 14). Relatively thin (less than 1 m) shale intervals, informally named Boas River Shale, are recognized on the northern edge of the basin and possibly offshore (Zhang, 2008). A single, but much thicker (11 m), calcareous shale interval is also recognized locally on the southwestern edge of the basin (Armstrong and Lavoie, 2010).

At the top of sequence 1, the presence of cyclic carbonate-evaporites in the latest Ordovician Red Head Rapids Formation indicates a relatively hypersaline shallow marine sedimentary environment and deposition in a confined setting rather than on a platform connected with deep water domains (sequence 1b in Fig. 14). Sequence 1 ended with sub-aerial

exposure and development of an unconformity (U_1), likely associated with the global sea-level lowstand associated with the end-Ordovician glaciation of Gondwana (Cherns and Wheeley, 2009). Time-wise, Sequence 1 covers the Late Ordovician and is correlative with the lower half of the Tippecanoe I Sequence of Sloss (1963).

2.5.2 Sequence 2 (lower Silurian)

Sequence 2 overlies the Ordovician-Silurian unconformity and includes shallow water carbonates (Severn River, Ekwan River and Kenogami River formations) deposited in a tectonically active basin (Fig. 14). Lower Silurian reefs belonging to the Attawapiskat Formation are recognized on the southern (Suchy and Stearn, 1993), central (Ramdoyal, 2012) and northern (Heywood and Sanford, 1976) edges of the basin. Mounded reflection patterns on marine seismic profiles indicate that reefs were also widely distributed in the basin and preferentially located atop fault-bounded blocks. The thickness of sequence 2 increases to the east, which may denote the tilting of the basin.

Sequence 2 ended with the large-scale emergence of Hudson Bay Basin onset of the central uplift, and development of the upper Silurian to lowermost Devonian U_2 unconformity that may reflect eustatic variations, far-field effects of Caledonian orogenesis, basement involved uplift associated with the thrust system of the Boothia Uplift to the north, or a combination of these elements (Pinet et al., 2013b) (Fig. 14). Sequence 2 covers the upper half of the Tippecanoe Sequence (Sloss, 1988) and its upper bounding unconformity correlates with the major Tippecanoe-Kaskaskia sequences boundary of Sloss (1963).

2.5.3 Sequence 3 (Lower Devonian)

Sequence 3 is highly variable in thickness and rock types and includes rocks of the Stooping River and Kwataboahegan formations. On structural highs (Netsiq, Walrus and Polar Bear wells), the ~ 125 m thick sequence consists mainly of carbonates with lesser amounts of salt, whereas in structural lows it corresponds to a thick (738 m in the Beluga well) salt-dominated interval (Fig. 14). In contrast to the underlying sequence, sequence 3 thickens westward, indicating an east-to-west reversal of basin tilting (Fig. 14).

During sequence 3a, faulting became localized along a few faults possibly through the linkage of favourably oriented structures and the central high became a prominent topographic feature that separated two sub-basins. Sediments onlap the western flank of the partially emergent central high (Fig. 14). During deposition of sequence 3b, the two sub-basins connected together and became a single broad confined basin (Fig. 14).

Sequence 3 ended with the formation of the U_3 unconformity that is marked by a ~ 4-10 Ma sedimentary hiatus. Time-wise, sequence 3 occurs in the lower part of Kaskaskia Sequence of Sloss (1963).

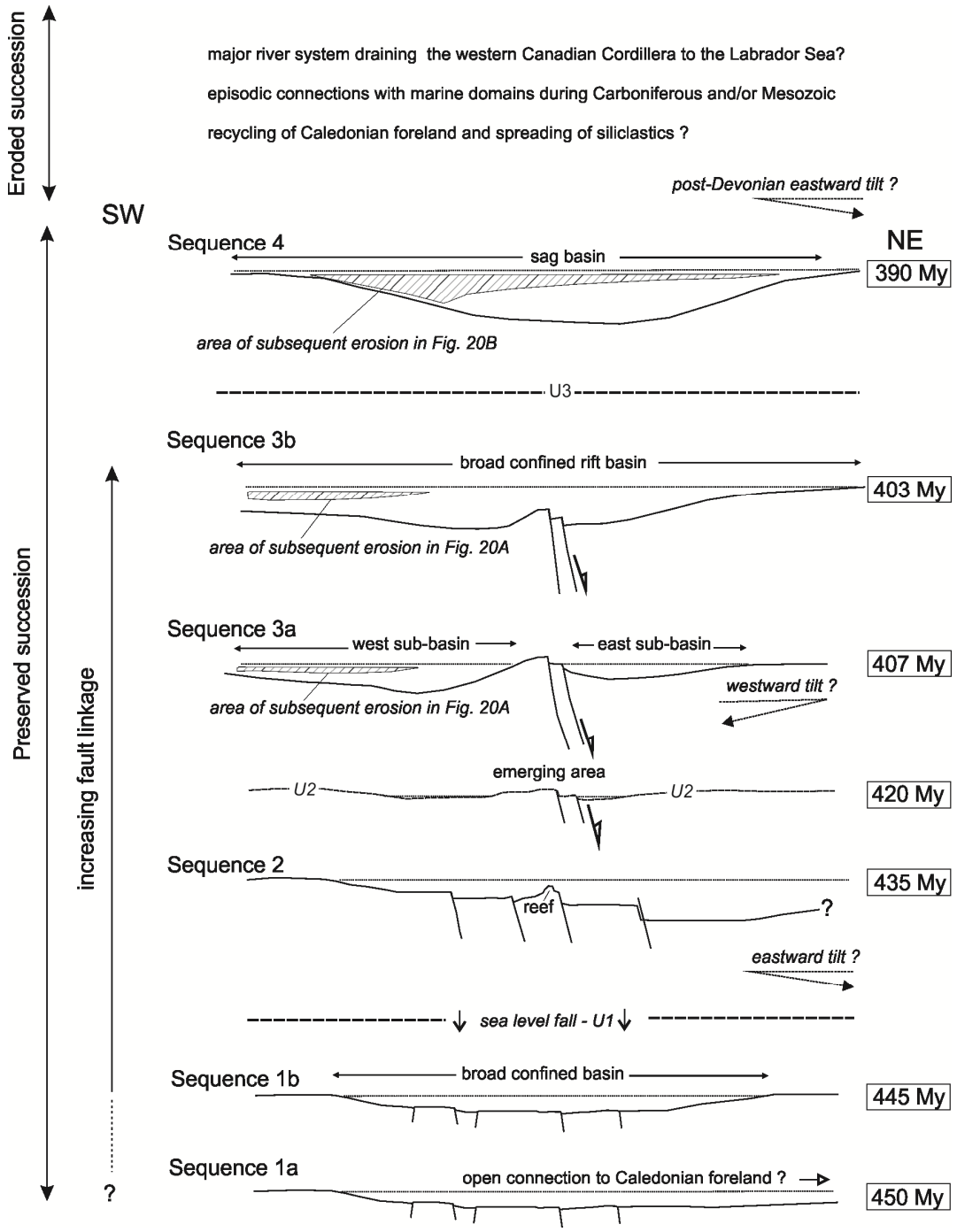

Figure 14. Schematic depositional setting of sedimentary sequences, Pinet et al. (2013a).

2.5.4 Sequence 4 (Middle-Upper Devonian)

Sequence 4 marks a drastic change in sedimentation and the beginning of sag basin

subsidence centred above the former central high. Sediments consist mainly of shale with limestone and minor sandstone, in the Moose River, Murray Island, Williams Island and Long Rapids formations (Fig. 14). Evaporites are only locally present in the Moose River Formation at the base of Sequence 4 and do not reappear upwards. . Moreover, seismic data provide no evidence of fault reactivation during deposition of sequence 4. A decrease in subsidence rates possibly characterized the end of sequence 4 (Fig. 14).

The youngest age of preserved Paleozoic strata is Late Devonian; this correlates with the end of Kaskaskia 1 sub-sequence of Sloss (1963).

2.5.5 Eroded successions

Following the deposition of sequence 4, an episode of post-Devonian northeastward tilting is required to account for higher exhumation on the southwest edge of the basin as indicated by organic maturation data (Manitoba and INCO-Winisk wells, see below). Post-Devonian sedimentation in the Hudson Bay area may have been influenced by the recycling of Caledonian foreland sediments and the spreading of siliciclastics (Patchett et al., 2004), episodic connections with marine domains during the Carboniferous (Tillement et al., 1976) and/or Mesozoic (White et al., 2000) and major river systems draining the western Canadian Cordillera to the Labrador Sea (Duk-Rodkin and Hugues, 1994).

3. HYDROCARBON SYSTEM ELEMENTS

In the first round of exploration, data and material pertinent to hydrocarbon system elements were gathered by the industry; this data was primarily acquired in the Hudson Bay Basin. These include thousands of linear kilometres of offshore seismic data, core and cuttings from onshore and offshore wells, various geophysical logs run in exploration wells and some limited Rock Eval[2] analyses; all this information was submitted to the National Energy Board. Moreover, after the first round of exploration and at the start of this research project, biostratigraphic and lithostratigraphic well and field data were acquired or available in various formats (GSC and provincial geological survey reports, scientific journals). The older reports served as the cornerstone of the last regional synthesis for the Hudson Bay Basin (Sanford and Grant, 1998). Hamblin (2008) presented a modern overview of the stratigraphy and available hydrocarbon system data as well as proposing some conceptual hydrocarbon plays to be eventually considered in any future exploration.

The National Energy Board provided access to the industry data for a re-evaluation as part of the Hudson Bay and Foxe Basin project of the Geomapping for Energy and Mineral Program of the Geological Survey of Canada. In the following sections, historical and new geoscience data are presented in the synthesis of all pertinent hydrocarbon system data.

3.1 Source rocks

The nomenclature of Upper Ordovician source rocks around Hudson Bay needs some clarification and precisions on how it is used in this report. Heywood and Sanford (1976) introduced the term Boas River Formation, for a thin black shale interval positioned at the contact between the Churchill and Bad Cache Rapids groups. Zhang (2008) failed to recognize a shale unit at this interval, but found those shales higher up in the stratigraphy in the Red Head Rapids Formation. In northern Ontario, Sanford and Grant (1990) identified the Boas River Shale in two mineral exploration wells; Armstrong and Lavoie (2010) confirmed the stratigraphic position of these shales between the Churchill and Bad Cache Rapids groups.

Based on conodont biostratigraphy (McCracken, 1990; Zhang, 2008, 2012), three distinct Upper Ordovician shale intervals with source rock potential are identified in the Hudson Bay Basin. The oldest one is late Mohawkian – late Edenian (Amadjuak Formation, south Baffin Island), the next one is Maysvillian (Boas River Formation, northern Ontario) and the youngest one is Richmondian (Red Head Rapids Formation, Southampton Island).

3.1.1 Ordovician – Southampton Island

Ordovician oil shales have been known for many years at the northern reach of the Hudson Bay Basin. Macauley (1986) described and sampled the oil shales from several localities on Southampton Island. Rock Eval[2] analyses of samples from these localities indicated

some significant genetic potential as well as an immature thermal rank. More recently, Zhang (2008) re-evaluated the stratigraphic setting of these shales on Southampton Island (see Zhang (2008) for a thorough review of the debate) as well as providing new biostratigraphic constraints on the age of the shales and detailed Rock Eval[6] analyses (see below). On Southampton Island, three thin oil shales intervals (total combined thickness less than 3 m over a *circa* 20 m stratigraphic interval) have been identified in the Red Head Rapids Formation of late Richmondian age (Zhang, 2008, 2011a).

Macauley et al. (1990) provided a petrographic description of the organic matter, which has a dominant matrix bituminite material and minor liptinite. A recent petrographic examination of the shales on Southampton Island (Reyes, unp. data) concluded that the organic-rich calcareous shales are characterized by an interconnected network of non-fluorescing granular to weak reddish fluorescing lamalginate (*Gloeocapsomorpha prisca*) showing trace amount of bright yellow to orange fluorescing unicellular alginite. Trace amount of orange fluorescing solid bitumen are also observed.

Rock Eval analyses of 63 samples collected by Zhang (2008) from Cape Donovan along the northern shore of Southampton Island are reported (Annex 1.1). Total Organic Carbon (TOC) is high with averages of 9.77%, 22.79% and 20.49% for the lower, middle and upper shale intervals. For the three shale intervals, Hydrogen Index (HI) are very high (averages of 567, 629 and 690) and Oxygen Index (OI) relatively low (averages of 28, 39, 23) (Annex 1.1). Average yields (S1 + S2) are high; 58.5, 145.9 and 128.7 kg HC/tonne (Zhang, 2008).

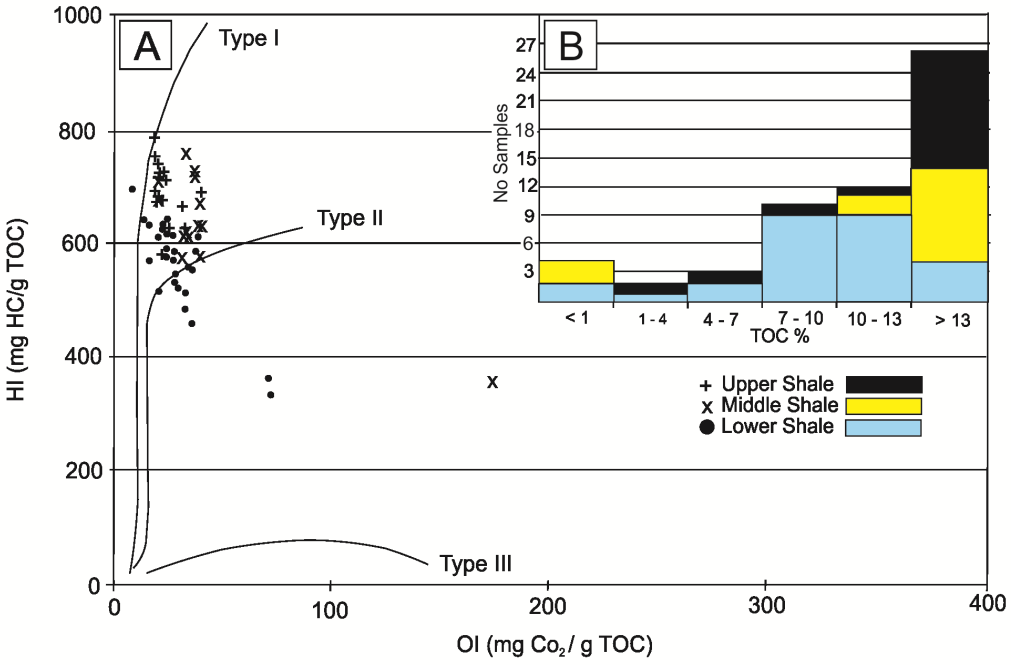

Figure 15: Modified van Krevelen diagram showing the relationship between Hydrogen Index (HI) and Oxygen Index (OI) for three shale intervals sampled near Cape Donovan, Southampton. Island. Inset: Histogram of TOC values for the same samples.

Six samples were selected for detailed organic geochemical characterization that includes: i) vitrinite reflectance and visual kerogen assessment, ii) kerogen carbon isotope; whole extract carbon isotope, and carbon isotope of saturates and aromatics fractions, iii) soxhlet extraction, iv) medium pressure liquid chromatography, v) whole extract bulk composition by Iatroscan analysis, vi) thermal extract gas chromatography and vii) high resolution gas chromatography. Results of this geochemical characterization are found in Zhang (2011a) and discussed below.

The HI *versus* OI graph (Fig. 15) provides a visual representation of the type of organic matter and its potential to generate oil (Type I and Type II) or gas (Type III). With the exception of limited number of samples (largely from the lower shale interval) located in the domain between typical Types II and III, the bulk of the results plot in the area between Type I and Type II organic matter. This observation suggests that the Ordovician shales at Southampton have a significant potential for oil generation (Macauley, 1986; Zhang, 2008). Interestingly, the HI increases upward from the lower to the upper shale intervals suggesting a slight increase of Type I organic matter through time possibly associated to variations in depositional environments with a slight decrease of hypersalinity

3.1.2 Ordovician – Baffin Island

Amadjuak Formation

Ordovician oil shales have been described from the Ordovician succession on south Baffin Island where Macauley (1987) reported a 12 to 14 m thick black shale interval (in place and as talus accumulations) of high quality marine Type II organic source rock. Rock Eval[2] analysis of 18 samples of laminated or massive oil shales produced TOC values between 2.9 to 14.8% (average of 9%), HI values between 462 to 691 (average of 566) and OI values between 22 and 80 (average of 42). Excellent yields of 15.8 kg HC/t to 99 kg HC/t were calculated. Based on Macauley (1987), Sanford and Grant (2000) tentatively correlated the Ordovician organic-rich interval to the 'Boas River Formation' they proposed on Southampton Island and northern Ontario and proposed that it is located between the Amadjuak and Akpatok formations. Zhang (2012) revisited the localities mentioned in the Macauley (1987) report, and attributed the organic-rich black shale (about 2 m of in-place thickness) to the lower part of Amadjuak Formation of latest Mohawkian – latest Edenian age.

41 samples from the Amadjuak Formation collected by Zhang (2012) were analysed with Rock Eval[6] (Annex 1.2); the TOC values range between 0.18 and 13.95% (average of 7.62%), HI values are between 97 and 640 (average of 439) and OI values are between 8 and 189 (average of 47). Yield values (S1 + S2) range between 0.32 kg HC/t and 85.18 kg HC/t. These values compare well with previous results of Macauley (1987), the slightly lower values being associated with a suite of sterile grey shale samples from one specific outcrop (Annex 1.2).

Petrography of Baffin Island oil shale was reported in Macauley (1987) and Macauley et al. (1990). Some petrographic differences are related to the rock type, with the laminated

material containing both fluorescent and non-fluorescent marine flora and fauna (acritarchs, tasmanite algae, chitinozoans and graptolites) with matrix bituminite, whereas the massive material consists of matrix bituminite and fluorescent marine fauna (acritarchs and tasmanites). Bituminite is the dominant kerogen type with secondary algal cysts, chitinozoans and graptolites of Type II (marine) origin. It is interesting to note that some bitumen was reported by Macauley from thin sections of samples with very high TOC. The HI *versus* OI diagram for the Amadjuak Formation (Fig. 16) indicates that the organic matter is Type II with some samples having slightly higher HI-lower OI values that would indicate presence of Type I OM material. The geochemical signature of the oil shales samples from the Amadjuak Formation indicates significant oil potential.

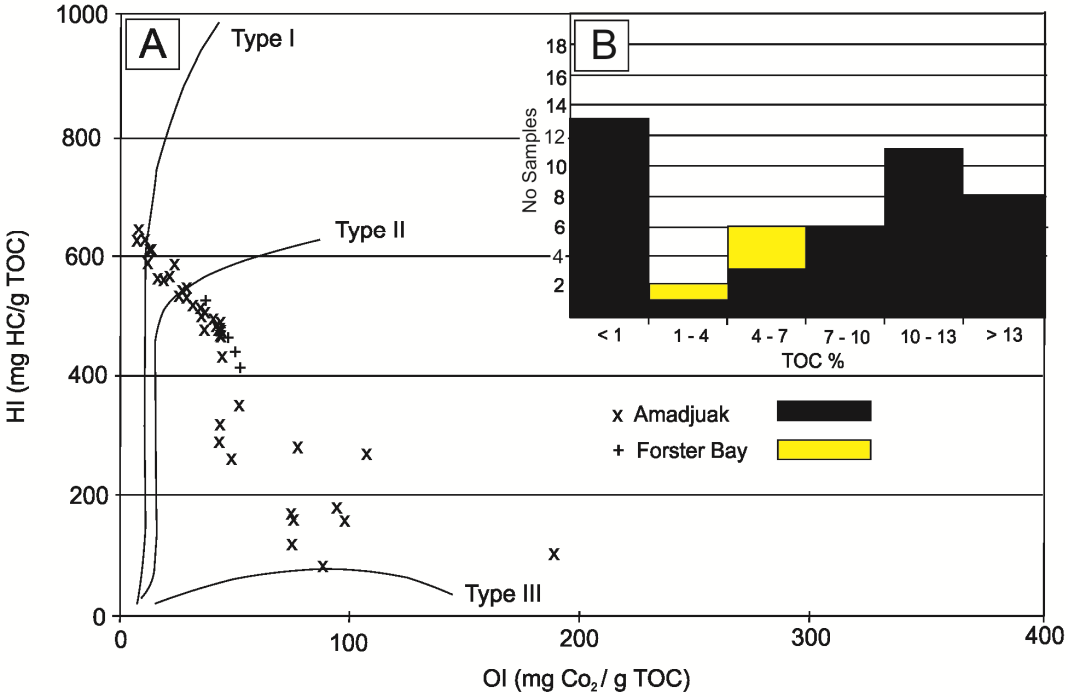

Figure 16: Modified van Krevelen diagram showing the relationship between Hydrogen Index (HI) and Oxygen Index (OI) for samples from South Baffin Island. Inset: Histogram of TOC values for the same samples.

Forster Bay Formation

Zhang (2012) reported the absence of Forster Bay Formation outcrops in areas assigned to that unit on the compilation map of Sanford and Grant (2000). However, rubble of brown argillaceous dolostone is found in that specific area. This rubble is described as being lithologically similar to unit 1 of the Red Head Rapids Formation of Southampton Island (Zhang, 2008, 2012) in which the three oil shale intervals are hosted.

4 rubble samples tentatively assigned to the Forster Bay Formation have been analysed with Rock Eval[6] (Annex 1.2); the TOC values range between 2.82 and 5.13% (average of

4.21%), HI values are between 403 and 536 (average of 463), and OI values are between 38 and 55 (average of 48). Hydrocarbon yields are lower compared with the Amadjuak Formation with values between 11.6 kg HC/t and 26.27 kg HC/t. The HI *versus* OI diagram (Fig. 16) indicates Type II organic matter.

3.1.3 Ordovician – Akpatok Island

Akpatok Island is located at the northern end of Ungava Bay and is close to the mouth of Hudson Strait (Fig. 6). Brown bituminous limestones have been described from Middle to Upper Ordovician carbonates on Akpatok Island. A well drilled on the island failed to core or recover material from this stratigraphic interval (Workum et al., 1976; Macauley, 1987). The brown to orange limestone forms a *circa* 60 m interval that was suggested to be of similar age to the Upper Ordovician Collingwood (Ontario) and the oil shales on Southampton Island (Workum et al., 1976). No true laminated oil shale was observed in these "bituminous" limestones, which were also correlated with the Amadjuak Formation on Baffin Island (Macauley, 1987).

Three samples (6 analyses) were evaluated with Rock Eval[2] (Annex 1.3); the TOC values are relatively low (0.51 to 2.11%) with low to good HI (39 to 529). Hydrocarbon yields (S1 + S2) range between 2.13 kg HC/t to 11.24 kg HC/t. The Hi vs OI diagram (Fig. 17) indicates Type II organic matter.

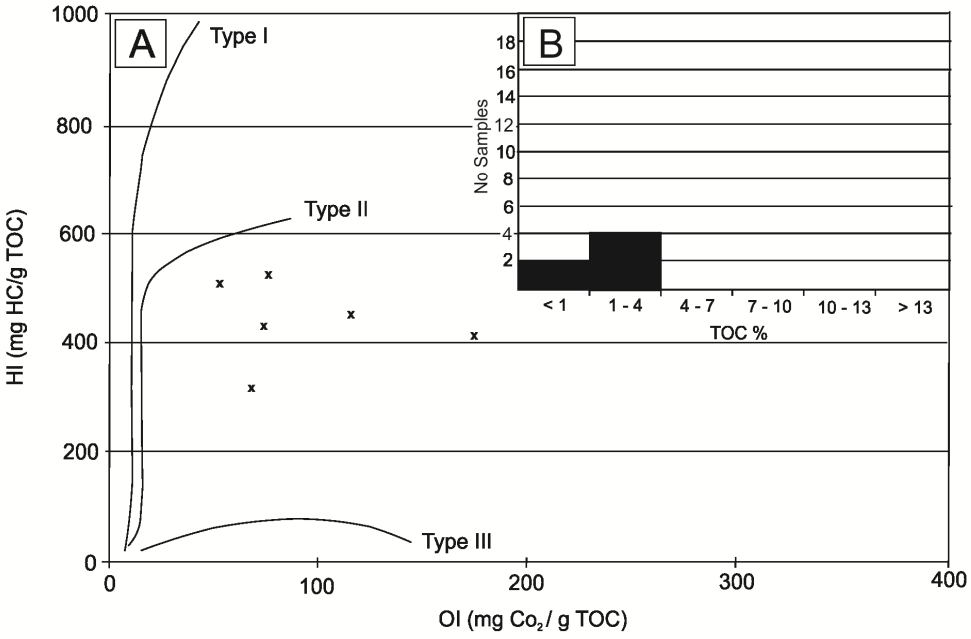

Figure 17: Modified van Krevelen diagram showing the relationship between Hydrogen Index (HI) and Oxygen Index (OI) for the Akpatok samples. Inset: Histogram of TOC values for the same samples.

3.1.4 Ordovician-Silurian – Northern Ontario

The potential presence of Upper Ordovician source rocks in Northern Ontario has been problematic for many years. The Hudson Bay Basin synthesis map of Sanford and Grant (1998) included a discontinuous band of interpreted Boas River Formation petroliferous limestone and shale between the Bad Cache Rapids and the Churchill River groups. However, no such unit was reported on the Ontario Geological Survey (1991) map of the area.

The Boas River shale was identified in two wells drilled in Northern Ontario (INCO-Winisk #49212 and #49204; McCracken, 1990) as well as in outcrop (Asheweig River; Armstrong, 2011; St-Jean, 2012). In the two INCO Winisk wells, the thickness of bituminous lime mudstone is 6 and 9.5 m, whereas an incomplete (base missing) stratigraphic section of 3.2 m of Boas River lime mudstone has been measured along Asheweig River. McCracken (1990) provided detailed conodont biostratigraphy of 12 samples from the INCO-Winisk wells that most likely indicates mid-Maysvillian age. From these 2 cores description and biostratigraphic data, the Boas River Formation occurs stratigraphically between the Churchill River and Bad Cache Rapids groups and not higher up in the Red Head Rapids Formation where oil shales have been identified on Southampton Island (Zhang, 2008, 2010). The INCO Winisk and other cores and the recently discovered outcrops have been sampled for organic petrography and detailed Rock Eval[6] analyses.

Polished thin sections were prepared from selected samples to evaluate the kerogen in these black organic matter rich fine-grained carbonates, as well as for an evaluation of the thermal rank of the successions through organic matter reflectance and UV observation (see thermal history section). The northern Ontario Boas River samples are rich in greenish to bright yellow fluorescing alginite *(Gloeocapsomorpha prisca*), fluorescing and non-fluorescing bitumen and abundant bioclasts (acritarchs, chitinozoans and conodonts). The organic matter in the fine-grained carbonate matrix is mostly chitinozoan, bitumen and alginite (Armstrong and Lavoie, 2010; Reyes et al., 2011).

INCO Winisk cores

17 samples from the two INCO Winisk wells were analyzed with Rock Eval[6] (Annex 1.4); the TOC values range between 2.61 and 12.84% (average of 7%), HI values are between 464 and 634 (average of 580) and OI values are between 17 and 37. Hydrocarbon yields (S1 + S2) range between 12.6 kg HC/t and 74.7 kg HC/t. These values are in close agreement with other reported values for Upper Ordovician source rocks on Southampton and Baffin islands (see above). The HI *versus* OI diagram (Fig. 18) indicates that the Boas River samples from the INCO Winisk wells are oil-prone Type I-II organic matter.

A few samples from the Bad Cache Rapids and Churchill groups that are located below and above the Boas River Formation respectively have been analysed (Annex 1.4). They contain little organic matter and are sterile for hydrocarbon potential.

Other Northern Ontario wells

Most core material available from the Hudson Lowlands in northern Ontario was re-logged to identify organic matter rich intervals (Annex 1.5). The succession in these wells is certainly less complete compared to wells in Hudson Bay itself and units are commonly thinner (see Ontario stratigraphy above). 21 samples from 7 wells were collected, focussing on dark coloured, fine-grained intervals in the Ordovician and Silurian succession. Of these, one sample assigned to the Bad Cache Rapids Group (Wallbridge WB-01-001 well; Annex 1.4) produced TOC (9.79%), HI (679), OI (12) and yields (67.9 kg HC/t); values that compare with the Boas River shale in the INCO Winisk wells. Another sample assigned to the Bad Cache Rapids Group (Mantle DDH-08-012 well; Annex 1.4) yielded high HI (761) and low OI (16) values although with a low TOC value of 1.65%. Hydrocarbon yields (S1 + S2) of 12.59 kg HC/t indicate good source rock potential. The few Silurian samples do not show any source rock potential.

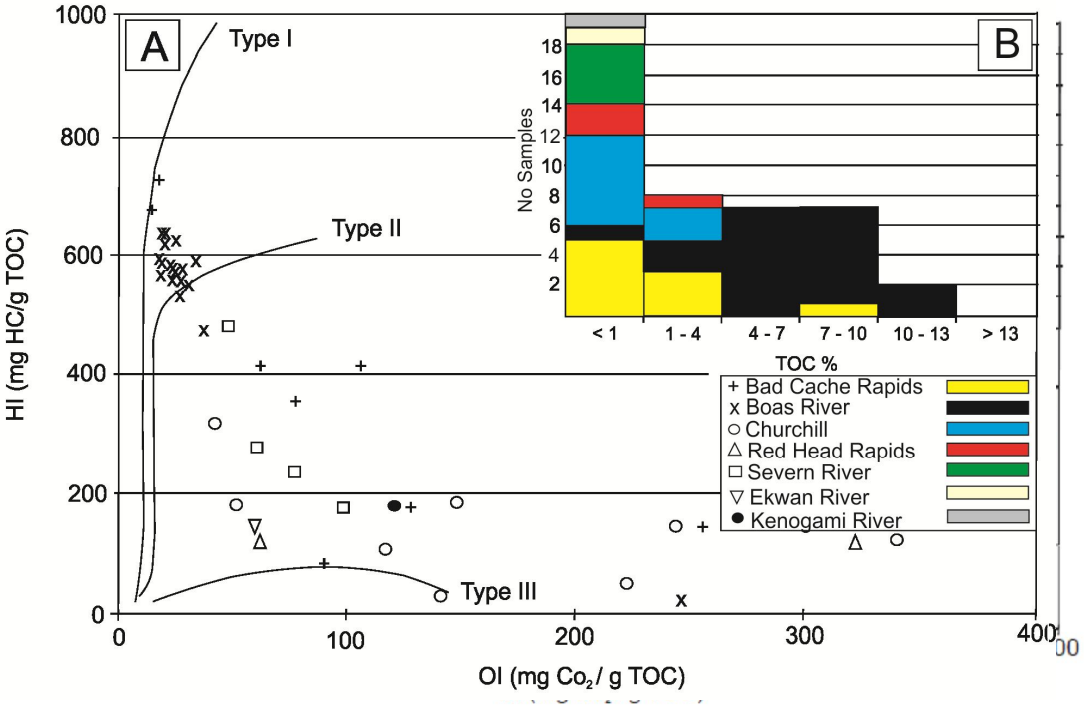

Figure 18: Modified van Krevelen diagram showing the relationship between Hydrogen Index (HI) and Oxygen Index (OI) for the Inco-Winisk and other Ontario well samples. Inset: Histogram of TOC values for the same samples.

Asheweig River

As part of a regional reconnaissance survey, an outcrop of black, laminated lime mudstone assigned to the Boas River Formation has been discovered along the Asheweig River (Armstrong, 2011; St-Jean, 2012). This is the first reported field occurrence of that unit. Interestingly, this outcrop occurs south of the map limit of the Paleozoic domain in northern

Ontario and likely represents the erosional remnant forming a Paleozoic outlier.

16 samples from that locality were analyzed with Rock Eval[6] (Annex 1.6); the TOC values range between 0.41 and 8.41% (average of 4.51%), HI values are between 180 and 616 (average of 516) and OI values range between 12 and 120 (average of 36). Hydrocarbon yields (S1 + S2) range between 0.75 kg HC/t and 51.58 kg HC/t. With the exception of one organic lean sample, these values are similar to other values reported for Upper Ordovician organic matter rich calcareous black shales in the Hudson Bay Basin. The HI versus OI diagram (Fig. 19) indicates that these Boas River samples are of Type I-II organic matter.

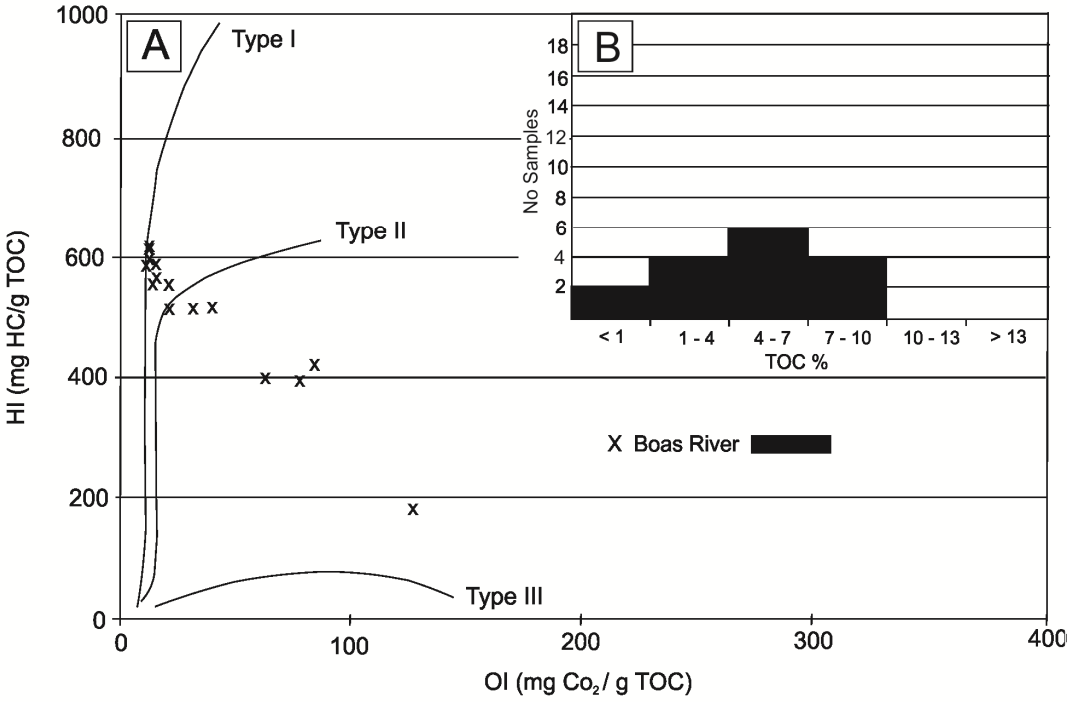

Figure 19: Modified van Krevelen diagram showing the relationship between Hydrogen Index (HI) and Oxygen Index (OI) for samples collected on the Asheweig River outcrops. Inset: Histogram of TOC values for the same samples.

3.1.5 Ordovician-Silurian – Northeastern Manitoba

There is no known outcrop of Upper Ordovician organic matter rich black shales in northeastern Manitoba. A detailed re-examination of hydrocarbon and mineral industry and government wells was carried out in the search of potential hydrocarbon source rocks. As with the Ontario onshore wells, the thicknesses of stratigraphic units are thinner compared to those from the correlative units in offshore wells (see Manitoba stratigraphic section above)

79 samples from 8 wells were analyzed with Rock Eval[6] (Annex 1.7). The TOC values for the 45 Ordovician samples (Bad Cache Rapids and Churchill groups and the Red Head Rapids Formation) are between 0.21 to 8.44%, HI values are between 21 and 730 and OI values range between 19 and 364. Two samples have good to excellent source rock potential, a sample

from the Red Head Rapids Formation (Whitebear Creek Provincial #1 well) yielded a high TOC value of 8.44%, HI of 355, OI of 19 with a hydrocarbon yield of 33.06 kg HC/t. The second sample, from the Churchill River Group (Comeault No 1 well) has TOC of 4.46%, HI of 730 and OI of 39; this sample has a HC yield of 32.93 kg HC/t. A few other Ordovician samples in the Comeault No 1 well have fair source rock potential with HC yields of 3.5 to 6.7 kg HC/t. The 34 Silurian samples (Attawapiskat, Ekwan River and Severn River formations) have TOC values between 0.07 and 6.38%, with HI values that range between 40 and 552 and OI values between 22 and 540. 11 samples of the Severn River Formation in three wells have fair to good hydrocarbon potential with TOC over 1% and hydrocarbon yields ranging between 3.98 kg HC/t to 29.33 kg HC/t. HI *versus* OI diagram (Fig. 20) illustrates that a significant number of samples from the Silurian Severn River Formation as well as from the Ordovician Churchill Group and Red Head Rapids Formation are Type II organic matter. The presence of potential Type II source rock in the Lower Silurian Severn River Formation had not been reported before.

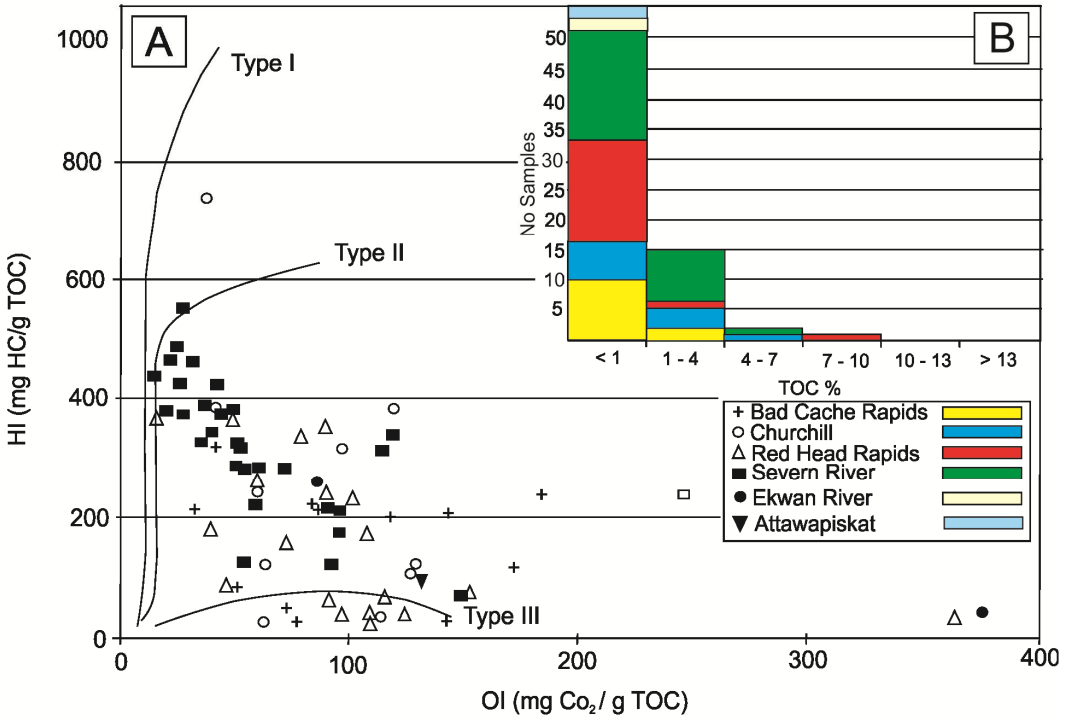

Figure 20: Modified van Krevelen diagram showing the relationship between Hydrogen Index (HI) and Oxygen Index (OI) for samples collected in Manitoba wells. Inset: Histogram of TOC values for the same samples.

3.1.6 Ordovician-Silurian – offshore Hudson Bay and Foxe Basin

The presence of Type I-II oil-prone Upper Ordovician source rocks has been documented for many years at various onshore localities surrounding Hudson Bay (see above). However, after six wells drilled onshore (Comeault No. 1, Pen Island No. 1 and Kaskattama No.

1) and offshore (Narwhal South O-58, Walrus, A-71 and Polar Bear C-11), the industry concluded that the presence of source rocks could not be demonstrated in the basin (Tillement, 1975).

There were very few cores recovered from the five wells drilled in the central part of Hudson Bay although cuttings were available. Conversely, the only well drilled in Foxe Basin was completely cored. An extensive sampling program of cores and cuttings of Ordovician-Silurian intervals was carried out for Narwhal South O-58, Polar Bear C-11 and Beluga O-23 wells in the Hudson Bay Basin as well as the Rowley M-04 well in the Foxe Basin (Zhang and Dewing, 2008). The selection of the sampling intervals and density were based on the known onshore stratigraphic position of Upper Ordovician oil shales as well as on reinterpretation of gamma ray logs in Hudson Bay offshore wells (Zhang, 2008; Hu et al., 2011) and for Foxe Basin Rowley M-04 well on Rowley Island (Trettin, 1975).

The gamma ray logs of the Polar Bear C-11, Narwhal South O-58 and Beluga O-23 (see stratigraphic section) have major kicks (increased radioactivity) in the Middle Devonian succession and significant kicks in the Silurian Severn River and in the Ordovician Red Head Rapids formations. The gamma ray kicks of the latter have been correlated with the three oil shales intervals on Southampton Island (Zhang, 2008). The significance of the gamma ray kicks in the Middle Devonian and Lower Silurian section of the three studied Hudson Bay wells (also present in the other offshore wells; Hu et al., 2011) has not been previously investigated.

For the Rowley M-04 well, a paper copy of the gamma ray log is available in Trettin (1975). The most significant kicks are found between 1120 and 1190 feet in the interpreted Middle Ordovician Ship Point Formation with minor kicks in the shallower section assigned to Map-Unit Ols between 1050 and 1060 feet.

Narwhal South O-58 well

81 Ordovician-Silurian samples were collected (Annex 1.8; Zhang and Dewing, 2008); 24 samples from the Silurian section (Kenogami River and Severn River formations) were collected at intervals that range between 3 m (10 ft) and 176 m (580 ft) with an average spacing of 21 m (67 ft). 57 samples were collected from the Ordovician section (Red Head Rapids Formation and Churchill River and Bad Cache Rapids groups) at intervals between 1.5 m (5 ft) and 24 m (80 ft) with an average spacing of 5.5 m (18 ft). In the Silurian section, the TOC are low and range between 0.08 and 0.81%, the HI values range between 37 and 412 whereas the OI values are between 84 and 911. One sample of the Severn River Formation could be qualified as a marginal source rock with TOC of 0.81%, HI of 412, OI of 84 and a hydrocarbon yield of 3.46 kg HC/t. In the Ordovician section, TOC values are also low (0.08 to 0.48%) with HI values ranging from 46 to 468 and OI values between 67 and 500. No Ordovician sample would qualify even as a poor hydrocarbon source rock.

HI *versus* OI diagram (Fig. 21) presents the general field of data for the Silurian and Ordovician samples. The very wide distribution of data mostly in the low HI and high OI field suggests that the cuttings that were analysed consisted primarily of very lean to sterile material.

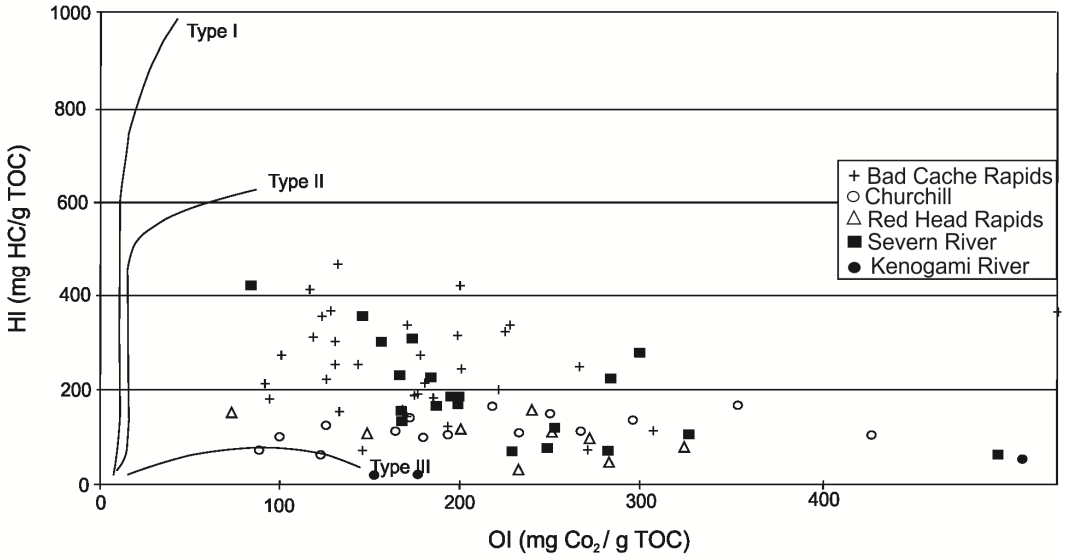

Figure 21: Modified van Krevelen diagram showing the relationship between Hydrogen Index (HI) and Oxygen Index (OI) for samples collected in the Narwhal well.

Polar Bear C-11 well

92 Ordovician-Silurian samples were initially collected by Zhang and Dewing (2008) (Annex 1.9), another sampling campaign was conducted later by Zhang (see further in text, samples C-457xxx). During the first sampling program, 37 samples were collected from the Silurian section (Kenogami River, Ekwan River and Severn River formations) at intervals that ranged between 1.5 m (5 ft) and 155 m (510 ft) with an average spacing of 13.5 m (44 ft). 55 samples were collected from the Ordovician section (Red Head Rapids Formation, Churchill and Bad Cache River groups) at intervals that ranged between 1.5 m (5 ft) and 23 m (75 ft) with an average spacing of 4.3 m (14 ft). TOC are uniformly low in the Silurian section, with values ranging between 0.05 to 0.56%, HI values range between 21 and 407 and OI values comprise between 67 and 1379. One sample of the Kenogami River Formation could qualify as a very marginal source rock with TOC value of 0.56%, HI value of 407 and OI of 71. This sample has a hydrocarbon yield of 2.47 kg HC/t. In the Ordovician interval, the TOC values are between 0.07 and 0.6%, HI values range between 85 and 329 and OI values are from 64 to 280. No Ordovician sample could be qualified as a potential source rock.

HI *versus* OI diagram (Fig. 22) presents the general field of data for the Silurian and Ordovician samples. As with the diagram for the Narwhal well, the wide distribution of data mostly in the low HI and high OI field suggests that the cuttings that were analysed consisted primarily of very lean to sterile material. It is interesting to observe that only three samples of the Lower Silurian Kenogami River Formation and three samples of the Upper Ordovician Red Head Rapids Formation are in a field of HI values over 270 and OI values below 90, these six

samples have slightly higher TOC values (0.3 to 0.56%) compared to the remaining of the data set (Annex 1.9).

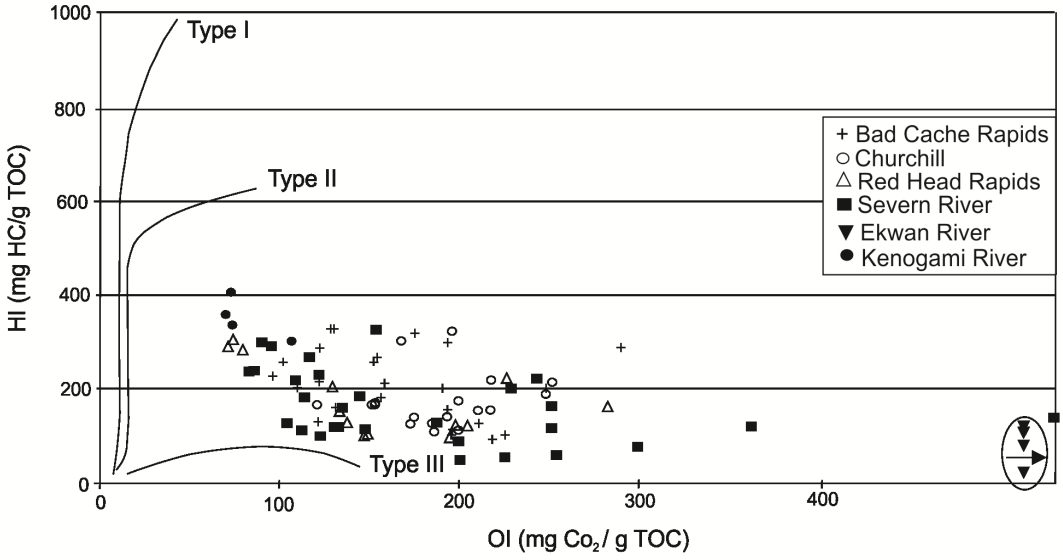

Figure 22: Modified van Krevelen diagram showing the relationship between Hydrogen Index (HI) and Oxygen Index (OI) for samples collected in the Polar Bear well.

Beluga O-23 well

38 samples were analysed from the Lower Silurian interval (Kenogami River, Ekwan and Severn River formations; Annex 1.10), samples were collected at intervals between 3 m (10 ft) and 6 m (20ft) with an average spacing of 3.1 m. TOC values range between 0.01 to 0.24%. No Silurian samples have source rock potential. 38 cutting samples were analysed from the Upper Ordovician interval (Red Head Rapids Formation, Churchill River and Bad Cache Rapids groups; Annex 1.10) at 3 m (10 ft) intervals. TOC values range between 0.01 and 0.40%. As for the Silurian samples, low TOC and S2 values result in erratic HI and OI results. No Ordovician samples have source rock potential.

Rowley M-04 well

30 core samples were collected from a 260 m (848 ft) Lower/Middle to Upper Ordovician section of the Rowley M-04 well (Annex 1.11; Zhang and Dewing, 2008). TOC values range from 0.1 to 1.67% with a noticeable exception of 7.26% in the Ship Point Formation. HI values are between 19 and 412 whereas OI values range between 22 and 240. A few Upper Ordovician samples have a very marginal source rock potential; three samples at 1050, 1055 and 1124 ft have slightly higher TOC (0.63, 0.51 and 0.6%, respectively), higher HI values (162, 214 and 412, respectively) and lower OI (79, 53 and 53, respectively) with a best hydrocarbon yields of 2.59 kg HC/t for the deepest sample. However, three samples (1159, 1162

and 1184 ft) of the Lower/Middle Ordovician Ship Point Formation have a fair to rich source rock potential with hydrocarbon yields between 4.84 to 14.61 kg HC/t. Interestingly, the samples with higher than background TOC and HI values are within or close to the gamma ray kicks in the well log (see above).

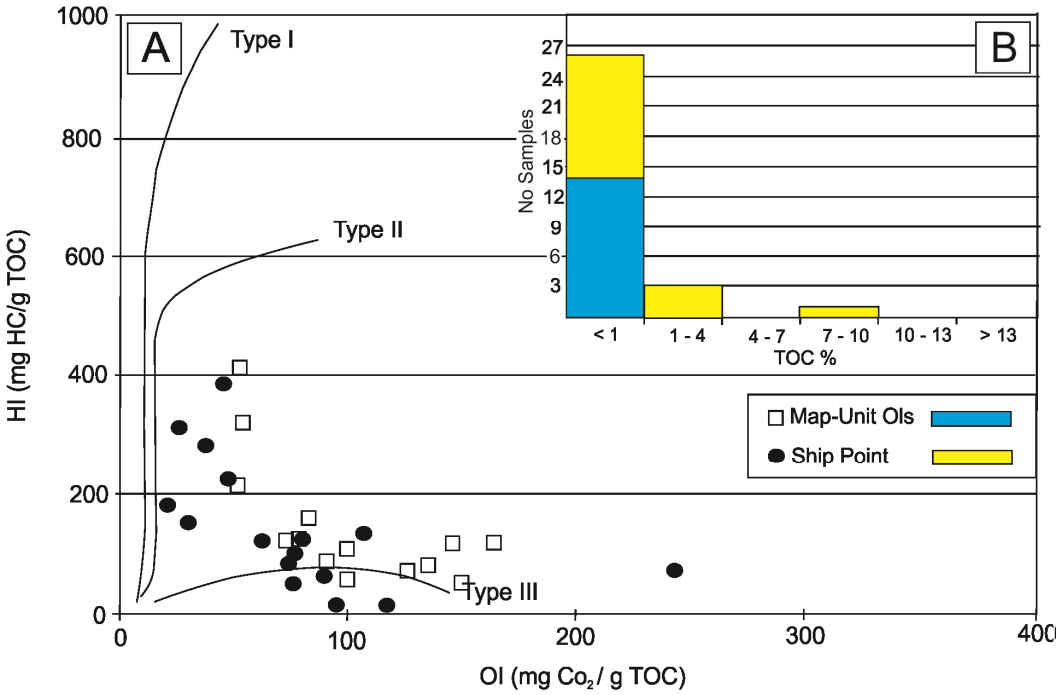

Figure 23: Modified van Krevelen diagram showing the relationship between Hydrogen Index (HI) and Oxygen Index (OI) for samples collected in the Rowley well. Inset: Histogram of TOC values for the same samples.

The HI versus OI (Fig. 23) shows that most samples have no hydrocarbon potential with the bulk of data being below HI of 200 and with elevated OI. However, nine samples (3 from Map Unit Ols and 6 from the Ship Point Formation) have intermediate values with HI between 160 and 400 and OI values below 80 that would suggest the presence of some Type II organic matter and marginal hydrocarbon potential.

3.1.7 Resampling of Upper Ordovician cuttings in Polar Bear C-11 – Offshore Hudson Bay

The lack of obvious source rock material correlative with the gamma ray kicks for the Hudson Bay offshore wells could be due to Ordovician oil shale intervals being thin (as on Southampton Island) and not effectively represented in the cutting samples collected at regular intervals, or diluted in the organic matter lean lithologies that comprise the bulk of the succession hosting the oil shales. Zhang (2008) re-examined all the cuttings for the interval

covering the three gamma ray kicks in the Polar Bear C-11 well and handpicked dark fragments. Annex 1.9 presents the Rock Eval[6] results for the dark cuttings; the 23 new samples are identified as C-457xxx series. Some of the samples are from the same intervals from which unsorted material was analysed (Annex 1.9) and new intervals were analysed in order to reduce the coarseness of the sampling interval. TOC values range between 0.29 to 5.73% compared to 0.07 and 0.36% for bulk cuttings, HI values are between 109 and 538 compared to 91 to 303 for bulk cuttings and OI values range between 27 and 321 compared to 64 to 278 for bulk material. Comparison of the best three results from the sorted cuttings (depth: 4365, 4370 and 4380 ft) with the unsorted cuttings shows a 2 to 4 fold increase in TOC indicating that dilution by organic-matter sterile cuttings reduced the TOC values of the initial analyses.

New samples were collected in the zone characterized by the deepest and most prominent gamma ray kick (at the contact between the Red Head Rapids Formation and the Churchill Group, as identified from electric logs for the Polar Bear C-11 well; see below). Samples at 4600, 4605 and 4615 ft (Annex 1.9) are characterized by the highest TOC values of the new data set (3.96, 5.61 and 5.73%) and high HI values (214, 458, 507). These samples have a high hydrocarbon yield ratio of 26.98 to 38.40 kg HC/t.

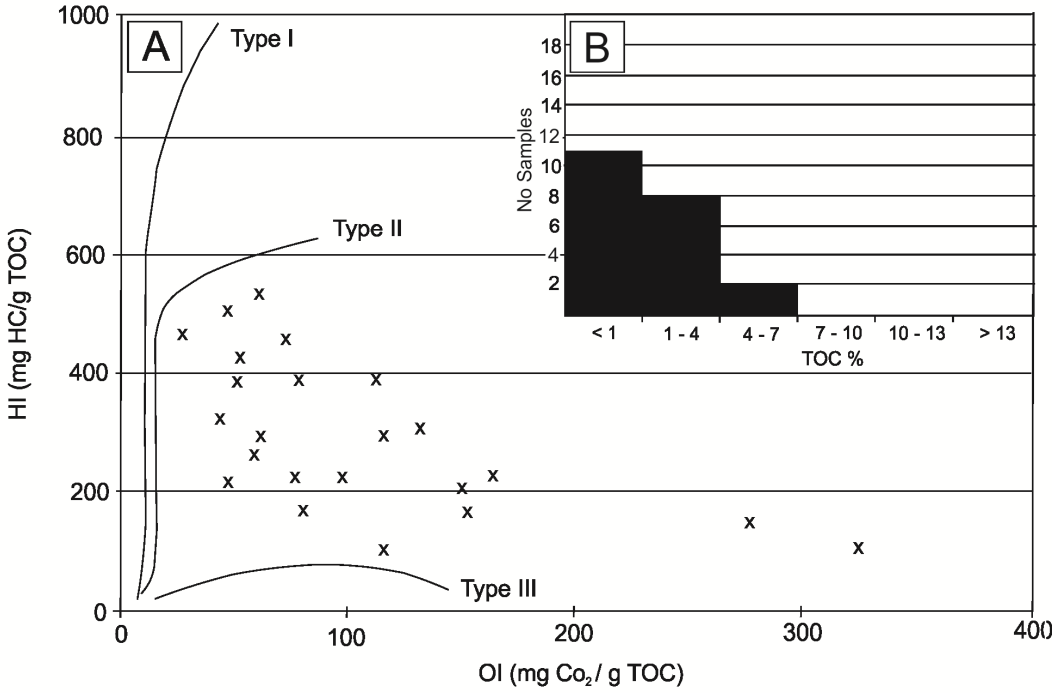

Figure 24: Modified van Krevelen diagram showing the relationship between Hydrogen Index (HI) and Oxygen Index (OI) for undiluted black cuttings collected in the Polar Bear well. Inset: Histogram of TOC values for the same samples.

When trying to correlate the 3 gamma ray kicks at *circa* 4430, 4480 and 4600 ft to geochemical results, it is noteworthy that only the deepest kick at 4600 ft can be easily correlated with elevated TOC, HI and HC yield values. The other two gamma ray kicks

exhibiting only slightly elevated values. The first gamma ray kick (4430 ft) could possibly be recorded in the sample at 4445 ft (2.29%, 237, 5.65 kg HC/t), whereas the second gamma ray kick (4480 ft) is possibly recorded in the sample at 4485 ft (1.07%, 329, 4.67 kg HC/t).

The HI vs OI diagram (Fig. 24) illustrates a wide distribution of data points with the best values (HI >400, OI<75) being most likely Type II organic matter. When compared to the diagram for unsorted cuttings (Fig. 22), a significant shift towards higher HI and lower OI values is discernable. However, the comparison with the diagram for the three oil shale intervals on Southampton Island (Fig. 15) would suggest degradation or alteration of the organic matter in the Polar Bear C-11 well.

3.1.8 Devonian source rock – Beluga well, offshore Hudson Bay

Based on fairly pronounced gamma ray kicks in the upper part of the Beluga O-23 well, 28 samples of handpicked black mudstone fragments were collected in the interval between 630 and 875 m (Annex 1.10; Zhang and Hu, 2013). Stratigraphically, this interval corresponds to the lower part of the Givetian Williams Island Formation to the upper part of the Emsian Stooping River Formation and is thus older than the Long Rapids Formation that is considered as a potential source rock in the Moose River basin (see below). This interval consists of interbedded shales (black and grey) with significant zones of evaporites and limestones.

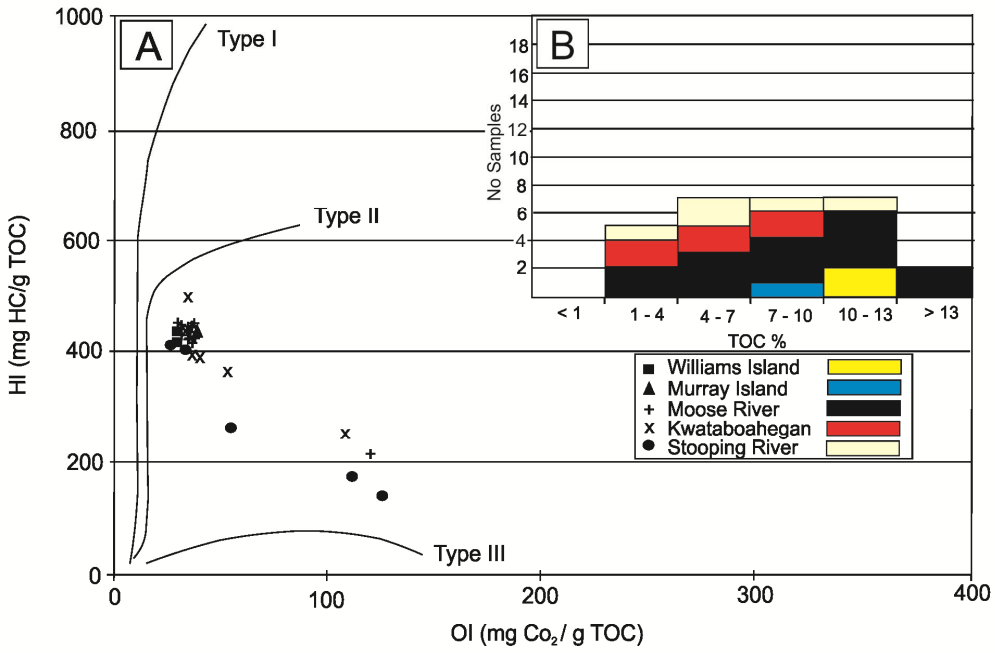

Figure 25: Modified van Krevelen diagram showing the relationship between Hydrogen Index (HI) and Oxygen Index (OI) for Devonian cuttings in the Beluga well. Inset: Histogram of TOC values for the same samples

For the entire interval (Annex 1.10), TOC values range between 1.6 and 17.64%

(average of 9.07%), with HI values between 142 and 495 (average of 390) and OI values from 26 to 135 (average of 46). Of the four stratigraphic units, the Moose River Formation has the highest average TOC (av. 9.17%). All the samples have high to very high yields (S1 + S2) that range from 5.52 to 86.67 kg HC/t and all samples would qualify as good to excellent hydrocarbon source rocks. An HI *versus* OI diagram (Fig. 25) shows that most of the samples are Type II organic matter. All but one sample for the Givetian interval plot in a narrow field of high HI and low OI, whereas the older Eifelian-Emsian succession yielded a slightly lower average HI value but still with some extremely high yield values. Detailed evaluations of the data are presented in Zhang and Hu (2013) who identified based on petrophysical analyses, 5 narrow distinct zones.

3.1.9 Devonian source rocks from the Moose River Basin

Upper Devonian hydrocarbon source rocks in the onshore Moose River Basin have been known for a long time. In this area, the Long Rapids Formation (85 m thick) includes beds of marine, organic-rich black mudstone, which alternate with grey-green mudstones (Bezys and Risk, 1990; Hamblin, 2008). The formation straddles the Frasnian-Famennian boundary as determined by conodonts (Bezys and Risk, 1990). TOC values range from 1.99 to 8.21% (averages 4.8%, 13 samples) (Bezys and Risk, 1990). Conversely, the Kwataboahegan Formation is described as a bituminous limestone (Telford, 1988). Four samples from the Upper Devonian Long Rapids Formation and 2 samples from the Middle Devonian Kwataboahegan Formation from the Moose River Basin were analysed (Annex 1.12).

The immature (T_{max} < 424°C) Long Rapids Formation has TOC values ranging between 2.42 and 11.21% with HI values between 175 and 519. These four samples are excellent source rocks with hydrocarbon yields from 5.47 kg HC/t to 59.53 kg HC/t of rock. The immature (Tmax < 431°C) Kwataboahegan Formation has low TOC values (0.43 and 0.45%) and is not a hydrocarbon source rock.

3.1.10 Conclusions concerning regional distribution of hydrocarbon source rocks

Upper Ordovician source rocks are widespread in eastern, central and Arctic North America, both in intracratonic (Michigan, Illinois, Williston) and foreland (Appalachians, Arctic platform) basins, where they are invariably associated with shallow marine carbonate platforms. Their thickness varies from a few metres to over 300 metres with thicker successions commonly found in foreland settings. The Upper Ordovician source rocks include the Utica Shale and Macasty Formation in the Appalachians foreland basin and the Collingwood, Red River-Stoney Mountain, Glenwood, Maquota, Boas River shales in intracratonic settings. These rocks are characterized by marine Type II organic matter. For some intracratonic basins, the accumulation of green algae (*Gloeocapsomorpha prisca*) results in the formation of extremely rich Type I source rocks or kukersite.

Silurian source rocks are not as widespread in North America as the Ordovician ones. In the Michigan basin, source rock intervals are described in the Niagaran (mid Llandovery to lower Ludlow) Salina Group (A1 carbonates).

Middle Devonian source rocks are widespread in central and western North America, including the marine Type II source rock of the Winnipegosis Formation in the Williston basin that occurs in a succession of carbonates and evaporites. The GSC Rock Eval database has 649 Rock Eval analyses of the Winnipegosis Formation, of these 424 are immature (T_{max} below 435°C) with S2 values over 0.35 mg HC/g rock. Average values from these 424 samples from the Williston Basin are TOC: 7.3%, HI: 395, OI: 48 and yields of 33.4 kg HC/t rocks; these average are very similar to the limited sample dataset of immature Middle Devonian black shales from the Beluga well.

Our study of the potential source rocks in the Hudson Bay, Foxe, Hudson Strait and Moose River basins has demonstrated, based on historical and new data that source rocks are widely distributed.

- Lower Ordovician source rocks (Type II) are likely present in the Ship Point Formation in the Foxe Basin (Rowley M-04 well). The source rock has modest hydrocarbon yields. Lower Ordovician rocks are unknown in the Hudson Bay Basin
- Upper Ordovician source rocks (Type I-II) are very rich in organic matter; they are documented in the onshore domain of the Foxe/Hudson Strait (Southampton, Baffin and Akpatok islands) and Hudson Bay (Manitoba and Ontario) basins and are also likely present in the central part of marine Hudson Bay (Zhang, 2008). If the regional presence of these source rocks is fairly well established, a potential issue with these source rocks resides in their thicknesses with only the Boas River Formation in Northern Ontario having a demonstrated fair thickness (up to 10 m). The Upper Ordovician source rocks have very high hydrocarbon yields. The variable thickness of Upper Ordovician organic-rich rock intervals and their possible patchy distribution is a major exploration issue. However, it should be noted that well control is extremely sparse, that the detailed paleogeography of the basin including the location of potential deeper depressions is presently unknown and that, considering the areal extent of the basins, the volume of potential source rocks may be high, even if the source rock interval is relatively thin.
- Lower Silurian source rocks (Type II) are identified in Manitoba and in Hudson Bay offshore wells. These relatively thin intervals have modest to fair hydrocarbon yields. The presence of these potential source rocks was mentioned in offshore well reports.
- Middle Devonian source rocks (Type II) have been identified in the Beluga O-23 well. Five thin intervals have been recognized in the Beluga well (Zhang and Hu, 2013). The Middle Devonian source rocks have significant hydrocarbon yields. The presence of these potential source rocks was previously unknown and significant gamma ray kicks similar to the one corresponding to the herein analysed Middle Devonian interval from the Beluga O-23 well are present in the other four offshore

wells.

- Upper Devonian source rocks in the Long Rapids Formation of the Moose River Basin have been previously identified; new Rock Eval data supports that interpretation of high hydrocarbon yield potential. The Long Rapids Formation is at the top of the Paleozoic succession and is immature.

3.2 Type of organic matter

Based on HI vs OI values, the TOC-rich samples from Upper Ordovician shales from Southampton and Baffin Islands as well those from the INCO Winisk well in northern Ontario qualify as Type I/II organic matter.

Macauley et al. (1990) reported that based on petrographic examination of organic rich shales in Southampton and Baffin islands, organic matter is dominated by marine liptinitic components of Type II origin. Recently, Reyes (unp.) documented *Gloeocapsomorpha prisca* in samples from Southampton Island and northern Ontario, suggesting that some Type I organic matter is locally present.

Gas chromatography was performed on extracts from samples from Southampton and Baffin islands (Macauley et al., 1990). Compared to well documented, *Gloeocapsomorpha prisca* –rich source rocks in southern Ontario (Collingwood Formation) and Saskatchewan (Yeoman Kukersites), the Upper Ordovician samples from the Arctic islands have relatively higher C_{19} + *n*-alkanes that indicate hypersaline depositional environments in which anaerobic bacterias reworked the organic matter. Gas chromatographs show: 1) lower Pr/Ph ratios (all lower than 1 compared to Upper Ordovician samples from southern Ontario and Saskatchewan suggesting very reducing conditions; 2) high abundances of acyclic isoprenoids in Southampton and Baffin islands samples, a characteristic not found in southern samples but documented in the Silurian hypersaline source rocks from the Michigan Basin (Summons and Powell, 1987); 3) a distribution of 17α(H), 21β(H)-hopane similar to hypersaline Silurian source rocks of the Michigan basin with lower abundance of C32 compared to C34 homohopanes; 5) the presence of 1-alkyl-2,3,6-trimethylbenzenes in the aromatic fraction of all samples from Southampton, Baffin and Akpatok island suggest highly reducing and hypersaline settings (Summons and Powell, 1987). This compound is associated with sulphur bacteria (Summons and Powell, 1987). New analyses of Southampton samples have confirmed the previous results (Zhang, 2011a).

All these elements allow a clear distinction between the source rocks at the northern end of Hudson Bay compared to coeval source rocks in southern Canada (southern Ontario, Québec, Saskatchewan). Overall, sedimentation in reducing and hypersaline settings is suggested; their presence in a succession dominated by carbonate-evaporite cycles agrees with the organic geochemistry information. The hypersaline setting conclusions based on biomarker results are supported by the shallow conodont association reported by Zhang and Hefter (2009) that indicate maximum regression in late Ordovician. Regionally, these Upper Ordovician source rocks are geochemically similar to Silurian source rocks of the hypersaline section of the

Michigan basin (Summons and Powell, 1987; Macauley et al., 1990). They would qualify as Type II-S (sulphur-rich).

The Boas River Formation in Northern Ontario is, based on biostratigraphic data, older than the shales on Southampton Island. The Boas River Formation is middle Maysvillian whereas the shales of the Red Head Rapids Formation on Southampton are late Richmondian. The Boas River Formation is part of a succession where limestone and dolostone prevail; evaporites are restricted to disseminated crystals in the upper part of the underlying Bad Cache Rapids Group. Evaporitive and hypersaline conditions are found in the lower part of the overlying Churchill Group and consist of desiccated dolostones with anhydrite nodules and beds together with gypsum-filled fractures.

Eight extracts were made from the Boas River Formation in the Inco Winisk cores of Northern Ontario and detailed analyses will be subject of future contributions. However, preliminary evaluation of some of the data indicates that:

1) Pristane to phytane (Pr/Ph) ratios range between 0.8 and 1.36 (average of 1.1), these values are higher than those of the Red Head Rapids shales of Southampton Island (0.48 to 0.75, average of 0.62; Zhang, 2011) (Table x). The Pr/Ph values of the Boas River shales are lower than the common range of values of 1.5 to 2.3 for Upper Ordovician source rocks of the Winnipeg and Yeoman formations in the Williston Basin and the Collingwood Formation of southern Ontario (Macauley et al., 1990). The Pr/Ph values of the Boas River Formation suggest reducing conditions but not as severe as those hypothesized for the Red Head Rapids shales.
2) Acyclic isoprenoids to n-alkanes ratios (Pr/n-C_{17}, table 1) in the Boas River shales are not as high (0.8 to 1.26; average of 1.07) compared to those of the Red Head Rapids shales (0.67 to 1.92; average of 1.24) (Zhang, 2011) but are significantly higher compared to values for Upper Ordovician source rocks of the Winnipeg and Yeoman formations in the Williston Basin and the Collingwood Formation of southern Ontario (0.07 to 1.66; average of 0.5, Macauley et al., 1990).
3) The 1-alkyl-2,3,6-trimethylbenzenes are present in all 8 samples of the Boas River Formation. This presence indicates reducing and hypersaline conditions for this carbonate source rock.

Figure 26 presents the Ph / *n*-C_{18} *versus* Pr / *n*-C_{17} values for shale samples from Southampton Island and northern Ontario. All, but one samples plot in the Marine – Algal Type II organic matter (data in Table 1). The distribution of the data would suggest possible oxidation of the Boas River material if of similar original nature, and considering averages of data, slightly more mature source rocks in northern Ontario.

Table 1: Selected organic geochemical data for the Red Head Rapids Formation, Southampton Island and Boas River Formation, Northern Ontario

Formation	Unit / **Well**	Sample	Pr/Ph	Pr/nC_{17}	Ph/nC_{18}	Tmax (°C)	$Ro_{equi.vit}$ (1)
Red Head Rapids	Upper shale	07CYA-Z044-10	0,48	1,72	3,36	418	0,51
Red Head Rapids	Upper shale	07CYA-Z044-12	0,75	0,73	1,41	415	0,5
Red Head Rapids	Middle shale	07CYA-Z040-08	0,62	0,9	1,79	417	0,48
Red Head Rapids	Middle shale	07CYA-Z040-10	0,73	0,67	1,3	415	0,49
Red Head Rapids	Lower shale	07CYA-Z043-03	0,54	1,92	4,86	415	0,55
Red Head Rapids	Lower shale	07CYA-Z043-04A	0,57	1,52	3,86	412	0,5
Average			***0,615***	***1,24***	***2,76***		
Boas River	**INCO 49212**	10DKA001a	1,36	0,86	1	423	N/A
Boas River	**INCO 49212**	10DKA001c	1,22	1,26	1,8	422	N/A
Boas River	**INCO 49212**	10DKA001d	0,98	1,12	1,8	423	N/A
Boas River	**INCO 49212**	10DKA001e	1,18	1,2	1,9	422	N/A
Boas River	**INCO 49204**	10DKA002k	1,19	1,2	1,4	422	N/A
Boas River	**INCO 49204**	10DKA002l	0,96	1,22	1,4	421	N/A
Boas River	**INCO 49204**	10DKA002n	1,08	0,9	1,05	426	N/A
Boas River	**INCO 49204**	10DKA002p	0,8	0,8	0,72	425	N/A
Average			***1,10***	***1,07***	***1,38***		

(1) From Reyes (unpublished)

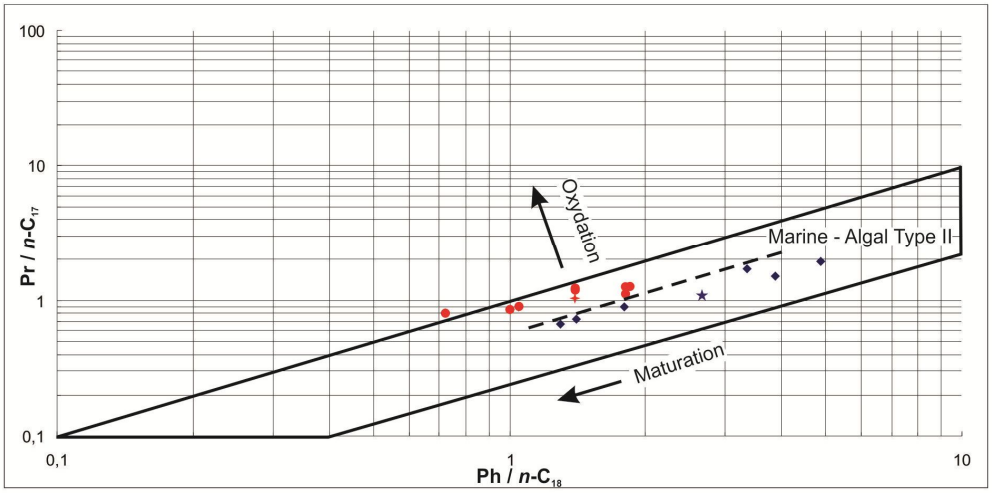

Fig. 26: Ph / n-C18 vs Pr / n-C17 graph of Southampton (blue lozenges) and Northern Ontario (red circles) shales. Stars are the average values. Modified from (Peters et al., 1999).

3.3 Thermal maturation – burial history

Together with the pessimistic evaluation of source rock presence in the Hudson Bay Basin (Tillement, 1975), the thickness of the succession, as imaged on seismic and confirmed by drilling, was deemed too thin to generate thermal conditions sufficient for oil generation. The maximum thickness present in the central part of the basin (where seismic information is available) is approximately 2.5 km, much thinner than the *circa* 4 km thick succession in the nearby Michigan and Williston basins. From a simplistic calculation, with a geothermal gradient of 20°C/km and a tropical seafloor temperature of 25°C, the very base of the succession for the thickest known succession in the basin would have merely reached the threshold of oil generation (75°C).

One of the scientific hypotheses that were defined at the start of the Hudson Bay – Foxe basins project focussed on evaluating if these basins have reached the oil window. Multiple tools and approaches have been used to evaluate the thermal history experienced by the Hudson Bay and Foxe basins, including a review of historical thermal data as well as strategic acquisition of new data. This section presents the summary of the results of the thermal indicators (CAI, Rock-Eval, organic matter reflectance, AFT and U-Th/He) that were gathered or re-evaluated in the course of this project.

3.3.1 Conodont Alteration Index (CAI)

Conodont Alteration Index (CAI) has been used by the hydrocarbon industry to evaluate the maximum thermal conditions reached by a sedimentary succession. The CAI is based on the alteration of colour of the phosphate test of conodonts with increasing thermal regime resulting

in darker colours. The change in color is irreversible and later exhumation does not affect the CAI value. CAI ranges between 1 (pale brown) and 5 (black) with rank 6 being characterized by a return to very pale colour (pale grey to white). At CAI of 1, the succession did not experience temperature above 80°C, with temperatures most commonly below 60°C whereas a CAI of 2 suggests temperature between 60 and 140°C. The oil window is assumed to start at 60 - 70°C depending on organic matter type and chemistry. For most researchers, a CAI of 1.5 is assumed to mark oil window conditions (50 - 90°C). Nonetheless, a CAI of 1 would be ambiguous given the range of accepted burial temperatures for that rank (<50 to 80°C)

Hudson Bay offshore wells

Geological reports for offshore wells (Dolby, 1986) and detailed assessment of conodonts in the Ordovician – Silurian succession (Zhang and Barnes, 2007) identified conodonts with CAI of 1.5 in the Polar Bear C-11 well at 1362 m (Ordovician Red Head Rapids Formation) and in the Beluga O-23 well between 1810 and 1920 m (Silurian Severn River Formation).

Northern Ontario Inco Winisk wells

McCracken (1990) documented conodonts with CAI of 1 to 2 and of 1.5 to 2 in two samples of the Churchill Group from INCO Winisk #49212 well. He noted that the lower CAI is associated with smaller conodont elements whereas the higher values occur for larger and robust conodonts with a common dark grey base. However, all remaining conodont samples were evaluated to have the ambiguous CAI of 1.

3.3.2 Rock Eval

Program pyrolysis is the most widely used technique to provide information on the thermal rank of a sedimentary succession. Details of the technique are summarized in Tissot and Welte (1984) and Espitalie et al. (1985). With progressive heating, the organic matter in the sample will release volatile and non-volatile hydrocarbons. Four major indices are measured and serve to quantify the type of organic matter as well as its thermal rank. S1 peak (mg HC/g rock) at 300°C provides information on the free hydrocarbon present in the sample. The S2 peak (mg HC/g rock) between 300 and 650°C results from the artificial maturation of the remaining organic matter in the sample and provides information on the remaining hydrocarbon potential of a sample; S2 is used in the calculation of the HI (HI = 100 * S2 / TOC). The S3 peak (mg CO-CO_2/g rock) between 300 and 390°C is the amount of CO_2 released from the thermal cracking of the organic matter; S3 is used in the calculation of the OI (OI = 100 * S3 / TOC). Finally, T_{max} is the temperature at which the maximum release of hydrocarbons during pyrolysis occurs, this is the highest value of the S2 peak. T_{max} is considered as a reliable indicator of thermal maturation of a rock succession, with the onset of oil window for Type II and Type II-S source rocks being set at 435°C and 430°C, respectively. A second thermal maturation indicator from the values obtained through program pyrolysis is the production index (PI) or

transformation ratio; this indicator (PI = S1 / [S1 + S2]) serves to evaluate the thermal degradation of the organic matter. It is commonly accepted that 0.1 < PI <0.4 indicates oil window condition (Peters, 1986).

Previous comparisons of Rock Eval results with other thermal indicators have led to the identification of some problematic issues with the T_{max} data, including incorrect evaluation of thermal rank in the case of Type I organic matter (T_{max} suppression); multiple studies (see Dewing and Sanei 2009 for a review) have documented that Rock Eval analysis of hydrogen-rich Type I organic matter will invariably produce a suppression of T_{max} values by up to 10 - 15°C (Dewing and Sanei, 2009). Non-reliable T_{max} values can result from too low organic matter content to generate a reliable S2 peak (Dewing and Sanei, 2009); it has also been proposed that only samples with S2 > 0.2 mg HC/g rock provide reliable T_{max} values (Peters, 1986). In their extensive study (T_{max} *versus* vitrinite reflectance) of Arctic Phanerozoic samples, Dewing and Sanei (2009) concluded that the threshold of valid S2 values should be raised to 0.35 mg HC/g rock. These samples are highlighted in grey in the Rock Eval tables in Annexes for the well results.

T_{max} suppression

Oil shales in the Upper Ordovician succession are characterised by high Hydrogen Index and are not true Type I organic matter. However, they do carry a significant percentage of liptinite/alginite (see petrography comments above), and T_{max} suppression is suggested in specific intervals for some succession (see below). These possibly suppressed T_{max} values are encircled on the T_{max} *versus* depth plots.

Increase in content of hydrogen-rich organic matter will be expressed by an anomalous increase of the (S1 + S2) / TOC values with respect to adjacent samples (Dewing and Sanei, 2009). This effect is present in Beluga O-23, Polar Bear C-11, Narwhal O-58, Comeault #1 and INCO Winisk wells. It occurs within the Upper Ordovician intervals associated with the oil shales, even if these source rocks are not entirely Type I.

The best well to document this T_{max} suppression effect is Polar Bear C-11 based on results of the re-sampling of dark cuttings by Zhang (2008) in the interval associated with oil shales on Southampton Island. Annex 1.9 documents multiple pairs of diluted and undiluted samples from the same interval; Tmax is suppressed by 7 to 12°C for undiluted (black) samples compared with values from immediately adjacent samples, a range of values that agrees well with observations by Dewing and Sanei (2009). In fact, almost all new samples from Zhang (2008) show suppressed values compared to adjacent diluted samples. This T_{max} suppression effect is not restricted to the Ordovician source rock, it is also observed for the Silurian Severn River Formation in the Comeault #1 well (Annex 1.7) where at least three samples with higher TOC, SI and S2 values have T_{max} values lower between 6 and 12°C compared to nearby samples. Finally, this effect can be detected in the INCO Winisk wells (Annex 1.4) with the T_{max} values of the Boas River samples being lower by 7 to 13°C compared to the immediately adjacent Churchill River group samples. This T_{max} suppression effect will be taken into account in the next section of vertical T_{max} trends.

T_{max} vertical trends

5 wells have sufficient to barely enough T_{max} data for an evaluation of vertical trends and interpretation of maximum thermal peak; as indicated above only data with S2 > 0.35 mg HC/g rocks and those with T_{max} above 410°C are considered here. For all these wells, except for the Beluga O-23, there are no T_{max} values for most of the Middle – Upper Devonian succession leading to very poor to non-significant R^2 values for the best-fit correlation line (see below). Given the relative closeness of the three offshore wells with T_{max} data, it is likely that the burial history of the Middle-Upper Devonian succession should be fairly similar. Therefore we are using the Middle-Upper Devonian T_{max} values from the Beluga O-23 well and utilize them, corrected for depth, especially for the Narwhal well were significant erosion of the Upper Devonian units is noted (Hu et al., 2011 and Fig. 26 herein). Moreover, suspected suppressed Tmax values were not included

Beluga O-23 well – This well has the most robust distribution of data with values from near the top of the well (Middle – Upper Devonian) and a fair number of values for the Ordovician-Silurian interval (Fig. 27). The Devonian samples are immature (from T_{max} and PI), whereas the highest T_{max} value for the Ordovician samples is 441°C (Annex 1.10). The best-fit line intercepts the 435°C and 430°C thresholds at *circa* 1900 m and 1600 m, respectively, with a R^2 correlation of 0.80. From T_{max}, the oil window threshold is in the upper part of the Red Head Rapids Formation for Type II OM and in the Lower Silurian Ekwan River Formation for Type II-S OM.

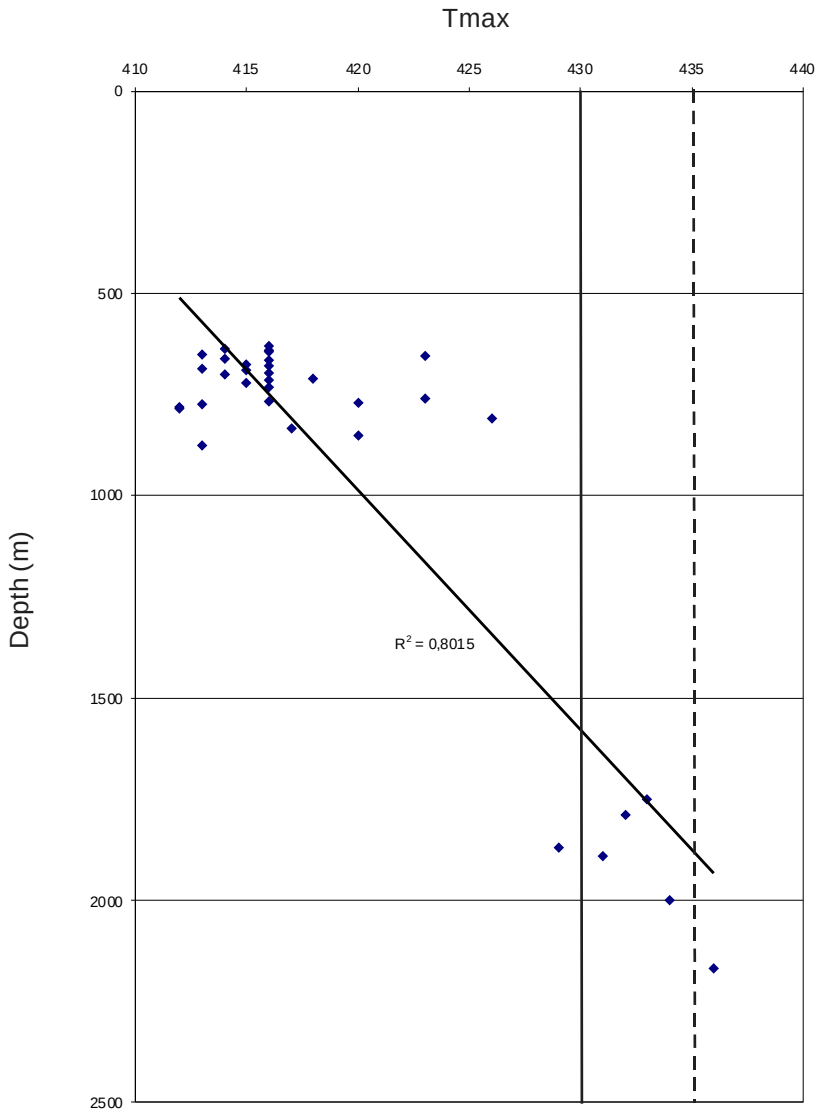

Figure 27: Diagram showing Tmax value vs depth in the Beluga well. The threshold of Tmax value of 435°C generally interpreted as indicator of the oil window for Type II OM is shown by the dashed line. The threshold of Tmax value of 430°C for Type IIS OM is also shown (full line).

Narwhal O-58 well – This well has a significant number of data from the top of the Silurian succession down to basement, an interval of 832 m (2730 ft). On figure 28, Tmax values from the Devonian section of the Beluga well (corrected for depth and thickness of units) have been added. The highest T_{max} value for the Ordovician samples is 445°C at the base of the well (Annex 1.8). The best-fit line intercepts the 435°C and 430°C thresholds at *circa* 1220 m (4000 ft) and at 1040 m (3400 ft), with a relatively good R^2 value of 0.84 (R^2 of 0.31 without the Devonian data). From T_{max}, the oil window threshold is within the Upper Ordovician Churchill River Group for Type II OM and at the top of the Upper Ordovician Red Head Rapids

Formation for Type II-S OM.

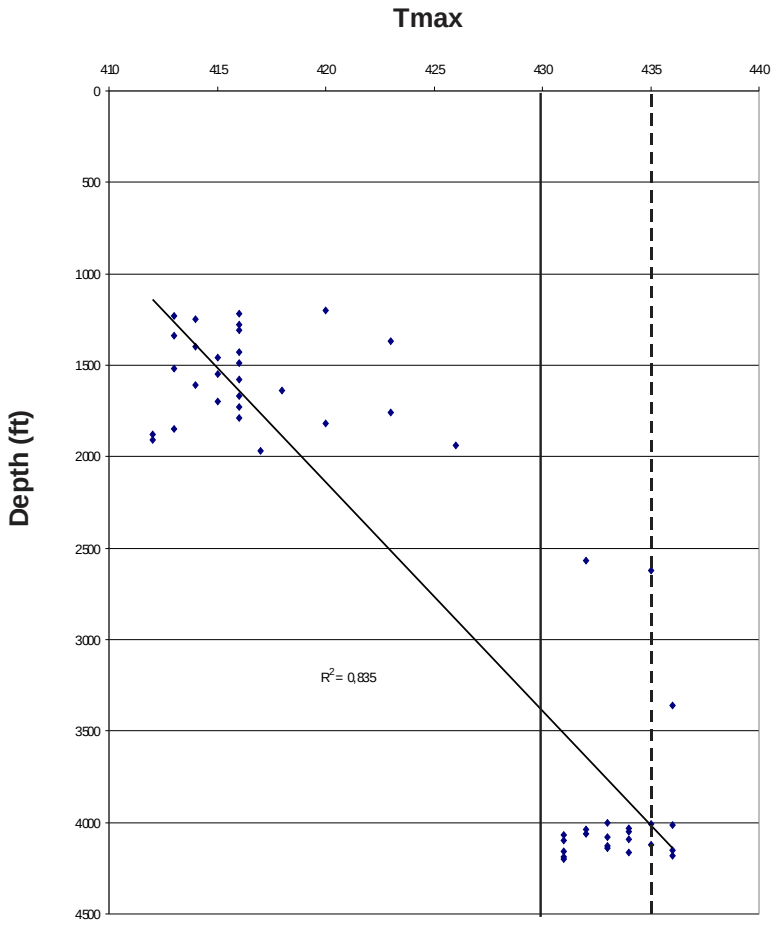

Figure 28: Diagram showing Tmax value vs depth in the Narwhal well. The threshold of Tmax value of 435°C generally interpreted as indicator of the oil window for Type II OM is shown by the dashed line. The threshold of Tmax value of 430°C for Type IIS OM is also shown (full line). Note that the data above 1000 m (3000ft) are from the Beluga well.

Polar Bear C-11 well – This well has a large number of analyses, with most of them concentrated in the lower part of the Lower Silurian interval down to basement, an interval of 740 m (2440 ft). Depth-corrected Devonian T_{max} data from the Beluga well were included for control at the top of the well. The highest T_{max} value for the Ordovician samples is 448°C in the Red Head Rapids Formation (Annex 1.9). The best-fit line intercepts the 435°C and 430°C thresholds at *circa* 1400 m (4600 ft) and 1220m (4000 ft), with a relatively good R^2 value of 0.70 (R^2 of 0.24 without the Devonian data). From T_{max}, the oil window threshold is at the contact between the Upper Ordovician Red Head Rapids Formation and the Churchill Group for Type II OM and in the middle part of the Severn River Formation for Type II-S OM (Fig. 29).

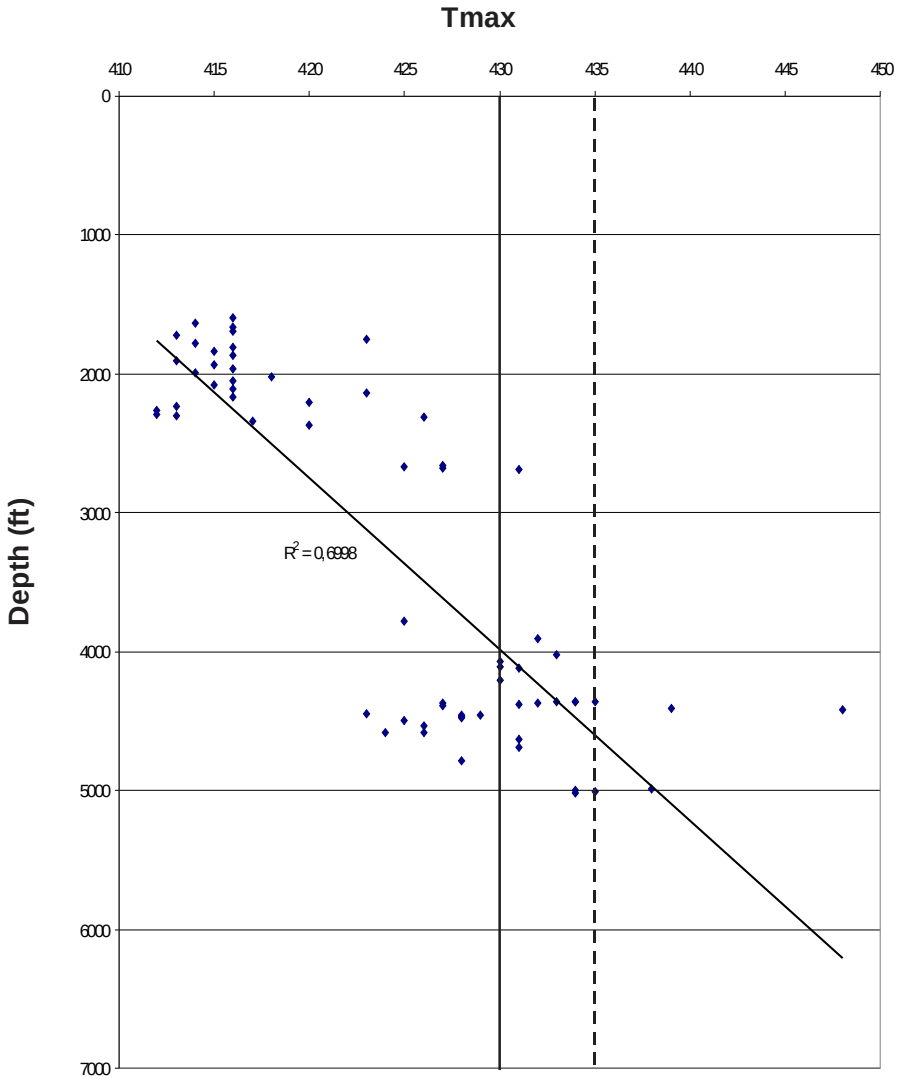

Figure 29: Diagram showing Tmax value vs depth in the Polar Bear well. The threshold of Tmax value of 435°C generally interpreted as indicator of the oil window for Type II OM is shown by the dashed line. The threshold of Tmax value of 430°C for Type IIS OM is also shown (full line). Note that the data above 1000 m (3000ft) are from the Beluga well.

Comeault #1 well – This onshore well is characterized by a thinner succession compared to offshore wells, with samples from the Silurian interval down to basement, an interval of 547 m (1795 ft). Given the significant distance from the offshore Beluga well, we do not use the Devonian data from the latter to better constrain the vertical trend. The highest T_{max} value is 440°C in the Bad Cache Rapids Group (Annex 1.7). The best-fit line intercepts the 435°C and 430°C thresholds at *circa* 490 m (1612 ft) and 410 m (1350 ft), respectively, with a poor R^2 value of 0.29, indicating a poor correlation between Tmax and depth. From T_{max}, the oil window threshold is in the Upper Ordovician Churchill River Group for Type II OM and in the Upper Ordovician Red Head Rapids Formation for Type II-S OM.

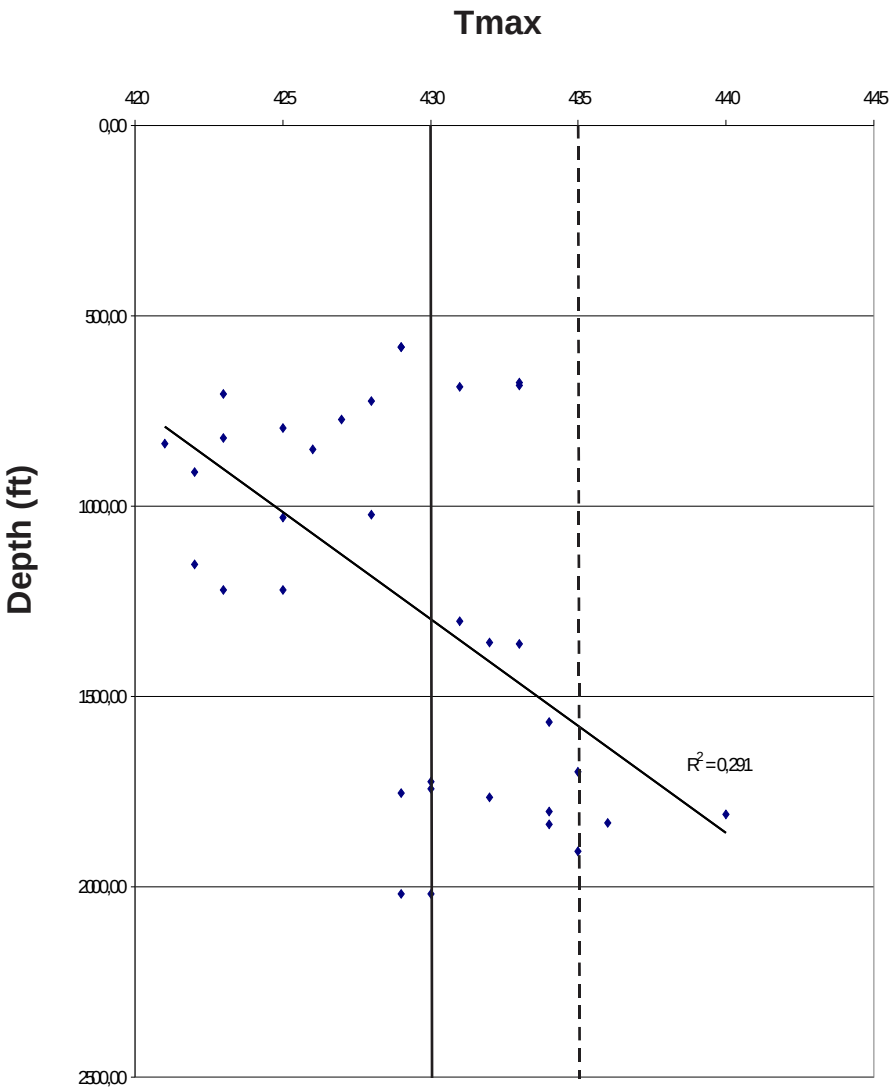

Figure 30: Diagram showing Tmax value vs depth in the Comeault well. The threshold of Tmax value of 435°C generally interpreted as indicator of the oil window for Type II OM is shown by the dashed line. The threshold of Tmax value of 430°C for Type IIS OM is also shown (full line).

Rowley M-04 well – This well in the Foxe Basin has the thinnest sedimentary succession of the analysed wells. Samples cover an interval of 260 m (848 ft) from the Middle to the Upper Ordovician interval. The highest T_{max} value is 435°C and occurs at the base of the Map-Unit Ols (Annex 1.11).

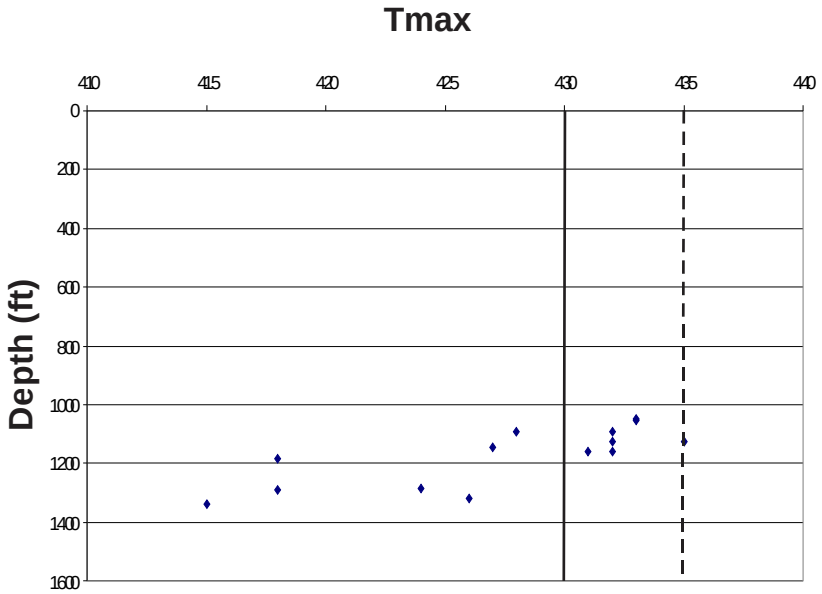

Figure 31: Diagram showing Tmax value vs depth in the Rowley well. The threshold of Tmax value of 435°C generally interpreted as indicator of the oil window for Type II OM is shown by the dotted line. The threshold of Tmax value of 430°C for Type IIS OM is also shown (full line).

Production index trends

The same 5 wells have been evaluated for the evolution of Production Index (PI) *versus* T_{max} values. Again, we have selected samples with S2 > 0.35 mg HC/g rock for the statistical analysis. Samples with PI > 0.1 and T_{max} > 435°C (Type II OM) or > 430°C (Type II-S OM) are considered mature (Peters, 1986).

The Beluga O-23 well has only on PI *versus* T_{max} 435°C values suggestive of thermal maturity (Annex 1.10 and Fig. 32), which is found in the Bad Cache Rapids Group. Four more values would be considered mature if a Type II-S OM (430°C) were chosen; three are found in the Severn River Formation and one in the Red Head Rapids. Three more samples have PI values over 0.4 with T_{max} lower than 430°C. This could indicate some hydrocarbon charge in the succession, resulting in higher S1 values with respect to the indigenous hydrocarbon expressed by S2. This phenomenon is present in the Severn River and Red Head Rapids formations. Hydrocarbon charge in the Ordovician-Silurian interval of the Beluga O-23 well has also been suggested from PI versus $Ro_{vit\text{-}equiv.}$ (Bertrand and Malo, 2012).

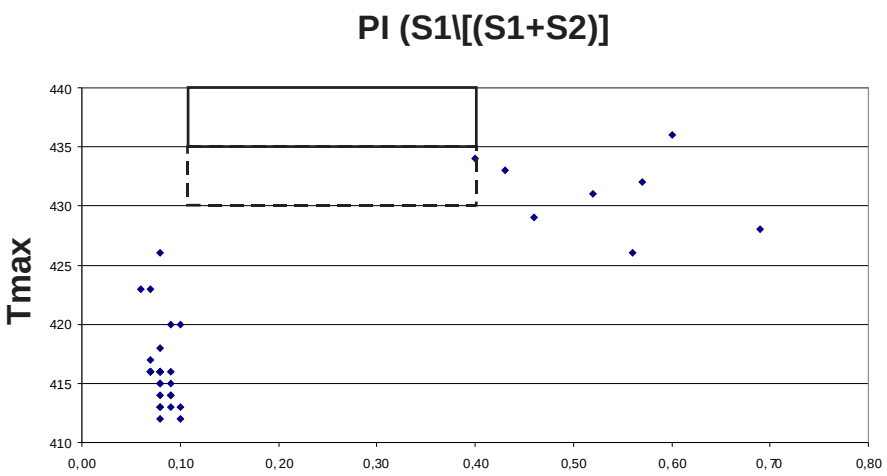

Figure 32: Diagram showing the production index (PI) vs Tmax for the Beluga well. The two boxes highlight mature condition for Type II (PI > 0.1 and Tmax > 435) and type IIS (PI> 0.1 and Tmax >430) respectively.

The Narwhal South O-58 well has all but two samples with PI < 0.1 suggesting immature stage. These two PI *versus* T_{max} value are suggestive of thermal maturity for Type II-S OM (Annex 1.8 and Fig. 33), both values occur in the Bad Cache Rapids Group. The possibility of some hydrocarbon charge in the Bad Cache Rapids Group in the Narwhal South O-58 well has been suggested from PI versus $Ro_{vit\text{-}equiv.}$ (Bertrand and Malo, 2012).

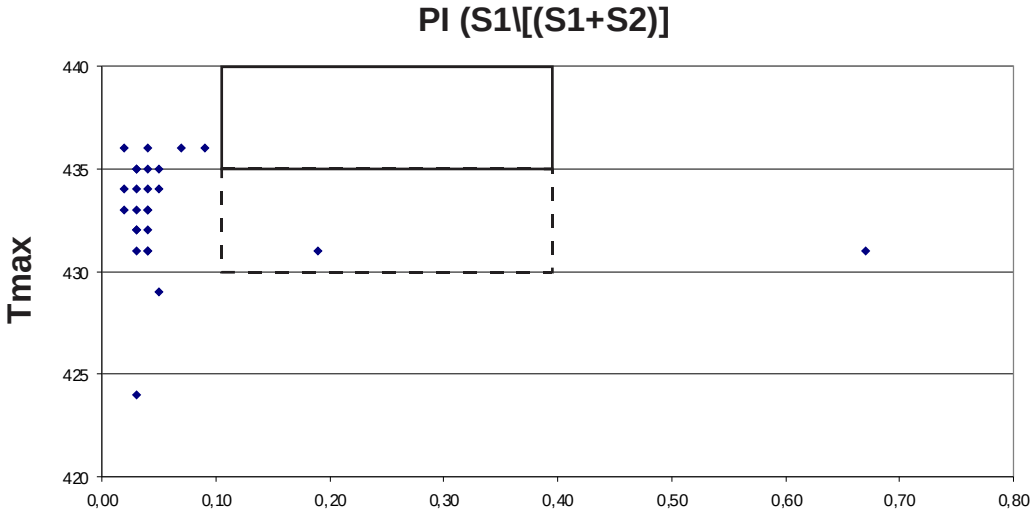

Figure 33: Diagram showing the production index (PI) vs Tmax for the Narwhal well. The two boxes highlight mature condition for Type II (PI > 0.1 and Tmax > 435) and type IIS (PI> 0.1 and Tmax >430) respectively.

The Polar Bear C-11 well has one PI *versus* T_{max} values from the Red Head Rapids Formation indicative of thermal maturity for Type II OM and 8 more for Type II-S OM (Annex 1.9 and Fig. 34), which are from the Lower Silurian Severn River Formation down to the Churchill Group.

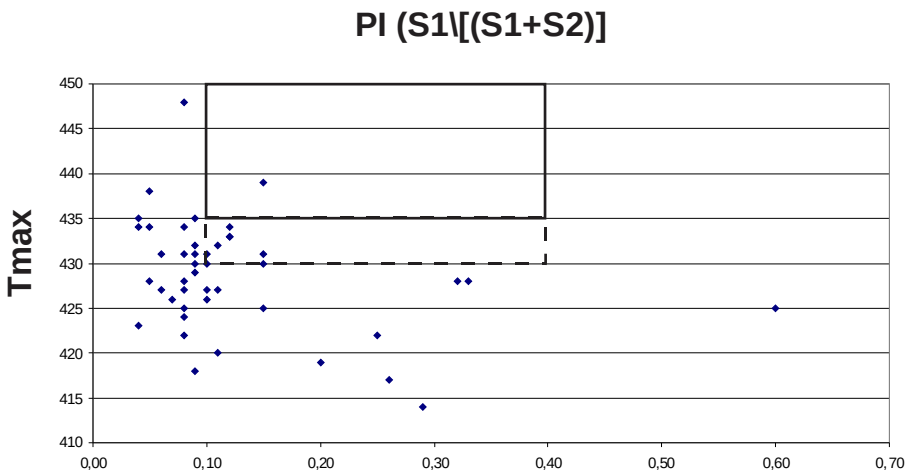

Figure 34: Diagram showing the production index (PI) vs Tmax for the Polar Bear well. The two boxes highlight mature condition for Type II (PI > 0.1 and Tmax > 435) and type IIS (PI> 0.1 and Tmax >430) respectively.

A large number of PI values are over 0.1 at Tmax below 430°C, these are found in all sedimentary units with the exception of the Bad Cache Rapids Group and could indicate hydrocarbon charge. Of interest are the obvious lower PI values (less than 0.1) from the middle part of the Churchill River Group down to the base of the well in an interval where T_{max} would suggest thermal maturity (Annex 1.9). This could suggest some hydrocarbon expulsion from that interval. The possibility of hydrocarbon charge in the Churchill River Group has been suggested from PI versus $Ro_{vit\text{-}equiv.}$ (Bertrand and Malo, 2012).

The Comeault #1 well has one PI *versus* T_{max} value indicative of thermal maturity for Type II OM and 4 more values for Type II-S OM (Annex 1.7 and Fig. 35) The value over 435 °C is found in the Churchill River Group, whereas values over 430°C are found from the Lower Silurian Severn River Formation and Churchill Group. The Comeault #1 well has 8 more PI values over 0.1 at Tmax lower that 430°C, these are found in the Severn River Formation (6) and Churchill Group.

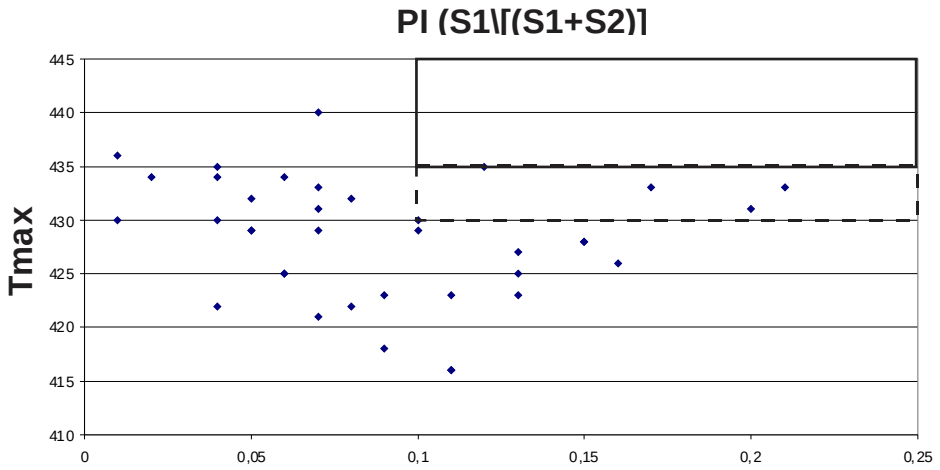

Figure 35: Diagram showing the production index (PI) vs Tmax for the Comeault #1 well. The two boxes highlight mature conditions for Type II (PI > 0.1 and Tmax > 435) and type IIS (PI> 0.1 and Tmax >430) respectively.

The Rowley M-04 well does not have PI *versus* T_{max} value indicative of thermal maturity for Type II organic matter but has two identical values for Type II-S (Annex 1.11 and Fig. 36), these samples are from Map Unit Ols. The Rowley M-04 well has a few more PI values over 0.1 at T_{max} values lower than 430°C, these values are found in the two sedimentary units of the well.

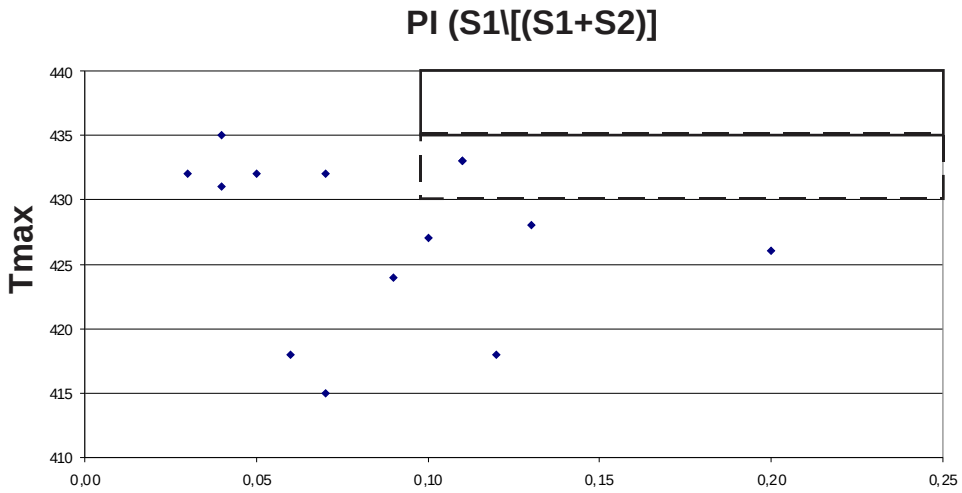

Figure 36: Diagram showing the production index (PI) vs Tmax for the Rowley well. The two boxes highlight mature condition for Type II (PI > 0.1 and Tmax > 435) and type IIS (PI> 0.1 and Tmax >430) respectively.

3.3.3 Organic matter reflectance

As with conodonts, an increase in thermal conditions will alter organic matter and

bitumen. When observed under the microscope, organoclasts and bitumen will become more reflective to incident light. As this process is not reversible, the reflectance of a specific element will be a relative indicator of the maximum burial temperature experienced by that specific component.

Vitrinite is the most commonly used organic material to evaluate the thermal rank of a succession. The onset of oil window (≈ 60°) corresponds to vitrinite reflectance (Ro) of 0.6%. However, vitrinite is only common in Devonian and younger sedimentary successions. In older sedimentary successions, the reflectance of other types of organic matter and kerogen are used. The reflectance of vitrinite and other types of organic matter are not the same at the same thermal rank. Based on statistically robust datasets from the Devonian and younger successions, where vitrinite and other organic matter occurs in the same sample, correlation equations between vitrinite and specific organoclasts and bitumen have been proposed (Jacob, 1989; Bertrand, 1990a, 1993; Tricker et al., 1992; Bertrand and Malo, 2001). The resulting value, known as $Ro_{vit\text{-}equiv.}$ has been used for evaluation of the thermal maturation of older than Devonian sedimentary successions. Dewing and Sanei (2009) from a very large database from the Canadian Arctic have published a table that links T_{max} values of sample with S2 > 0.35 mg HC/g rock with $Ro_{vit\text{-}equiv.}$.

Petrographic evaluation of organic matter reflectance has been done for three wells in Hudson Bay (Beluga O-23, Polar Bear C-11 and Narwhal South O-58; Bertrand and Malo, 2012). Similar analyses have been done for the two INCO Winisk wells in Northern Ontario (Armstrong and Lavoie, 2010; Reyes et al. 2011) as well as on samples from the three shale intervals on Southampton Island (Zhang, 2011; Reyes, unp. data).

Beluga O-23 well

18 samples were prepared and petrographically examined (Bertrand and Malo, 2012); of these 9 were from the Devonian succession, 5 from the Silurian and 4 from the Ordovician. The total number of samples is relatively low for such a thick succession (2200 m). The $Ro_{vit\text{-}equiv.}$ values of the Devonian samples range between 0.45 to 0.67%, the Silurian samples range from 0.55 to 0.69% and the Ordovician samples range between 0.61 to 0.91%. Bertrand and Malo (2012) concluded that the threshold of Type II OM oil window occurs close to the Silurian-Devonian contact (Fig. 36).

A comparison was made between petrographic results and intervals with Rock Eval results (Bertrand and Malo, 2012). Some reflectance measurements were made from composite samples covering 10 to 20 m interval to produce more robust statistical results from the low amount of organic matter in specific samples. It is not expected that thermal conditions (and organic matter reflectance) should vary over such a short interval making direct comparison possible. Table 2 is modified from Bertrand and Malo (2012) with the addition of two columns based on Dewing and Sanei (2009) correlation between T_{max} and $Ro_{vit\text{-}equiv.}$ (columns T_{max} from $Ro_{vit\text{-}equiv}$ and $Ro_{vit\text{-}equiv.}$ from T_{max}). For the 2 paired samples with S2 > 0.35 mg HC/g (highlighted in grey in Table 2) the difference between T_{max} from $Ro_{vit\text{-}equiv}$ and measured T_{max} is -1 and -2°C. The two Bertrand and Malo (2012) values are from various organoclasts and are

considered more precise than reflectance measurements taken only on inertitite or bitumen. This difference is minor and both techniques suggest similar results.

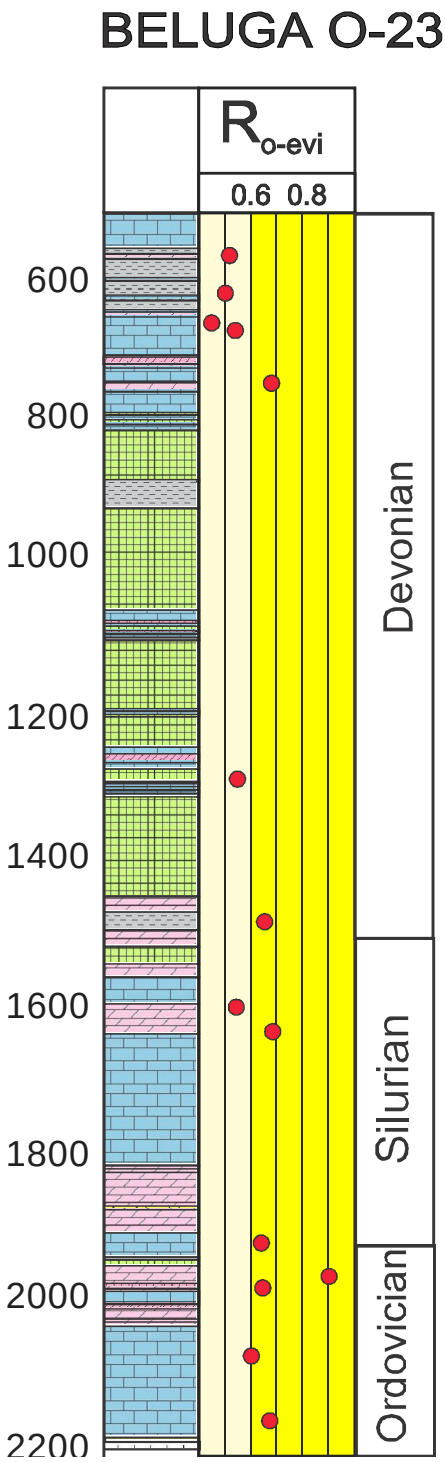

Figure 37: $Ro_{vit\text{-}equiv}$ in the Beluga well (from Bertrand and Malo, 2012). The yellow box ($Ro_{vit\text{-}equiv}$ > 0.6) indicates the oil window.

The integration of $Ro_{vit\text{-}equiv.}$ from Bertrand and Malo (2012) with Rock Eval data (Tmax transferred in $Ro_{vit\text{-}equiv.}$) for samples from the same interval (Table 2) is represented on Figure 38. The plot suggests that the threshold of oil window for Type II OM is reached at 2000 m (Upper Ordovician Red Head Rapids Formation) and at 1000 m (Lower Devonian Stooping River Formation) for Type II-S. This threshold for Type II-S is significantly higher up compared to results from Rock Eval. From the line equation, the eroded succession is around 2390 m (for a initial background value of 0.25%). R2 is 0,56 would be qualified as fair.

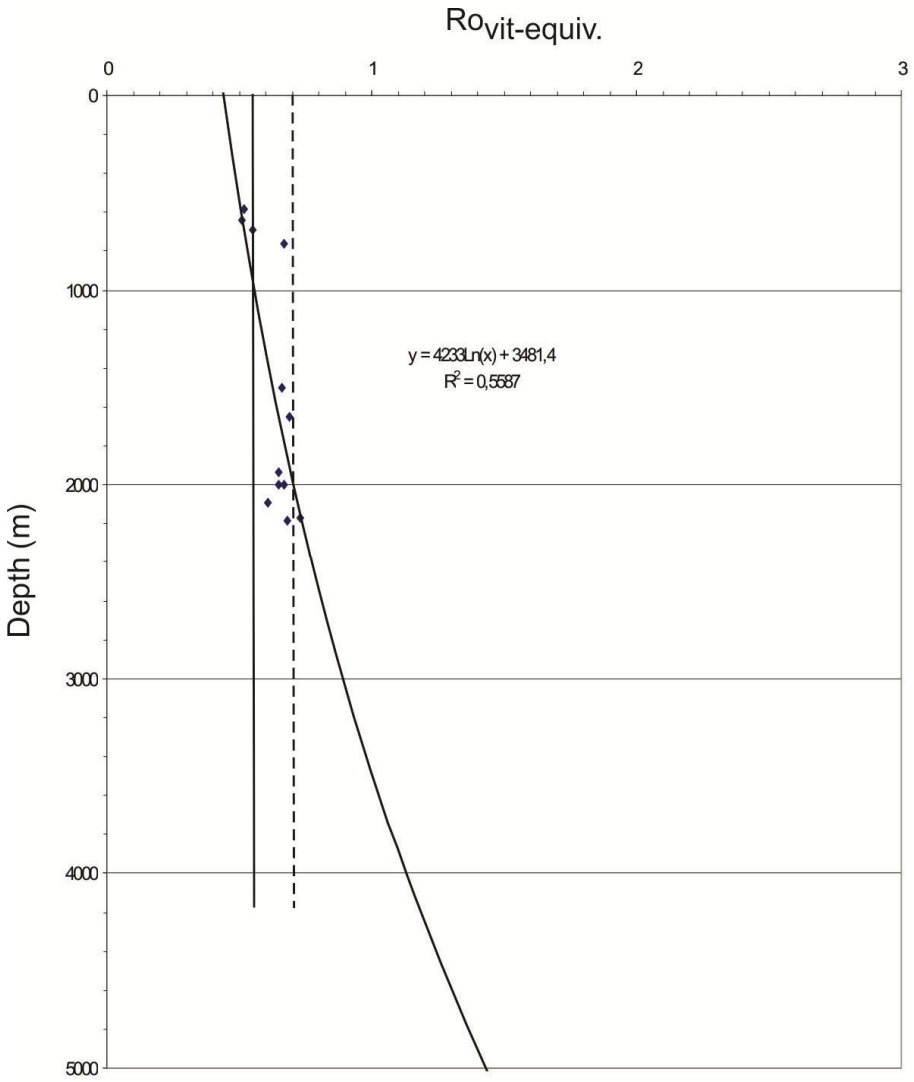

Figure 38: $Ro_{vit\text{-}equiv}$ from Bertrand and Malo (2012) with $Ro_{vit\text{-}equiv.}$ from Rock Eval Tmax values for Beluga well. Thresholds of oil window for Type II OM and II-S are shown by the dashed line and full line, respectively.

Well	Unit	Depth	**Ro vit-equiv. - Bertrand and Malo (2012)**	**Tmax from Ro vit-equiv.**	TOC(%)	PI	**Tmax**	**Ro vit-equiv. from Tmax**	S1	S2	S3	HI	OI
Beluga O-23	Red Head Rapids	2000	0.65	**433**	0.21	0.40	434	**0,67**	0.39	0.59	1.12	280	533
Beluga O-23	Churchill River	2170	0,68	**434**	0.27	0.60	436	**0,73**	1.45	0.95	1.15	351	425
Polar Bear C-11	Kenogami River	2690	0,68	**434**	0.36	0.09	431	**0,58**	0.11	1.10	0.39	306	108
Polar Bear C-11	Bad Cache Rapids	5020	0,7	**435**	0.14	0.04	434	**0,67**	0.02	0.46	0.19	329	136
Narwhal South O-58	Severn River	2570	0,74	**436**	0.27	0.04	432	**0,61**	0.03	0.85	0.45	315	167
Narwhal South O-58	Severn River	2600	0,66	**434**	0.81	0.03	424	**0,32**	0.12	3.34	0.68	412	84
Narwhal South O-58	Bad Cache Rapids	4040	0,76	**437**	0.22	0.03	432	**0,61**	0.03	0.80	0.28	364	127
Narwhal South O-58	Bad Cache Rapids	4070	0,76	**437**	0.21	0.04	431	**0,58**	0.02	0.54	0.27	257	129
Narwhal South O-58	Bad Cache Rapids	4080	0,74	**436**	0.20	0.04	433	**0,64**	0.02	0.45	0.24	225	120
Narwhal South O-58	Bad Cache Rapids	4200	0,69	**435**	0.17	0.19	431	**0,58**	0.09	0.39	0.30	229	176

Table 2: Comparison of offshore well intervals with both Rock-Eval[6] analyses (with S2>0.35) and $Ro_{equi\text{-}vit}$ values.

Polar Bear C-11

14 samples were examined for organic matter maturation (Bertrand and Malo, 2012), of these 2 were from the Devonian interval (Kwataboahegan Formation), 4 from the Silurian (Kenogami River, Ekwan River and Severn River formations) and 8 from the Ordovician (Red Head Rapids Formation, Churchill River and Bad Cache Rapids groups). The $Ro_{vit\text{-}equiv.}$ values of the 2 Devonian samples is 0.68%, the range for the Silurian is from 0.62 to 0.72% and the range for the Ordovician samples is from 0.57 to 0.77%. Bertrand and Malo (2012) indicated that there is no correlation of $Ro_{vit\text{-}equiv}$ with depth because of some anomalous high values in the Devonian and anomalous low values in the Ordovician (Fig. 38).

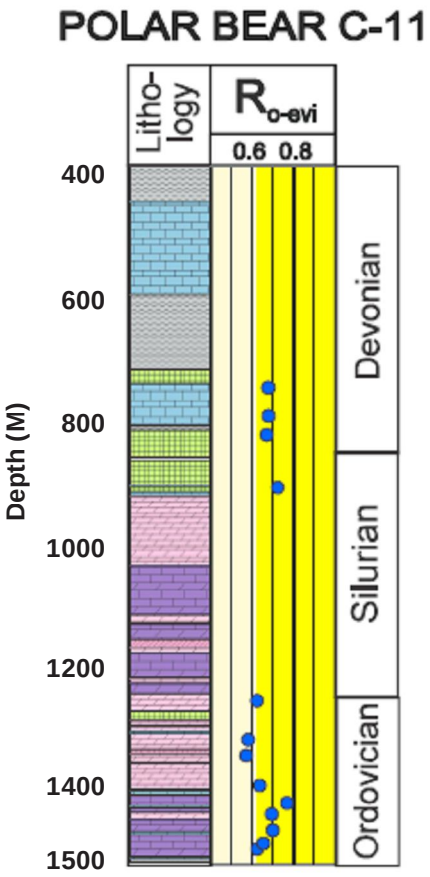

Figure 39: $Ro_{vit\text{-}equiv}$ in the Polar Bear well (from Bertrand and Malo, 2012). The bright yellow box ($Ro_{vit\text{-}equiv}$ > 0.6) indicates the oil window

Table 2 presents the correlation between $Ro_{vit\text{-}equiv}$ values of Bertrand and Malo (2012) *versus* the T_{max} results for correlative samples with S2 > 0.35 mg HC/g rock for the Polar Bear samples. Only 2 samples meet the S2 criteria; the difference between T_{max} from $Ro_{vit\text{-}equiv}$ and measured T_{max} is +1 and +3°C. From Bertrand and Malo (2012) the two Ro values in table 2 are from various organoclasts and not from inertitite or bitumen only, the difference between Rock Eval T_{max} and organic matter reflectance is minor.

The integration of $Ro_{vit\text{-}equiv.}$ from Bertrand and Malo (2012) with Rock Eval data (Tmax transferred in $Ro_{vit\text{-}equiv.)}$ for samples from the same interval (Table 2) is represented on Figure 40. The plot suggests that there is no correlation between $Ro_{vit\text{-}equiv.}$ and depth as indicated by the negative logarithmic curve and the R^2 value.

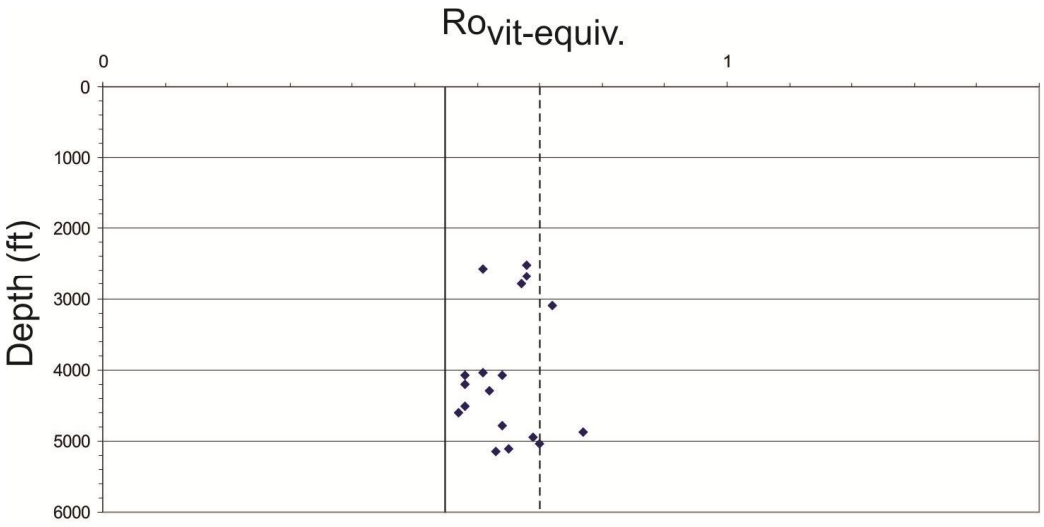

Figure 40: $Ro_{vit\text{-}equiv}$ from Bertrand and Malo with $Ro_{vit\text{-}equiv.}$ from Rock Eval Tmax values for Polar Bear well. Thresholds of oil window for Type II OM and II-S are shown by the dashed line and full line, respectively.

Narwhal South O-58

A total of 19 samples were examined for organic maturation (Bertrand and Malo, 2012), of these 10 were from the Silurian interval (Kenogami River and Severn River formations) and 9 from the Ordovician succession (Red Head Rapids Formation, Churchill River and Bad Cache Rapids groups). The $Ro_{vit\text{-}equiv.}$ values of the Silurian samples range between 0.51 and 0.78% and the Ordovician data range between 0.66 to 0.76%. Bertrand and Malo (2012) indicated that the correlation of $Ro_{vit\text{-}equiv}$ with depth is poor and suggested the Type II OM oil window threshold in the Lower Silurian Severn River Formation (Fig. 39).

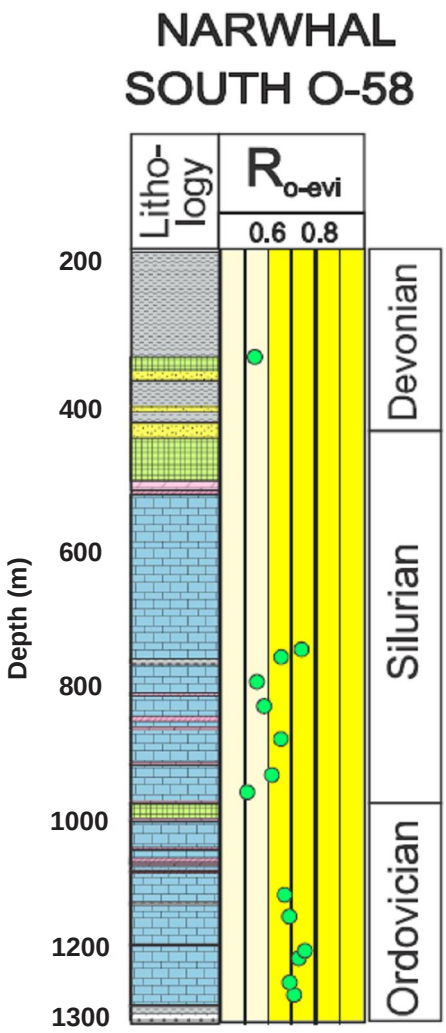

Figure 41: $Ro_{vit\text{-}equiv}$ in the Narwhal well (from Bertrand and Malo, 2012). The bright yellow box ($Ro_{vit\text{-}equiv}$ > 0.6) indicates the oil window.

Table 2 presents the correlation between $Ro_{vit\text{-}equiv}$ values of Bertrand and Malo (2012) *versus* the T_{max} results for correlative samples with S2 > 0.35 mg HC/g rock for the Narwhal samples. Six samples are correlated; the difference between T_{max} from $Ro_{vit\text{-}equiv}$ and measured T_{max} is between -3 and +10°C. In 5 cases, the $Ro_{vit\text{-}equiv}$ values suggest higher maturation level compared to Rock Eval values. Data from Bertrand and Malo (2012) for the Narwhal well in Table 2 is derived from a mixture of organoclasts, inertitite and bitumen.

The integration of $Ro_{vit\text{-}equiv.}$ from Bertrand and Malo (2012) with Rock Eval data (Tmax transferred in $Ro_{vit\text{-}equiv.)}$ for samples from the same interval (Table 2) is represented on Figure 42. The plot suggests that the threshold of oil window for Type II OM is reached at 3600 ft (1100 m; Lower Silurian Severn River Formation) and at 2750 ft (849 m; Lower Devonian Stooping River Formation) for Type II-S. This threshold for Type II and II-S is significantly higher up compared to results from Rock Eval. From the line equation, the eroded succession would be around 300 m (for a initial background value of 0.25%); this casts serious doubts on

the validity of the correlation. R2 at 0.25 is poor.

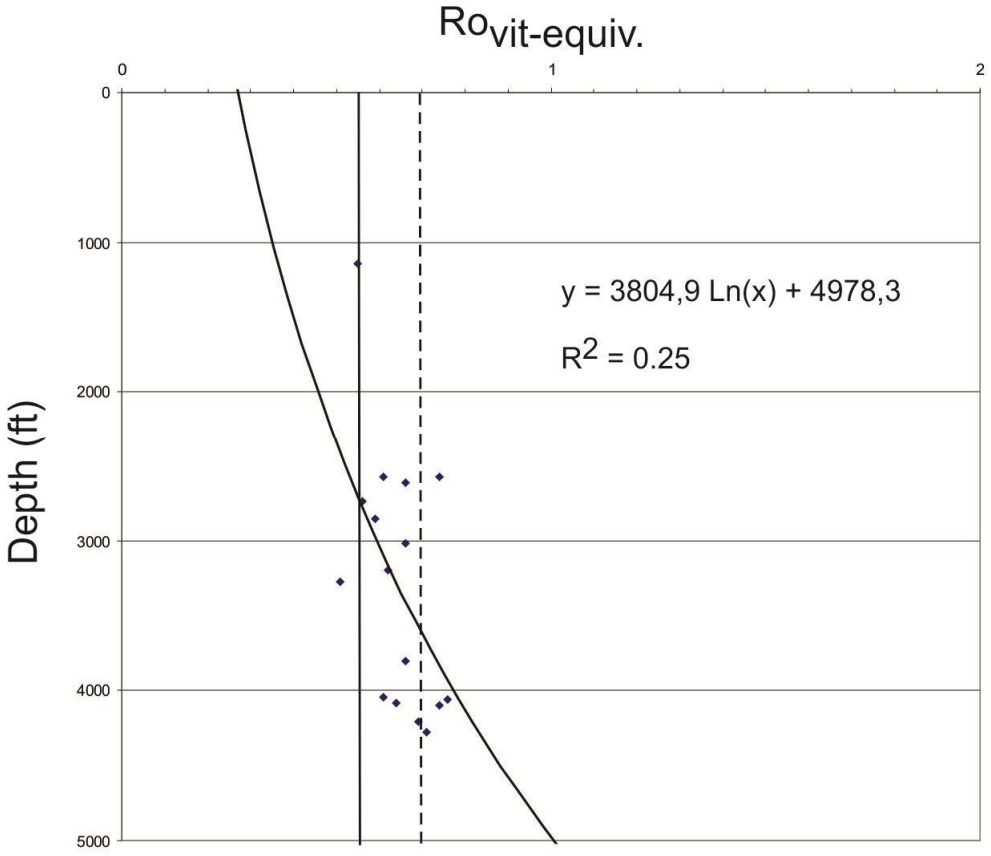

Figure 42: $Ro_{vit\text{-}equiv}$ from Bertrand and Malo with $Ro_{vit\text{-}equiv.}$ from Rock Eval Tmax values for Narwhal well. Thresholds of oil window for Type II OM and II-S are shown by the dashed line and full line, respectively.

Inco Winisk wells

10 samples from the Ordovician succession were petrographically examined in the two wells (Reyes, unp. data). 8 samples are from the Boas River Formation with one sample each from the Churchill River and Bad Cache Rapids groups (Table 3). Organic matter reflectance measurements were taken on vitrinite (corpohuminite/corpogellinite), bitumen, and chitinozoans. $Ro_{vit\text{-}equiv}$ values range between 0.55 and 0.69% (Table 3; Figs. 43 and 44)

Table 3 presents the correlation between $Ro_{vit\text{-}equiv}$ values of Reyes (unp. data) *versus* the T_{max} results from the same sample. The columns T_{max} from $Ro_{vit\text{-}equiv}$ and $Ro_{vit\text{-}equiv.}$ from T_{max} are from Dewing and Sanei (2009). A direct correlation between T_{max} and $Ro_{vit\text{-}equiv}$ is noted for the Churchill River Group sample, the only one in this suite of samples to have low S2 and TOC. For all remaining samples, the Rock Eval T_{max} values are considerably lower to what would be expected from the $Ro_{vit\text{-}equiv}$.

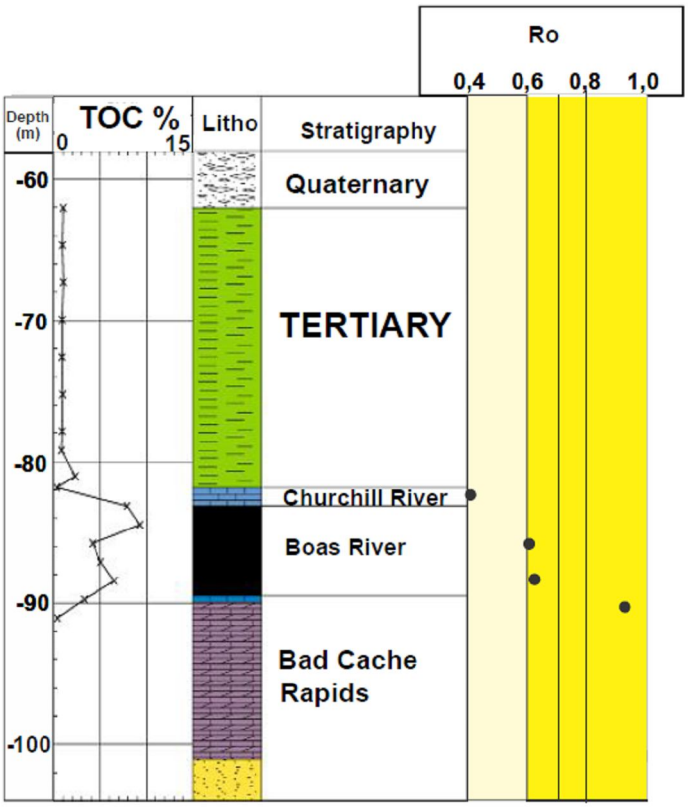

Figure 43: $Ro_{vit\text{-}equiv}$ in the Winisk #49204 well. The bright yellow box ($Ro_{vit\text{-}equiv}$ > 0.6) indicates the oil window.

Sample	Strat. unit	Depth (m)	Ro vit-equiv. - Reyes et al (2011)	Tmax from Ro vit-equiv.	TOC(%)	PI	Tmax	Ro vit-equiv. from Tmax	S1	S2	S3	HI	OI
INCO Winisk # 49212													
10DKA001b	Boas River	105,31	0,63	433	8,71	0,04	425	0,35	2,14	51,97	1,60	597	18
10DKA001f	Boas River	111,34	0,66	434	7,92	0,04	420	0,14	1,96	42,35	2,04	535	26
10DKA001g	Boas River	112,44	0,62	432	6,29	0,04	424	0,32	1,72	36,61	1,51	582	24
10DKA001h	Boas River	113,76	0,67	434	5,93	0,04	426	0,38	1,59	37,59	1,37	634	23
10DKA001i	Boas River	114,81	0,68	434	4,98	0,03	426	0,38	0,91	30,41	1,13	611	23
!0DKA001j	Boas River	116,20	0,69	435	4,71	0,04	423	0,27	1,11	26,02	1,48	552	31
INCO Winisk # 49204													
10DKA002m	Boas River	85,79	0,6	432	4,19	0,05	423	0,27	1,34	23,31	1,16	556	28
10DKA002o	Boas River	88,42	0,62	433	6,51	0,05	422	0,23	2,15	37,76	1,77	580	27

Table 3: Comparison of INCO-Winisk well intervals with both Rock-Eval[6] analyses with S2 > 0.35 mg HC/g rock and $Ro_{equi\text{-}vit}$ values.

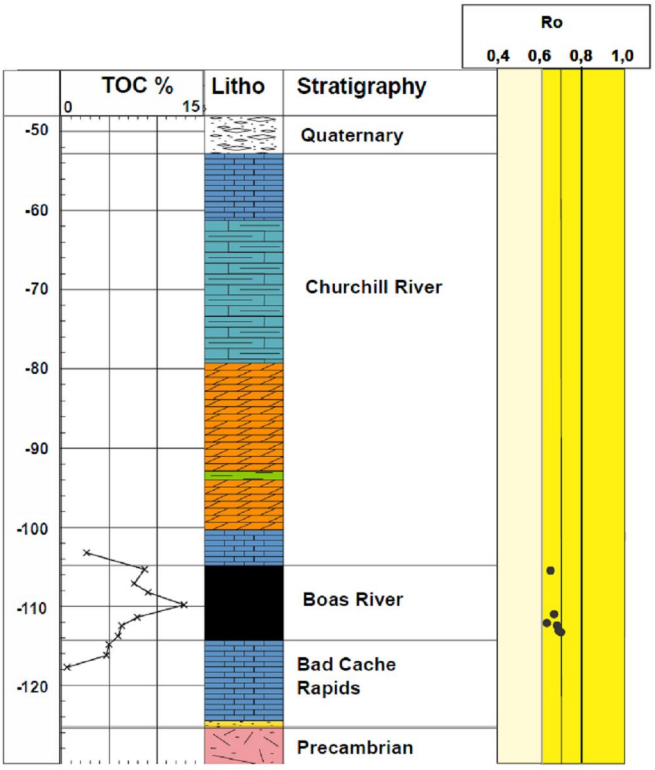

Figure 44: $Ro_{vit\text{-}equiv}$ in the Winisk #49212 well. The bright yellow box ($Ro_{vit\text{-}equiv}$ > 0.6) indicates the oil window.

The difference in measured T_{max} and the one calculated from $Ro_{vit\text{-}equiv}$ is between 8 and 14°C, and falls in the range of T_{max} suppression from hydrogen-rich source rocks as reported in other studies (10-15°C; Dewing and Sanei, 2009).

Southampton shale outcrops

6 samples from Cape Donovan, on the northern coast of Southampton Island were petrographically examined (Zhang, 2011b and Reyes, unp. data). The suite consists of 2 samples each from the lower, middle and upper oil shale intervals (Table 3). The average organic matter reflectance values reported in Zhang (2011b) are, with the exception of one sample, all lower than the values measured by Reyes (unp. data). Zhang (2011b) concluded that one sample in the lower shale interval was at the onset of oil window and all the others were immature. Values of Reyes (unp. data) suggest late immature stage to onset of oil window.

Table 4 presents the correlation between $Ro_{vit\text{-}equiv}$ values of Zhang (2011b) and Reyes (unp. data) *versus* the T_{max} results from the same sample. The columns T_{max} from $Ro_{vit\text{-}equiv}$ and $Ro_{vit\text{-}equiv.}$ from T_{max} are from Dewing and Sanei (2009) equation. For all samples, the Rock Eval T_{max} values are considerably lower to what would be expected from $Ro_{vit\text{-}equiv}$. The difference between the measured and calculated T_{max} is between 11 and 17°C and is in the range of T_{max} suppression from hydrogen-rich source rocks as reported in other studies (10-15°C; Dewing and Sanei, 2009).

Sample	Strat unit	Ro vit-equiv. - Zhang (2011)	Ro vit-equiv. - Reyes (unp. data)	Tmax from Ro vit-equiv. of Reyes	TOC(%)	PI	Tmax	Ro vit-equiv. from Tmax	S1	S2	S3	HI	OI
07-CYA-Z043-03B	**Lower Shale**	0,56	0,55	430	10,51	0,02	415	0	1,49	61,78	2,16	588	21
07-CYA-Z043-04A	**Lower Shale**	0,49	0,5	429	9,25	0,03	412	0	1,46	52,16	1,73	564	19
07CYA-Z040-08	**Middle Shale**	0,35	0,48	428	21,62	0,03	417	0	4,23	139,21	4,96	644	23
07-CYA-Z040-10	**Middle Shale**	0,43	0,49	429	29,65	0,04	415	0	6,21	168,79	7,71	569	26
07-CYA-Z044-10	**Upper Shale**	0,43	0,51	429	31,97	0,03	418	0,04	6,12	210,29	5,48	658	17
07-CYA-Z044-12	**Upper Shale**	0,4	0,5	429	26,61	0,03	415	0	5,52	159,83	5,24	601	20

Table 4. Comparison of Southampton shale intervals with both Rock-Eval[6] analyses and $Ro_{vit\text{-}equiv.}$ values. Calculation of Tmax from $Ro_{equi\text{-}vit}$ and $Ro_{equi\text{-}vit}$ from Tmax is based on Dewing and Sanei (2009).

3.3.4 Low-temperature geothermochronology (AFT and U-Th/He)

Geothermochronology using apatite grains is a tool that provides time / temperature estimates based on a reasonable understanding of the geological history of a sedimentary basin (stratigraphy, unconformities and tectonic scenario). Apatite Fission Tracks analysis (AFT) provides detailed information in the 60 to 120°C thermal range, which is correlative to the oil window. The evaluation of the U-Th/He ratios in the apatite provides time / temperature constraints in the 50 to 80°C range, and thus provide important information on the cooling history (exhumation) of a sedimentary basin.

55 samples were submitted for analyses (Annex 2), of these 17 were from Phanerozoic sandstones (15 Ordovician, 1 Devonian, 1 Jurassic) and 38 from Precambrian metamorphic or volcanic rocks. The samples originate from the Hudson Bay and Foxe basins and from various surrounding basement localities in Nunavut, Quebec, Ontario and Manitoba (Fig. 47). Workable apatites were only found in 12 samples; 1 Ordovician sandstone and 6 Precambrian samples had enough apatites for AFT and U-Th/He analyses (Table 5) and 2 sandstones and 3 Precambrian samples had enough for U-Th/He only (Table 5). Samples included outcrops and well samples ranging from depths of ~365-2200 m (Table 5).

All mineral processing and analytical work was carried out in the School of Earth Sciences, University of Melbourne, Australia. Details on the methodology can be found in Annex 2.

Apatite fission track thermochronology

This method is based on the spontaneous fission of ^{238}U in uranium-bearing apatite, producing narrow trails of intense damage. Tracks in apatite have approximately the same length when formed (~16±1 μm) and are produced continuously through geological time. If the mineral is subjected to a sufficiently high temperature for a long period of time, all existing fission tracks will fade (anneal) and eventually disappear, effectively resetting the fission track clock. On cooling below the annealing temperature, continuously formed tracks are shortened in accordance with the prevailing time-temperature conditions, providing a length distribution that contains a record of the cooling history. Only under conditions of rapid cooling through the entire annealing zone will AFT ages date a 'specific' geological event. The analysis becomes more complicated when samples have experienced multiple heating episodes or very slow exhumation. Useful summaries of the principles of fission track thermochronology, the interpretation of data and their application to geological problems have been presented by Wagner & Van den haute (1992), Gallagher et al, (1998), Gleadow et al, (2002) and Donelick et al, (2005).

Apatite (U-Th-Sm)/He thermochronometry

The (U-Th-Sm)/He method is based on α-decay of isotopes of the actinides, i.e. ^{238}U, ^{235}U, ^{232}Th and ^{147}Sm. Each of these isotopes produces a series of α-particles (^{4}He), which are

retained in the crystal lattice below a certain temperature. Knowing the amount of U-Th-Sm and the amount of retained helium will provide an estimate of the age at which it passed below the retention temperature. Detailed summaries of (U-Th-Sm)/He apatite dating and its applications are given by Farley (2002) and Farley & Stockli (2002).

Results

Seven apatite fission track (AFT) results (six from crystalline basement and one from sediment) are summarized in Table 6 and shown on Figure 45. For most samples, grain quality was good to excellent, allowing for age determinations based on 10-29 apatite grains, measurement of up to 101 horizontal confined track lengths and 152 Dpar measurements.

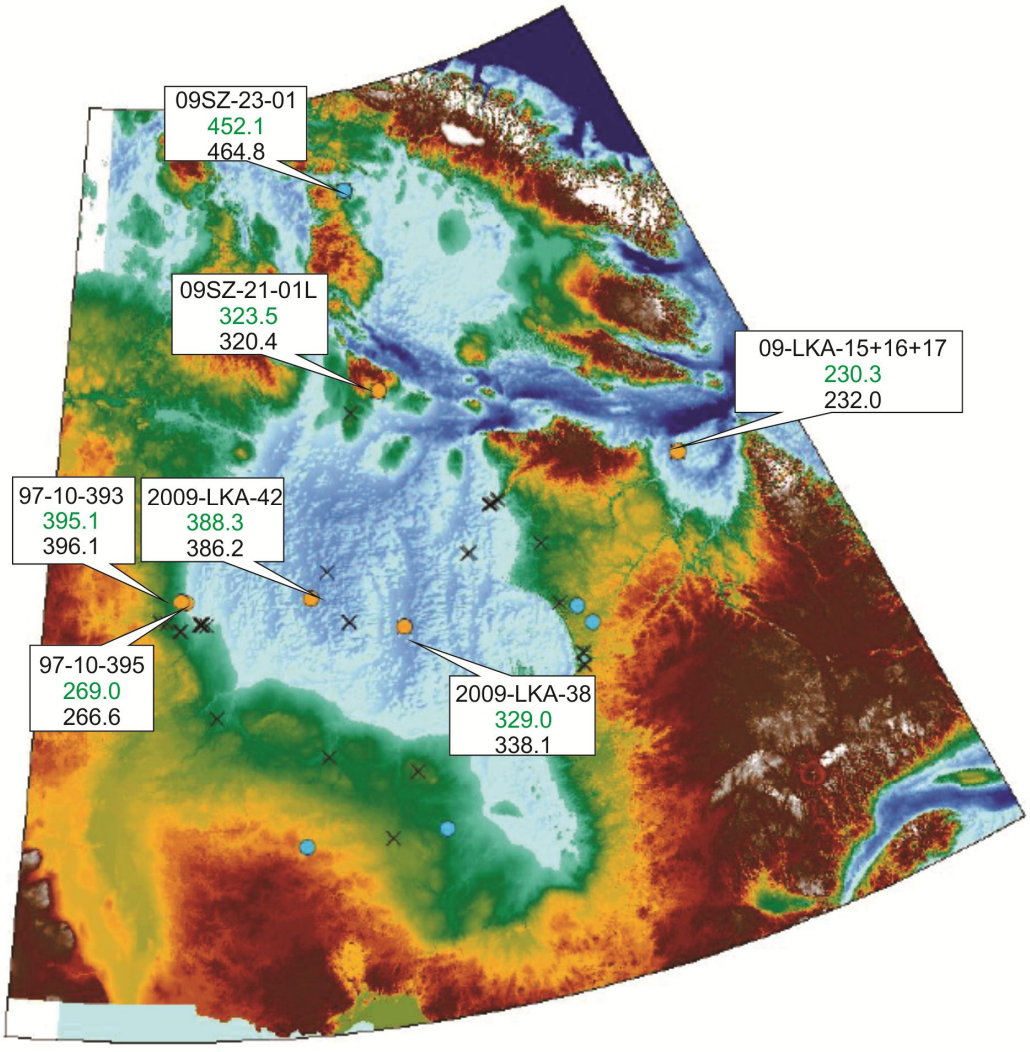

Figure 45: Apatite fission track results. For each samples, the sample number, the pooled age (in green) and the central age are indicated. Orange dots for samples with AFT and U-Th/He results, blue dots for samples with U-Th/He results only and x for samples with no results.

Sample No.	Lithology	Age	Location (**Bold = well)**	Easting	Northing	Latitude °N	Longitude °W	Depth or elevation (m)	Apatite yield	Analyses carried out	
										AFT	***AHe***
Sediments											
09SZ-21-01L	Paleozoic Sandstone	Ord	Southampton Island			64,28469	-83,10660	150	excellent	✔	✔
03 GRS 0022A	Quartz rich arenite grit	Ord	Attawapiskat River			52,80801	-83,97570	272-283	rare	X	✔
2009-LKA-52	Mesozoic Sandstone	Juras.	Victor Mine	305987	5856166	52,82030	-83,87934	82	sparse	X	✔
Crystalline											
09SZ-23-01	Granite	PreCamb	Melville			69,49660	-82,84220	15	excellent	✔	✔
09SZ-24-01	Granite	PreCamb	Melville			69,49580	-82,84350	9	rare	X	✔
2009-LKA-15+16+17	Gneiss	PreCamb	**Akpatok F-26**			60.424606	-68.33575	-365	excellent	✔	✔
2009-LKA-38	Gneiss	PreCamb	**Narwhal South O-58**			58.133442	-84.134053	-1310	good	✔	✔
2009-LKA-42	Gneiss	PreCamb	**Beluga O-23**			59.215175	-88.557453	-2200	good	✔	✔
03-JY-7117-B2	Mafic	PreCamb	Northern Quebec	479576	6326424	57,08070	-75,79820	258	good	X	✔
03-JV-9017-A1 and A2	Mafic	PreCamb	Northern Quebec	452281	6383083	57,58760	-75,79820	176	rare	X	✔
97-10-395	K-spar porphyritic granite	PreCamb	Outcrop - Manitoba	383712	6580690	59,34891	-95,04501	35	excellent	✔	✔
97-10-393	K-spar porphyritic granite	PreCamb	Outcrop - Manitoba	396670	6575164	59,30268	-94,81463	10	excellent	✔	✔

Table 5: Samples with enough apatite for AFT and/or (U-Th-Sm)/He analyses.

Sample	No. of grains	U	Fossil track density	Pooled age	X^2	Dis-persion	Central age	Mean track length [µm ±1SE]	SD [µm]	Dpar µm [±1SD]	Cl wt% range [mean]
Comments		**a**	**b**	**c**	**d**	**e**	**f**		**g**		**h**
2009-LKA-15+16+17	18	6,4	0.8229 (1113)	**230.3 ± 13.7**	28,89	**19**	**232.0 ± 13.0**	12.12 ± 0.32 (51)	2,28	1.36 ± 0.08 (122)	0.00-0.04 [0.01]
2009-LKA-38	25	17,9	3.105 (5697)	**329.0 ± 16.9**	29,21	**24**	**338.1 ± 16.8**	11.08 ± 0.26 (64)	2,15	1.56 ± 0.13 (125)	0.02-0.27 [0.14]
2009-LKA-42	29	8,5	1.814 (4302)	**388.3 ± 18.0**	41,18	**20**	**386.2 ± 16.2**	10.37 ± 0.22 (60)	1,78	1.51 ± 0.10 (152)	0.00-0.07 [0.04]
09SZ-21-01L	10	18,0	3.112 (1788)	**323.5 ± 30.7**	28,90	**32**	**320.4 ± 34.2**	12.36 ± 0.23 (51)	1,65	1.61 ± 0.21 (54)	0.01-0.30 [0.13]
09SZ-23-01	29	3,6	0.8726 (2376)	**452.1 ± 24.5**	38,98	**23**	**464.8 ± 24.6**	12.18 ± 0.15 (100)	1,59	1.48 ± 0.11 (147)	0.02-0.12 [0.05]
97-10-393	29	17,0	3.561 (10079)	**395.1 ± 8.1**	38,12	**9**	**396.1 ± 7.7**	11.95 ± 0.18 (101)	1,83	1.46 ± 0.08 (145)	0.00-0.07 [0.02]
97-10-395	21	17,4	2.554 (3401)	**269.0 ± 28.8**	52,43	**46**	**266.6 ± 27.2**	11.81 ± 0.18 (100)	1,83	1.48 ± 0.12 (105)	0.00-0.03 [0.01]

a) Pooled uranium content (ppm) of all grains measured by LA-ICP-MS.

b) Fossil track density (10^6 cm^{-2}) Nos. in brackets are no. of tracks counted, track lengths measured or Dpars measured.

c) Pooled AFT grain age (My ±1σ) calculated from pooled counts and U of all grains (Hasebe et al., 2004).

d) P value for χ^2 for (n-1) degrees of freedom, % (Galbraith, 2005).

e) Percentage variation or dispersion between single grain ages (%).

f) Central age (My ±1σ) calculated from single grain ages after Galbraith (2005).

g) Standard deviation of track length distribution.

h) Range of Cl content determined by electron microprobe, means in bracket – for analytical conditions, see the Annex 2.

Table 6: Apatite fission track results. Location of samples is given on Table 5

The chi-square (χ^2) test calculated for each sample analysed (Table 6) is a standard test for homogeneity of single grain estimates. It provides an assessment of whether the FT counts were derived from a Poissonian distribution with a common mean value. If the χ^2-statistic $P(\chi^2)$ is ≥ 5%, (as is the case for all samples discussed here) it can be taken as evidence that all grains counted derive from a single age population. Therefore, in this case it is appropriate to use the pooled uranium age, rather than the central age (also shown in Table 6), which is a calculation to estimate the age dispersion (Galbraith & Laslett, 1993), essentially a weighted-mean age.

Figure 46 shows the radial plots that are a means of graphically presenting the value and precision of an analysis simultaneously (Galbraith, 1990). The distribution of track lengths measured for each sample is also shown in Fig. 43. All samples show a broad horizontal confined track length distribution, with sample 97-10-393 showing a distinctly negatively skewed distribution, due to a tail of shorter track lengths (Fig. 43). All samples exhibit narrow etch pits, suggesting that the predominant composition of the grains analysed is fluorapatite. This was confirmed by electron microprobe analyses of apatites on which ATF ages were determined

Crystalline basement rocks yield AFT pooled ages ranging from 230.3 ± 13.7 to 452.1 ± 24.5 Ma. The oldest AFT age is from the Melville Peninsula, close to the Foxe Basin western margin. The youngest AFT is age is from the Akpatok well, the sample that is the closest to the Atlantic margin. The single sedimentary sample (09SZ-21-01L) analysed from an Ordovician sandstone sample from Southampton Island, yields an AFT age of 323.6 ± 30.7 Ma. All AFT ages are substantially younger than the metamorphic/magmatic or deposition age of their host rocks.

Mean horizontal confined track lengths range from 10.37 ± 0.22 to 12.36 ± 0.23 µm for crystalline basement rocks and is 12.36 ± 0.23 µm for the sandstone sample from Southampton Island. Standard deviations of the length distributions are intermediate in range (1.45-1.65 µm).

The relatively young AFT age and short mean track length indicate that the sample has experienced substantial annealing and that they experienced temperature > 60°C. This is in agreement with other thermal indicators discussed above.

Single grain apatite (U-Th-Sm)/He results are presented in Table 7 and shown on Figure 47, which also shows weighted mean values for multi-single grain analyses. Single grain ages are often widely dispersed in that the AHe age variation between different grains from the sample often exceeds the analytical uncertainties. Most apparent AHe ages are Paleozoic or early Mesozoic, reflecting slow cooling over a relatively long time span. The oldest weighted mean (U-Th-Sm)/He age is from a Manitoba basement sample. Interestingly, the youngest weighted mean (U-Th-Sm)/He age is from the deepest sample located at the base of the Beluga O-23 well.

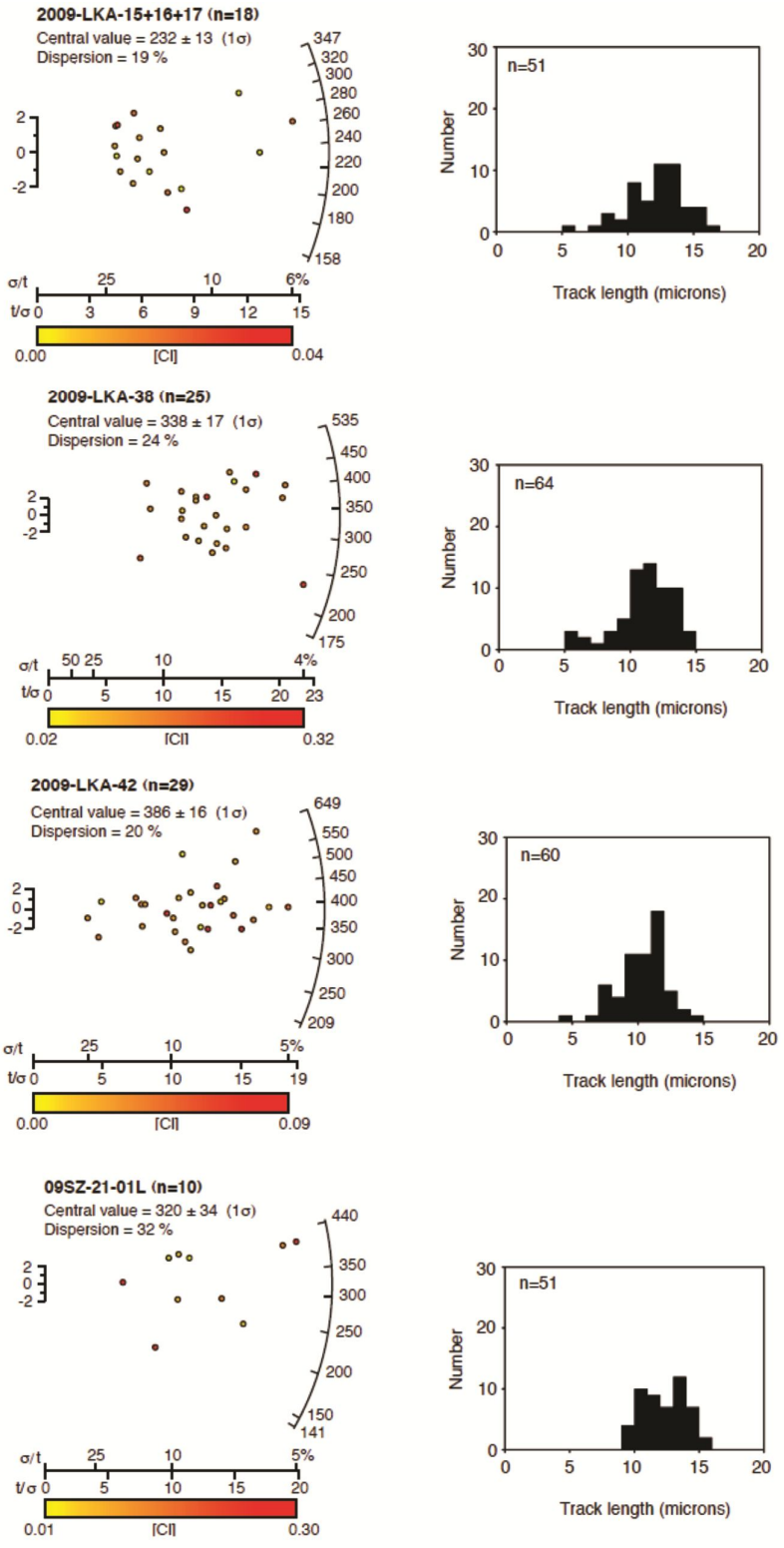
2009-LKA-15+16+17 (n=18)
Central value = 232 ± 13 (1σ)
Dispersion = 19 %
347
320
300
280
260
240
220
200
180
158
2
0
-2
σ/t
25
10
6%
t/σ 0 3 6 9 12 15
0.00
[Cl]
0.04
n=51
Number
Track length (microns)
2009-LKA-38 (n=25)
Central value = 338 ± 17 (1σ)
Dispersion = 24 %
535
450
400
350
300
250
200
175
50 25
10
4%
t/σ 0 5 10 15 20 23
0.02
0.32
n=64
2009-LKA-42 (n=29)
Central value = 386 ± 16 (1σ)
Dispersion = 20 %
649
550
500
450
400
350
300
250
209
5%
t/σ 0 5 10 15 19
0.09
n=60
09SZ-21-01L (n=10)
Central value = 320 ± 34 (1σ)
Dispersion = 32 %
440
350
300
250
200
150
141
t/σ 0 5 10 15 20
0.01
0.30
n=51

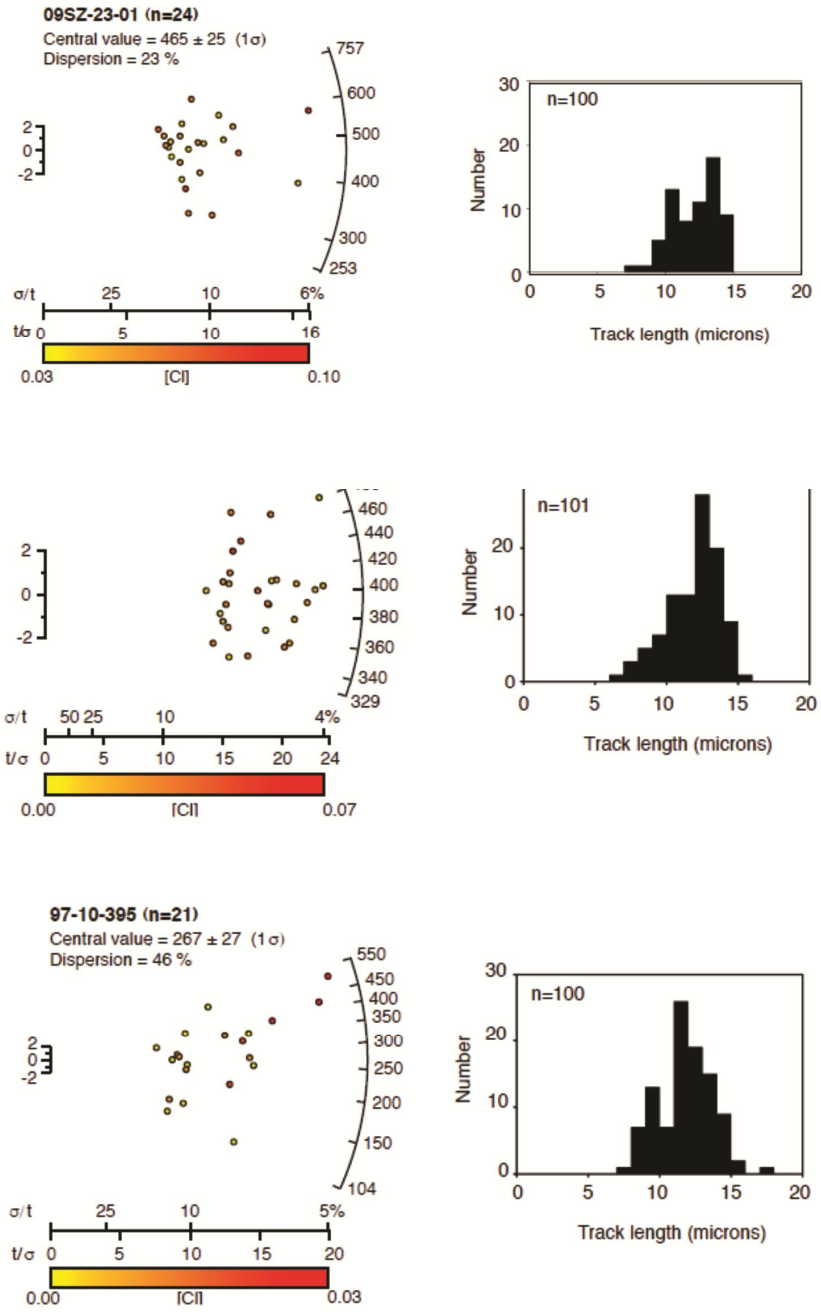

Figure 46: Plots showing measured single-grain AFT age data distributions as radial plots (Galbraith, 1990) of single-grain AFT age data (left-hand side) and histograms showing confined track length distributions (right hand side) for all samples. In radial plots, the slope of a straight line from the origin (0) through a particular data point yields the AFT age read off radially around the perimeter of the plot. A horizontal line drawn from the origin to the perimeter yields the central value (age). The *x-axis* value and the percent relative error measure the precision of each grain age, also plotted along this axis is the Cl content range, which is color coded for each grain according to its Cl value. The further a point plots to the right of the origin, the more precise the individual grain age.

Sample No.	He #	[a]F_T	[4]He (ncc)	Mass (mg)	Th/U ratio	U ppm	Th ppm	Sm ppm	[b][eU]	Corrected age (Ma)	Error (±1s)	[c]Weighted mean age (Ma)	Grain radius (mm)	Grain length (mm)	[d]*Rs*
2009-LKA-15+16+17	17062	0,79	7,294	0,0086	0,44	15,3	6,7	55,5	16,9	**394.9**[x]	**24,2**		71,5	167,8	75,2
2009-LKA-15+16+17	17068	0,83	1,053	0,0152	0,56	2,0	1,1	36,6	2,3	**239.2**[y]	**14,8**		84,9	210,2	90,7
2009-LKA-15+16+17	17071	0,80	0,924	0,0108	0,82	2,1	1,8	26,3	2,5	**265.5**[y]	**16,4**		69,0	226,5	79,3
2009-LKA-15+16+17	18119	0,74	0,417	0,0038	1,79	2,3	4,1	194,1	3,3	**251.9**[y]	**15,6**		58,8	171,2	65,7
2009-LKA-15+16+17	18122	0,69	1,911	0,0026	0,60	17,6	10,6	96,9	20,1	**288.9**[x]	**17,9**		43,5	138,1	49,6
2009-LKA-15+16+17	18125	0,70	1,619	0,0031	0,69	22,1	15,2	128,6	25,7	**162.9**[x]	**10,1**		46,4	144,2	52,7
												232±73			
2009-LKA-38	17079	0,74	5,316	0,0048	3,64	11,9	43,4	209,3	22,1	**398.4**[x]	**24,7**		54,8	227,5	66,2
2009-LKA-38	17082	0,77	12,027	0,0092	1,35	28,1	38,1	278,4	37,1	**280.0**[x]	**17,3**		53,9	316,1	69,1
2009-LKA-38	17085	0,80	18,822	0,0115	2,90	20,3	58,8	162,6	34,1	**381.8**[x]	**23,6**		70,1	233,6	80,9
2009-LKA-38	17088	0,81	20,468	0,0124	3,15	18,9	59,5	375,7	32,9	**395.6**[x]	**24,5**		77,5	301,1	92,5
2009-LKA-38	17556	0,77	29,994	0,0086	6,34	35,5	225,2	212,2	88,4	**317.9**[y]	**19,7**		69,5	176,9	74,8
2009-LKA-38	18157	0,75	18,150	0,0050	2,65	48,3	127,9	330,4	78,4	**366.6**[y]	**22,7**		57,4	221,9	68,4
2009-LKA-38	18160	0,73	8,328	0,0050	1,91	22,1	42,1	305,9	32,0	**413.6**[x]	**25,6**		53,0	175,6	61,1
												352±49			
2009-LKA-42	17094	0,75	0,871	0,0051	6,46	4,7	30,2	499,3	11,8	**111.6**[x]	**6,6**		63,9	194,2	72,1
2009-LKA-42	17097	0,77	0,578	0,0087	2,43	3,5	8,6	218,8	5,5	**92.4**[x]	**5,7**		68,9	221,2	78,8
2009-LKA-42	17103	0,80	1,200	0,0119	2,81	4,0	11,3	273,3	6,7	**117.0**[x]	**7,2**		79,9	225,1	88,5
2009-LKA-42	17106	0,75	4,037	0,0051	4,98	13,0	64,9	970,2	28,3	**216.5**[y]	**13,4**		58,3	220,8	69,2
2009-LKA-42	18163	0,80	0,354	0,0128	3,30	1,5	5,0	127,5	2,7	**80.0**[x]	**5,0**		72,7	240,5	83,7
2009-LKA-42	18169	0,81	3,074	0,0129	4,11	4,2	17,3	340,2	8,3	**222,3**	**13,8**		85,3	176,5	86,3
												107±44			

2009-LKA-52	18184	0,84	0,166	0,0217	1,28	0,2	0,2	1,9	0,2	**242,2**	**15,0**		119,3	151,6	100,1
2009-LKA-52	18213	0,86	0,288	0,0328	1,42	0,2	0,3	0,1	0,3	**218,2**	**13,5**		105,6	292,7	116,4
												223±34			
09SZ-21-01L	18193	0,80	21,541	0,0103	0,67	37,4	24,9	660,4	43,3	**377.1**[y]	**23,4**		77,5	169,9	79,8
09SZ-21-01L	18196	0,79	3,758	0,0093	1,62	8,6	13,9	44,2	11,9	**272,6**	**16,9**		76,4	159,1	77,4
09SZ-21-01L	18199	0,79	1,792	0,0104	1,23	3,9	4,8	82,0	5,0	**268.6**[x]	**16,7**		67,5	226,3	78,0
09SZ-21-01L	18202	0,69	4,533	0,0030	2,79	20,2	56,3	839,2	33,4	**347,2**	**21,5**		47,1	136,7	52,5
09SZ-21-01L	18205	0,72	5,154	0,0033	0,54	25,6	13,8	171,6	28,8	**422,3**	**26,2**		49,8	133,5	54,4
												317±78			
09SZ-23-01	17034	0,80	6,132	0,0096	0,54	15,3	8,3	150,6	17,3	**292.7**[x]	**18,1**		73,9	174,9	77,9
09SZ-23-01	17040	0,85	10,078	0,0220	0,33	8,5	2,8	87,2	9,2	**392,6**	**24,3**		91,4	182,8	91,4
09SZ-23-01	17043	0,85	8,489	0,0233	0,50	6,0	3,0	35,3	6,7	**428.0**[z]	**26,5**		96,2	250,9	104,3
09SZ-23-01	17046	0,84	1,959	0,0207	0,85	1,9	1,6	67,1	2,3	**323,8**	**20,0**		86,3	172,6	86,3
09-SZ-23-01	18116	0,76	2,735	0,0062	0,44	8,7	3,8	51,6	9,6	**362.2**[y]	**22,5**		54,8	284,8	68,9
												347±65			
09SZ-24-01	17049	0,79	3,886	0,0087	2,41	5,8	13,9	174,9	9,1	**385,2**	**23,8**		74,8	155,2	75,7
09SZ-24-01	17054	0,69	2,579	0,0034	8,22	10,1	83,3	174,5	29,7	**203,4**	**12,6**		48,2	147,8	54,5
09SZ-24-01	17056	0,73	2,744	0,0047	5,58	4,0	22,2	95,7	9,2	**498,2**	**30,8**		54,3	159,1	60,7
09SZ-24-01	17059	0,78	4,432	0,0072	0,41	14,1	5,8	68,3	15,5	**317,5**	**19,7**		67,9	154,8	70,8
09SZ-24-01	17547	0,69	1,046	0,0030	5,21	6,3	32,9	201,7	14,0	**196,9**	**12,2**		52,3	110,2	53,2
09-SZ-24-01	18107	0,69	2,230	0,0030	5,02	11,8	59,1	130,1	25,7	**233,0**	**14,4**		45,6	142,4	51,8
09-SZ-24-01	18110	0,64	1,900	0,0018	6,31	24,2	152,5	367,3	60,0	**143,8**	**8,9**		41,3	153,4	48,8
												211±80			
03-JY-7117-B2	17111	0,76	1,119	0,0087	11,20	1,3	14,8	234,6	4,8	**204,5**	**12,7**		68,9	221,2	78,8
03-JY-7117-B2	17113	0,79	0,936	0,0109	9,77	0,6	6,2	142,3	2,1	**304,8**	**18,9**		73,0	203,1	80,5
03-JY-7117-B2	17116	0,79	0,954	0,0119	11,30	0,6	6,8	141,9	2,2	**275,3**	**17,0**		79,9	225,1	88,5
03-JY-7117-B2	17119	0,74	0,818	0,0051	7,40	1,2	9,1	245,2	3,3	**349,0**	**21,6**		58,3	220,8	69,2
03-JV-7117-B2	18151	0,72	0,469	0,0046	4,03	1,3	5,4	162,3	2,6	**293,3**	**18,2**		50,3	182,2	59,1
03-JV-7117-B2	18154	0,75	0,498	0,0060	8,05	0,9	7,2	192,5	2,6	**239,5**	**14,8**		61,4	157,9	66,3
												261±53			
03-JV-9017-A1&A2	17128	0,68	0,672	0,0032	4,61	2,4	11,2	335,7	5,0	**306,4**	**19,0**		43,2	172,0	51,8
03-JV-9017-A1&A2	17131	0,69	1,769	0,0029	0,50	10,6	5,2	41,4	11,8	**402,9**	**24,9**		49,2	145,8	55,2

03-JV-9017-A1&A2	17137	0,73	0,377	0,0042	0,67	3,0	2,0	19,8	3,5	**208,3**	**12,9**		53,0	150,5	58,8
03-JV-9017-A1&A2	17140	0,77	0,800	0,0064	0,62	2,3	1,4	21,6	2,6	**381,2**	**23,6**		64,3	153,9	68,0
03-JV-9017-A1&A2	18207	0,70	0,941	0,0036	8,19	1,6	12,9	339,4	4,6	**415,5**	**25,8**		50,9	139,8	56,0
												296±120			
03-GRS-0022A	18131	0,75	0,170	0,0065	2,38	0,5	1,3	0,5	0,8	**255,6**	**15,8**		55,3	211,6	65,8
97-10-393	19752	0,77	28,121	0,0065	0,26	101,3	26,0	470,1	107,4	**319.1**[x]	**19,8**		58,2	270,1	71,8
97-10-393	19754	0,76	14,202	0,0043	0,13	49,9	6,3	343,4	51,4	**495.0**[y]	**30,7**		54,1	214,1	64,8
97-10-393	19756	0,76	14,397	0,0056	0,18	54,1	9,8	306,6	56,4	**362.4**[y]	**22,5**		53,4	193,7	62,8
97-10-393	19735	0,81	15,110	0,0104	0,09	22,8	2,0	269,9	23,3	**481.6**[z]	**29,9**		71,1	204,2	79,1
97-10-393	19733	0,79	15,290	0,0085	0,20	30,2	5,9	250,6	31,6	**442.5**[z]	**27,4**		60,0	235,5	71,7
												396±96			
97-10-395	19728	0,78	20,350	0,0084	1,86	26,1	48,7	257,6	37,5	**502.5**[x]	**31,2**		67,9	181,6	74,1
97-10-395	19724	0,79	52,865	0,0094	1,71	60,1	102,9	288,0	84,3	**521.4**[y]	**32,3**		65,3	220,0	75,5
97-10-395	19832	0,76	15,283	0,0073	1,91	21,4	40,8	204,2	31,0	**531.7**[x]	**33,0**		55,0	238,4	67,0
97-10-395	19834	0,78	47,063	0,0086	1,84	55,6	102,5	383,9	79,7	**539.1**[y]	**33,4**		60,4	233,9	72,0
												523±32			

a) Fγ is the α-ejection correction after Farley et al. (1996)

b) (eU) is the effective uranium concentration (U ppm + 0.235 Th ppm)

c) Weighted means calculated using Isoplot v. 3.3 (Ludwig, 1991) – errors at 95% confidence level

d) *Rs* is radius of a sphere with the equivalent surface – area - to - volume ratio as cylindrical crystals [Meesters and Dunai, 2002]

Table 7: U-Th results. Location of samples is given on Table 5.

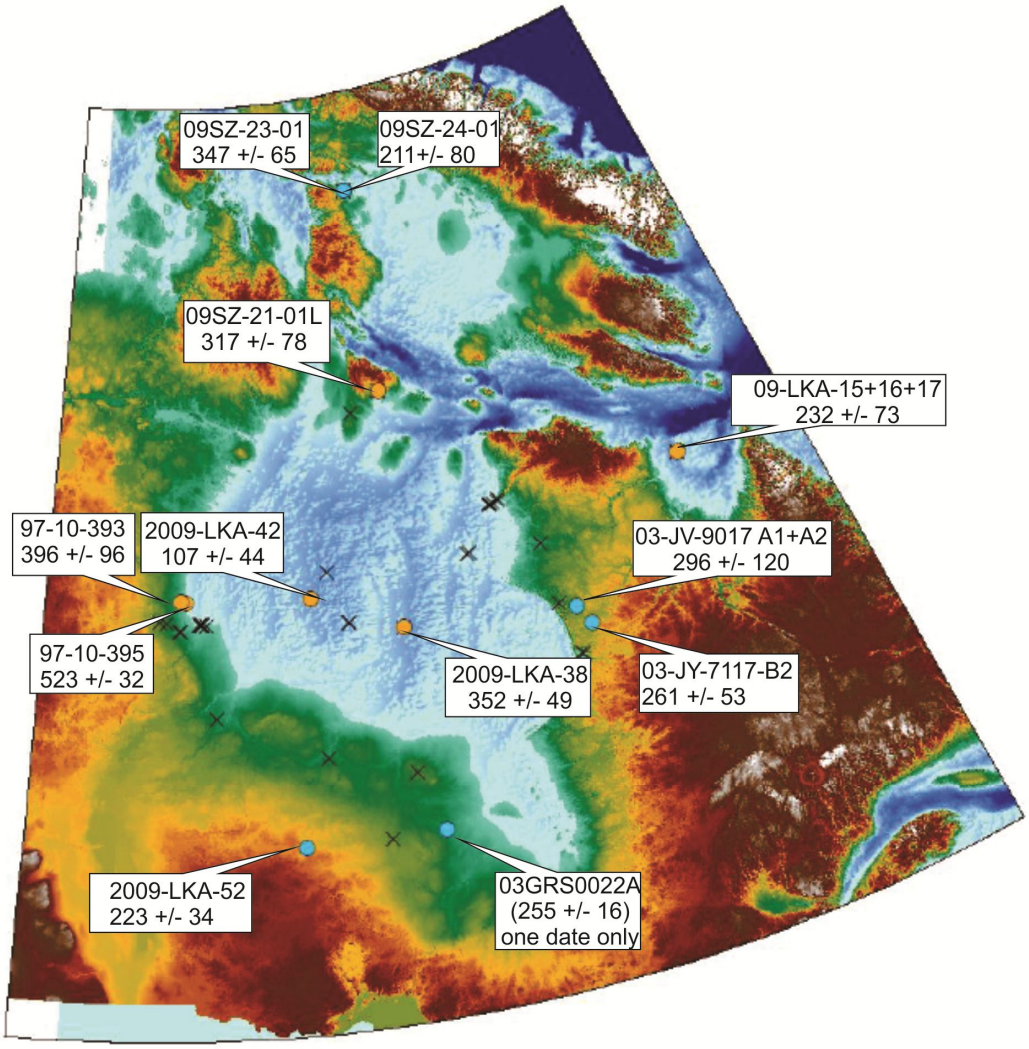

Figure 47: U-Th/He results. For each samples, the sample number, the pooled age (in green) and the central age are indicated. Orange dots for samples with AFT and U-Th/He results, blue dots for samples with U-Th/He results only and x for samples with no results.

Among the seven samples with both AFT and single grain (U-Th-Sm)/He ages, 3 show grossly the same ages with both methods, 2 show (U-Th-Sm)/He ages significantly younger than AFT ages and two show (U-Th-Sm)/He ages significantly older than their AFT age counterparts. The expected relationship of AFT>He age is thus not always respected. This may be due to a range of possible issues discussed in several studies (Lippolt et al, 1994, Fitzgerald et al, 2006, Shuster et al, 2006, Spiegel et al, 2009, Shuster & Farley, 2009, Flowers et al, 2009, Farley et al, 2011, Flowers & Kelley, 2011, Ault & Flowers, 2012, Brown et al, 2013). Most of the issues outlined in these studies will result in increased He accumulation resulting in ages, which are too old.

3.3.5 Conclusions regarding burial and thermal history of the Hudson Bay and Foxe basins

A detailed re-evaluation of historical maturation data and acquisition of new data from diverse thermal indicators result in a more precise understanding of burial and thermal history of the Hudson Bay and Foxe basins.

- No new specific evaluation of Conodont Alteration Index (CAI) was attempted; historical data suggest CAI of 1.5 (indicative of oil window) in 2 offshore wells, in the Silurian section (Beluga O-23 well; 1810 m and downward) and in the Ordovician succession (Polar Bear C-11; 1362 m and downward). CAI values of 1.5 – 2 have been reported in the Ordovician interval in one Winisk well.
- A re-evaluation of historical and new T_{max} values from Rock Eval[6] analyses has been done using only samples with S2 > 0.35 mg HC/g rock. The Ordovician successions of the four wells with enough data for statistical treatment are all interpreted to have entered the oil window. Using the oil window threshold of 435°C for Type II organic matter or 430°C for Type II-S organic matter, it is suggested that: i) for the Beluga O-23 well, the threshold is either at 1900 m (Silurian-Ordovician contact) or at 1600 m (upper part of Lower Silurian Ekwan River Formation), ii) for the Polar Bear C-11 well, the threshold is either at 1400 m (base of the Upper Ordovician Red Head Formation) or at 1220 m (middle part of the Lower Silurian Severn River Formation), iii) for the Narwhal South O-58 well, the threshold is either at 1220 m (Upper Ordovician Churchill River Group) or at 1040 m (upper part of the Upper Ordovician Red Head Rapids Formation) and iv) for the Comeault #1 well, the threshold is either at 490 m (Upper Ordovician Churchill River Group) or at 410 m (Upper Ordovician Red Head Rapids Formation).
- Production index (PI) values of samples with S2 > 0.35 mg HC/g rock for the same four wells suggests that few samples reached thermal maturity. All wells have at least one sample of the Churchill River Group in the field of PI > 0.1 and Tmax > 435°, as with Tmax (above); assuming a Type II-S organic material (P1>0.1 and Tmax > 430°C) significantly increases the number of samples considered to be thermally mature - for all four wells the oil window would extend below the Lower Silurian Severn River Formation. The well that has the most PI values indicative of thermal maturity is Polar Bear C-11 with samples of the Silurian Severn River Formation and Ordovician Red Head Rapids Formation and Churchill River Group. For all four wells, a significant number of Silurian and Ordovician values have PI well over 0.1 with T_{max} below 430°C or 435°C. This is commonly interpreted to result from elevated S1 values from volatiles in the sample with respect to the amount of residual organic matter expressed by the S2 value; this likely indicates some hydrocarbon charge in sedimentary units. Conversely, a significant number of PI values for the Bad Cache Rapids Formation are characterized by the inverse

relationship with PI values lower than 0.1 at T_{max} over 435°C; this could suggest hydrocarbon expulsion.

- Limited organic matter reflectance data ($Ro_{vit\text{-}equiv}$) were gathered for the first time from three offshore wells in Hudson Bay. From this dataset, Bertrand and Malo (2012) concluded that the oil window in the Beluga O-23 well is at the Devonian-Silurian contact, the Narwhal South O-58 enters the oil window in the Lower Silurian Severn River Formation and the data from the Polar Bear C-11 are inconclusive. A re-evaluation of the $Ro_{vit\text{-}equiv}$ values with correlative T_{max} from Rock Eval results with S2>0.35, led to a significant displacement of the oil window threshold; for the Beluga O-23 well, it is placed in the Upper Ordovician Red Head Rapids Formation (2000 m) and in the Lower Devonian Stooping River Formation for Type II and II-S, respectively; for the Polar Bear C-11, the Type II and II-S oil window threshold are respectively in the Lower Silurian Severn River (1100 m) and Lower Devonian Stooping (850 m) formations; the data for Narwhal South O-58 are inconclusive as significant discrepancies are noted with organic matter reflectance yielding significantly higher thermal results. From Dow's method, significant erosion of close to 2400 m is proposed for the Beluga O-23 well.
- $R_{ovit\text{-}equiv}$ values for the INCO Winisk wells in Northern Ontario indicate that the Boas River Formation is in the oil window.
- Values from the onshore wells (Comeault #1 and INCO Winisk) suggest that these onshore localities have been significantly buried in Paleozoic time.
- $Ro_{vit\text{-}equiv}$ data were also measured from six oil shale samples from Southampton Island, the results indicate that these shales are late immature to very early mature.
- All Apatite Fission Track (AFT) ages are younger than the age of the host rocks indicating that samples experienced significant annealing and were subjected to temperature > 60°C. The track length distribution suggests slow cooling.
- AFT pooled ages range from 230.3 ± 13.7 to 452.1 ± 24.5 Ma. The sample from the Akpatok well exhibits the youngest AFT, suggesting that the burial/exhumation history of this area may be different from the Hudson Bay Basin.

3.4 Hydrocarbon generation model

To evaluate the possible magnitude and timing of oil generation in the Hudson Bay Basin, a series of one-dimensional subsidence - thermal maturation models were derived from known or estimated basin stratigraphy, lithology, source rock thickness, organic matter type and burial depths. The models were generated using ZetaWare Genesis modelling software.

3.4.1 Source rocks parameters

The main hydrocarbon source rocks in the Hudson Bay Basin occur in the Upper

Ordovician succession (see above). Petrophysical logs and limited sample data indicate the Upper Ordovician succession in the offshore domain contains several, thin organic-rich beds (estimated cumulative thickness of 14 m in the Beluga O-23 well; Lavoie et al., 2013). Geochemical data (hydrogen-oxygen indices) indicate Upper Ordovician onshore and offshore source rocks contain a predominance of Type II organic matter (OM). Gas chromatogram data (Macauley et al., 1990; Zhang, 2011b; Lavoie et al., 2013) indicate Upper Ordovician strata contain Type II-S (sulphur-enriched) OM. The presence of Type II-S source rocks may be significant in that this type of OM will generate oil at lower maturation levels than Type II or Type I OM. Given the limited information on distribution of organic matter types, the hydrocarbon generation models incorporate possible Type II or Type IIS organic matter.

3.4.2 Subsidence and basin history parameters

The stratigraphy and lithology models were derived from the Beluga O-23 well (Fig. 48), the deepest well drilled in the basin and the one with the best biostratigraphic control. Two burial scenarios have been considered. In model 1, the eroded succession is thinner (1500 m; 4900 ft), the erosion estimate is based on Rock Eval data (Dietrich et al, 2009). In model 2, the thickness of the eroded succession is 2400 m (7900 ft) in agreement with the estimate derived from organic matter reflectance and Rock Eval analysis using the Dow's method (see above). These two models represents approximate minimum and maximum amounts of missing sections based on available maturation data. The age of the missing section(s) is not well constrained, but was assumed to be Late Devonian and a constant rate of post-Devonian erosion was assumed (Fig. 48). For modeling (models 1 and 2), both Type IIS and Type II organic matter have been considered.

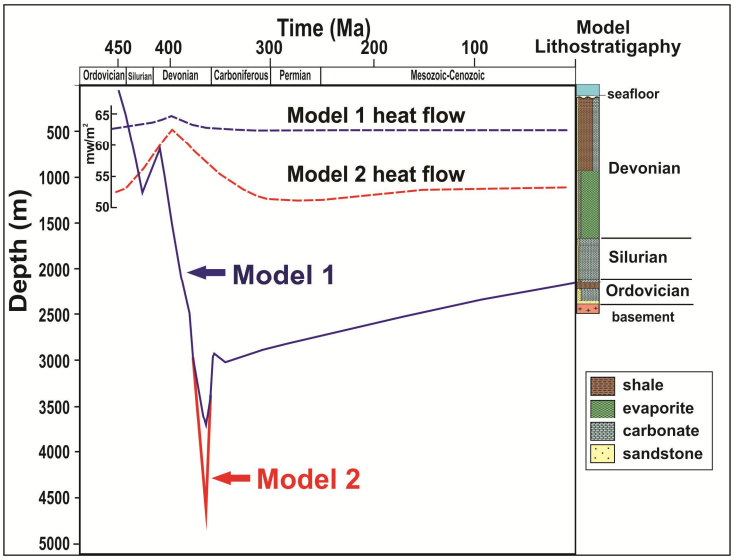

Figure 48. Subsidence models for the offshore Hudson Bay Basin, based on lithostratigraphy of the Beluga 0-23 well. Models 1 and 2 include interpreted 1500 m and 2400 m of post-Devonian uplift/erosion, respectively. The timing of maximum burial is not known but was assumed to be latest Devonian. Subsidence curves depict the top of the Upper Ordovician interval. Heat flow profiles are derived from rift models constrained by maturity in the Beluga well.

An important model parameter is the measured (present-day) maturation values. Two maturation (Ro equivalent) values from the Beluga O-23 well were used as model inputs; 0.45 % Ro at the top of Devonian section (basin surface) and 0.65 % Ro at the top of the Lower Silurian Severn River Formation. A good fit between the observed and calculated Ro values is reached for model thermal gradients of 18 to 23° C/km. Based on the recognition of extensional tectonics in the early phases of basin evolution, a rift model was used to derive heat flow history (Fig. 48).

3.4.3 Model results

The models outline the oil generation potential for the most deeply buried parts of the Hudson Platform, as currently known. In the models, Silurian and Ordovician strata are within the oil window (Fig. 49), with the maturation of Ordovician source rocks varying from 0.76% to 0.80 % Ro in agreement with measured Ro values. The models indicate the source rocks entered the oil window during the late sag phase of basin subsidence (Fig. 49), providing a good timing relationship for potential charging of most structures/traps in the basin. The hydrocarbon generation models indicate there is very low oil expulsion (11- 17 mg/g-TOC, 16-18 % transformation) for Type II source rocks in the Model 1 scenario, and modest oil expulsion (48-56 mg/g-TOC, 23-25 % transformation) for Type II source rocks in the Model 2 scenario (Fig. 50). In contrast, there is good oil expulsion (130-142 mg/g-TOC, 38-40 % transformation) for Type IIS source rocks in the Model 1 scenario, and very good oil expulsion (180-190 mg/g-TOC, 48-50 % transformation) for Type IIS source rocks in the Model 2 scenario. The models also indicate that most of the oil expulsion occurred in the Late Devonian to Early Carboniferous.

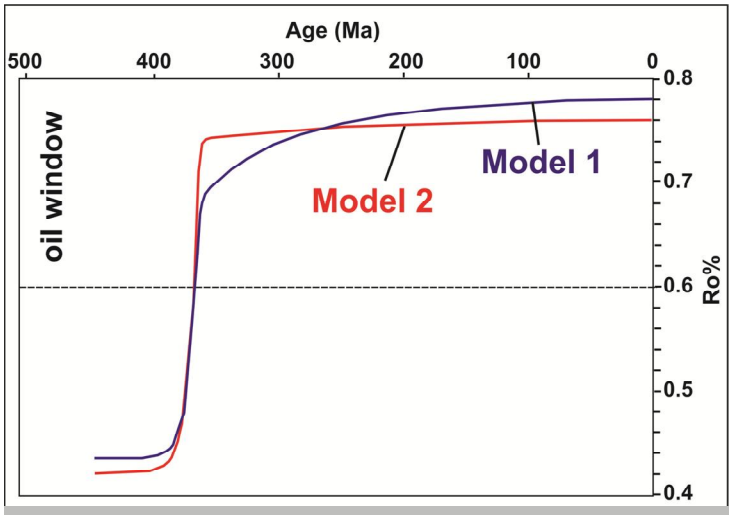

Figure 49. Model derived maturation profiles (top of source-rock interval) for Model 1 (1500 m erosion) and Model 2 (2400 m erosion). Upper Ordovician source rocks entered the oil window in the Late Devonian in both model scenarios. The Model 2 (deeper burial) scenario has increased maturation levels in the Late Devonian-Carboniferous, resulting in higher oil expulsion volumes than in Model 1 (Fig. 50).

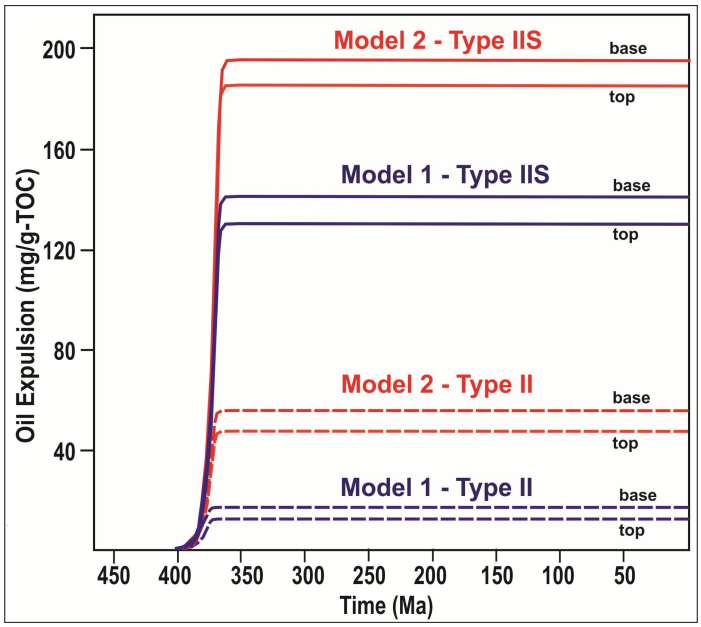

Figure 50. Calculated oil expulsion (top and base of Ordovician source rock interval) for Type II and IIS source rocks in subsidence models 1 and 2 (see text for discussion)

The best oil generation scenarios currently interpreted in the Hudson Platform are associated with the presence of Type IIS source rocks. Other optimistic oil generation scenarios may be associated with the presence of deeper subbasins (not mapped with existing seismic data) and increased paleo-temperatures due to hydrothermal fluid flow in/near fault zones. The known occurrences of fault sags and hydrothermal dolomite in the Hudson Platform indicate the latter scenario is likely, but the spatial and temporal links between hydrothermal fluid flow and hydrocarbon generation are not well constrained.

3.5 Reservoirs and migration

The onshore Hudson Platform has very few outcrops and hydrocarbon seeps are unknown. Bitumen has been reported in vugs in Upper Ordovician reefs (Procter et al., 1984). Live oil has recently been reported in the Severn River Formation in the Kaskattama Prov. #1 well and dead oil in the same formation in the Comeault #1 well (Nicolas and Lavoie, 2012). No commercial oil or gas reservoirs have been identified in the onshore and offshore wells drilled in the Hudson Bay and Foxe basins. However, evidence for the presence of hydrocarbons has been reported in all offshore wells. In Walrus A-71, gas shows were reported from the Devonian Kwataboahegan Formation carbonates with presence of bitumen-impregnated dolomite in a cored interval. In Narwhal South O-58, shows of methane were reported in carbonates of the Silurian Kenogami and Attawapiskat formations as well as in the Ordovician Churchill River

Group. In the Polar Bear C-11, minor gas shows were reported from the carbonates of the Silurian Severn River Formation. In the Beluga O-23 well, oil-stained limestone sidewall cores were observed in the Devonian Stooping River Formation. Finally, in the Netsiq N-01 well, gas shows are reported in the Devonian carbonates of the Devonian Williams Island, Kwataboahegan and Stooping River formations. It is important to remember that the 3 of the 5 offshore wells were drilled on the crest of fault-block highs, testing a limited number of potential plays/reservoirs (see later) with a thin section of Lower Devonian strata (Sanford and Grant, 1990; Sanford et al., 1993).

The Hudson Platform is dominated by diverse carbonate facies, including platform limestones, reefs and various types of dolomites; evaporites are locally abundant whereas siliciclastics are dominated by fine-grained lithologies with a relatively thin interval of coarse-grained sandstone above the basal unconformity with the Precambrian. The Hudson Bay and Foxe basins sedimentary successions share strong similarities with those of the Michigan and Williston basins, where carbonates are significant hydrocarbon reservoirs. Some potential reservoir units, primarily in the Ordovician-Silurian successions, are documented from detailed outcrop description and data, and supplemented by seismic and well petrophysical analysis. On the other hand, potential Devonian reservoirs are primarily identified on seismic and petrophysical data. This is a brief summary of potential reservoirs in the succession, more details are provided in the following sections:

- The carbonates of the Upper Ordovician succession (Red Head River Formation, Bad Cache Rapids and Churchill River groups) locally share characteristics with Upper Ordovician hydrothermal dolomite reservoirs in the Michigan Basin.
- The Red Head Rapids Formation contains large reefal structures of microbial-algal origin with large vugs filled with bitumen.
- The Lower Silurian succession is characterized by bioherms and reefs, with significant metazoan buildups in the Attawapiskat Formation which is correlative to productive reefs of the Guelph Formation of Southern Ontario
- The Middle Devonian platform carbonates with reefs of the Kwataboahegan and Williams Island formations also form potential reservoirs.

This section presents field, petrographic, geochemical and geophysical (magnetotelluric) data to document potential Upper Ordovician and Lower Silurian carbonate reservoirs. This will be followed by a summary of a detailed core and petrophysical analyses of onshore and offshore wells (Hu and Dietrich, 2012). The seismic expression of most of these reservoirs is presented in the Conventional Hydrocarbon Plays section.

3.5.1 Upper Ordovician hydrothermal dolomites (HTD)

Fault-controlled dolostone bodies are reservoirs for significant oil and gas deposits in North America (Davies and Smith, 2006). The first technical description of this type of reservoir is found in Hurley and Budros (1990) from the Michigan basin in the USA. It was demonstrated that extensional to transtensional faulting was responsible for brecciation and dissolution of

carbonate units resulting in local collapse of the affected areas and formation of U-shaped synform features visible on the seismic for which the term “sag” was introduced. Within these sags, highly porous dolostone zones were irregularly distributed in the limestone host. Detailed petrographic and geochemical studies resulted in the proposition that high-temperature brines were responsible for limestone dissolution and replacement by dolomite, with local massive to imperfect cementation by saddle dolomite (Searl, 1989). The distribution of dolostone zones and intensity of cementation were linked to active upward circulation of hot brines along fault planes and lateral migration in porous limestone intervals leading to the development of dolostone reservoirs (Davies and Smith, 2006).

Field and core occurrence of HTD

Fault-controlled porous dolostone and dolostone breccia interpreted to be related to circulation of hydrothermal fluids have been identified at two localities along the northern shore of Southampton Island (Lavoie et al., 2011). The dolostone occurs in the Upper Ordovician Red Head Rapids Formation and consists of a 10 – 15 m thick massive dolostone breccia (Fig. 51) with dolostone and limestone clasts. The highly brecciated zones irregularly alternate with meter-scale areas where the well-bedded facies is preserved. Carbonate fragments can make up to 90% of the breccia and the clasts range from 1 cm to 20 cm in diameter. Fragments are highly angular, unsorted and have a jigsaw-puzzle fabric that suggest little displacement and hydraulic fracturing; this type of breccia would be described as crackle and mosaic types of Morrow (1982). The breccia is associated with fractures and faults.

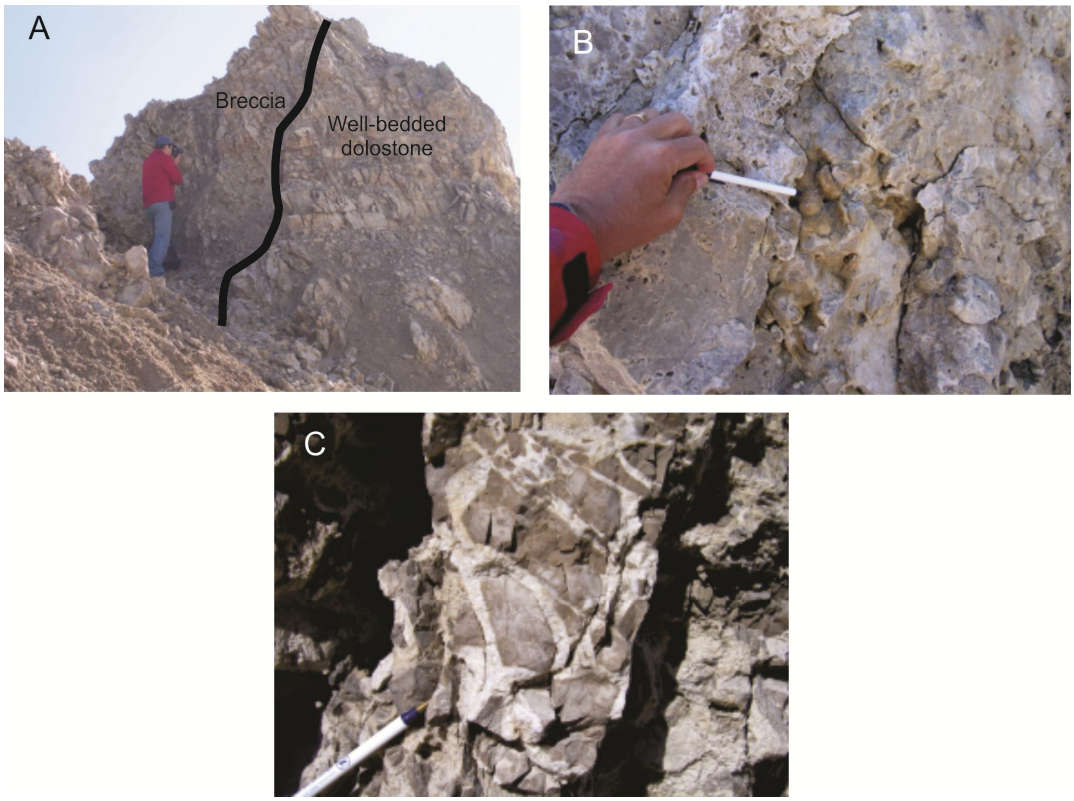

Figure 51: Field photographs of dolomite breccia near Cape Donovan, Southampton Island.

Dolomite cement imperfectly fills the pore space between carbonate clasts resulting in a highly irregular distribution of pore space in the outcrop with values visually estimated to vary between 5 to 25% (Fig. 51). Open pore space can be fairly large, up to a few centimetres in diameter; although the effective connectivity between the pores is currently unknown. The abundance of cement is seemingly controlled by its location within the fracture zone with decreasing cement abundance moving away from the main fault; eventually, the breccia is essentially clast-supported with no visible cement.

In northeastern Manitoba, in close vicinity of the town of Churchill, a few shallow wells were drilled by the Manitoba Government. One well (M-04-03) was drilled to a depth of 102.8 m with the contact between the Precambrian metamorphic basement and the overlying Paleozoic succession at 99.6 m. The Ordovician succession is dominated by various dolomitic facies with dolomicrite as the dominant lithology with subordinate cryptomicrobial mats, bioclastic dolopackstone and dolowackestone and sulphate nodules (Lavoie et al., 2011). Over a 14 metre interval (53 m to 67 m), brecciated and porous dolomitic facies form up to 30 % of the core. Decimetric porous and locally brecciated intervals are irregularly found in the dolomicrite facies (Fig. 52). Dissolution porosity is present at some intervals and cm-wide open pore space can be significant, going up to 20 %. Locally, alteration (dolomitization and subordinate silicification) is controlled by vertical fractures.

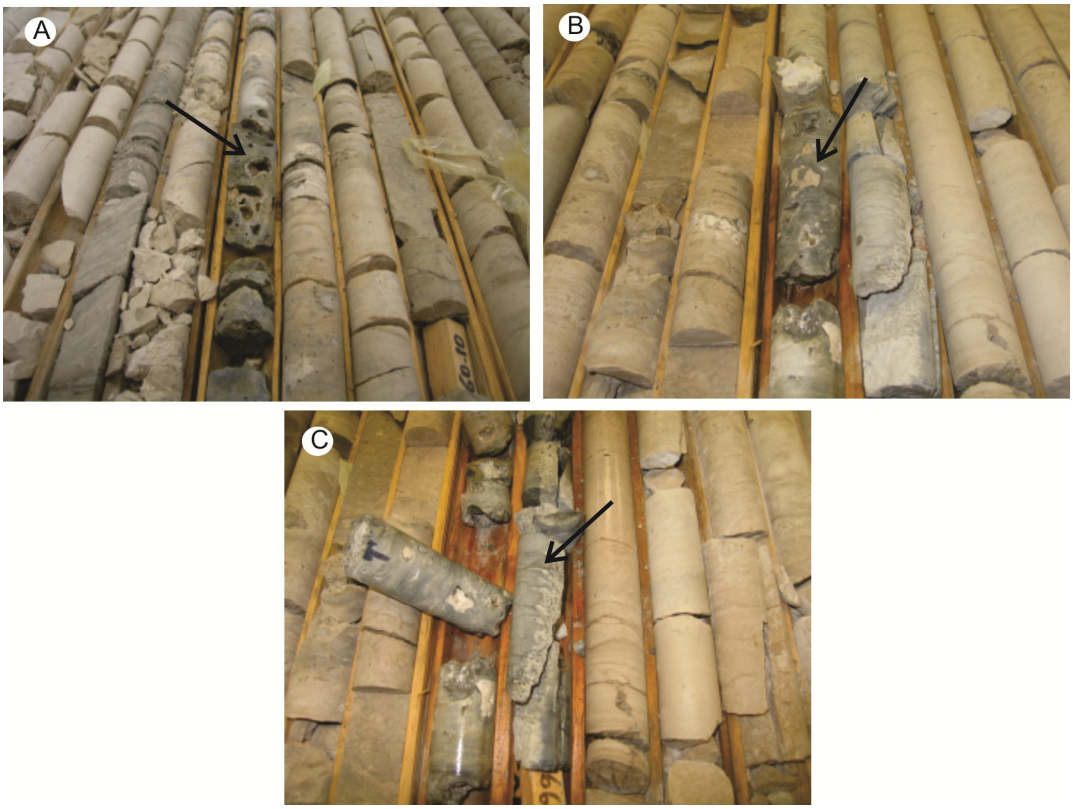

Figure 52: Photographs of cores from the M-04-03 well in Manitoba showing dolomite breccia with significant porosity.

Oxygen, Carbon and Magnesium stable isotopes

$\delta^{18}O$ and $\delta^{13}C$ values are routinely acquired to provide preliminary ideas on the origin of the dolomite phases. The GSC has recently pioneered the development of $\delta^{26}Mg$ and $\delta^{25}Mg$ values in order to provide ideas about the nature of the dolomitizing fluids and more importantly, the source of Mg^{2+} for dolomitization (Lavoie et al., submitted). 20 dolomite samples from Southampton Island, M-04-03 and M-05-03 wells in Manitoba and Rowley well in the Foxe Basin have been analyzed for their $\delta^{18}O$ and $\delta^{13}C$ values (Table 8 and Fig 53), and 3 dolomite samples from Southampton have been analyzed for their $\delta^{26}Mg$ and $\delta^{25}Mg$ values (Annex 3 and Fig 54). This dataset consists of 6 interpreted HTD samples from Southampton, 7 interpreted HTD samples from the M-04-03 well and 7 groundmass dolomicrite (non-HTD) from M-04-03 and M-05-03 wells in Manitoba and Rowley well.

Preliminary interpretation of stable isotope ratios

The oxygen and carbon stable isotope ratios of the saddle dolomite cements and the fabric-retentive groundmass dolomites define two very distinct $\delta^{18}O$ fields (Fig. 53). The saddle dolomites are characterized by very negative ratios whereas the groundmass dolomite is significantly less negative. However, both types of dolomites have $\delta^{13}C$ values that largely overlap and are characterized by a significant scatter of values.

It is hazardous to interpret dolomite origin only based on $\delta^{18}O$ and $\delta^{13}C$ values as a detailed analysis would necessitate an understanding of the temperature of precipitation and / or

of the isotopic composition of the diagenetic fluid. This is commonly done through microthermometric analyses of fluid inclusions, a type of study which is not yet available for the Hudson Platform dolostone. The $\delta^{18}O$ values of the saddle dolomites are more widespread than those of the groundmass dolomite, however, they are significantly more negative than the latter and are in the general range of $\delta^{18}O$ values for saddle dolomite cements in the Upper Ordovician successions ("Trenton-Black River") in southern Quebec (Lavoie and Chi, 2010) and New York (Smith, 2006).

Locality	**Sample ID**	**Nature**	**$\delta^{18}O$ (l)**	**$\delta^{13}C$ (l)**
Southampton	DL-1	Saddle dolomite	-13,3	-3,8
Southampton	DL-1	Saddle dolomite	-12,4	-3,4
Southampton	DL-2	Saddle dolomite	-13,9	-3,1
Southampton	DL-2	Saddle dolomite	-14,2	-3,4
Southampton	DL-15	Saddle dolomite	-13,7	-4,3
Southampton	DL-15	Saddle dolomite	-13,3	-4,6
M-04-03 core	DL-7	Saddle dolomite	-15	-2,6
M-04-03 core	DL-7	Saddle dolomite	-16,2	-4,1
M-04-03 core	DL-8	Saddle dolomite	-15,4	-1,6
M-04-03 core	DL-8	Saddle dolomite	-10,3	-1,4
M-04-03 core	DL-9	Saddle dolomite	-16	-5,4
M-04-03 core	DL-10	Saddle dolomite	-14,1	-4,6
M-04-03 core	DL-12	Saddle dolomite	-17,4	-8,3
M-04-03 core	DL-3	Groundmass dolomite	-7	1,4
M-04-03 core	DL-4	Groundmass dolomite	-6,3	-0,4
M-04-03 core	DL-5	Groundmass dolomite	-6,1	0
M-04-03 core	DL-6	Groundmass dolomite	-6	0,2
M-05-03 core	DL-11	Groundmass dolomite	-7,8	-1
Rowley core	DL-13	Groundmass dolomite	-4,7	-5,1
Rowley core	DL-14	Groundmass dolomite	-4,5	-2,9

Table 8: Oxygen and carbon stable isotopes for samples from the Cape Donovan area (Southampton Island) and M-04-03 core (Manitoba).

The $\delta^{13}C$ ratios for both type of dolomites are very scattered and range from near normal marine bicarbonate source to very negative; the latter values are commonly found associated with the presence of biogenic-derived HCO_3^- in the diagenetic fluid.

The $\delta^{26}Mg$ and $\delta^{25}Mg$ values for the Red Head Rapids Formation saddle dolomites are similar to those of coeval Upper Ordovician saddle dolomites from southern Quebec. However, as stated above, we do not have fluid inclusion microthermometry to evaluate if temperature of precipitation is more or less similar to that of southern Quebec HTD. As proposed by Lavoie et al. (submitted), the $\delta^{26}Mg$ and $\delta^{25}Mg$ values are controlled primarily by the Mg isotope composition of the hydrothermal fluids which is largely controlled by the lithological nature of the basement from which the large volume of Mg^{2+} needed for dolomitization is derived.

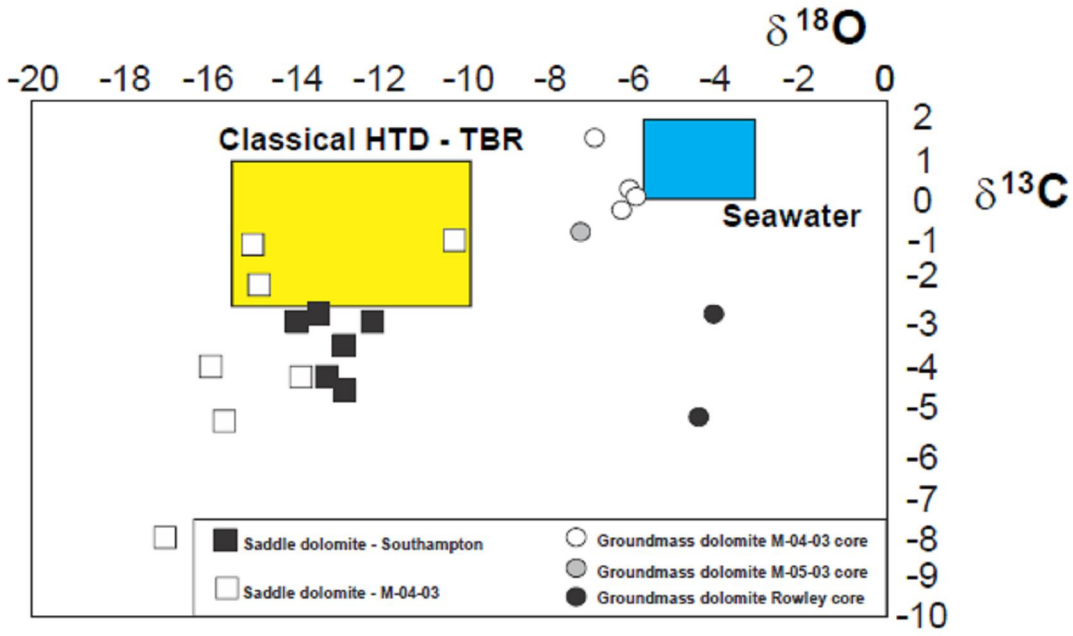

Figure 53: $\delta^{18}O$ versus $\delta^{13}C$ diagram of dolomite samples. The blue (seawater) and yellow (classical hydrothermal dolomite in the Trenton – Black River Group) are from Shields et al. (2003) and Smith (2006), respectively

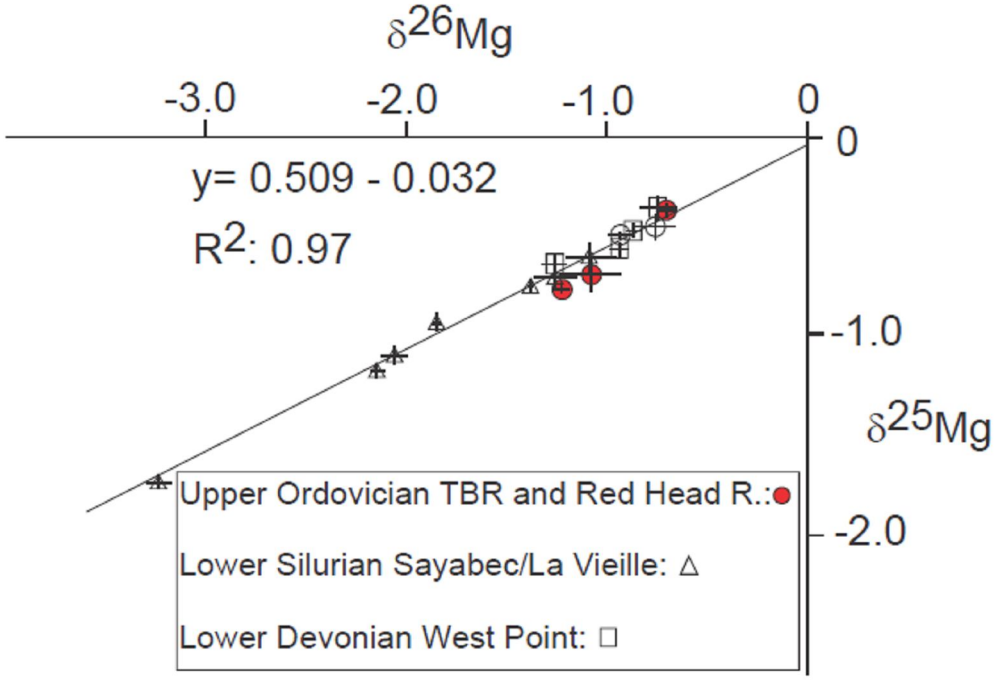

Figure 54: $\delta^{26}Mg$ versus $\delta^{25}Mg$ diagram for dolomite from various localities: Red Head Rapid Formation from Southampton Island, Trenton-Black River Group from southern Quebec, Sayabec/La Vieille and West Point formations from Gaspé Peninsula.

Recognition of HTD in the subsurface with magnetotelluric data

The magnetotelluric (MT) method provides information on the electrical conductivity of the subsurface through the measurement of the natural time-varying electric and magnetic fields at the surface. Due to the dependence of the depth of investigation of the fields on their frequency, an estimate of conductivity variation with depth can be attained. The technique was tested for identification of potential porous rock units at shallow depth; the test was conducted in the area of Churchill (northeastern Manitoba) where Lavoie et al. (2011) have identified the presence of porous hydrothermal dolomites in the Upper Ordovician carbonates (Roberts and Craven, 2012).

A total of 46 high frequency audio-magnetotelluric (AMT) sites were collected, 38 along one approximately N-S corridor perpendicular to the coastline and 8 in a more E-W direction closer to the town of Churchill. The MT data have been edited and processed to produce response functions at all sites, and the data have been input to a 3D inversion program. Preliminary 3D resistivity volumes have been generated along with an estimate of 3-D porosity variations (Fig. 55; Roberts and Craven, 2012).

The analysis of the data shows that the MT method can successfully image some of the more conductive zones within the Paleozoic strata in the Hudson Bay Platform (Roberts and Craven, 2012). Modeling has provided a consistent image of a shallow zone of enhanced conductivity that seems to be related to high porosity layers in the Paleozoic section, and also, the transition to Archean basement is reasonably well defined. In general, the section appears to thicken to the south. One –dimensional inversion (not shown) images a conductive feature in the deeper part of the sedimentary section. The depth to this feature is reasonably well resolved and is consistent across the profile suggesting that it is likely to be related to lithology. It could either be enhanced porosity within a unit or a conductive shale unit. At shallow (< 100 m) depths in the northern portion of the profile the structure is more complicated and correct geometries and accurate estimate of the resistivity can only be revealed through 3-D modelling. It is assumed from the limited physical rock property measurements (resistivity) available in the area that the dolomitized sedimentary rocks of the Ordovician Churchill River Group comprise the section at these depths. Calculation of bulk porosity values from the modeled conductivities indicated that values up to 25% are certainly possible within the sedimentary section. The more resistive rocks above the porous layer may be Silurian limestones from the Severn River Formation. The MT results have demonstrated the possibility that such porosity is regional and identified complex structure, possibly faults related to high porosities with main “feeders” splitting in complex frameworks at shallower depths (Craven and Roberts, 2012). The depth of the enhanced porosity is similar to what has been observed in the cores extracted from stratigraphic wells near the survey.

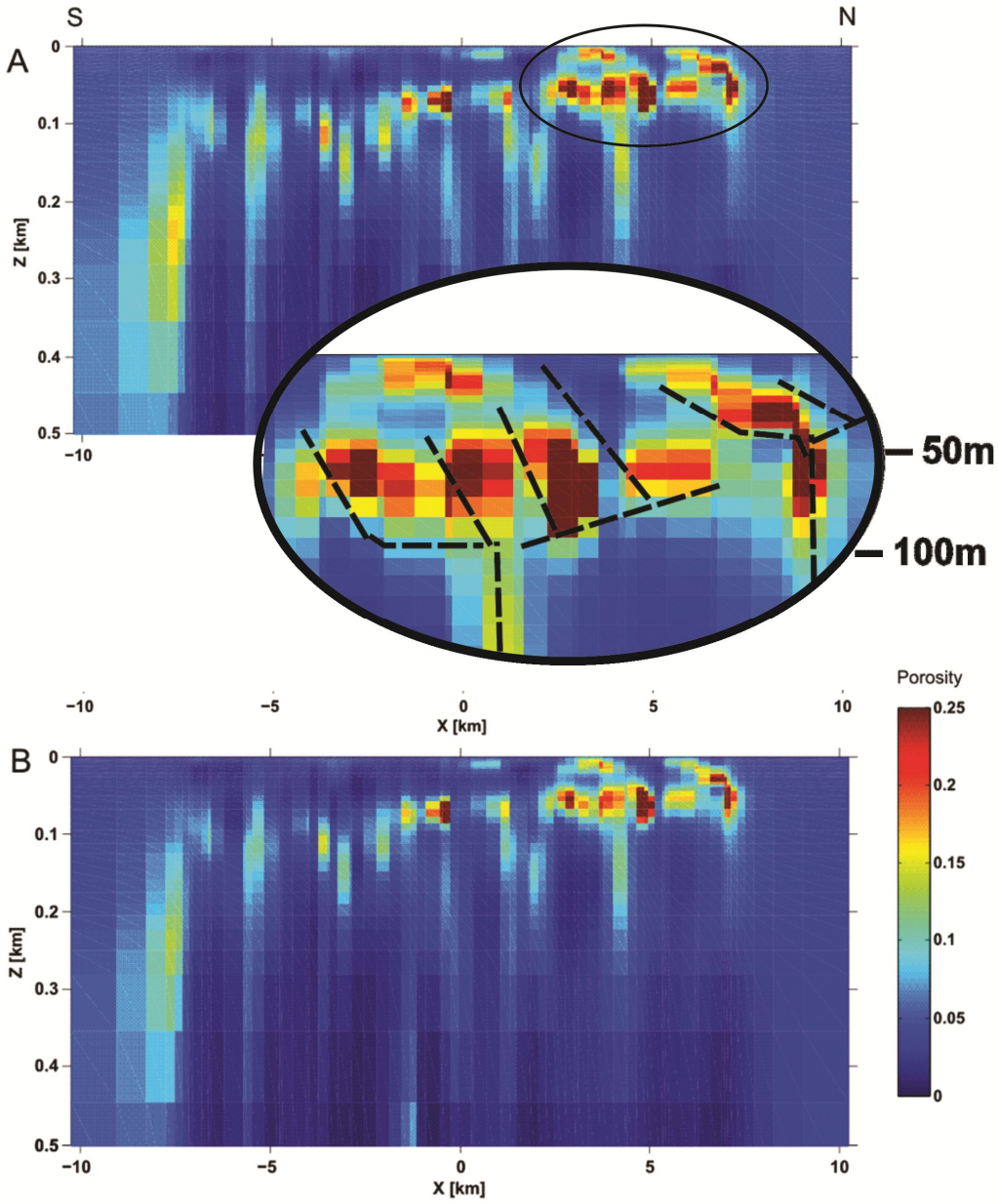

Figure 55: MT pseudo-section with conductivity values converted to porosity; A) for a brine solution conductivity (Cw) = 3.3 S-m, and B) Cw = 5.0 S-m. The shallow encircled area on A presents an interpretation with shallow faults splaying from a deeper feeder. Modified from Roberts and Craven (2011).

3.5.2 Upper Ordovician microbial-algal reefs – Red Head Rapids Formation

On Southampton Island, small and large reefal structures are developed in the Red Head Rapids Formation. These mound-shaped structures have a maximum exposed size of 450 m long by 250 m wide and 25 m high (Fig. 56) (Heywood and Sanford, 1976), with similar or larger sized structures identified on seismic profiles (see below). These mounds are flanked by

bioclastic dolopackstones and dolowackestones. The contact between the mound and the encasing beds is not well exposed, so the synoptic relief of these mounds on the seafloor is unknown. No detailed internal facies architecture study has been done on these structures. Preliminary field observations indicate that the structure is dominated by a thrombolite-like framework with patches of possible *Renalcis* visible at many places. The mounds are partly dolomitized although the origin of the dolomitization is unknown. These mounds are locally highly porous with porosity visually estimated to be up to 25%. The size of some pores is centimeter in scale although it is unknown if connectivity between the pores is good or not. The origin of the porosity is poorly constrained, even if the fine-grained nature of the matrix between the bioframework may suggest a secondary origin.

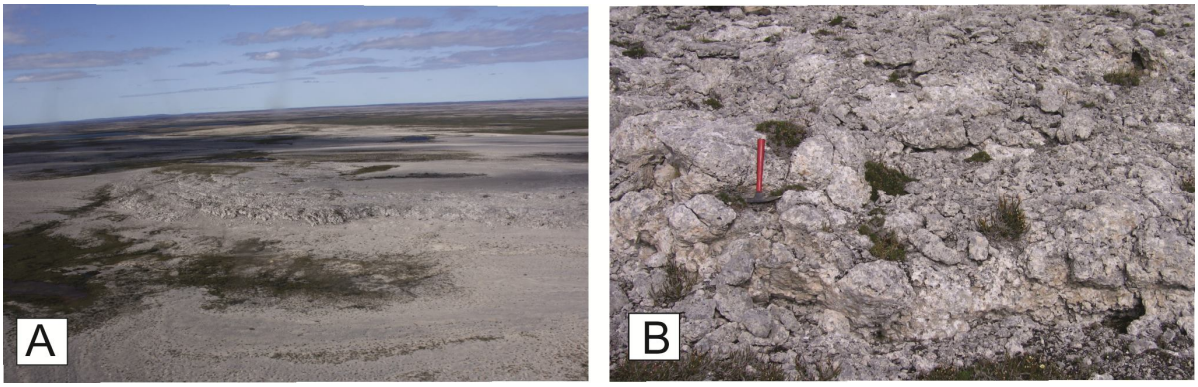

Figure 56: Helicopter (A) and outcrop (B) views of Upper Ordovician reef belonging to the Red Head Rapids Formation, Southampton Island.

On Southampton Island, these mounds occur near the top of the Red Head Formation (Zhang, 2008; 2010), as such, they are stratigraphically over the three oil shales intervals. Heywood and Sanford (1976) mentioned the presence of dead oil filling large vugs.

3.5.3 Lower Silurian metazoan reefs

Small to large bioherms are known in Lower Silurian rocks. Small stromatolite-coral bioherms are known in the Severn River Formation (Sanford and Norris, 1973), although the development of reefal structures becomes more significant in the overlying Ekwan River and Attawapiskat formations. The latter two units are exposed on Southampton Island (Heywood and Sanford, 1976) and in Northern Ontario (Suchy and Stearn, 1992; Armstrong, 2011). The Attawapiskat reefs are identified in drill holes in Manitoba (Ramdoyal, 2012). For many years, the reefs of the Attawapiskat Formation have been considered as the main hydrocarbon reservoir target for the Hudson Bay Basin. In the Hudson Bay offshore wells, the Ekwan River and Attawapiskat formations are commonly lumped together because of similar limestone facies composition (marine bioclastics limestones and bioherms) with the Attawapiskat being slightly

more dolomitic and dominated by bioconstructions. The fact that bioherms and biostromes are also present in the Ekwan River Formation makes the distinction fairly equivocal and these two units are considered as lateral equivalents (Sanford and Norris, 1973). In the Ekwan River Formation, the small coral-stromatoporoid bioherms and biostromes have been described on Southampton Island (Heywood and Sanford, 1976) where they consist of isolated metazoan bioherms surrounded by bioclastic limestones.

The Attawapiskat Formation was first defined on the basis of presence of bioherms (Attawapiskat Coral Reef; Savage and Van Tuyl, 1919). The formation consists of cyclic succession of locally dolomitized inter-reef sediments made up of various open marine to intertidal facies (bioclastics, oolitic, intraclastic peloidal wackestones to rudstones) associated with stromatoporoids and corals bioherms and biostromes (Suchy and Stearn, 1993; Ramdoyal, 2012). In well exposed field sections (Fig. 57), the Attawapiskat Formation was described as forming atoll-like metazoan buildups, up to 200 meters in diameters and with significant vertical relief (up to 10 m; Suchy and Stearn, 1993).

Figure 57: Photograph illustrating Attawapiskat mounds in northern Ontario.

The Attawapiskat Formation is locally very porous (up to 35%, Hamblin, 2008). However, detailed diagenetic studies aimed at identifying the origin of the porosity are few (Chow, 1986; Chow and Stearn, 1989). A recent detailed facies and diagenetic study of the Attawapiskat reefs in 3 northeastern Manitoba wells (Ramdoyal, 2012) has documented significant porosity (up to 55%) that consists of both primary (preserved depositional) and secondary (dolomitization and dissolution) phases (Fig. 58). Most of the lithofacies (inter-reef and bioherms) are porous in the Manitoba wells and log analysis of Penn No. 1 well (see further) has documented significant porosity and possible hydrocarbons in the Attawapiskat / Ekwan River formations. However, at other localities, the Attawapiskat Formation has been described as having little to no porosity, (Chow and Stearn, 1989) which suggests diverse burial-diagenetic scenarios.

Oil shows in the Attawapiskat Formation have been reported from some wells drilled in Manitoba and Ontario (Johnson, 1971). The Llandoverian Attawapiskat reefs have been correlated, facies-wise, to the slightly younger (Wenlockian) Guelph Formation in the Michigan

basin (Suchy and Stearn, 1993); reefs of the Guelph Formation are major hydrocarbon producers in the Michigan Basin.

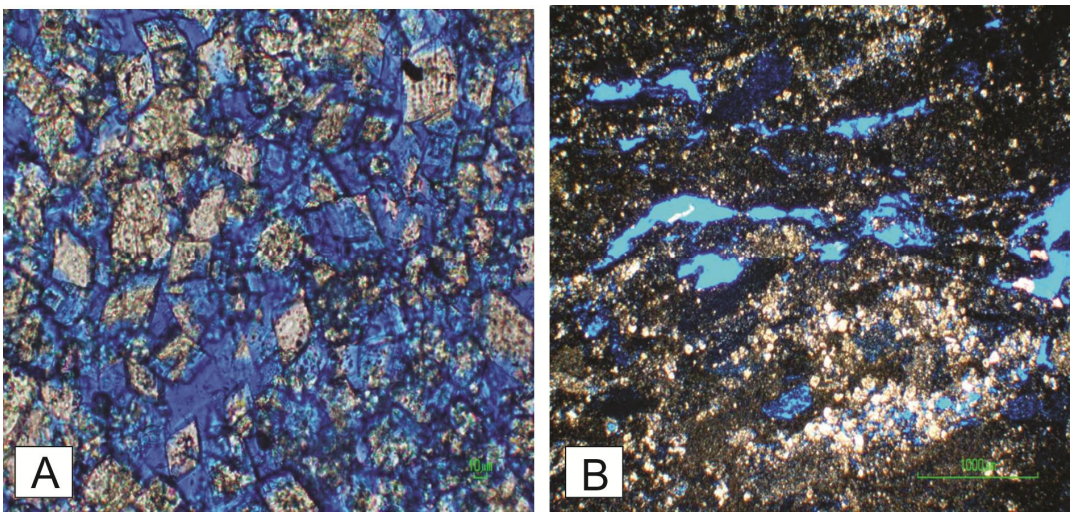

Figure 58. Thin sections showing secondary (A) and primary (B) porosity in the Attawapiskat Formation of Manitoba.

3.5.4 Late Early to Middle Devonian platform carbonates and reefs

The Lower to Middle Devonian succession does not outcrop in the onshore extension of the Hudson Bay Basin. The reservoir potential for the Devonian carbonates is primarily based on field observations in the Moose River Basin and on petrophysical core data and interpreted reef structures seen in seismic (see below),

The upper Lower Devonian (Emsian? to Givetian) Kwataboahegan Formation in the Moose River Basin has been described as a bituminous limestone forming massive and thick metazoan buildups (Telford, 1987). There is no detailed understanding of diagenetic evolution of the reefal units. The Kwataboahegan Formation has been encountered in most of the industry onshore and offshore wells.

The Middle Devonian (Givetian) Williams Island Formation is the youngest known carbonate formation in the Paleozoic succession of the Hudson Bay Platform. As seen in the Moose River Basin (Telford, 1987) and in the offshore wells, the formation consists of interbedded fine- and coarse-grained clastics, evaporites and porous and brecciated marine limestones and dolostones (Telford, 1987; Hu et al., 2011). The succession of the Williams Island Formation has similarities to the Winnipegosis Formation and Prairie Evaporites in the Williston Basin (Norris et al., 1982); locally high porosity reef facies are developed in the Winnipegosis Formation (Dietrich and Magnusson, 1988).

3.5.5 Reservoir evaluation from well logs

The hydrocarbon reservoir potential in the Hudson Bay Basin has been evaluated from petrophysical log analyses of five offshore wells (Walrus A-71, South Narwhal O-58, Polar Bear C-11, Beluga O-23 and Netsiq N-01; Hu and Dietrich, 2012) and one onshore well (Pen No.1, Ontario). The petrophysical analyses of wireline logs, integrated with core and thin section data, provide information on lithology, porosity, permeability and water saturation. The analyses indicate that many limestone, dolomite, sandstone, and conglomerate intervals within the succession have sufficient porosity and permeability to form good quality hydrocarbon reservoirs. The best reservoir characteristics occur in carbonates in the Devonian Williams Island and Kwataboahegan formations and Silurian Attawapiskat and Severn River formations. Formation pressure and permeability data indicate effective seals are present in the basin. Water saturation calculations from log data indicate that possible hydrocarbon zones occur in all wells and at many stratigraphic intervals. Well history records indicate hydrocarbon shows were encountered in some reservoir intervals.

Core data

Porosity and permeability analyses of 109 core samples were compiled from the offshore Walrus A-71, Narwhal O-58 and Beluga O-23 wells (Fig. 59) and 676 porosity measurements and 527 permeability (maximum) data have been acquired from the Pen No.1 well (Fig. 60).

For the offshore wells, most core samples are from the Devonian Williams Island, Kwataboahegan and Kenogami River formations and the Ordovician Red Head Rapids Formation. Most samples are from limestone or dolomite units, with a few samples from the thin basal sandstone interval. Most core samples from the Walrus A-71 well have porosity and permeability between 8 and 16% and 0.1 to 10 mD, respectively. The Narwhal O-58 core samples display a narrow range of porosity values (<4 to 8%) but a wide range of permeability values (<0.01 to >1000 mD). The high permeability values in the Narwhal well (1000+ mD) may be inaccurate or spurious measurements due to the poor quality of some core material. Porosity in the Beluga O-23 core samples varies from less than 4% to over 20%, with permeability values varying from less than 0.01 mD to 10 mD. Well samples show generally poor correlation between porosity and permeability. Statistical correlations of increasing permeability with increasing porosity occur in samples from the Devonian Williams Island and Murray Island formations and the Ordovician Red Head Rapids Formation. The Devonian carbonates of the Williams Island and Kwataboahegan formations have the best-paired porosity -permeability values (Fig. 61).

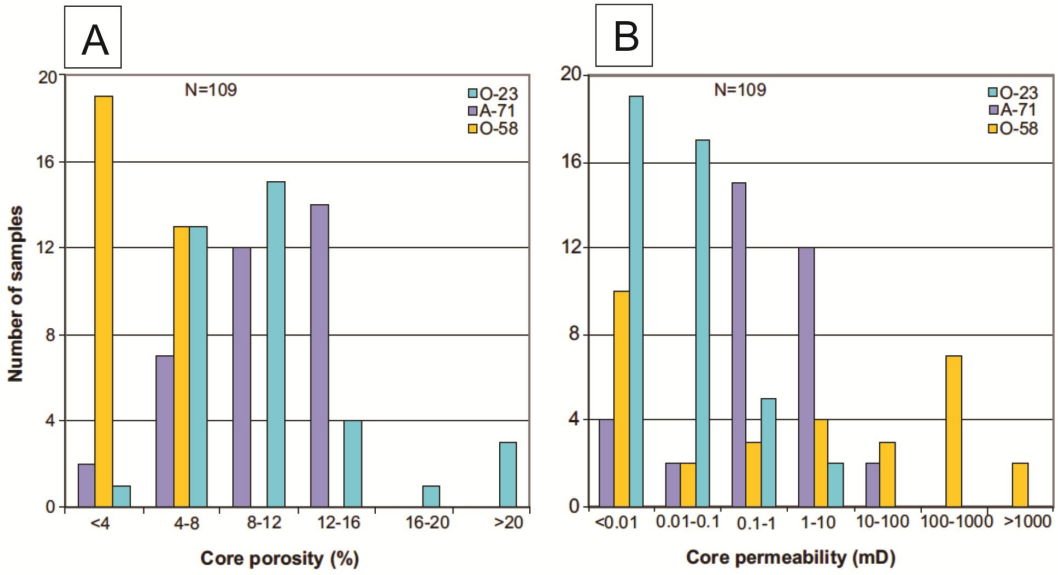

Figure 59: Porosity (A) and core maximum permeability (B) for the Beluga (O-23), Walrus (A-71) and Narwhal (O-58) wells

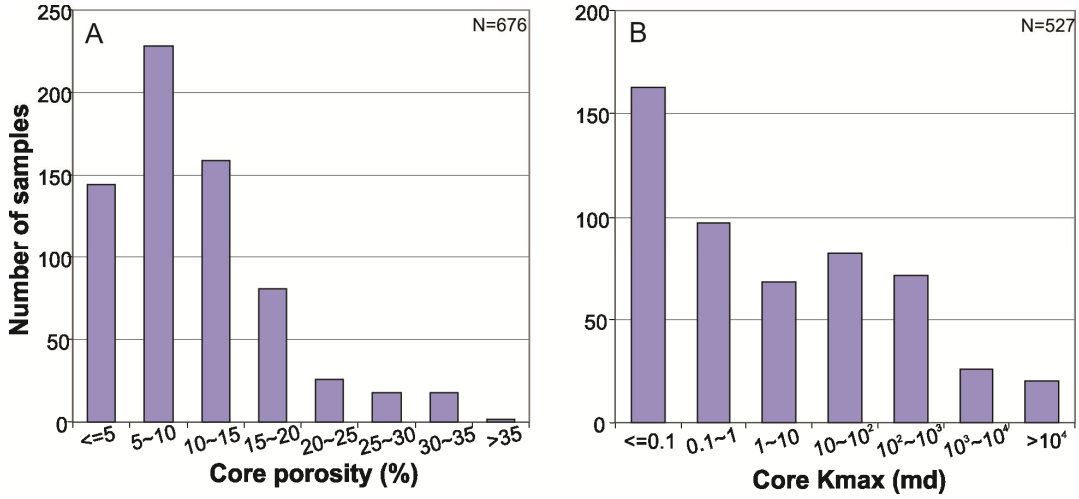

Figure 60: Porosity and core maximum permeability for Pen No. 1 well, Ontario.

For the Pen No. 1 well, all units except for the Bad Cache Rapids Formation have core analyses (Figs. 62 and 63). The Upper Ordovician to Devonian succession is dominated by carbonates; limestones are more abundant than dolostones. Core porosity distribution indicates that ~9% of the samples have porosity above 20% (Fig. 62 and 63). The core maximum permeability distribution shows that 49% of samples have low permeabilities (<0.1 to 10 mD). However, 9% of samples have permeabilities over 1000 mD. The Kenogami River Formation have porosity and permeability between < 5 and 35% and < 0.1 and 1000 mD, respectively; some very high permeability values (>10 000 mD) are reported. The Lower Silurian

Attawapiskat, Ekwan River and Severn River have porosity and permeability values between <5 and >35% and <0.1 and >10 000 mD; the reefal facies of the Attawapiskat and Ekwan River formations are more porous and permeable than the Severn River Formation. Finally the Ordovician Red Head Rapids Formation and Churchill Group have porosity and permeability between < 5 and 25% and <0.1 and 10 mD. The Attawapiskat and Ekwan River formations have the highest porosity and permeability values, whereas the Severn River and Red Head Rapids formations and the Churchill Group have the lowest values (Figs. 61 and 62). Various types of pores have been documented including interparticle, pin-point vugs, vugs and fractures; the highest permeabilities values are associated with the presence of vugs.

Petrophysical log analyses

Evaluations of log data in the six wells included new processing and interpretation of digital gamma ray (GR), gamma-ray spectroscopy (SGR), caliper (CAL), density (RHOB), sonic (DT), photoelectric index (PEF), spontaneous potential (SP), neutron (NEUT) or neutron porosity (PHIN) and resistivity wireline logs, utilizing commercial log-analysis software (Halliburton-GeoGraphix PRIZM™) (Hu and Dietrich, 2012). Porosity values were calculated from the sonic, density and neutron logs, with shale corrections applied for shaly sandstone intervals. In wells with core data, core and log calculated porosity and permeability values generally matched very well, providing a high level of confidence in the log-derived data. Water saturation values were calculated from deep induction log or deep laterolog (or shallow laterolog if deep resistivity log not available) using the Archie equation (Schlumberger, 1989). Water resistivity (Rw), a critical parameter for water saturation calculations, was derived from available water analyses (2 samples in each of the Polar Bear and Narwhal South wells). Due to the limited number of water resistivity measurements in the basin, the log calculations of water and hydrocarbon saturations are considered tentative interpretations. Permeability values in carbonate intervals were estimated from porosity data (Crain, 1986). Permeability values in sandstone intervals were calculated using the Timur equation (Schlumberger, 1989). The identification of possible hydrocarbon zones was based on porosity, permeability and water saturation data. With the absence of testing or production data in the Hudson Bay Basin, it is not possible to determine definitive reservoir parameters for delineating hydrocarbon pay zones. However, based on state of the art log analysis and empirical evidence from other basins, the selected cut-off values for this study (porosity above 4% or 6%, permeability above 1 mD, and water saturation below 55%) are considered reasonable values for identifying possible hydrocarbon zones in conventional reservoirs. The results of the log analyses for the five wells are illustrated in figures 64 to 68. Possible hydrocarbon zones (indicated in red in the right columns of figures) are based on the cut-off values cited above. The Walrus A-71, Beluga O-23 and Netsiq N-01 analyses include core measurements of porosity, permeability and water saturation compiled from well history reports. The porosity (PHI) curves depicted in the well figures represent filtered porosity measurements (4 point averages of 0.25 metre data points) and do not always depict maximum porosity values. Detailed analyses and descriptions can be found in Hu and Dietrich (2012).

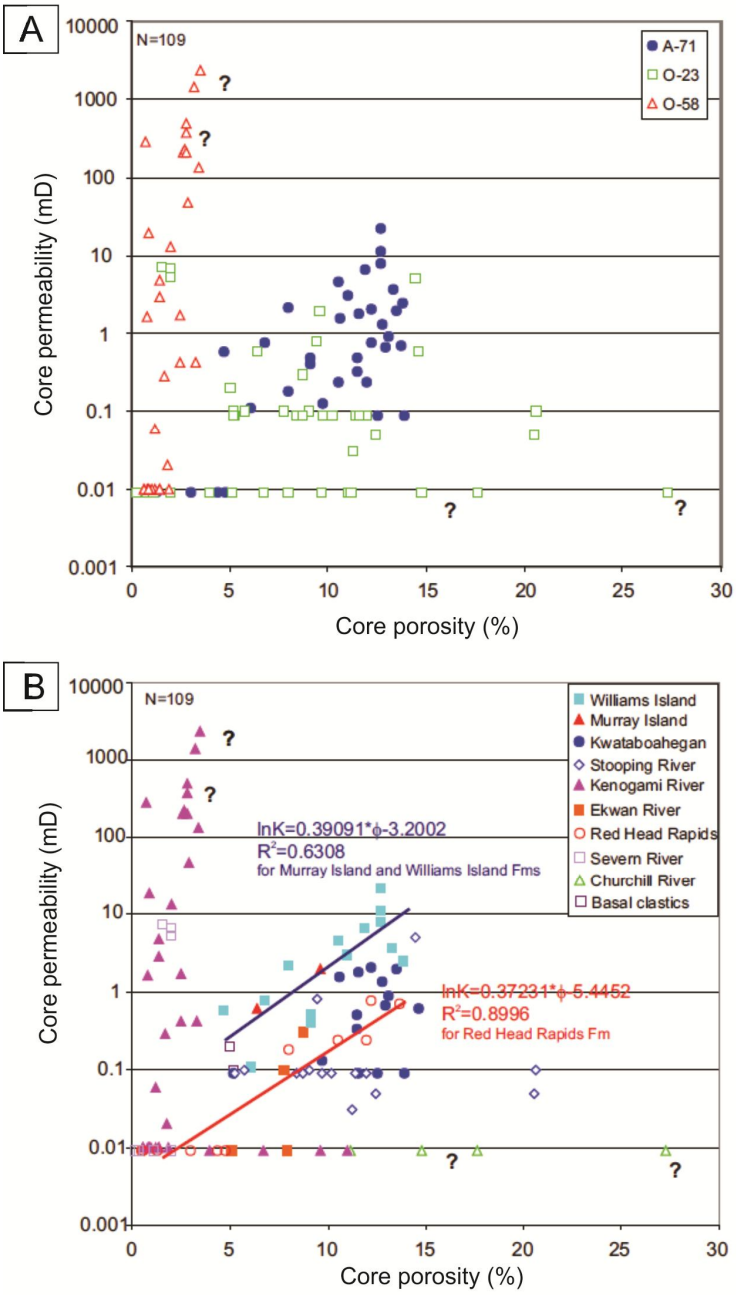

Figure 61: Core porosity versus core maximum permeability for three offshore wells (A) and for the various formations (B).

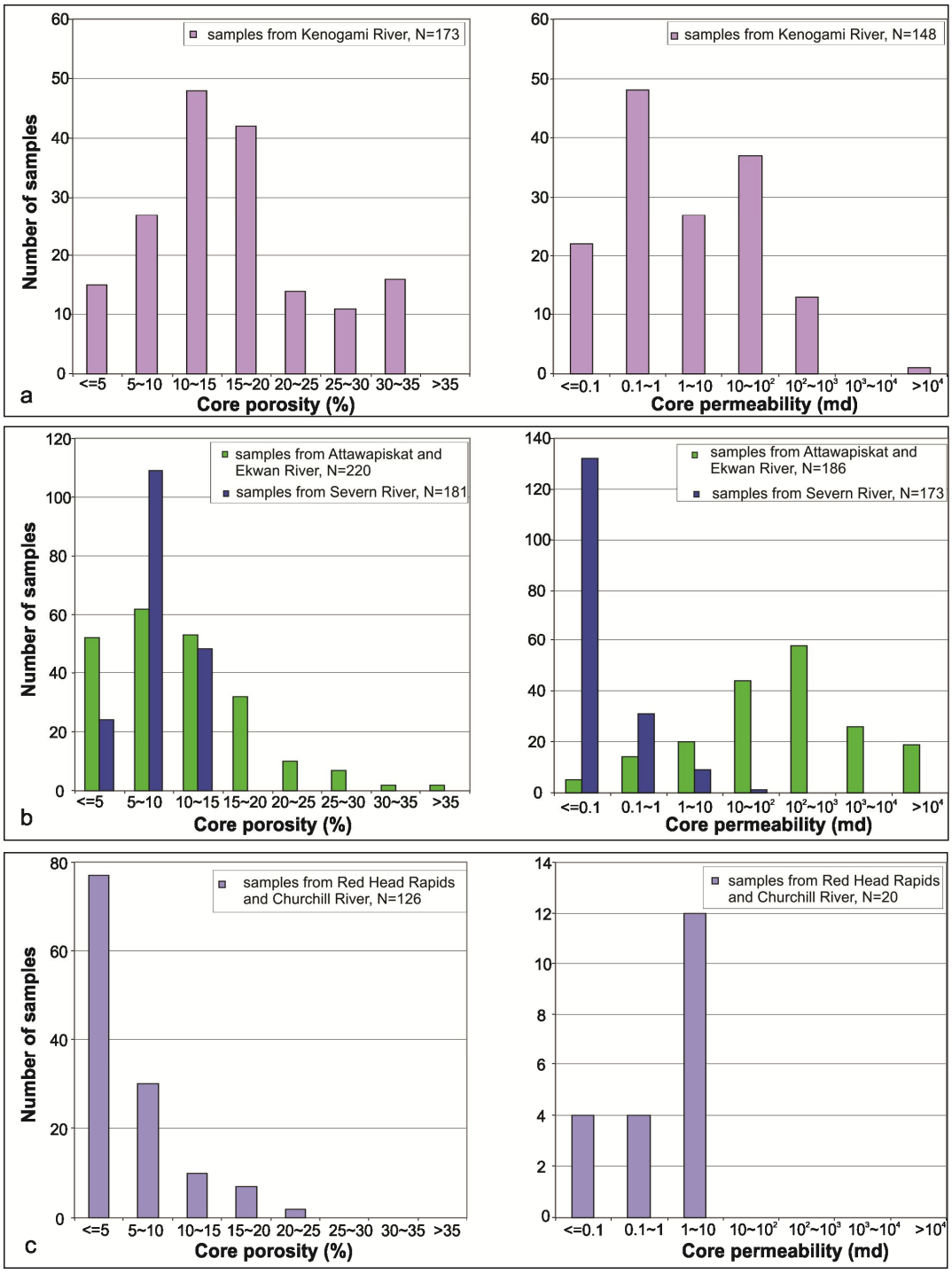

Figure 62: Porosity and maximum permeability for various formations, Pen No.1 well, Ontario.

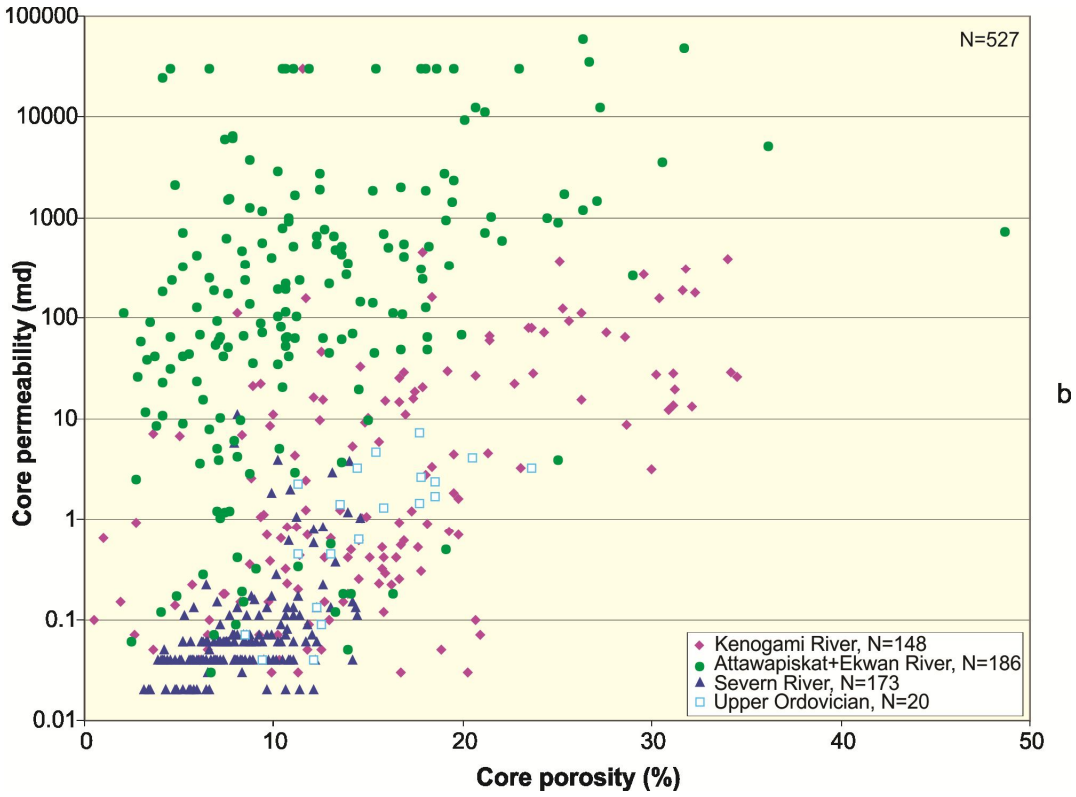

Figure 63: Core porosity versus Core permeability for the Pen No. 1 well.

The porosity-depth profile for the five Hudson Bay offshore wells provides information on reservoir characteristics and trends between different wells and stratigraphic units (Hu and Dietrich, 2012). An overall trend of decreasing porosity with depth is detected for all wells. The highest log porosity occurs in Devonian carbonates (including the Williams Island, Murray Island, Kwataboahegan and Stooping River formations), with porosities above 10%, and very high porosity values (≥ 20%) in carbonate intervals in the Beluga O-23 and Walrus A-71 wells. The maximum log-measured porosity is 24% in the Williams Island Formation in the Walrus A-71 well. Good porosity values (10 to 15%) occur in carbonates in the Silurian Severn River Formation, in the Netsiq N-01, Polar Bear C-11 and Narwhal South O-58 wells.

A

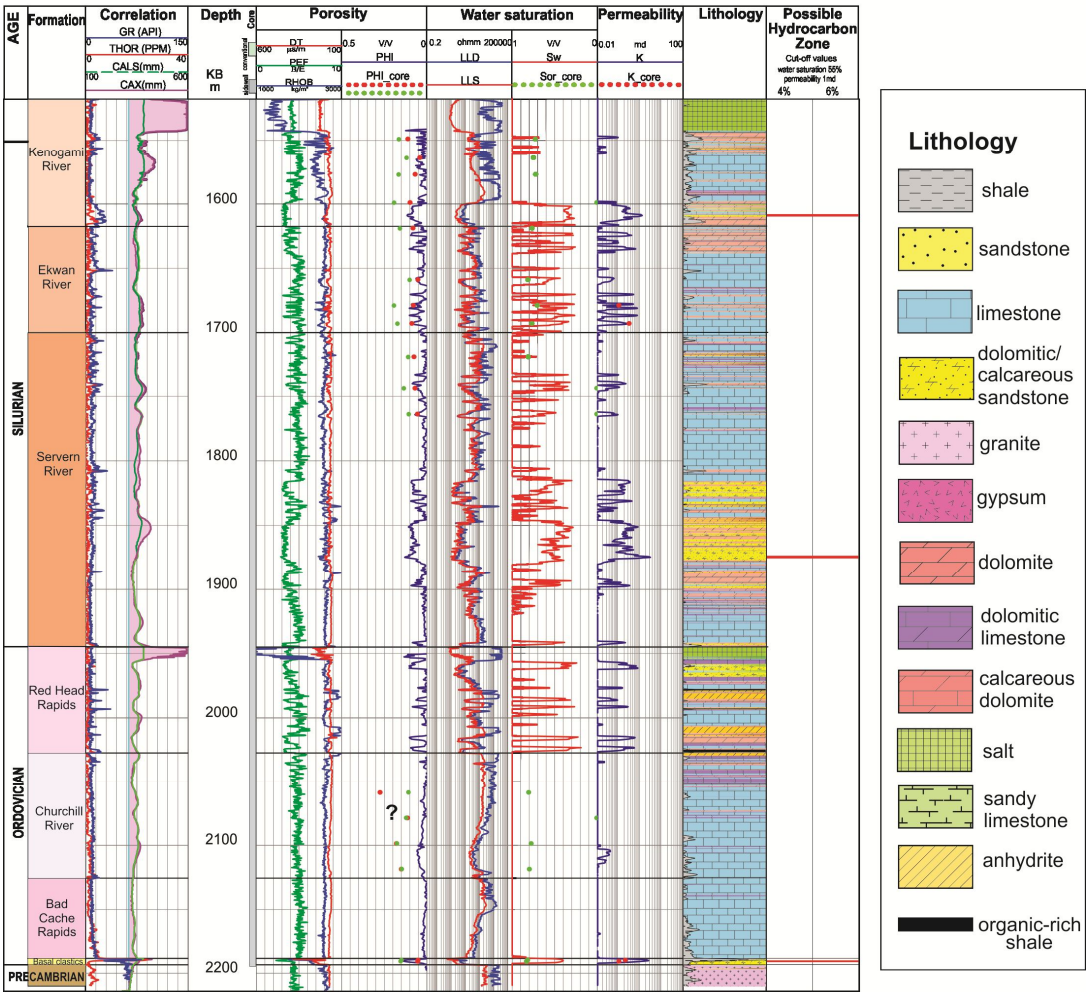
AGE
Formation
Correlation
GR (API)
THOR (PPM)
CALS(mm)
CAX(mm)
Depth
KB
m
Core
Porosity
DT
PHI
PEF
RHOB
PHI_core
Water saturation
LLD
Sw
LLS
Sor_core
Permeability
K
K_core
Lithology
Possible Hydrocarbon Zone
Cut-off values
water saturation 65%
permeability 1md
4%
6%
SILURIAN
ORDOVICIAN
PRECAMBRIAN
Kenogami River
Ekwan River
Servern River
Red Head Rapids
Churchill River
Bad Cache Rapids
Basal clastics
1600
1700
1800
1900
2000
2100
2200
?
Lithology
shale
sandstone
limestone
dolomitic/ calcareous sandstone
granite
gypsum
dolomite
dolomitic limestone
calcareous dolomite
salt
sandy limestone
anhydrite
organic-rich shale

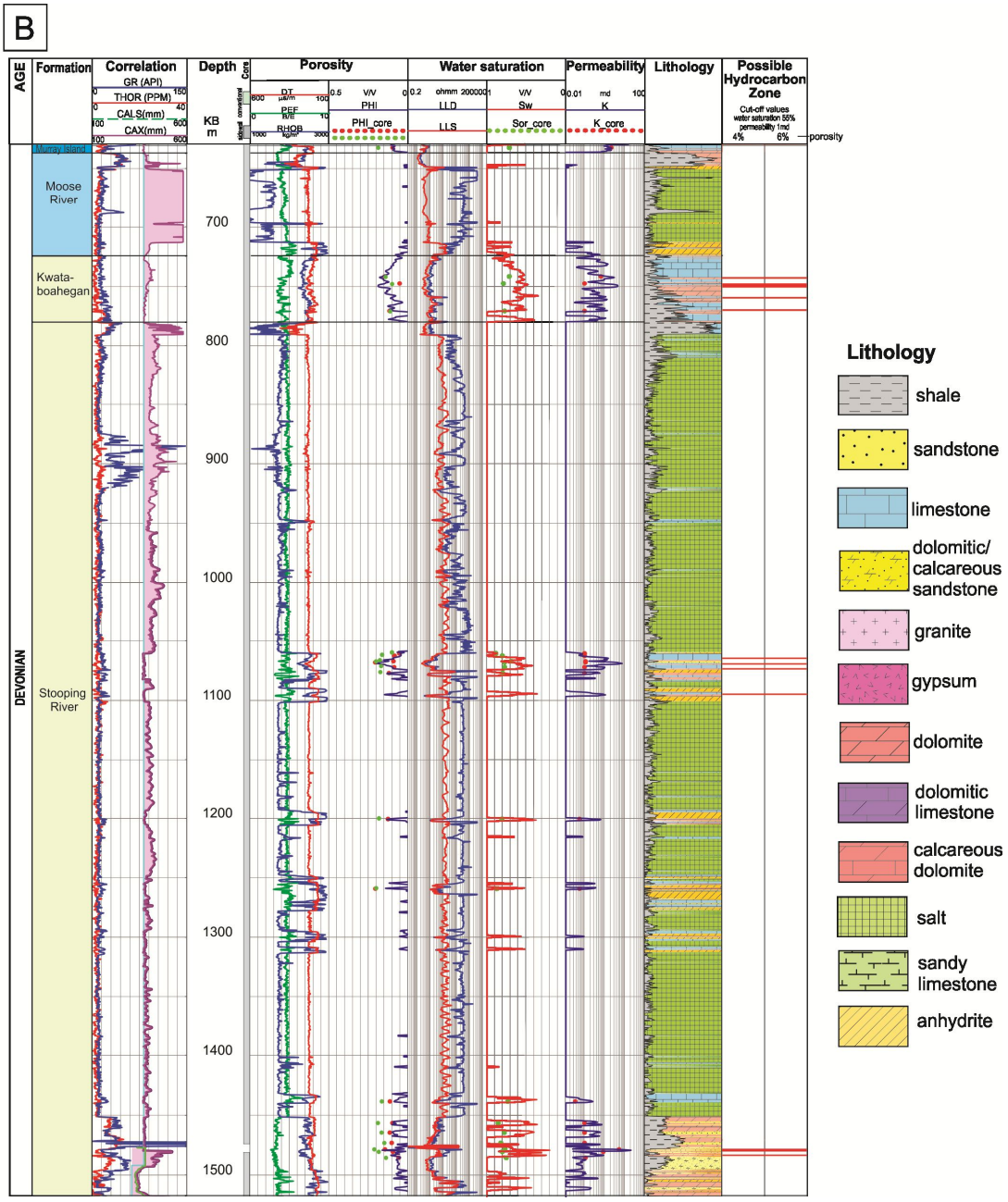

Figure 64: Log data for the Beluga well. A- Ordovician and Silurian strata; B- Devonian strata Possible hydrocarbon zones are indicated in red in the right column.

A

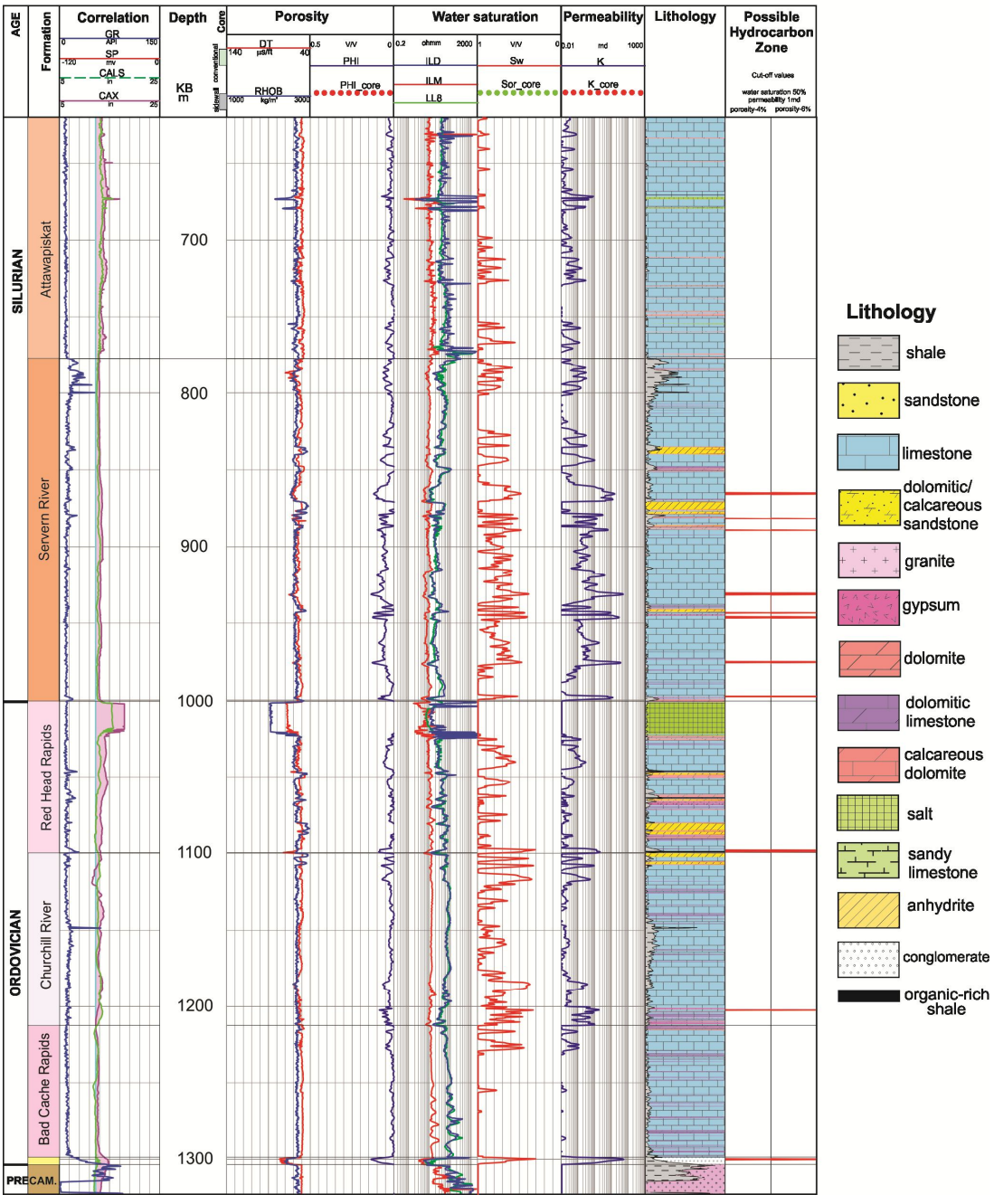
AGE
Formation
Correlation
GR
API
SP
mv
CALS
in
CAX
in
Depth
KB
m
Core
conventional
sidewall
Porosity
DT
µs/ft
PHI
RHOB
kg/m³
PHI_core
Water saturation
ohmm
ILD
ILM
LLS
V/V
Sw
Sor_core
Permeability
md
K
K_core
Lithology
Possible Hydrocarbon Zone
Cut-off values
water saturation 50%
permeability 1md
porosity-4%
porosity-6%
SILURIAN
Attawapiskat
Severn River
ORDOVICIAN
Red Head Rapids
Churchill River
Bad Cache Rapids
PRECAM.
700
800
900
1000
1100
1200
1300
Lithology
shale
sandstone
limestone
dolomitic/ calcareous sandstone
granite
gypsum
dolomite
dolomitic limestone
calcareous dolomite
salt
sandy limestone
anhydrite
conglomerate
organic-rich shale

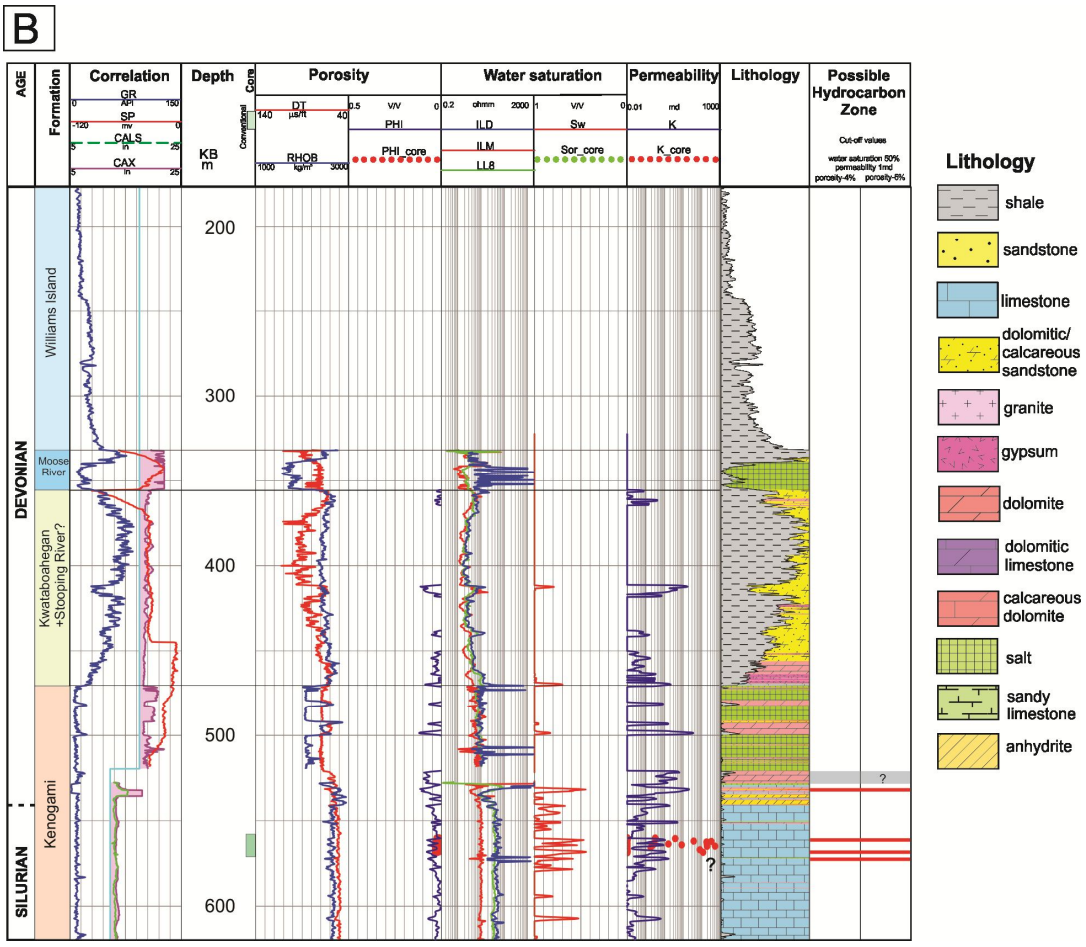

Figure 65: Log data for the Narwhal well. A- Ordovician-Silurian strata; B- Devonian strata. Possible hydrocarbon zones are indicated in red in the right column.

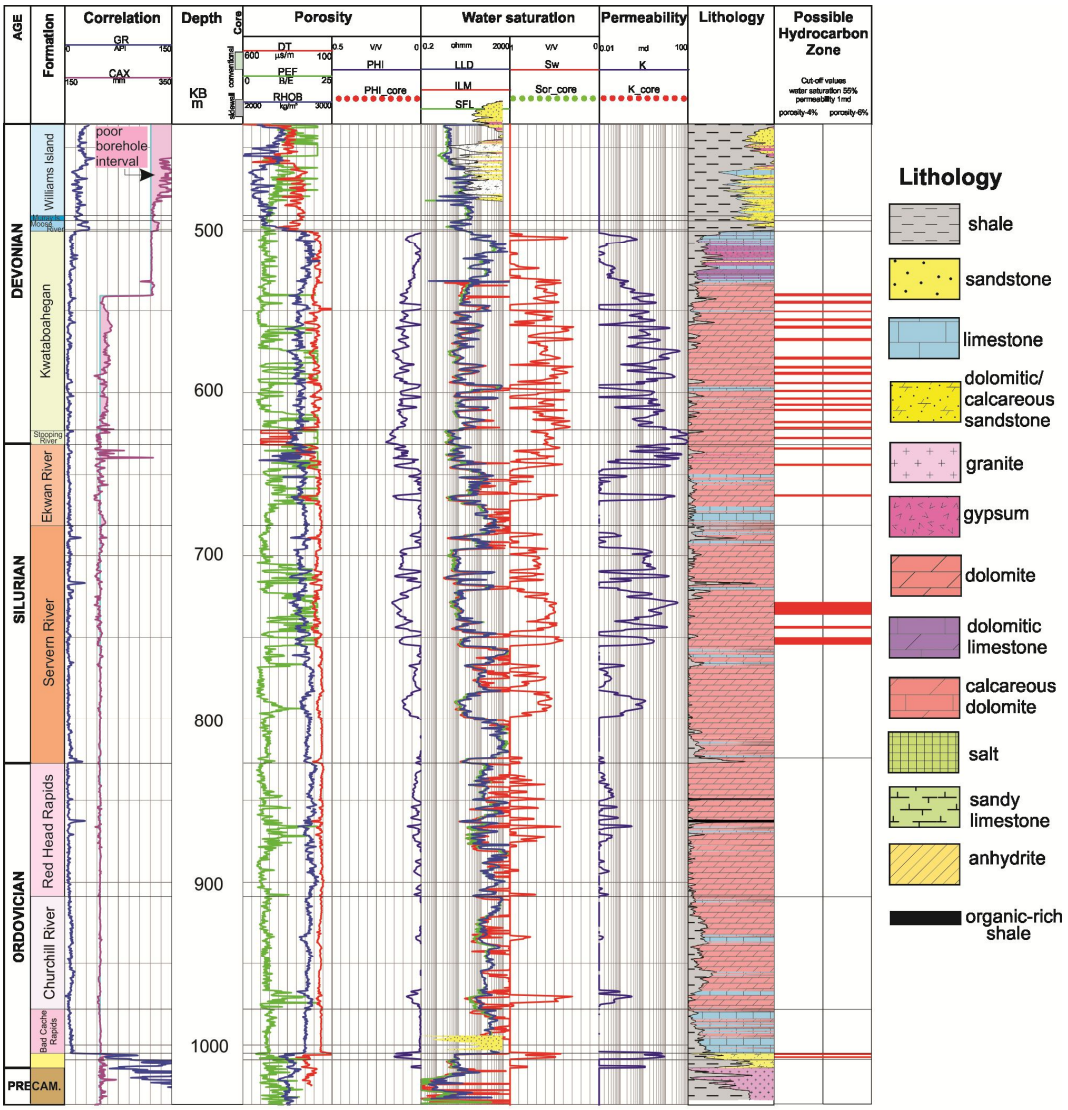

Figure 66: Log data for the Netsiq well. Possible hydrocarbon zones are indicated in red in the right column.

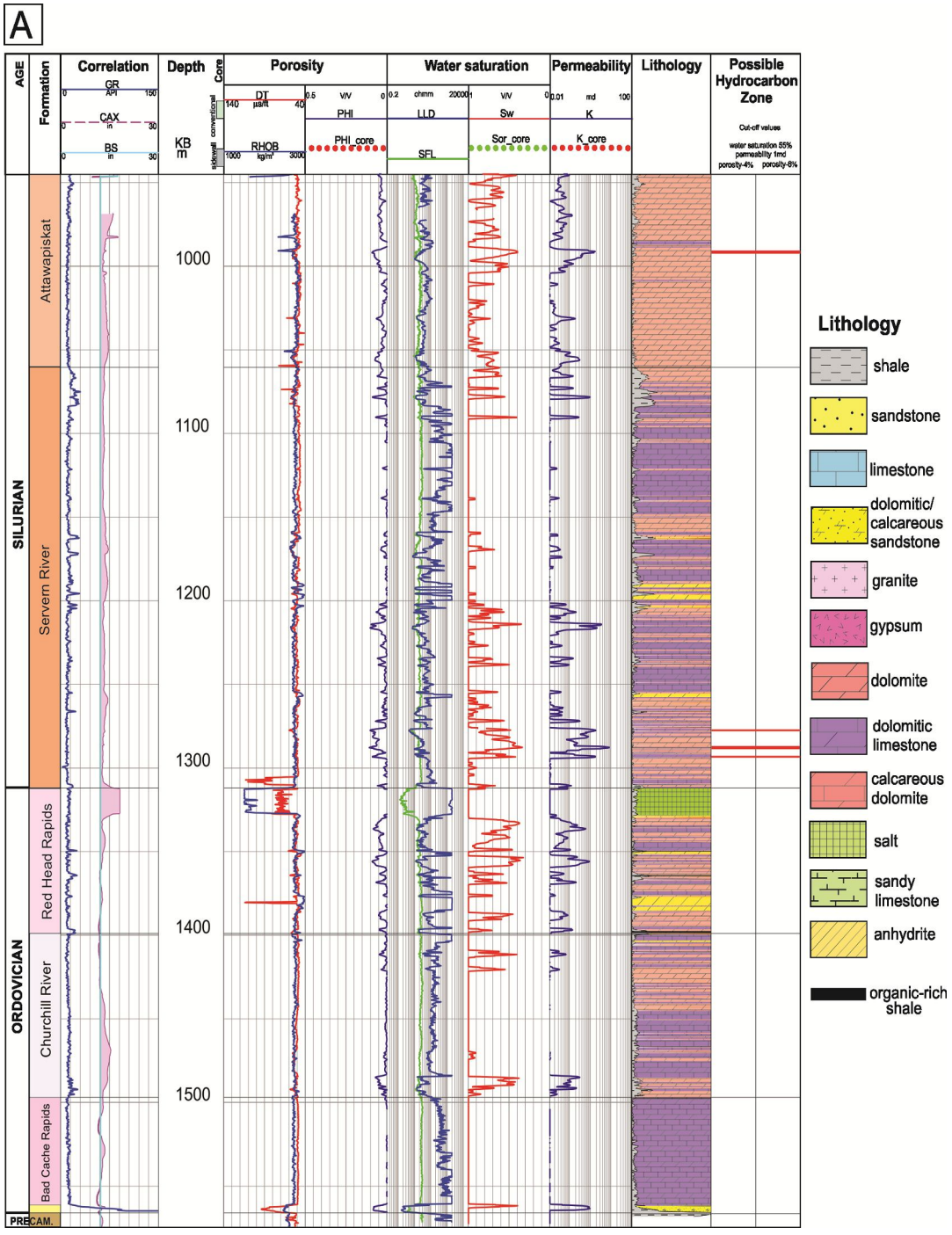
A
AGE
Formation
Correlation
Depth
Porosity
Water saturation
Permeability
Lithology
Possible Hydrocarbon Zone
GR
CAX
BS
KB
m
DT
RHOB
PHI
PHI_core
LLD
SFL
Sw
Sor_core
K
K_core
Cut-off values
water saturation 55%
permeability 1md
porosity-4%
porosity-8%
SILURIAN
ORDOVICIAN
PRECAM.
Attawapiskat
Servern River
Red Head Rapids
Churchill River
Bad Cache Rapids
1000
1100
1200
1300
1400
1500
Lithology
shale
sandstone
limestone
dolomitic/ calcareous sandstone
granite
gypsum
dolomite
dolomitic limestone
calcareous dolomite
salt
sandy limestone
anhydrite
organic-rich shale

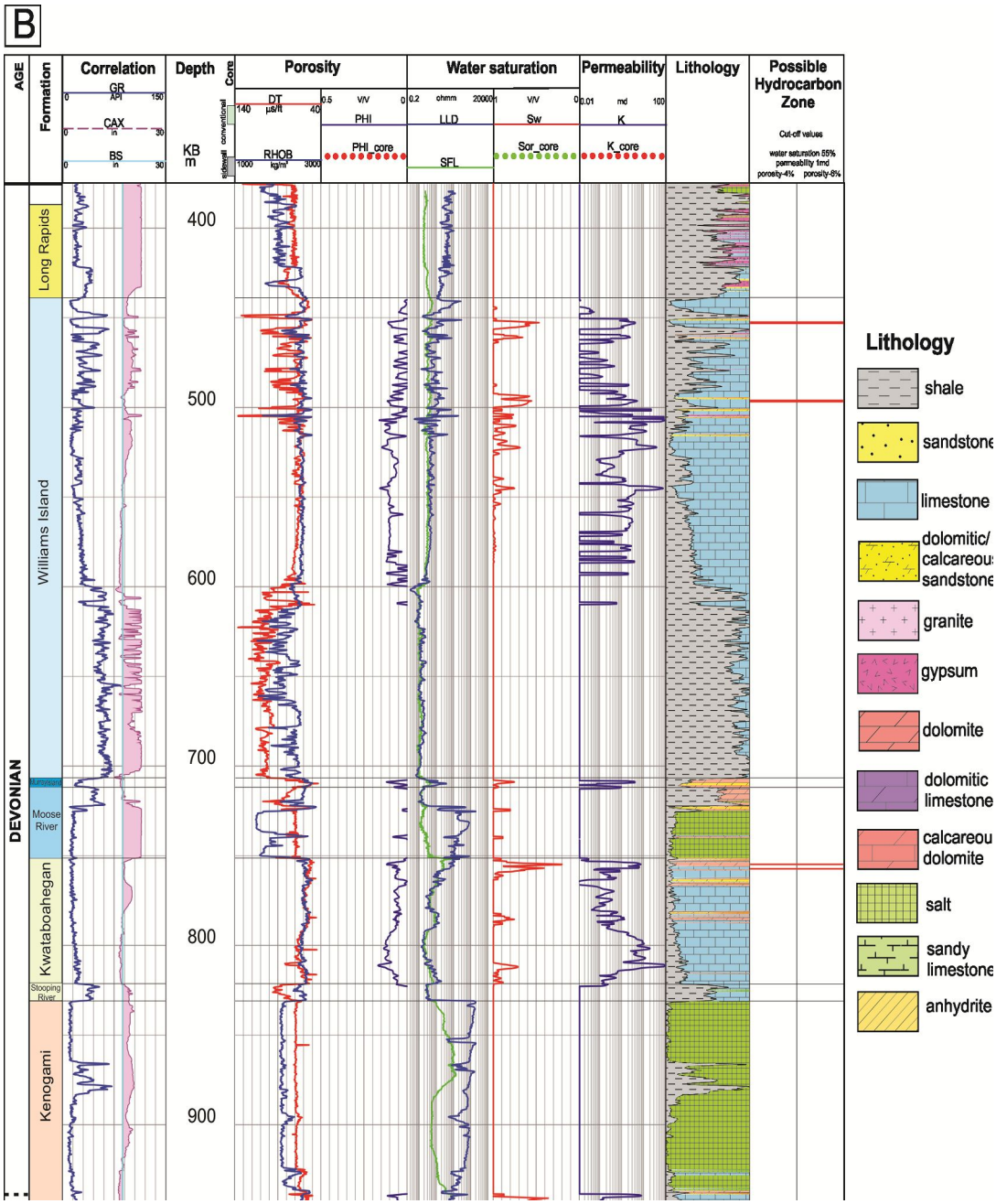

Figure 67: Log data for the Polar Bear well. A- Ordovician-Silurian strata; B- Devonian strata. Possible hydrocarbon zones are indicated in red in the right column.

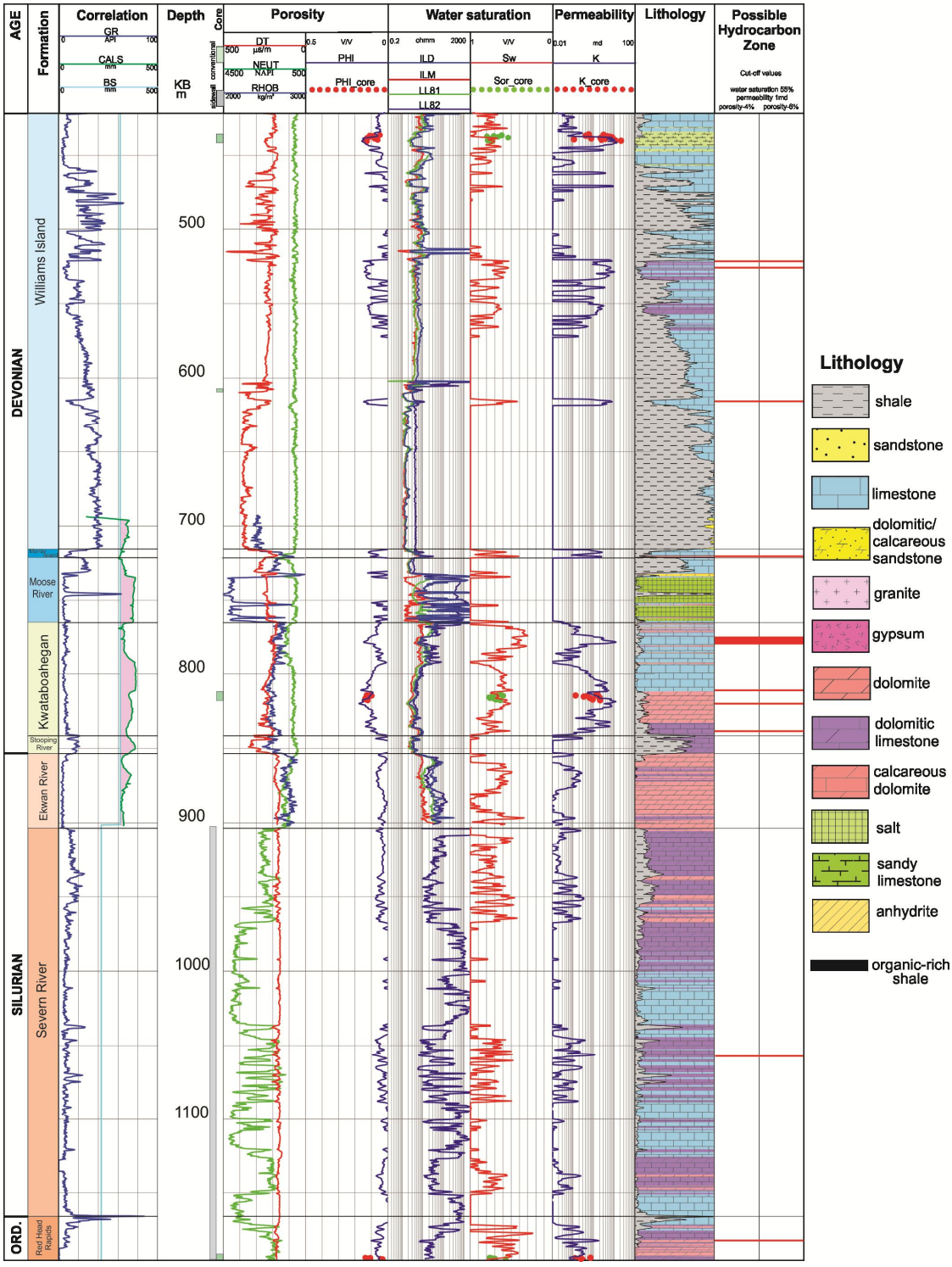

Figure 68: Log data for the Walrus well. Possible hydrocarbon zones are indicated in red in the right column.

Hydrocarbon zones in the Hudson Bay offshore and onshore wells

The petrophysical analysis of Hu and Dietrich (2012) indicates that possible hydrocarbon zones (with porosity above 4 and 6% for dolostone and limestone, respectively, permeability above 1 mD, and water saturations less than 55%) are present in all six wells and at many stratigraphic levels. Most of the log-indicated hydrocarbon zones are < 5 m.

Possible hydrocarbon zones are common in Silurian-Devonian carbonates in the Kwataboahegan Formation (Walrus A-71, Beluga O-23 and Netsiq N-01 wells), in the Attawapiskat Formation (Pen Island #1 and Polar Bear C-11 wells) and Severn River Formation (Narwhal South O-58 and Netsiq N-01 wells), and in Ordovician basal clastics. The Netsiq N-01 well encountered the largest number of log-indicated hydrocarbon zones whereas the Polar Bear C-11 well has the fewest. The highest calculated hydrocarbon saturations (Sw < 25%) occur in reservoirs in the Kwataboahegan Formation in the Netsiq N-01 and Polar Bear C-11 wells, the Stooping River Formation in the Beluga O-23 well, and the Red Head Rapids Formation in the Walrus A-71 and Beluga O-23 wells. One of the more prospective hydrocarbon zones overall (good porosity and permeability, relatively low water saturation and associated hydrocarbon shows) occurs in limestones in the upper part of Kwataboahegan Formation in the Walrus A-71 well (Fig. 69).

The presence of anomalously high Production Index (PI) values combined with low (immature level) T_{max} values of some Ordovician and Silurian units is interpreted to indicate the presence of migrated hydrocarbons (see above). Table 9 presents the T_{max} and PI values of intervals of the three wells (Narwhal South O-58, Beluga O-23 and Polar Bear C-11) for which petrophysical log data suggest the possible presence of hydrocarbon zones. Only hydrocarbon log picks with correlative Rock Eval data are presented. The potential hydrocarbon intervals associated with immature T_{max} (<435°C) and high PI (>0.1) are highlighted in grey.

In the Narwhal South O-58 wells, 2 out of 10 log picks have T_{max}-PI values suggestive of hydrocarbons; they are found near the top of the Severn River Formation. In the Beluga O-23, 3 out of 6 log picks have T_{max}-PI values suggestive of possible hydrocarbon charge, they occur in the Kenogami River and Severn formations as well as in the Bad Cache Rapids Group. Interestingly, the picks in the Kwataboahegan Formation, even if immature, are at the limit of anomalous PI values (0.08 and 0.09). In the Polar Bear, the 2 picks in the Severn River Formation are associated with T_{max}-PI values indicative of a hydrocarbon charged interval.

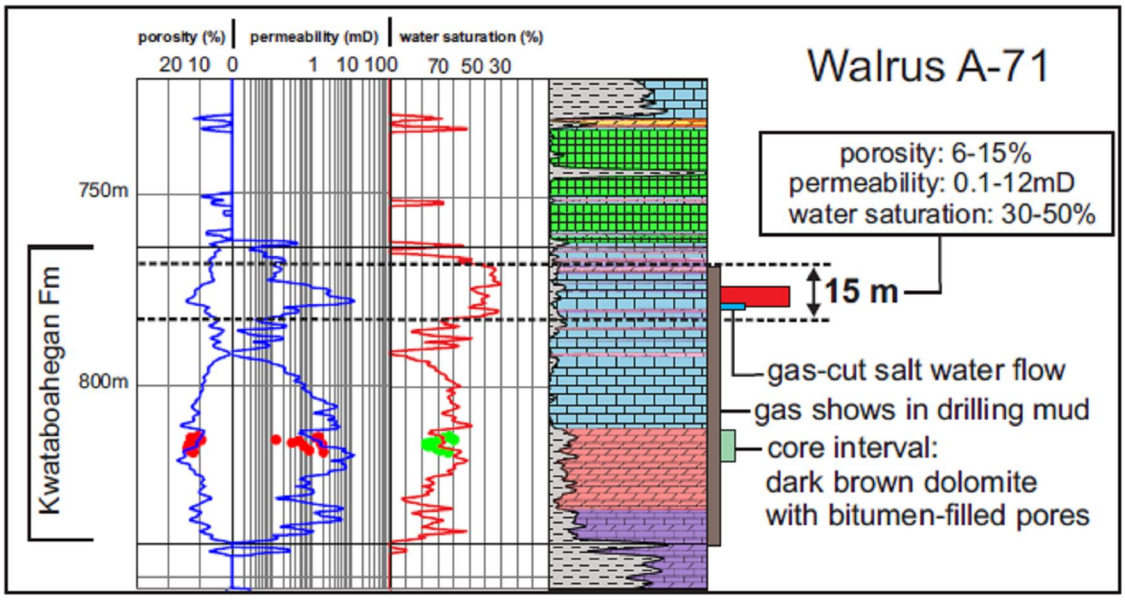

Figure 69: Porosity, permeability and water saturation interpreted from well logs in the interval corresponding to the Kwataboahegan Formation, Walrus well. Dashed lines indicate possible 15 m thick hydrocarbon zone (with permeability above 0.1 mD) in Kwataboahegan limestones. Red bar indicates same zone with 1.0 mD cut-off.

One interval in the Narwhal South O-58 well (515-520 m, Fig. 65) with high porosity and permeability could not be identified as a possible hydrocarbon zone, as no Sw data were available. However, this interval is characterized by high PI values (PI of 0.2 to 0.3; Annex 1.8). In the Beluga O-23 well, a significant number of intervals have porosity, permeability and water saturation values that are at the threshold of being classified as potential hydrocarbon zones; these are found in the Ekwan River Formation from 1670 to 1700 m and in the Red Head Rapids Formation from 1960 to 2025 m (Fig. 64). For the Ekwan River Formation, this interval is associated with immature T_{max} and high (>0.3) PI values (Annex 1.10). Rock Eval data for the Red Head Rapids Formation, in the 1990 to 2020 m interval includes 7 results (4 samples) with immature T_{max} (425 to 434°C) and very high PI values (0.38 to 0.69; Annex 1.10).

Overall, a significant number of possible hydrocarbon zones identified from well logs have associated Rock Eval data indicating immature strata that may contain migrated hydrocarbons.

Reservoir pressures

Well drilling records (mud weights, repeat formation tests, and well kick occurrences) indicate that reservoir strata penetrated in deeper parts of the Hudson Bay Basin are overpressured (Hu and Dietrich, 2012). The highest reservoir pressures occur in the Walrus A-71 and Netsiq N-01 wells (pore pressures up to 70% above hydrostatic pressure). The elevated pressures indicate that effective seals are present in the basin. Impermeable strata (potential seals) identified from log data include evaporites, shales and tight limestones. Fault zones may also provide seals in structured parts of the basin.

Well	Stratigraphic unit	Depth	Tmax	PI
Narwhal South O-58	Kenogami River	1742 ft	444	0.31
	Kenogami River / Severn River	1837 ft	422	0,22
	Kenogami River / Severn River	1870 ft	430	0,16
	Severn River	2877 ft	428	0,06
	Severn River	2903 ft	429	0,05
	Severn River	3083 ft	426	0,07
	Severn River	3264 ft	433	0,07
	Churchill River	3608 ft	433	0,06
	Churchill River	3937 ft	437	0,1
	Bad Cache Rapids	4281 ft	445	0,04
Beluga O-23	Kwataboahegan	740 m	416	0,08
	Kwataboahegan	765 m	416	0,09
	Kwataboahegan	770 m	420	0,09
	Kenogami River	1620 m	423	0,4
	Severn River	1870 m	429	0,46
	Bad Cache Rapids	2190 m	432	0,17
Polar Bear C-11	Severn River	4190 ft	433	0,13
	Severn River	4215 ft	430	0,15

Table 9: Tmax and Production Index (PI) values of samples located in log-indicated hydrocarbon zones.

3.5.6 Conclusions regarding reservoir potential of the Hudson Bay and Foxe basins

A detailed re-evaluation of historical well logs and acquisition of significant new data provide a more precise understanding of reservoir potential in the Hudson Bay Basin.

- The presence of Upper Ordovician hydrothermal dolomites had been first hypothesized by Sanford and Grant (1990). Outcrops of interpreted hydrothermal dolomites in the Red Head Rapids River Formation on Southampton Island have been studied. The petrography and stable isotopes characteristics of the dolomites are indicative of a hydrothermal origin. Hydrothermal dolomites in the Upper Ordovician Bad Cache

Rapids Group have also been identified in a core from a well drilled in northeastern Manitoba.

- Porous reef facies are recognized in the field (Upper Ordovician and Lower Silurian), in cores (Lower Silurian) and from electric log data (Lower Silurian and Devonian). Historical and new reports of live and dead oil are known from Ordovician and Silurian reefs and carbonates and log data suggest the presence of possible hydrocarbons in intervals commonly associated with reef facies.
- Detailed log analyses has documented the presence of porous and permeable intervals in all offshore wells in Hudson Bay and for the Pen No. 1 well in Ontario. For the offshore wells, the most porous facies are Devonian and a decrease of porosity is recognized with depth; dolostone is the most porous carbonate facies. For the Pen No. 1 well, the most porous and permeable unit is the limestone-dominated Attawapiskat / Ekwan River interval.
- Based on porosity cut-off values of 4% for limestone and 6% for dolostone, coupled with permeability values over 1 mD and water saturation lower than 55%, numerous zones with potential hydrocarbons have been identified in all well logs. A significant number of these zones are in Devonian strata. They are also abundant in Silurian rocks and less abundant in Ordovician strata. These log-based hydrocarbon-bearing intervals are often associated with Rock Eval data indicating immature strata containing migrated hydrocarbons.
- Pressure indicators from drilling records indicate significant overpressure zones, suggestive of efficient sealing capacity.

3.6 Hydrocarbon indicators

Without direct production or positive well testing, the presence of potential hydrocarbons in a sedimentary basin can be evaluated from indirect indicators visible on seismic profiles or through physical expression of leakage out of the sedimentary basin. The latter can be expressed in the formation of onshore seeps, pockmarks on the seafloor and oil slicks on water surface.

3.6.1 Seafloor pockmarks

Pockmarks are circular or elliptical seafloor features with diameters varying from a few metres to more than 300 m (Hovland *et al.,* 1984). Pockmarks on soft seabed have been known since the 1970s and have been found worldwide in water depths ranging from 30 m to over 3000 m (King and MacLean 1970; Hovland and Judd 1988; Pinet et al., 2008). These features normally occur where the seafloor consists of sandy to silty clay sediments and they are assumed to be the result of fluids expulsion out of the seabed (Hovland, 1989). A significant volume of the interstitial fluids found within shallow, unconsolidated sediment pore space

consists of methane either from biogenic-process (microbial decay of organic matter) in relatively shallow sediments (<1000 m) or from thermogenic-process in deep-lying organic matter rich hydrocarbon source rocks (Hovland, 1989); besides methane, water and liquid hydrocarbons can locally fill the available pore space. Fluid escape seafloor features have been reported in several producing hydrocarbon domains worldwide (Logan et al., 2010) and in some cases they may represent an open window to petroleum systems and provide indirect evidence for the presence of mature source rocks (Hunt, 1996; Pinet et al., 2008).

Pockmarks are recognized at two sites on multibeam bathymetry data that were collected on board the icebreaker CCGS Amundsen using a Kongsberg-Simrad EM302 system: 1) off the northern part of Mansel Island (Fig. 70) in the central part of Hudson Bay (Fig. 71) (Roger et al., 2011). The data provided an integral image of the seafloor with a relative depth accuracy of 2 to 5 m. It is important to note than less than 1% of the entire seafloor of Hudson Bay and Strait and Foxe Basin are covered by high-resolution sea-floor bathymetric data.

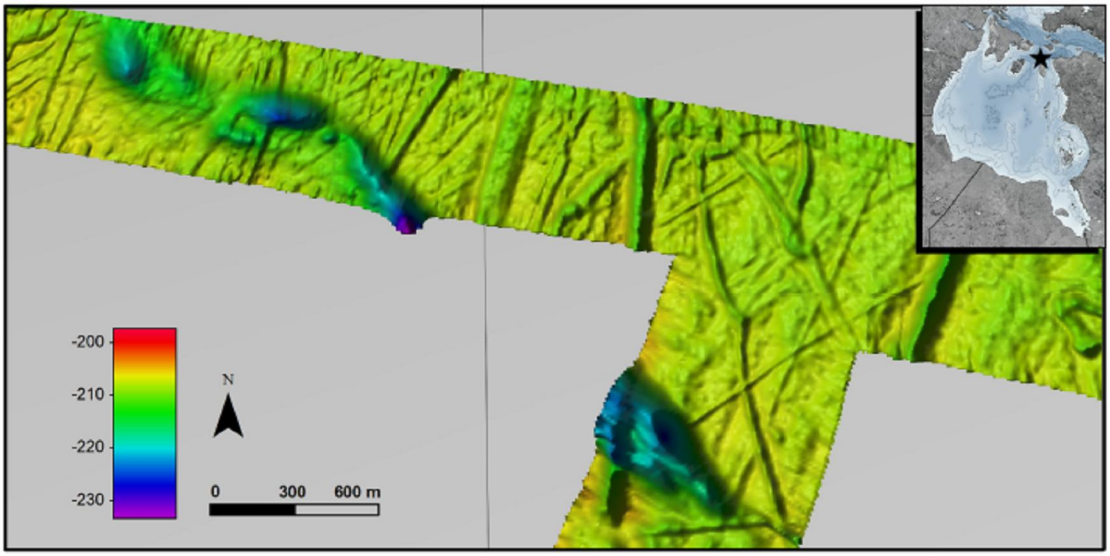

Figure 70: Multibeam bathymetry image showing pockmarks that post-date elongated iceberg scours, north Mansel Island.

North of Mansel Island

An area characterized by a ± 2 km long seafloor depression associated with fluid escape features has been identified on multibeam bathymetry data collected north of Mansel Island (Fig. 70). Circular depressions are grossly aligned with an average diameter of 100 m and average depth of 10 m, under a mean water depth of 200 m. These structures formed in surficial sediments that consist of a 6 to 20 m-thick sorted sands (Henderson, 1990). North-south striking icebergs scours seem to be cut by the pockmarks suggesting that the pockmark formation is a recent (post-glacial) event. This site is located over a set of east-west trending normal faults, which extend over more than 200 km (Sanford and Grant, 1998).

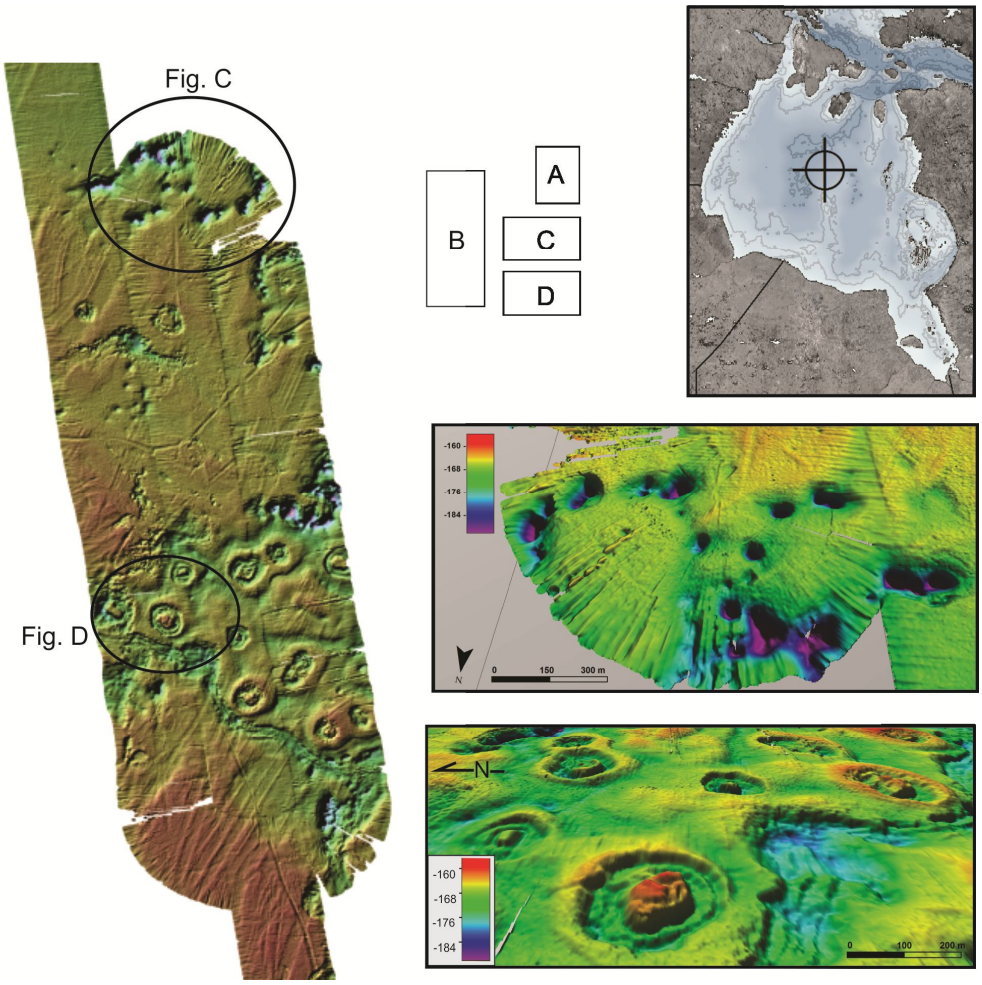

Figure 71: Multibeam bathymetry images of pockmarks (C) and ring structures (D) in the central Hudson Bay.

Central Hudson Bay, north of Polar-Bear C-11 and Narwhal 0-58 wells

Multibeam data collected in central Hudson Bay show a sector characterized by an impressive quantity of pockmarks and ring-like features (Fig. 71). These features are located at an average water depth of 200 m and surficial sediments consist of mixed diamicton and sandy mud (Henderson, 1990). This area is divided into two distinct sectors. The sector to the North is characterized by a significant number of pockmarks with an average diameter of 100 m and at average depth of 20 m (Figs 71 B and C). The second sector to the south is dominated by a large number of circular features showing a ring-like morphology (Figs. 71 B and D). These structures exhibit a central high, are more than 200 m in diameter, up to 10 m in depth and are

surrounded by dipping off aprons (Fig. 71D). The northern sector is affected by south-north oriented icebergs scours. Scours also occur in the southern sector, but they are less prominent on and around the ring structures.

Considerations on Hudson Bay seafloor pockmark-like and ring structures

The crater-like features observed north of Mansel Island and in the central part of Hudson Bay have all the physical characteristics of fluid escape pockmarks. For both areas, it is currently unknown if these structures are actively venting hydrocarbons (gas or liquids).

The ring structures in the central part of Hudson Bay are morphologically different than common pockmarks, being significantly larger and having an internal central high. Their formation mechanism is presently poorly constrained (Rogers et al., 2011).

3.6.2 Potential oil slicks from satellite RADARSAT imaging

RADARSAT – 2 data were acquired to provide a background set of synthetic aperture radar (SAR) images. Space-borne radar data, provide some preliminary information at relatively low cost, aimed primarily at determining if persistent natural oil seeps occur in the area.

The Wide mode beam of RADARSAT - 2, with 12.5 m resolution and a swath of 150 km, was chosen for its appropriate mid incidence angle range and area of coverage. Vertical (VV) polarization was selected because it provides a superior clutter-to-noise ratio (CNR) over horizontal (HH) polarization for dark target detection in ocean images. Data was collected during ice-free periods (early September to late October) in each of the years 2010, 2011 and 2012 exceeding a total of 360 scenes. With adequate coverage obtained over almost the entire area of interest as of November 2012, a systematic search for small dark patches (dark targets) was carried out. A visual identification of suspected seeps was made from geo-referenced 8-bit images (median filtered) in strip mosaics from each satellite pass. Dark targets were defined as potential or suspect oil seeps that require further validation. Repeat observations of dark targets at or near the same location at different periods of time are one criterion that increases the likelihood that the feature is related to seeps of a subsurface hydrocarbon source.

In this study, 41 dark targets were identified which met semi-quantitative criteria known to be associated with natural oil seeps. These criteria include a sharp boundary defining a small-enclosed region (< 1,000 ha); sufficient backscatter contrast (i.e. - 10 dB) between the background sea state and the dark region; absence of other oceanographic phenomena recognizable that result in dark features in SAR images. The suspected seep areas were then extracted as vector features. A number of parameters were computed for each suspected seep based on its morphological and physical features. A few examples of dark target, or suspect oil seeps are shown in Figure 72 from the database. A more detailed discussion of this project and the database entries is given in Decker et al. (2013).

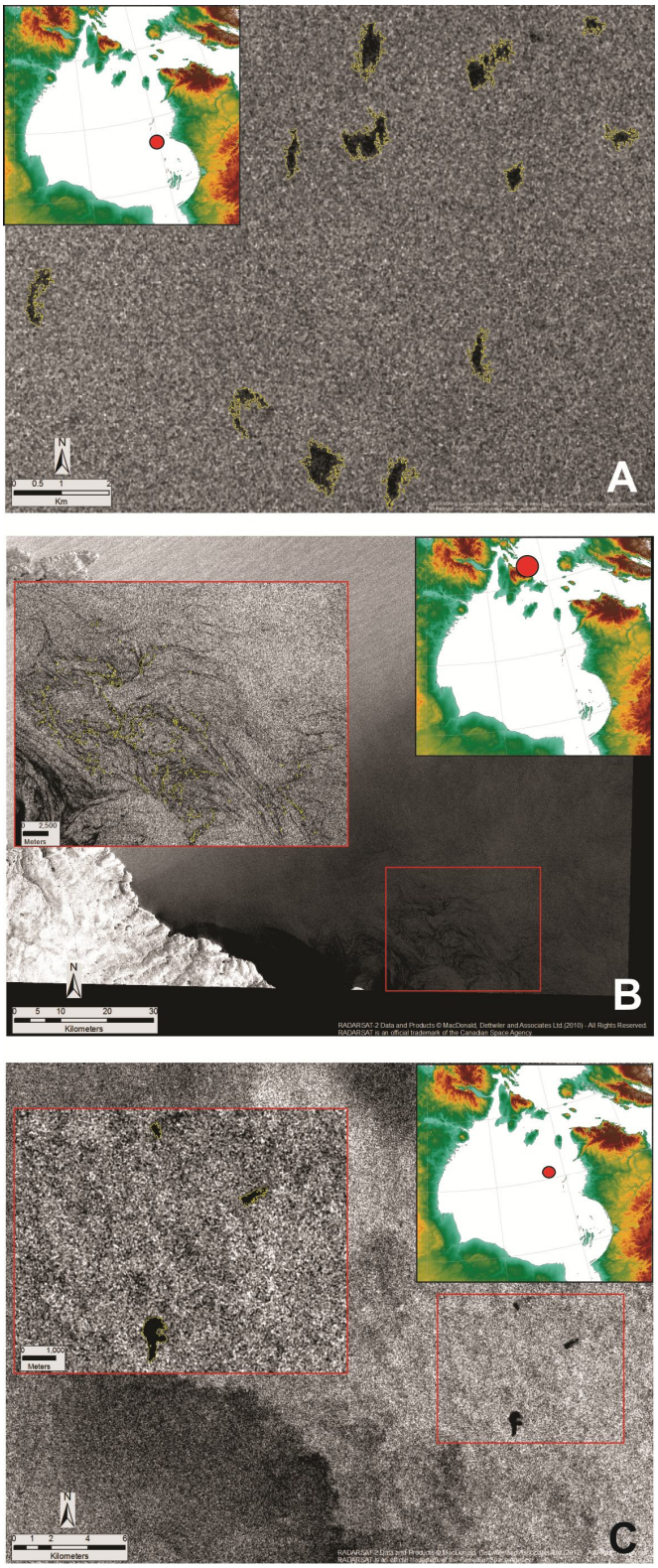

Figure 72: SAR images showing dark targets. A, Cluster of discrete dark targets, eastern Hudson Bay, outlined in yellow; B, Large feature covering an area of 900 hectares off Cape Donovan, Southampton Island; C, Group of three dark targets, northeast Hudson Bay.

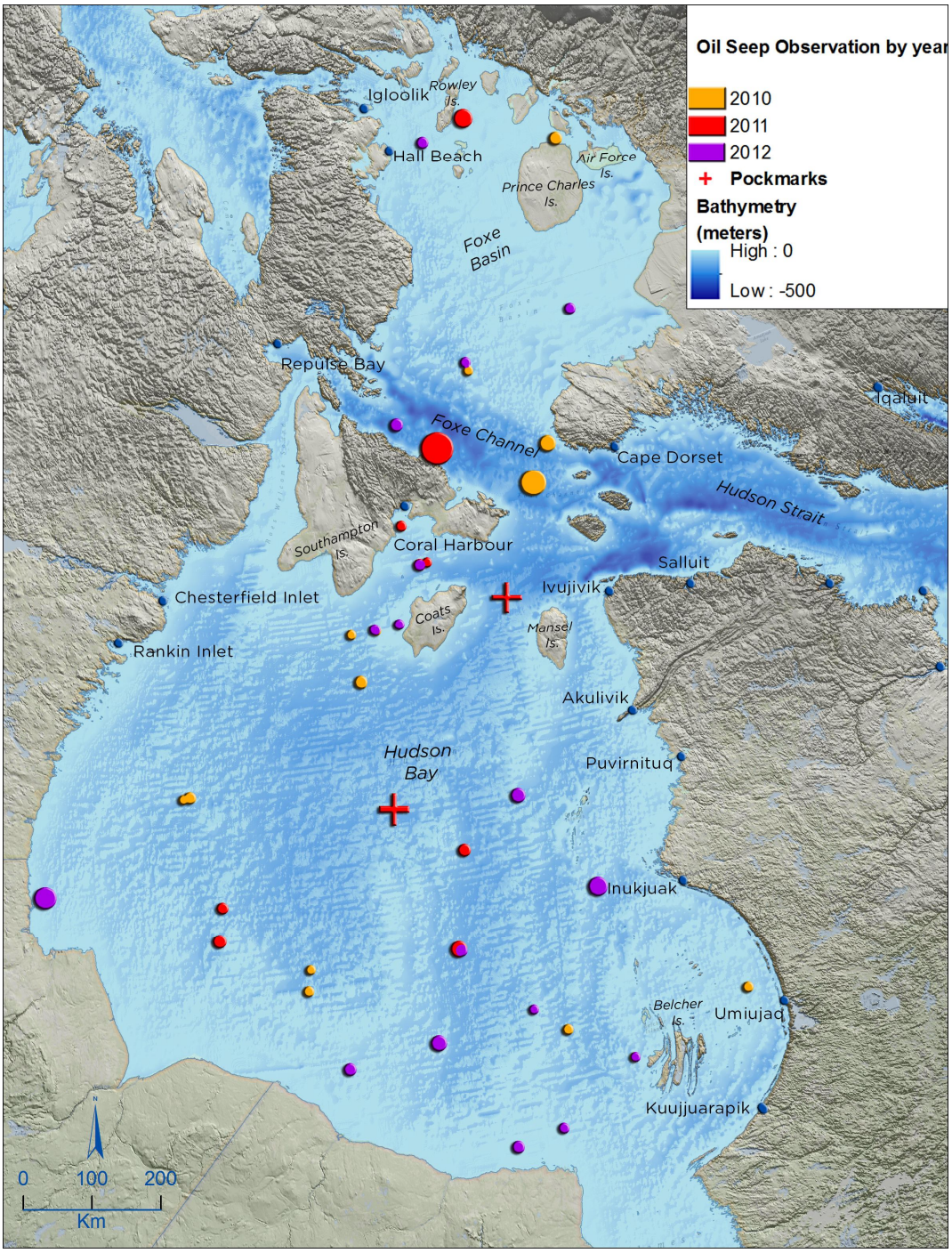

Figure 73: Locations of identified dark targets observed on SAR images collected during 2010-2012 over Foxe Basin and Hudson Bay (size of circles shows a slight exaggeration compared to observed features for visualisation purposes).

In summary, the locations of all dark target results identified are given in Figure 73 in association with seafloor bathymetry and the location of “pockmarks” discussed above. Repeat observations of potential slicks in the same zones (e.g. north of Foxe Channel, 2010 to 2012; north of Coats Island, 2011 and 2012; central Hudson Bay, 2011 and 2012) lend support to the interpretation of phenomena causing certain dark targets to persist from year to year. Other examples include repeated observations of dark targets in the same location, but on different days during the same season (e.g. western Hudson Bay, 2010).

This project provides intriguing initial results and has established a collection of historic data that is ultimately required as a basis for any further investigation or monitoring in the region.

3.7 Conceptual hydrocarbon plays

3.7.1 Conventional Plays

Five conventional petroleum plays and two unconventional plays are identified in Paleozoic strata in the Hudson Bay and Moose River basins. The conventional play types include fault blocks, reefs, fault-bounded sags (with associated hydrothermal dolomites), unconformity traps, and salt dissolution structures (Fig. 74). The unconventional plays are associated with oil shale and biogenic shale gas. A conventional petroleum play may also be present in Proterozoic strata beneath the eastern Hudson Bay Basin.

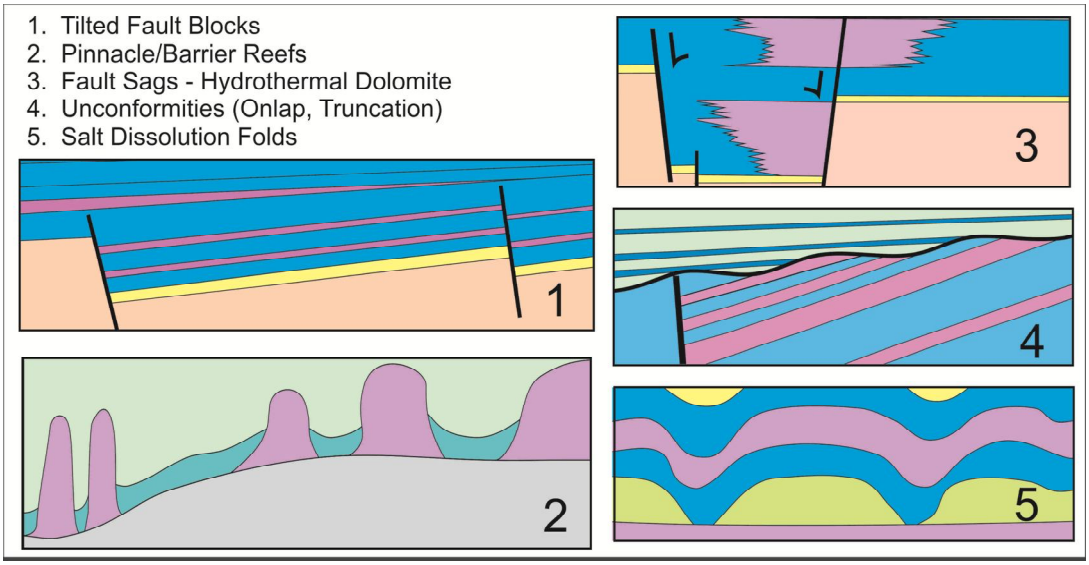

Figure 74: Schematic depiction of Paleozoic conventional petroleum plays in the Hudson Bay Basin.

Fault Block Play

The main exploration targets of early drilling in the offshore Hudson Bay Basin were fault block highs, with three wells (Netsiq, Polar Bear and Walrus) drilled on the central high trend (Figs. 75, 76). Seismically mapped fault blocks are abundant in this part of the basin. Most of the large-offset faults are oriented north-northwest and are downthrown to the east-northeast, with associated westward tilting of fault blocks. Many of the regional faults appear to occur in a right-stepping en-echelon pattern (Fig. 75), indicating a possible transtensional tectonic setting. The fault blocks developed during deposition of Upper Ordovician (?), Silurian and Lower Devonian strata. Flat lying or gently draped Middle and Upper Devonian strata occur over fault block highs.

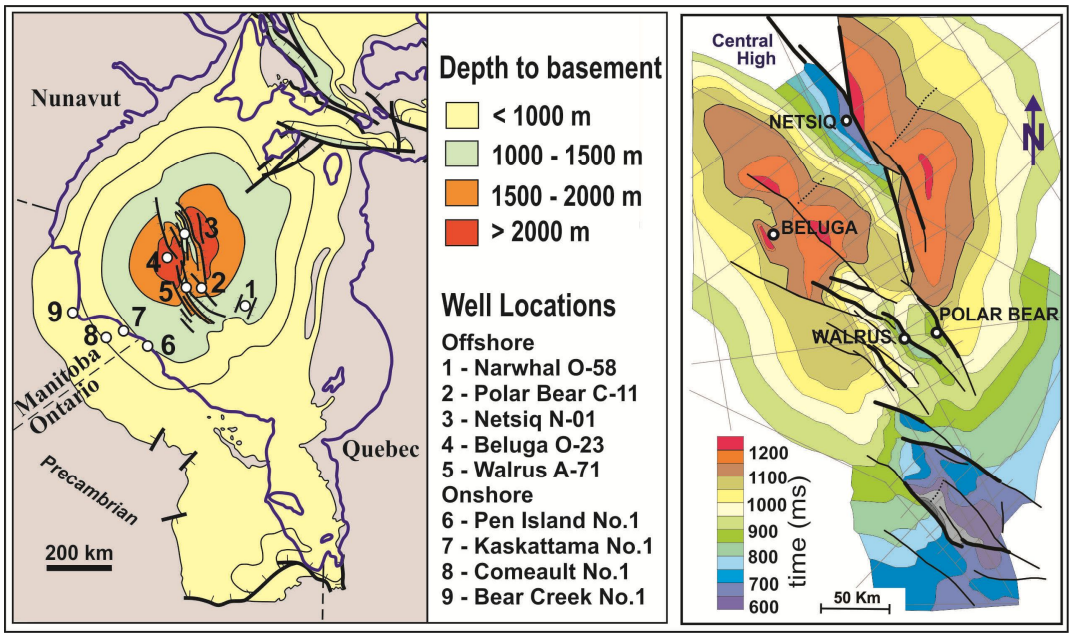

Figure 75: Well location and regional sedimentary isopach map of the Hudson Bay Basin (left panel; modified from Sanford and Grant, 1990) and detailed map of faults and subbasins in the central part of the basin (right panel; modified from Pinet et al., 2013a). The mapped horizon in the detail map is at/near the base of the Ordovician succession (top basement) - time structure contours of 1100 ms and higher indicate sedimentary sections greater than 2000 m thick.

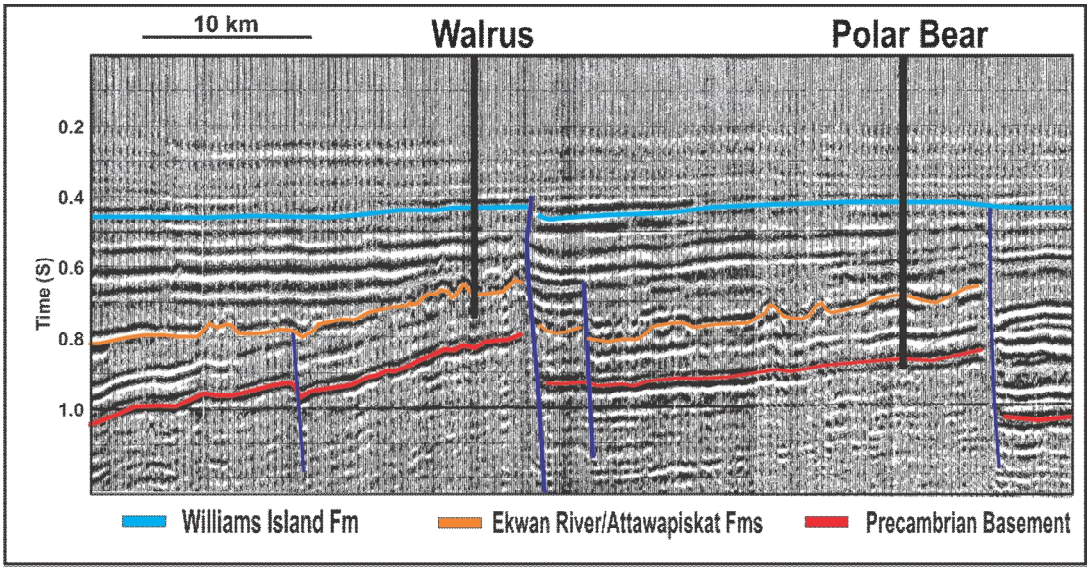

Figure 76: Seismic profile across tilted Lower Paleozoic fault blocks tested by the Walrus and Polar Bear wells in the central Hudson Bay Basin. Mounded seismic features at the Ekwan/Attawapiskat formation interval are drilled or interpreted reefs.

Reef Plays

The reef plays include pinnacle, patch or barrier reefs that occur at several stratigraphic levels in the basin, including the Devonian Williams Island and Kwataboahegan formations, the Lower Silurian Attawapiskat Formation, and the Upper Ordovician Red Head Rapids Formation. Devonian and Silurian reefs were penetrated in the Walrus, Polar Bear and Narwhal wells, with hydrocarbon shows encountered in a Devonian reef section in the Walrus A-71 well (Hu and Dietrich, 2012). Seismic indications of Devonian and Silurian reefs (mounded reflection patterns; Figs. 77, 78) occur in abundance in many parts of the basin, indicating these reefs are numerous and widespread. Reefs appear to be abundant over many fault block highs (Fig. 76), indicating paleotopographic controls on reef development. Reefs in the Ordovician Red Head Rapids Formation are difficult to identify seismically, but may be the most prospective (of the reef plays) due to the close stratigraphic proximity of potential reservoir and source rocks (Fig. 79).

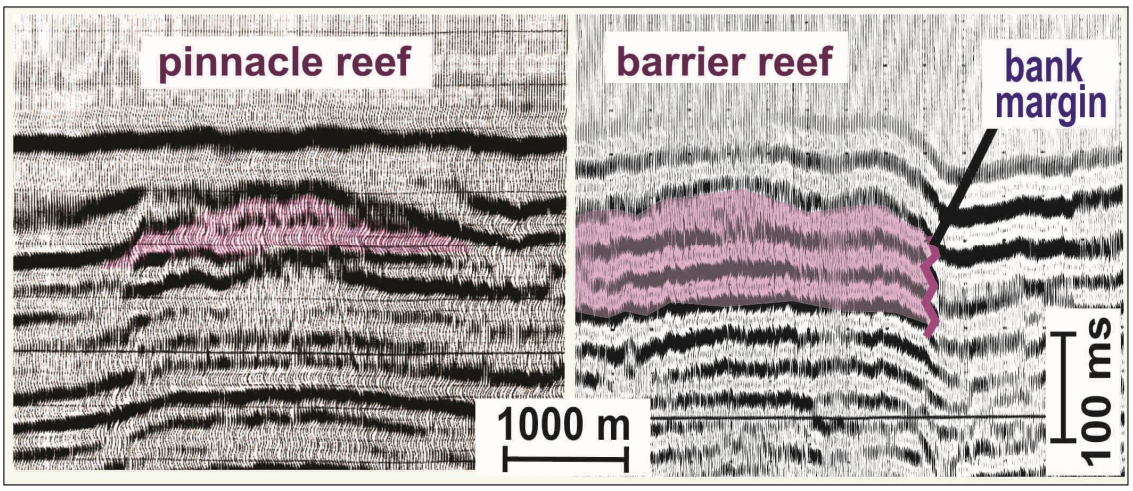

Figure 77: Seismic profiles illustrating mounded features interpreted as Devonian (Williams Island Formation) pinnacle and barrier reefs.

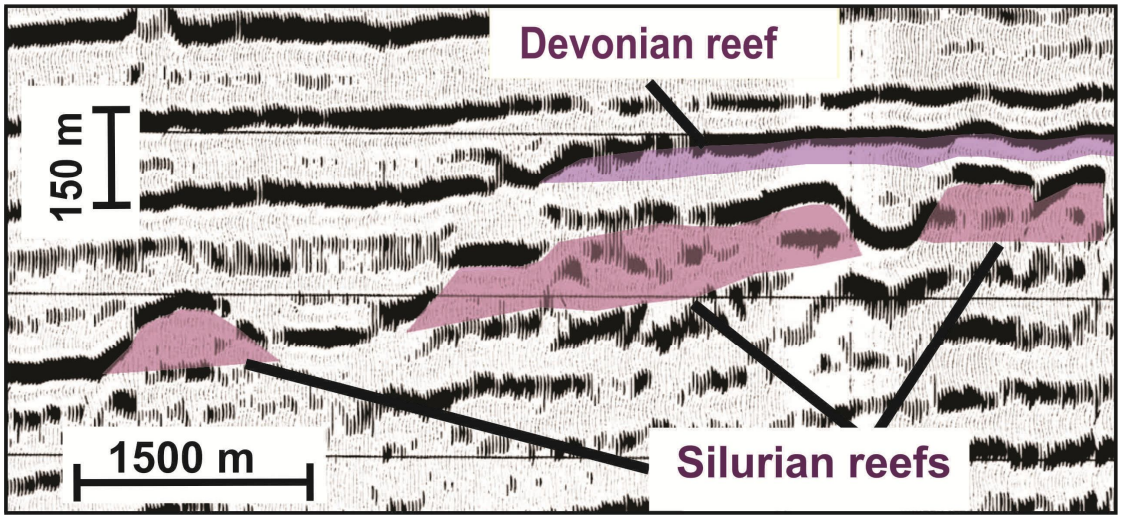

Figure 78: Seismic profile illustrating stacked mounded features interpreted as Devonian (Kwataboahegan Formation) and Silurian (Attawapiskat Formation) reefs.

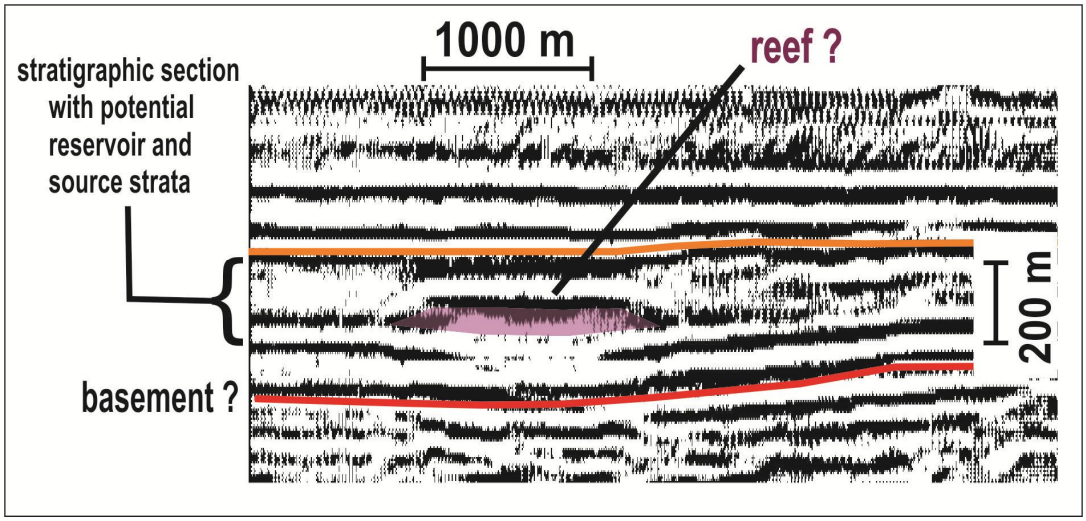

Figure 79. Interpreted seismic profile illustrated a stratigraphic anomaly (possible reef) in the Upper Ordovician Red Head Rapids Formation. This section contains organic-rich intervals that have oil generation potential.

Fault Sag - Hydrothermal Dolomite Play

Several petroleum play types were not tested in early exploration drilling in the Hudson Bay Basin. The most prospective of these untested plays is a hydrothermal dolomite play associated with fault zones. Fault-controlled dolostones are significant conventional reservoirs for oil and gas in many North American basins, including the intracratonic Michigan and Illinois basins (Davies and Smith, 2006). The development of hydrothermal dolostone reservoirs is commonly associated with basement-involved extensional or transtensional faulting and associated platform collapse zones (referred to as "sags" in seismic data interpretations). The fault zones provided conduits for high temperature fluids that altered the adjacent sedimentary sections. The hydrothermal fluids may have increased local maturation levels and oil generation in organic-rich units within or adjacent to fault sags.

In the Hudson Bay Basin, fault-controlled hydrothermal dolomites in Ordovician and Silurian strata have been identified from onshore field and core samples (Lavoie et al., 2011). Seismic data indicate fault sags are common features in the offshore Hudson Bay Basin, with some of the sag features displaying seismic expressions similar to hydrocarbon-producing sags in other cratonic basins (Fig. 80). The interpreted transtensional tectonic setting in the central part of the Hudson Bay Basin is consistent with fault sag development models. Seismic-stratigraphic interpretations indicate more than one phase of fault-sag development. Many of the fault zone/sag features in the basin are associated with local seismic amplitude anomalies, indicating fault-controlled lateral variations in lithology and/or porosity (Fig. 81). Some of the anomalous reflection intervals could be related to the presence of porous hydrothermal dolomites, including possible hydrocarbon charged intervals.

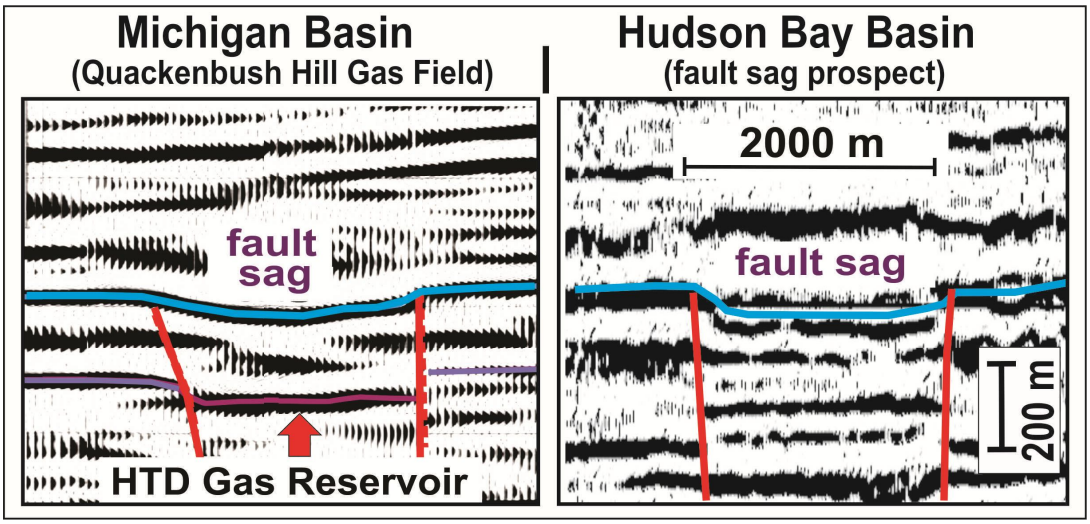

Figure 80: Seismic profiles illustrating fault sags in the Michigan and Hudson Bay basins. The Michigan Basin sag contains gas-bearing hydrothermal dolomites (Quackenbush Hill Field; Davies and Smith, 2006).

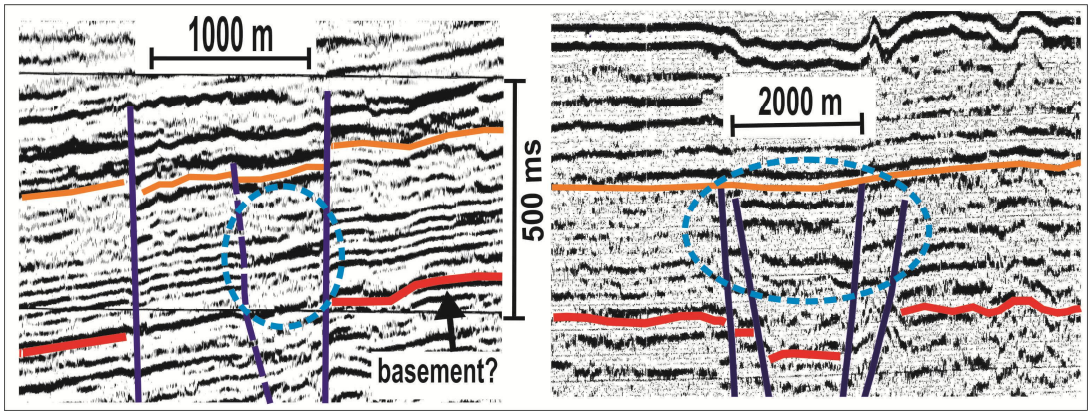

Figure 81: Seismic profiles in the Hudson Bay Basin illustrating fault sags with internal amplitude and frequency anomalies (blue dashed circles) in Ordovician-Silurian sections, below the sub-Devonian unconformity (orange marker).

Unconformity Play

A second untested play type in the Hudson Bay Basin is an unconformity play, associated with stratal truncation or onlap (Fig. 82). Major regional unconformities in the basin occur in the Middle Devonian (base Williams Island Formation) and at the Devonian-Silurian boundary. A variety of potential stratigraphic-structural traps may be associated with these unconformities, particularly where dipping strata occur on the flanks of tilted fault blocks.

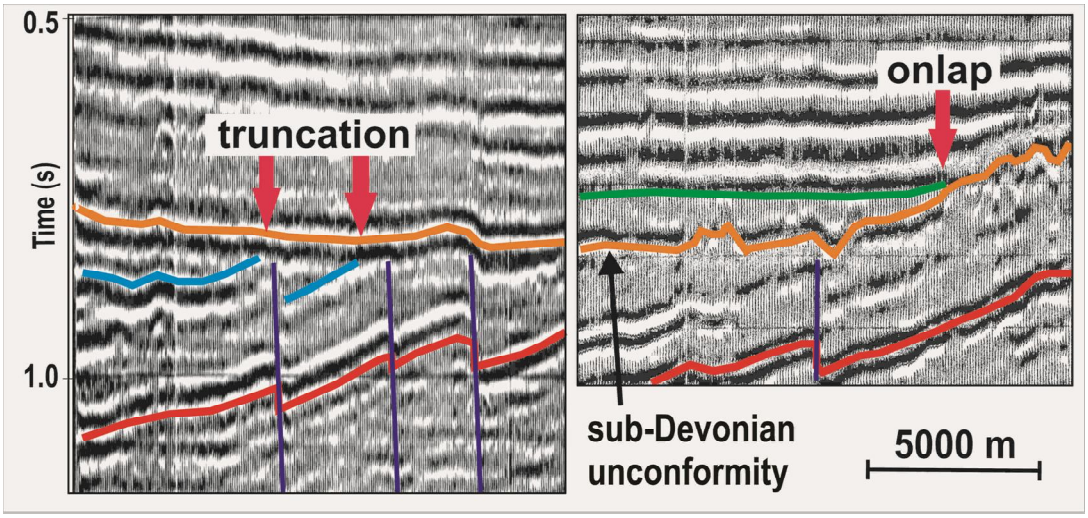

Figure 82. Interpreted seismic profiles illustrating truncation of Silurian strata and onlap of Lower Devonian strata across a base-Devonian unconformity. The profiles also illustrates the fault block play in Silurian-Ordovician strata (red horizon is at/near top of basement).

Salt Dissolution Play

A third untested play may be associated with salt dissolution structures. Evaporites occur at several stratigraphic intervals in the basin, with thick salt sections known to occur locally in the Devonian Stooping River Formation. Unusual structural features imaged in seismic profiles in a few parts of the basin may be related to salt dissolution (Fig. 83). Salt dissolution features occur in other cratonic basins, including the Williston Basin where Devonian salt dissolution is widespread. Some oil and gas fields in the Williston Basin are associated with salt-dissolution structures.

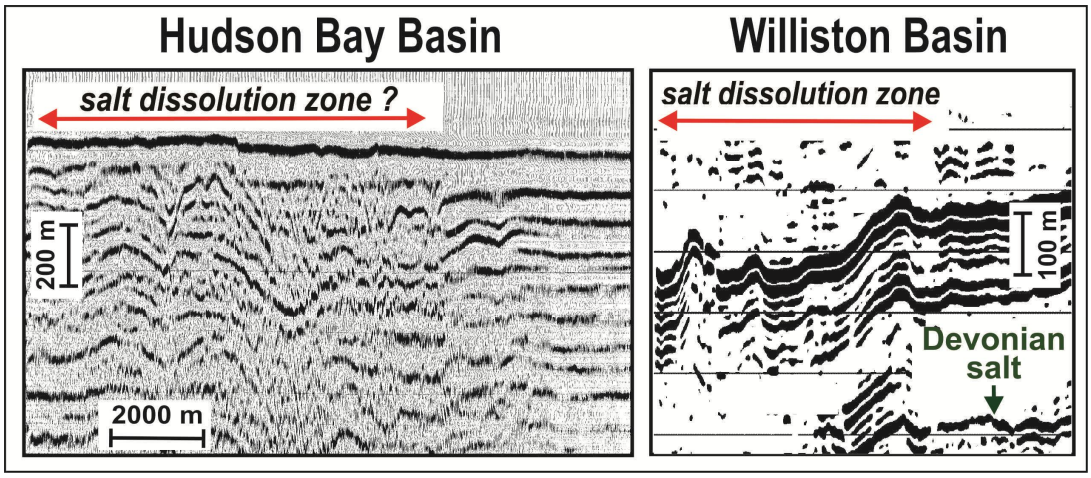

Figure 83: Seismic profiles illustrating deformation in Paleozoic strata in the Hudson Bay Basin (left panel; this study) and Williston Basin (right panel; Hamid et al., 2005) related to possible and known salt dissolution. The structural features in the Williston Basin section (anticlines, synclines and faults) formed as a result of dissolution of Middle Devonian salt.

3.7.2 Unconventional Oil Shale Plays

Oil shale plays may be present in Ordovician and Devonian strata, in the Hudson Bay and Moose River basins, respectively (Fig. 84). Mining or in-situ extraction of oil-shale resources may be possible where low maturity, organic-rich shales occur at or near surface, such as known in the Upper Ordovician Red Head Rapids Formation in Southampton Island (northern Hudson Bay Basin) and Upper Devonian Long Rapids Formation in the James Bay Lowlands (Moose River Basin). Geochemical analyses indicate some Ordovician oil shales in Southampton Island have high oil-yield potential (>100 kg hydrocarbon/tonne; Macauley, 1986; Zhang, 2008).

The economic potential of oil shales in these remote regions is not well known. Macauley (1986) considered the mapped high-yield shale beds on Southampton Island to be too thin for commercial development. Limited analyses indicate the (thicker) Devonian oil shales in the Moose River Basin have oil yields and organic content that are generally below (geochemical) thresholds for economic extraction of oil resources (Macauley, 1981; Bezys and Risk, 1990).

3.7.3 Unconventional Shale Gas Play

A shallow biogenic shale gas play, similar to the Antrim Shale Play in the Michigan Basin, may be present in Upper Devonian strata (Long Rapids Formation) in parts of the Hudson Platform (Fig. 85; Hamblin, 2006). The Long Rapids Formation is a shale-dominant, thermally immature succession in the upper part of the offshore Hudson Bay Basin and onshore Moose River Basin. The formation contains organic-rich black shales, with measured TOC values up to 11%. The Antrim Play (unconventional analog) is associated with fractured Upper Devonian shales, at the northern margin of the Michigan Basin (Fig. 85). Organic-rich black shales comprise both the source and reservoir for the gas accumulations. Antrim organic units are thermally immature and the contained hydrocarbons are considered to be part of a late-generation biogenic gas system (Shurr and Ridgley, 2002). Gas generation is believed to be related to near-surface microbial activity, controlled in part by incursions of glacial melt waters into organic-rich beds (Martini et al., 1998). Quaternary glacial loading and unloading controlled key aspects of play development, including formation fracturing and gas generation. Post-glacial rebound/uplift may have enhanced fracturing and gas production potential. Over 9000 wells have been drilled in the Antrim Shale Play in northern Michigan, with cumulative gas production (to 2008) of 2.5 Tcf and estimated total recoverable gas resources of 20 Tcf (Dolton and Quinn, 1996; Goodman and Maness, 2008).

The geology and glacial history of the Hudson Platform indicates the potential for biogenic gas plays, similar to the Antrim Shale. The Long Rapids Formation in the onshore Moose River Basin (northern Ontario) may be the most prospective unconventional play, in terms of exploration viability.

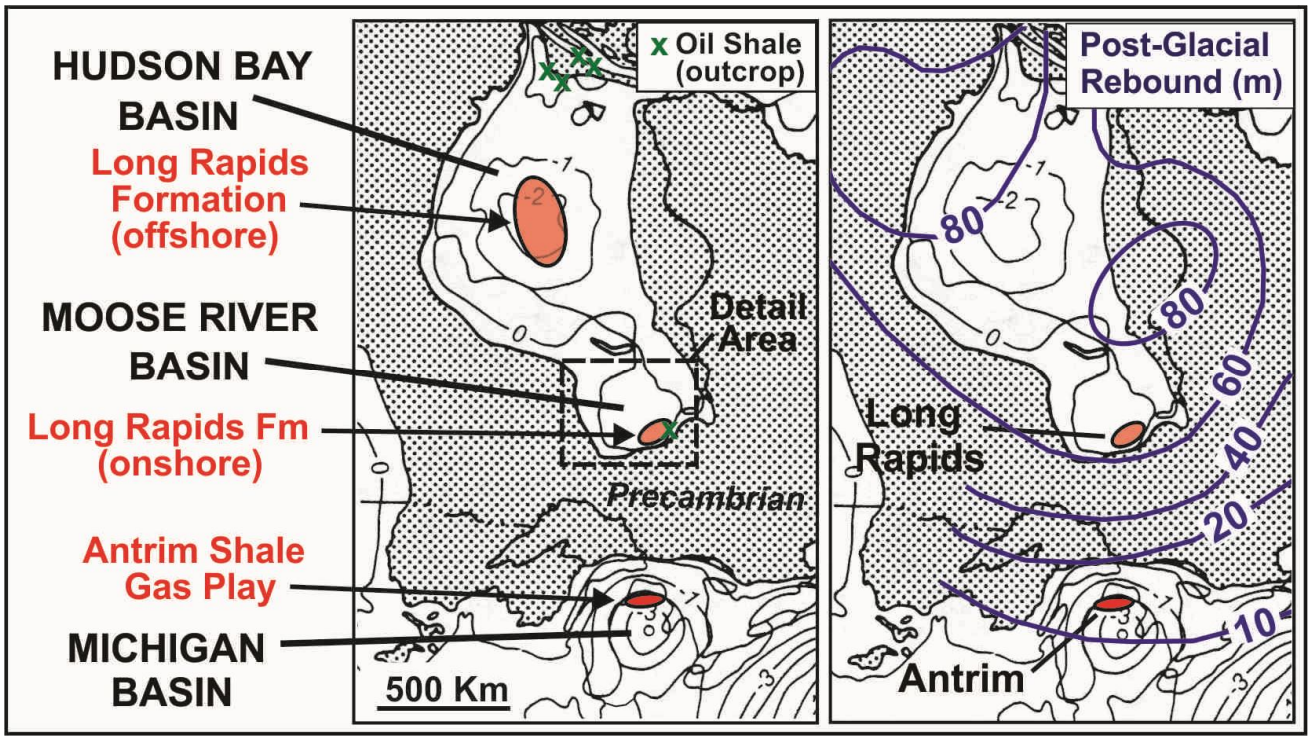

Figure 84. Sedimentary isopach map of the Hudson, Moose River and Michigan basins, with locations of known or possible unconventional petroleum plays, including Ordovician oil shale in the northern Hudson Bay Basin, Devonian oil shale in the Moose River Basin, and Upper Devonian biogenic shale gas in the Hudson and Moose River basins (Long Rapids Formation) and Michigan Basin (Antrim Shale). Detail map of the Moose River Basin illustrated in Figure 13. Right panel illustrates approximate magnitude of post-glacial uplift/rebound in the Hudson and Michigan basin areas (modified from Dutch, 2011). Glacial loading and unloading (rebound) are considered important factors in development of the Michigan Basin Antrim Shale Gas Play.

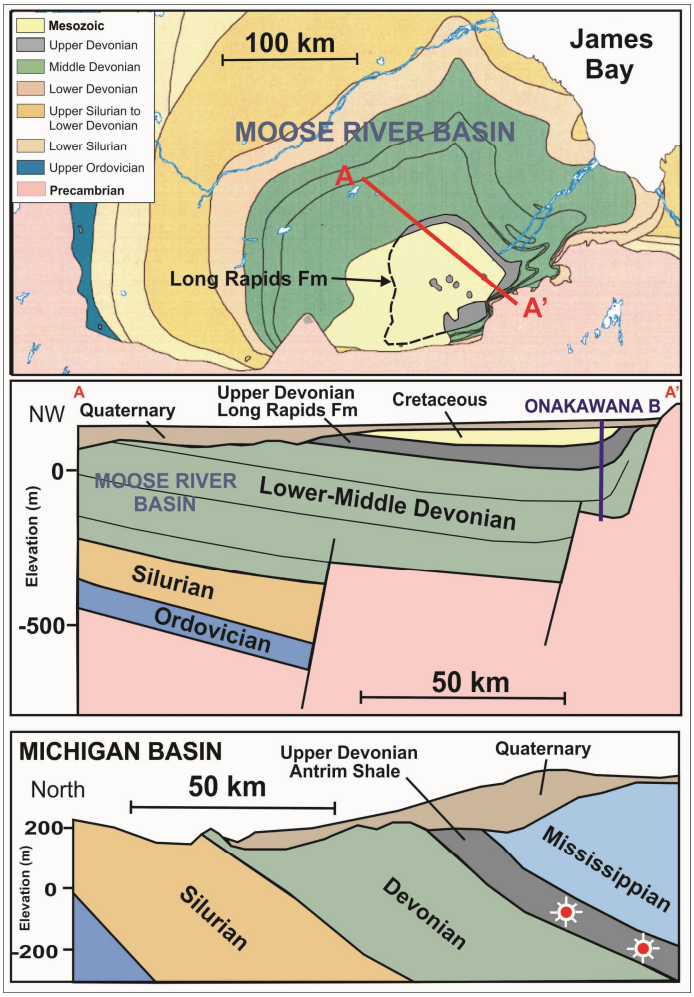

Figure 85: Geological map of the onshore Moose River Basin (top panel; adapted from Armstrong and Lavoie, 2010), with location of the Upper Devonian Long Rapids Formation (outcrop and subcrop) and illustrated cross-section A-A' (middle panel; modified from Sanford and Grant, 1998). The Onakawana B well penetrated 80 m of Upper Devonian (Long Rapids) strata, including abundant organic-rich black shale intervals (Bezys, 1989). Bottom panel illustrates a comparative cross-section of the northern Michigan Basin and geological setting of the Antrim Shale Gas Play (modified from Martini et al., 2008). Gas trapping may be controlled by hydrodynamic flow and water blocking at the formation subcrop (Dolton and Quinn, 1996).

3.7.4 Proterozoic Structure Play

The Hudson Bay Basin overlies an indented segment of the Paleoproterozoic Trans-Hudson Orogen (Fig. 86). In eastern Hudson Bay, the margin of the Trans-Hudson Orogen (Churchill-Superior Boundary Zone) is marked by the Belcher and Cape Smith fold belts.

Surface exposures indicate these tectonic belts consist of tightly folded and reverse faulted metasedimentary and igneous rocks (with little or no petroleum potential). Seismic data indicate an adjacent tectonic domain (referred to as the Winisk Basin) contains broad open folds, few or no faults, and a more stratified succession, indicating the possible presence of

younger (Mesoproterozoic or Neoproterozoic) strata. The presence of petroleum reservoir and source rocks in the Winisk Basin succession is unknown, but other Middle-Late Proterozoic cratonic basins in central North America and Greenland (including the Borden, Hecla-Fury and Thule basins, and the Mid-Continent Rift; Fig. 86) contain thick sequences of unmetamorphosed carbonate and clastic strata, including organic-rich black shales (potential petroleum source rocks). If similar petroleum system elements were present in the Proterozoic Winisk Basin, the large anticlinal structures would form a prospective exploration play.

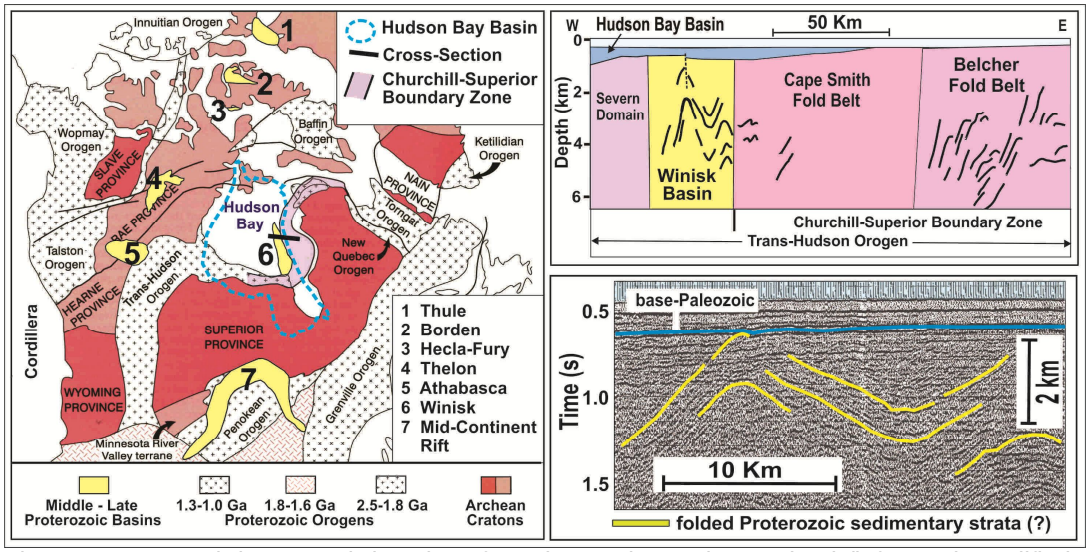

Figure 86: Precambrian crustal domains of North America and Greenland (left panel; modified from Card and Poulsen, 1998) with locations of Middle-Late Proterozoic sedimentary basins, including the geophysically interpreted Winisk Basin in Hudson Bay. A cross-section derived from seismic and potential field data (top right panel; modified from Roksandic, 1987) illustrates interpreted Precambrian crustal domains and structures beneath eastern Hudson Bay. Numerous, large anticlinal structures occur in the Winisk Basin (example in bottom right panel).

ACKNOWLEDGEMENTS

Many other people and organizations were associated to this project. First and foremost, sincere thanks to Keith Dewing (GSC-C) for his leadership of the GEM program, his comments and advice throughout the course of this project and his in-depth, patient and critically important review of this report. Martin Fowler (former GSC-C) provided important guidance at the start of this program and helped in focussing this project. Andy Mort (GSC-C) kindly reviewed the "type of organic matter" section. Brent Hogue of the National Energy Board (NEB) helped us to access the historical exploration database stored at NEB. Nancy Chow and Bob Elias (Manitoba University) defined and supervised number of B.Sc. Honours theses dealing with this project. Eric Prosh (recently deceased) and Peter Frampton (Nunavut government) for their continued support and interest in that project. ESS and provincial surveys managers who believed in that

project in a real frontier area. Finally, to all ESS, academia and provincial geologists who helped in various ways during that project.

REFERENCES

Allen, P.A., Armitage, J.J., 2012. Cratonic basins. In: Tectonics of sedimentary basins: recent advances, Busby, C., and Azor, A. eds, Blackwell Publishing Ltd, p. 602-620.

Armitage, J.J., Allen, P.A., 2010. Cratonic basins and the long-term subsidence history of continental interiors. Journal of the Geological Society, London, 167, 61-70.

Armstrong, D.K., 2011. Re-evaluating the hydrocarbon resource potential of the Hudson Platform: interim results from northern Ontario. In: Summary of field work and other activities 2011, Ontario Geological Survey, Open File Report 6270, p.27-1 to 27-11.

Armstrong, D., 2012. Project Unit 10-028. Update on the Hudson Platform Paleozoic mapping project: Results from the Northwestern Moose River Basin. In: Summary of field work and other activities 2012, Ontario Geological Survey, Open File Report 6280, p.30-1 to 30-8.

Armstrong, D.K. and Lavoie, D. 2010a. Re-evaluating the hydrocarbon resource potential of the Hudson Platform: project introduction and preliminary results from northern Ontario. In: Summary of field work and other activities 2010, Ontario Geological Survey, Open File Report 6260, p. 39-1 to 39-9.

Armstrong, D.K. and Lavoie, D. 2010b. Re-appraisal of the hydrocarbon resource potential of the Hudson Platform: project introduction and preliminary results from northern Ontario. In: Proceedings of the Ontario Petroleum Institute, 49th Annual Conference, Niagara Falls, Ontario, Technical Paper 15, 12p.

Armstrong, D.K. and Lavoie, D. in preparation. The Hudson Platform in northern Ontario: New insights into a frontier region. In: Proceedings of the Ontario Petroleum Institute, 51st Annual Conference, Niagara Falls, Ontario, Technical Paper 17.

Bell, R., 1884. Observations on the geology, mineralogy, zoology and botany of the Labrador Coast, Hudson's Strait and Bay. Geological Natural History Survey, Annual Report 1885, part DD.

Bell, R., 1885. Report of the second Hudson Bay's expedition under the command of Lieutenant A.R. Gordon, R.N., 1885. Canada Department of Marine Fisheries.

Bell, R. 1887. Report on an exploration of portions of the At-ta-wapish-kat and Albany Rivers, Lonely Lake to James' Bay. Geological Survey of Canada, Summary Report 1886, Part G, p. 1-38

Bertrand, R. 1990. Correlations among the reflectance of vitrinite, chitinozoans, graptolites and scolecodonts. Organic Geochemistry, v. 15, p. 565-574.

Bertrand, R. 1993. Standardization of solid bitumen reflectance to vitrinite in some Paleozoic sequences of Canada. Energy Sources Journal, v. 15, p. 269-288.

Bertrand, R. and Héroux, Y. 1987. Chitinozoan, graptolite, and scolecodont reflectance as an alternative to vitrinite and pyrobitumen reflectance in Ordovician and Silurian strata, Anticosti Island, Quebec, Canada. American Association of Petroleum Geologists Bulletin, v. 71, p. 951-957.

Bertrand R. and Malo, M. 2001. Source rock analysis, thermal maturation, and hydrocarbon generation in the Siluro-Devonian rocks of the Gaspé Belt basin, Canada. Bulletin of Canadian Petroleum Geology, v. 49, p. 238-261.

Bertrand, R. and Malo, M. 2012. Dispersed organic matter reflectance and thermal maturation in four hydrocarbon exploration wells in the Hudson Bay Basin: regional implications; Geological Survey of Canada, Open File 7066, 52 p.

Bezys, R.K., 1989. The Onakawana B Drillhole, District of Cochrane: Report on drilling operations and preliminary geological findings. Ontario Geological Survey, Open File 5708.

Bezys, R.K. and Risk, M.J., 1990. The Long Rapids Formation: an Upper Devonian black shale in the Moose River Basin, northern Ontario; Canadian Journal of Earth Sciences, v. 27, p. 291-305.

Blackadar, R.G., 1956. Geological reconnaissance of Admirality Inlet, Baffin Island, Arctic Archipelago, Northwest Territories. Geological Survey of Canada paper 55-6.

Blackwell, D. and Richards, M., 2004. Geothermal Map of North America. American Association of Petroleum Geologist, 1 sheet, 1:6,500,000.

Card, K.D. and Poulsen, K.H., 1998. Geology and mineral deposits of the Superior province of the Canadian shield. In Geology of the Precambrian Superior and Grenville Provinces and Precambrian fossils in North America. Geological Society of America, The geology of North America, v. C-1, p. 15 – 204

Cherns, L., and Wheeley. J.R., 2009. Early Palaeozoic cooling events: Peri-Gondwana and beyond. Geological Society Special Publication, v. 325, p. 257-278.

Chow, A.M.C., 1986. Sedimentology and paleontology of the Attawapiskat Formation (Silurian) in the type area, northern Ontario. M.Sc. thesis, McGill University, Montréal.

Chow, A.M.C. and Stearn, C.W., 1989. Attawapiskat patch reefs, Lower Silurian, Hudson Bay Lowlands, Ontario. In: Reefs, Canada and Adjacent Area, H.H.J. Geldsetzer, N.P. James and G.E. Tebbutt (eds.); Canadian Society of Petroleum Geologists, Memoir 13, p. 263-270.

Christie, R.L., 1972. Central stable region. In The Canadian Arctic Islands and the Mackenzie region. XXIV International Geological Congress, Canada, 1972. Excursion A66, p. 40-87.

Crain, E.R., 1986. The log analysis handbook, vol.1, Quantitative log analysis methods, p.220, p.301.

Craven, J., and Roberts, B. 2012. High resolution audiomagnetotelluric investigation of the porosity at the margin of the Hudson Bay Basin, Canada. Fall meeting American Geophysical Union, San Francisco. Abstract.

Cumming, L.M. 1971. Ordovician strata of the Hudson Bay Lowlands in northern Manitoba. In: Geoscience Studies in Manitoba. A.C. Turnock (ed.). Geological Association of Canada, Special Paper no. 9, p. 189-197.

Cumming, L.M. 1975. Ordovician strata of the Hudson Bay Lowlands; Geological Survey of Canada, Paper 74-28, 93p.

Davies, G.R. and Smith, L.B. 2006. Structurally controlled hydrothermal dolomite facies: An overview. Bulletin of the American Association of Petroleum Geologists, v. 90, p. 1641-1690.

Decker, V. Budkewitsch, P. and Tang, W., 2013. Reconnaissance mapping of suspect oil seep occurrences in Hudson Bay and Foxe Basin using satellite radar. Geological Survey of Canada, Open File 7070, 23 p.

Dewing, K. and Sanei, H., 2009. Analysis of large thermal maturity datasets: Examples from the Canadian Arctic Islands. International Journal of Coal Geology, v. 77, p. 436-448.

Dietrich, J.R. and Magnusson, D.H., 1988. Basement controls on Phanerozoic development of the Birdtail-Waskada salt dissolution zone, Williston Basin, Southwestern Manitoba. In: J.E. Christopher, C.F. Gilboy, D.F. Paterson and S.J. Bend, (eds.) Eight International Williston Basin Symposium. Saskatchewan Geological Society Special Publication No. 13, p. 166-174.

Dolby, G. 1986. The micropaleontology, palynology and the stratigraphy of the Trillium et al. Beluga O-23 well. Report for Cantera Energy by Dolby Canada Ltd. 7 p.

Dolton, G.L. and Quinn, J.C., 1996. An initial resource assessment of the Upper Devonian Antrim Shale in the Michigan Basin. U.S. Geological Survey, Open File 95-75K.

Douglas, R.J.W., Gabrielse, H. Wheeler, J.O., Stott, D.F., and Belyea, H.R., 1970. Geology of western Canada. In: Geology and economic minerals of Canada. Geological Survey of Canada, Economical Geology Report 1., 5th edition, p. 367-488.

Duncan, B.J. 2012. Stratigraphy and facies analysis of uppermost Ordovician to lowermost

Silurian strata in the Whitebear core, Hudson Bay Basin, northern Manitoba; University of Manitoba, Department of Geological Sciences, B.Sc. Honours Thesis, 192 p.

Duk-Rodkin, A., Hugues, O.L., 1994. Tertiary-Quaternary drainage of the pre-glacial Mackenzie Basin. Quaternary International, vol. 22/23, p. 221-241.

Dutch, S., 2011. Crustal Deformation. University of Wisconsin-Green Bay, Earth Science (102), Notes and Presentations

Dyer, W.S., 1928. Geology and economic deposits of the Moose River Basin, Ontario. Department of Mines, Vol. XXXVII, pt. 6, p. 1-69.

Dyer, W.S. 1929: Limestones of the Moose River and Albany River basin. Ontario Department of Mines, Vol. XXXVIII, pt. 4, p. 31-33

Dyer, W.S., and Crozier, A.R. 1933. Lignite and refractory clay deposits of the Onakawana lignite field. Ontario Department of Mines, Vol. XLII, pt. 3, p. 46-78.

Eaton, D.W., Darbyshire, F., 2009. Lithospheric architecture and tectonic evolution of the Hudson Bay region, Tectonophysics, vol. 480, p. 1-22.

Espitalie, J., Deroo, G., Marquis, F., 1985. Rock Eval pyrolysis and its applications. Preprint; Institut Français du Pétrole, Géologie No. 27299, 72 p. English translation of: La pyrolyse Rock-Eval et ses applications, Première, Deuxième et Troisième Parties. Revue de l'Institut Français du Pétrole v. 40, 563–579 and 755–784; v. 41, 73–89.

Galloway, J.M., Armstrong, D.A. and Lavoie, D. 2011. Palynology of the INCO-Winisk #49204 core (54˚18’30”N, 87˚02’30”W, NTS 43L/6) Open File 7065, 51 p.

Gao, C., McAndrews, J.H., Wang, X., Menzies, J., Turton, C.L., Wood, B.D., Pei, J. and Kodors, C. 2012. Glaciation of North America in the James Bay Lowland, Canada, 3.5 Ma. Geology, vol. 40, p. 975-978.

Goodman, W.R. and Maness, T.R., 2008. Michigan’s Antrim gas shale play - a two decade template for successful Devonian gas development. American Association of Petroleum Geologists, Search and Discovery Article 10158.

Hamblin, A.P., 2006. The Shale Gas concept in Canada: a preliminary inventory of possibilities. Geological Survey of Canada, Open File 5384.

Hamblin, A.P. 2008. Hydrocarbon potential of the Paleozoic succession of Hudson Bay Bay/James Bay: Preliminary conceptual synthesis of background data. Geological Survey of Canada, Open File 5731, 12 p., 3 figs.

Hamid, H., Morozov, I.B., and Kreis, L.K., 2005. Seismic delineation of the Prairie Evaporite dissolution edge in south-central Saskatchewan. In: Summary of Investigations 2005, Volume 1, Saskatchewan Geological Survey, Saskatchewan Industry Resources, Misc. Rep. 2005-4.

Henderson, P.J. 1990. Provenance and depositional facies of surficial sediments in Hudson Bay, a glaciated epeiric sea. Thesis of Ottawa-Carleton Geoscience Centre, 288 p.

Heywood, W.W. and Sanford, B.V. 1976: Geology of Southampton, Coats, and Mansel Islands, District of Keewatin, Northwest Territories. Geological Survey of Canada, Memoir 382, 35 p.

Hovland, M., Judd, A.G., and King, L.H. 1984. Characteristic features of pockmarks on the North Sea Floor and Scotian Shelf. Sedimentology, vol. 31, p. 471-480.

Hovland, M. and Judd, A. 1988. Seabed pockmarks and seepages. Graham and Trotman Inc., Sterling House, London, 293pp

Howell, P.D., van der Pluijm, B.A., 1999. Structural sequences and styles of subsidence in the Michigan basin. Geological Society of America Bulletin, vol. 111, p. 974-991.

Hu, K., Dietrich, J., Dewing, K., Zhang, S., Asselin, E., Pinet, N. and Lavoie, D. 2011. Stratigraphic correlations for five offshore wells in the Hudson Bay Basin, northern Canada; Geological Survey of Canada, Open File 7031. doi:10.4095/289545.

Hu, K. and Dietrich, J. 2012. Reservoir characterization of five offshore wells in the Hudson Bay Basin, Northern Canada. Geological Survey of Canada, Open File 7052.

Hunt, J.M. 1996. Petroleum geochemistry and geology. Second edition. Freeman and Company, New-York, 743 p.

Hurley, N.F. and Budros, R. 1990. Albion-Scipio and Stoney Point fields – USA Michigan Basin. In: Stratigraphic traps 1. E.A. Beaumont and N.H. Foster (eds.). American Association of Petroleum Geologists, Treatise of Petroleum Geology, Atlas of Oil and Gas fields, p. 1-38.

Jacob, H.J., 1989. Classification, structure genesis and practical importance of natural solid oil bitumen (« migrabitumen »). International Journal of Coal Geology, v. 11, p. 65-79.

Jefferson, C.W., Hamilton, S.M., 1987. Structure and stratigraphy of the Paleozoic-Precambrian contact zone on White and Southampton islands, district of Keewatin. In: Current Research, Part A, Geological Survey of Canada, Paper 87-1A, p. 451-455.

Jin, J., Caldwell, W.G.E., and Norford, B.S. 1993. Early Silurian brachiopods and biostratigraphy of the Hudson Bay Lowlands, Manitoba, Ontario, and Quebec. Geological Survey of Canada, Bulletin 457, 221 p.

Jin, J., Caldwell, W.G.E., and Norford, B.S. 1997. Late Ordovician brachiopods and biostratigraphy of the Hudson Bay Lowlands, northern Manitoba and Ontario; Geological Survey of Canada, Bulletin 513, 115 p.

Johnson, M.D., Armstrong, D.K., Sanford, B.V., Telford, P.G. and Rutka, M.A. 1992. Paleozoic and Mesozoic geology of Ontario. In: Geology of Ontario, Ontario Geological Survey, Special Volume 4, Part 2, p.907-1008.

Johnson, R.D., 1971. Petroleum potential of Hudson Bay Basin studied. Oilweek, v. 22, no. 12, p. 40, 43, 52.

Johnson, R. D. and Nelson, S. J. 1969. Sogepet-Aquitaine Kaskattama Province No. 1 well, Hudson Bay Lowland, Manitoba; Geological Survey of Canada, Paper 68-53, 215-226 p.

Kaminski, E., and Jaupart, C., 2000. Lithospheric structure beneath the Phanerozoic intracratonic basins of North America. Earth and Planetary Science Letters, vol. 178, pl 139-149.

Keele, J. 1920. The Abitibi and Mattagami rivers north of the National Transcontinental Railway, III. Clay and shale deposits; Ontario Bureau of Mines, Vol. XXIX, pt. 2, p. 31-55.

Kindle, E.M., 1924. Geology of a portion of the northern part of Moose River Basin, Ontario. Geological Survey of Canada, Summer Report 1923, part C1, p. 21-24.

King, L.H. and MacLean, B. 1970. Pockmarks on the Scotian Shelf. Geological Society of America Bulletin, vol. 81 p. 3141-3148.

Klapper, G., Uyeno, T.T., Armstrong, D.K. and Telford, P.G. 2004. Conodonts of the Williams Island and Long Rapids formations (Upper Devonian, Frasnian-Famennian) of the Onakawana B drillhole, Moose River Basin, northern Ontario, with a revision of Lower Frasnian species. Journal of Paleontology, vol. 78, p.371-387.

Larsson, S.Y., and Stearn, C.W. 1986. Silurian stratigraphy of the Hudson Bay Lowlands in Quebec. Canadian Journal of Earth Sciences, vol. 23, p. 288-299.

Lavoie, D., and Chi, G. 2010. Lower Paleozoic foreland basins in eastern Canada: tectono-thermal events recorded by faults, fluids and hydrothermal dolomites. Bulletin of Canadian Petroleum Geology, vol. 58, p. 17-35.

Lavoie, D., Pinet, N. and Zhang, S. 2011. Hydrothermal dolomites in Hudson Bay platform: preliminary field and geochemical data. Geological Survey of Canada, Open File 7002, 22 p.

Lavoie, D., Jackson, S., and Girard, I. submitted. Magnesium isotopes in high-temperature saddle dolomite cements in the Lower Paleozoic of eastern Canada. Journal of Sedimentary Research.

LeFèvre, J. A., Barnes, C. R. and Tixier, M. 1976. Paleoecology of Late Ordovician and Early Silurian conodontophorids, Hudson Bay Basin. In: Conodont Paleoecology, C.R. Barnes (ed.), Geological Association of Canada, Special Paper, no. 15, p. 69-89.

Lemon, R.R.H., and Blackadar, R.G., 1963. Admirality Inlet area, Baffin Island, District of Franklin. Geological Survey of Canada, Memoir 328, 84 p.

Levman, B.G., and von Bitter, P.H. 2002. The Frasnian–Famennian (mid-Late Devonian) boundary in the type section of the Long Rapids Formation, James Bay Lowlands, northern Ontario, Canada. Canadian Journal of Earth Science, vol. 39, p.1795–1818.

Logan, G.A., Jones, A.T., Kennard, J.M., Ryan, G.J., and Rollet, N. 2010. Australian offshore natural hydrocarbon seepage studies, a review and re-evaluation. Marine and Petroleum Geology, vol. 27, p. 26-45.

Macauley, G., 1981. Geology of the Oil Shale deposits of Canada. Geological Survey of Canada, Open File 754.

Macauley, G. 1986. Geochemistry of the Ordovician Boas Oil Shale, Southampton Island, Northwest Territories. Geological Survey of Canada, Open File 1285, 15 p.

Macauley, G., 1987. Geochemistry of organic-rich Ordovician sediments on Akpatok and Baffin Islands, Northwest Territories. Geological Survey of Canada, Open File 1502, 27 p.

Macauley, G., Fowler, M.G., Goodarzi, F., Snowdon, L.R., and Stasiuk, L.D. 1990. Ordovician oil shale — source rock sediments in the central and eastern Canada mainland and eastern Arctic areas, and their significance for frontier exploration. Geological Survey of Canada, Paper 90-14.

Martini, A.M., Walter, L., Budai, J., Ku, T., Kaiser, C., and Schoell, M., 1998. Genetic and temporal relations between formation waters and biogenic methane - Upper Devonian Antrim Shale, Michigan Basin, USA. Geochimica et Cosmochimica Acta, vol. 62, p. 1699-1720.

Martini, A.M., Walter, L.M., and McIntosh, J.C., 2008. Identification of microbial and thermogenic gas components from Upper Devonian black shale cores, Illinois and Michigan basins. Bulletin of the American Association of Petroleum Geologists, vol. 92, p. 327-339.

Martiniuk, C.D. 1992. Lower Paleozoic sequence, southwestern Manitoba - an overview; Manitoba Energy and Mines, Petroleum Branch, Petroleum Open File POF 13-92, 40 p.

Martison, N.W. 1953. Petroleum possibilities of the James Bay Lowland area; Ontario Department of Mines, Annual Report, v. 61, p. 1-58.

McCabe, H.R. 1971. Stratigraphy of Manitoba, an introduction and review; *in* Geoscience Studies in Manitoba, Special Paper 9, A. C. Turnock (ed.), Geological Association of Canada, p. 167-187.

McCracken, A.D. 1990. Report on 38 Ordovician conodont samples from drill core of the Bad Cache Rapids Formation, Boas River Formation, and Churchill River Group in the Hudson Bay Lowlands (Clendenning River Map Sheet, Winisk River area), northern Ontario submitted by B.V. Sanford (GSC-LCSD) and A.C. Grant (GSC-AGC) (NTS 43L/6, 43L/12); Geological Survey of Canada, Paleontological Report 03-ADM-1990, 30p.

McCracken, A.D. 2000: Middle and Late Ordovician conodonts from the Foxe Lowland of southern Baffin Island, Nunavut. Geological Survey of Canada, Bulletin 557, p. 159-216.

McCracken, A.D. and Bolton, T.E. (eds.), 2000: Geology and Paleontology of the southeast Arctic Platform and southern Baffin Island, Nunavut. Geological Survey of Canada, Bulletin 557, 248 p.

McCracken, A.D. and Nowlan, G.S. 1989. Conodont paleontology and biostratigraphy of Ordovician carbonates and petroliferous carbonates on Southampton, Baffin, and Akpatok islands in the eastern Canadian Arctic. Canadian Journal of Earth Sciences, vol. 26, p. 1880–1903.

McGregor, D.C. and Camfield, M., 1976. Upper Silurian? to Middle Devonian spores of the Moose River Basin, Ontario. Geological Survey of Canada, Bulletin 263, 63p.

McGregor, D.C., Sanford, B.V. and Norris, A.W. 1970. Palynology and correlation of Devonian formations in the Moose River Basin, northern Ontario. Geological Association of Canada, Proceedings, vol. 22, p. 45-54.

Morrow, D.W., 1982. Descriptive field classification of sedimentary and diagenetic breccia fabrics in carbonate rocks. Bulletin of Canadian Petroleum Geology, vol. 30, p. 227-229.

Nelson, S. J. 1963. Ordovician paleontology of the northern Hudson Bay Lowland; Geological Survey of Canada, Memoir 90, 152 p.

Nelson, S.J., 1964. Ordovician stratigraphy of northern Hudson Bay Lowland, Manitoba; Geological Survey of Canada, Bulletin 108, 36 p.

Nelson, S.J. and Johnson, R.D. 1966. Geology of Hudson Bay Basin. Bulletin of Canadian Petroleum Geology. v. 14, p. 520–578.

Nicolas, M.P.B. 2011. Stratigraphy of three exploratory oil-well cores in the Hudson Bay Lowland, northeastern Manitoba (parts of NTS 54B10, F8, G1). In: Report of Activities 2011, Manitoba Innovation, Energy and Mines, Manitoba Geological Survey, p. 165-170.

Nicolas, M.P.B. 2012. Stratigraphy and regional geology of the Late Devonian-Early Mississippian Three Forks Group, southwestern Manitoba (NTS 62F, part of 62G, K); Manitoba Innovation, Energy and Mines, Manitoba Geological Survey, Geoscientific Report GR2012-3, 92 p.

Nicolas, M P.B. and Barchyn, D. 2008. Williston Basin Project (Targeted Geoscience Initiative II): summary report on Paleozoic stratigraphy, mapping and hydrocarbon assessment, southwestern Manitoba. Manitoba Science, Technology, Energy and Mines, Manitoba Geological Survey, Geoscientific Paper GP2008-2, 21 p.

Nicolas, M.P.B. and Lavoie, D. 2009. Hudson Bay and Foxe Basins Project: introduction to the Geo-mapping for Energy and Minerals, GEM–Energy initiative, northeastern Manitoba (parts of NTS 54). In: Report of Activities 2009, Manitoba Innovation, Energy and Mines, Manitoba Geological Survey, p. 160–164.

Nicolas, M.P.B. and Lavoie, D., 2010. Hudson Bay and Foxe Basins Project: update on a Geo-mapping for Energy and Minerals program (GEM) initiative, northeastern Manitoba (part of NTS 54). In: Report of Activities 2010, Manitoba Science, Technology, Energy and Mines, Manitoba Geological Survey, p. 186-192.

Nicolas, M.P.B. and Lavoie, D. 2012a. Oil shale and reservoir rocks of the Hudson Bay Lowland, northeastern Manitoba (part of NTS 54). In: Report of Activities 2012, Manitoba Innovation, Energy and Mines, Manitoba Geological Survey, p. 124-133.

Nicolas, M.P.B. and Lavoie, D. 2012b. Oil shale and reservoir rocks of the Hudson Bay Lowland, northeastern Manitoba (part of NTS 54). Manitoba Innovation, Energy and Mines, Manitoba Geological Survey, Data Repository Item DRI2012002, Microsoft® Excel® file.

Nicolas, M.P.B., Lavoie, D. and Armstrong, D.K. 2012. Oil shale and reservoir rocks of the Hudson Bay Lowland, northeastern Manitoba. Manitoba Innovation, Energy and Mines, Manitoba Geological Survey, Manitoba Mines and Minerals Convention, Nov. 15-17, 2012, poster.

Norford, B.S. 1971. Silurian stratigraphy of northern Manitoba. In: Geoscience Studies in Manitoba, A. C. Turnock (ed.), Geological Association of Canada, Special Paper 9, p. 199-207.

Norford, B.S., Nowlan, G.S., Haidl, F.M. and Bezys, R.K. 1998. The Ordovician-Silurian boundary interval in Saskatchewan and Manitoba. In: Eighth International Williston Basin Symposium, Saskatchewan Geological Society Special Publication No. 13, J. E. Christopher and C. F. Gilboy (eds.), p. 27-45.

Norris, G. 1977. Palynofloral evidence for terrestrial Middle Jurassic in the Moose River Basin, Ontario. Canadian Journal of Earth Sciences, vol. 14, p.1 53-158.

Norris, A.W. 1986. Chapter 2 : Review of Hudson Platform Paleozoic Stratigraphy and Biostratigraphy. Elsevier Oceanography Series, v. 44, Issue C, p. 17-42.

Norris, A.W. 1993. Hudson Platform – Geology. In: Sedimentary cover of the craton in Canada. D.F. Stott and J.D. Aitken (eds.). Geological Survey of Canada, Geology of Canada, no.

5, p. 653–700 (also Geological Society of America, The Geology of North America, vol. D-1).

Norris, A.W., Uyeno, T.T., and McCabe, H.R. 1982. Devonian rocks of the Lake Winnipegosis - Lake Manitoba outcrop belt, Manitoba. Geological Survey of Canada, Memoir 392, 280 p.

Ontario Geological Survey 1991a. Bedrock geology of Ontario, northern sheet; Ontario Geological Survey, Map 2541, scale 1:1 000 000.

Ontario Geological Survey 1991b. Bedrock geology of Ontario, east-central sheet; Ontario Geological Survey, Map 2543, scale 1:1 000 000.

Parry, W.E., 1824. Journal of a second voyage for the discovery of a north-west passage from the Atlantic to the Pacific performed in the years 1821-22-23 in His Majesty's ship Fury and Hecla under the orders of Captain William Edward Parry… Commander of the expedition. John Murray, London, 601 p.

Parry, W.E., 1825. Journal of a third voyage for the discovery of a north-west passage from the Atlantic to the Pacific performed in the years 1824-25 in His Majesty's ship Fury and Hecla under the orders of Captain William Edward Parry… Commander of the expedition. John Murray, London, 179 p.

Patchett, P.J., Embry, A.F., Ross, G.M., Beauchamp, B., Harrison, J.C., Mayr, U., Isachsen, C.E., Rosenberg, E.J., and Spence, G.O. 2004. Sedimentary cover of the Canadian Shield through Mesozoic time reflected by Nd isotopic and geochemical results for the Sverdrup Basin, Arctic Canada. The Journal of Geology, vol.112, p. 39-57.

Peters, K..E. 1986: Guidelines for evaluating petroleum source rock using programmed pyrolysis; American Association of Petroleum Geologist Bulletin, v. 70, p. 318-329.

Peters, K.E., Fraser, T.H., Amris, W., Rustanto, B., Hermanto, E., 1999. Geochemistry of crude oil from eastern Indonesia, American Association of Petroleum Geologists Bulletin v. 83, p. 1927–1942.

Pietrus, E. 2013. Sedimentological analysis and petroleum reservoir potential of the Hudson Bay Basin, northeastern Manitoba. University of Manitoba, Department of Geological Sciences, B.Sc. Honours Thesis, 73 p.

Pinet, N., Duchesne, M., Lavoie, D., Bolduc, A., and Long, B. 2008. Surface and subsurface signatures of gas seepage in the St. Lawrence Estuary (Canada): Significance to hydrocarbon exploration. Marine and Petroleum Geology, vol. 25 p. 271-288.

Pinet, N., Lavoie, D., Dietrich, P., Hu, K., and Keating, P. 2013a. Architecture and subsidence history of the Hudson Bay intracratonic basin. Earth Science Reviews, v. 125, p. 1-23.

Pinet, N., Keating, P., Lavoie, D., 2013b. Did the Hudson Strait in Arctic Canada record the opening of the Labrador Sea? Marine and Petroleum Geology, v. 48, p. 354-365.

Powell, T. G. and Snowdon, L. R., 1983. A composite hydrocarbon generation model. Erdöl und Kohle, Erdgas, Petrochemie, vol. 36, p. 163-170.

Procter, R.M., Taylor, G.C., and Wade, J.A., 1984. Oil and Natural Gas resources of Canada; Geological Survey of Canada, Paper 83-31, 59 p.

Quinlan, G.M., 1987. Models of subsidence mechanisms in intracratonic basins, and their applicability to North American examples. In: Beaumont, C. and Tankard, A.J., (Eds.), Sedimentary basins and basin-forming mechanisms, Canadian Society of Petroleum Geologists, Memoir 12, p. 463-481

Ramdoyal, A., 2012. Lithofacies Analysis, Diagenesis and Petroleum Reservoir Potential of the Lower Silurian Attawapiskat Formation, Hudson Bay Basin, Northeastern Manitoba. Bsc thesis, University of Manitoba, 124 p.

Reyes, J., Armstrong, D. and Lavoie, D. 2011. Organic petrology of James Bay Basin. Ontario Petroleum Institute, 50th Annual meeting.

Roberts, B. and Craven, J., 2012. Results of a magnetotelluric survey in Churchill, Manitoba: GEM Energy, Hudson Bay. Geological Survey of Canada, Open File 7151, 21 p. doi: 10.4095/291442

Roksandic, M.M., 1987. The tectonics and evolution of the Hudson Bay region. In: Beaumont, C. and Tankard, A.J., Eds, Sedimentary basins and basin-forming mechanisms, Canadian Society of Petroleum Geologists, Memoir 12, p. 507-518.

Roger, J., Duchesne, M.J., Lajeunesse, P., St-Onge, G., and Pinet, N. 2011. Imaging pockmarks and ring-like features in Hudson Bay from multibeam bathymetry data. Geological Survey of Canada Open File 6760, 19 p.

Rudkin, D. M., Young, G. A., Elias, R. J. and Dobrzanski, E. P. 2003. The world's biggest trilobite - *Isotelus rex* - new species from the Upper Ordovician of northern Manitoba, Canada. Journal of Paleontology, vol. 77, p. 99-112.

Sanford, B.V. 1977. Ordovician rocks of Melville Peninsula, southeastern District of Franklin. In: Geology of Ordovician rocks, Melville Peninsula and region, southeastern District of Franklin. *by* T.E. Bolton, B.V. Sanford, M.J. Copeland, C.R. Barnes, and Rigby, J.K. (eds.) Geological Survey of Canada Bulletin 269, pp. 7–21.

Sanford, B.V. 1987: Paleozoic geology of Hudson Platform. In: Beaumont, C. and Tankard, A.J. (Eds.), Sedimentary basins and basin forming mechanism. Canadian Society of Petroleum Geologists, Memoir 12, p. 483-505.

Sanford, B.V. and Grant, A.C. 1990: New findings relating to the stratigraphy and structure of the Hudson Bay Platform. Current Research, Part D; Geological Survey of Canada, Paper 90-1D, P. 17-30.

Sanford, B. V. and Grant, A.C. 1993. Recent Advances in the geology of the Hudson Platform. In: Sedimentary Cover of the Craton in Canada, D. F. Stott and J. D. Aitken (eds.), Geological Survey of Canada, Geology of Canada (Seventh Edition), no. 5, p. 687-689.

Sanford, B.V., and Grant, A.C. 1998. Paleozoic and Mesozoic Geology of the Hudson Bay and Southeast Arctic Platforms. Geological Survey of Canada, Open File 3595, 2 sheets.

Sanford, B.V. and Grant, A.C. 2000: Geological framework of the Ordovician System in the southeast Arctic Platform, Nunavut. Geological Survey of Canada, Bulletin 557, p. 13-38.

Sanford, B.V. and Norris, A.W. 1973. Devonian stratigraphy of the Hudson Platform. Geological Survey of Canada, Memoir 379.

Sanford, B.V. and Norris, A.W. 1973: The Hudson Platform – their geology and potential. In: Future petroleum provinces of Canada. R.G. McCrossan (ed.), Canadian Society of Petroleum Geologists, Memoir 1, p. 387-409.

Sanford, B.V. and Norris, A.W., 1975. Devonian rocks of the Moose River basin, Ontario/Quebec. Geological Survey of Canada, Open File 291,

Sanford, B.V., Norris, A.W. and Bostock, H.H. 1968. Geology of the Hudson Bay Lowlands (Operation Winisk); Geological Survey of Canada, Paper 67-60, 118p.

Savage, T. E. 1918. Correlation of the Early Silurian rocks in the Hudson Bay Region; Journal of Geology, vol. 26, p. 334-340.

Savage, T.E. and Van Tuyl, F.M., 1919. Geology and stratigraphy of the area of Paleozoic rocks in the vicinity of Hudson and James bays. Geological Society of America Bulletin, vol. 30, p. 339-378

Schlumberger, 1989. Log Interpretation Principles/Applications, p.8-1, p.10-3.

Searl, A. 1989. Saddle dolomite: a new view of its nature and origin. Mineralogical Magazine, vol. 53, p. 547-555.

Shields, G.A., Carden, G.A.F., Veizer, J., Meidla, T., Rong, J.-Y. and Li, R-Y. 2003. Sr, C and O isotope geochemistry of Ordovician brachiopods: A major isotopic event around the Middle-Late Ordovician transition. Geochimica et Cosmochimica Acta, vol. 67, p. 2005-2025.

Shurr, G.W. and Ridgley, J.L. 2002. Unconventional shallow biogenic gas systems. Bulletin American Association of Petroleum Geologists, vol. 86, p. 1939-1969.

Sloss, L.L., 1988. Tectonic evolution of the craton in Phanerozoic time. *In* Sloss, L.L. (ed), Sedimentary Cover – North America Craton, US. Geological Society of America, The Geology of North America, vol. D2, p. 25-51.

Smith, L.B. 2006. Origin and reservoir characteristics of Upper Ordovician Trenton-Black River hydrothermal dolomite reservoirs in New York, USA. Bulletin of the American Association of Petroleum Geologists, vol. 90, p. 1691-1718.

S.N.P.A., 1975. Aquitaine et al., Polar Bear C-11 well (Hudson bay, Canada) Geological and geochemical study. Available at the National Energy Board, 31 p.

St. Jean, N.F. 2012. Mineralogical, Petrographic and Geochemical Characterization of Organic-Rich Carbonate of the Upper Ordovician Boas River Formation in Northern Ontario: Implications for Petroleum Exploration; unpublished Bachelor of Science thesis, University of Ottawa, 61p.

Stoakes, F.A. 1978. Lower and Middle Devonian strata of the Moose River Basin, Ontario; Ontario Petroleum Institute Proceedings, vol. 17, Paper 4, 29p.

Suchy, D.R. 1992. Hudson Bay Platform: Silurian sequence stratigraphy and paleoenvironments. Ph.D. thesis, McGill University, Montreal, 192p.

Suchy, D.R., Stearn, C.W., 1992. Lower Silurian sequence stratigraphy and sea-level history of the Hudson Bay platform. Bulletin of Canadian Petroleum Geology, vol. 40,p. 335-355.

Suchy, D.R., Stearn, C.W., 1993. Lower Silurian reefs and post-reefs beds of the Attawapiskat Formation, Hudson Bay Platform, northern Ontario. Canadian Journal Earth Sciences, vol. 30, p. 575-590.

Summons, R.E. and Powell, T.G. 1986. Chlorobiaceae in Paleozoic seas revealed by biological markers, isotopes and geology. Nature, vol. 319, p. 763-765.

Summons, R.E. and Powell, T.G. 1987. Identification of aryl isoprenoids in source rocks and crude oils: biological markers for the green sulphur bacteria. Geochimica Cosmochimica Acta, vol. 51, p. 557-566.

Telford, P.G., 1988. Devonian stratigraphy of the Moose River Basin, James Bay Lowlands, Ontario. In: Devonian of the World, N.J. McMillan, A.F. Embry and D.J. Glass (eds.); Canadian Society of Petroleum Geologists, Memoir 14, Volume I, p. 123-132.

Telford, P.G. and Long, D.G.F. 1986. Mesozoic geology of the Hudson Platform; in Canadian Inland Seas, Elsevier Oceanographic Series 44, Elsevier Science Publishers, New York, p. 43-54

Telford, P.G., Long, D.G.F., Norris, G., Zippi, P., and Griffis, R. 1991. Mesozoic geology and lignite potential of the Moose River Basin; Ontario Geological Survey, Open File Report 5777, 184p.

Telford, P.G. and Verma, H. (eds.) 1982. Mesozoic geology and mineral potential of the Moose River Basin; Ontario Geological Survey, Study 21, 193p.

Telford, P.G., Vos, M.A. and Norris, G. 1975. Geology and mineral deposits of the Moose River Basin, James Bay Lowlands, Preliminary Report; Ontario Division of Mines, Open File Report 5158.

Thorpe, J.E., 1988. The Devonian of the Hudson Bay. In: Devonian of the world, N.J. McMillan, A.F. Embry and D.J. Glass (eds), Canadian Society of Petroleum Geologists, Memoir 14, p. 133-153.

Thorsteinsson, R., and Uyeno, T.T., 1980. Stratigraphy and conodonts of Upper Silurian and Lower Devonian Rocks in the Environs of the Boothia Uplift, Canadian Arctic Archipelago. Geological Survey of Canada Bulletin 292, 75 p.

Tillement, B.A., 1975: Hydrocarbon potential of Hudson Bay Basin - 1975 evaluation: report prepared by Aquitaine Company of Canada Ltd., on behalf of the Aquitaine-Acro Group. Available from Information Services, Canterra Energy Ltd., 202, 505-4th Avenue S.W., Calgary, 35 p.

Tillement, B.A., Peniguel, G. and Guillemin, J.P. 1976. Marine Pennsylvanian rocks in Hudson Bay. Bulletin of Canadian Petroleum Geology, vol. 24, p. 418-439.

Tissot, B. P. and Welte, D. H. 1984. Petroleum Formation and Occurrence. Second Ed. Springer-Verlag, Berlin, 699 p., 327 figs.

Trettin, H.P. 1969. Lower Paleozoic sediments of northwestern Baffin Island. Geological Survey of Canada, Bulletin 157.

Trettin, H.P. 1975. Investigation of lower Paleozoic geology, Foxe Basin, northeastern Melville Peninsula and parts of northwestern and central Baffin Island. Geological Survey of Canada, Bulletin 251, 177p.

Tricker, P. M., Marshall, J.E.A. and Badman, T.D. 1992. Chitinozoan reflectance : a Lower Paleozoic thermal maturity indicator. Marine and Petroleum Geology, vol. 9, p. 302-307.

Try, C.F., Long, D.G.F. and Winder, C.G. 1984. Sedimentology of the Lower Cretaceous Mattagami Formation, Moose River Basin, James Bay Lowland, Ontario, Canada. In: The Mesozoic of Middle North America, Canadian Society of Petroleum Geologists, Memoir 9, p. 345-359.

Uyeno, T.T., 1989. Report on 55 conodont samples from four offshore wells in the Hudson Bay. Geological Survey of Canada, Paleontological Report 02-TTU-89, 14 p.

Uyeno, T.T. and Bultynck, P. 1993. Lower to Middle Devonian conodonts of the Jaab Lake well, Moose River Basin, northern Ontario. In: Geological Survey of Canada, Bulletin 444, p. 7-35.

White, T.S., Witzke, B.J., Ludvigson, G.A., 2000. Evidence for an Albian Hudson arm connection between the Cretaceous western interior seaway of North America and the Labrador Sea. Geological Society of America Bulletin, vol. 112, p. 1342-1355.

Williams, G.L. and Barss, M.S. 1976. Palynological analysis of the interval 1130 – 1260 feet from Aquitaine et al., Narwhal O-58, Hudson Bay. Geological Survey of Canada, Paleontological Report EPGS-PAL. 11-77GLW, 4 p.

Wilson, A.E., Stewart, J.S., and Caley, J.F., 1941. Sedimentary Basins of Ontario: Possible Sources of Oil and Gas. Proceedings and Transactions of the Royal Society of Canada, 3rd series, vol. 35, p. 167-185.

Wong, M.E. 2011. Lithofacies analysis and stratigraphic correlation of the Upper Ordovician Red Head Rapids Formation, Hudson Bay Basin, northeastern Manitoba; University of Manitoba, Department of Geological Sciences, 72 p.

Workum, R.H., Bolton, T.E. and Barnes, C.R. 1976. Ordovician geology of Akpatok Island, Ungava Bay, District Franklin. Canadian Journal of Earth Sciences, vol. 13, p. 157–178.

Zhang, S. 2008. New insights into Ordovician oil shales in Hudson Bay Basin: their number, stratigraphic position, and petroleum potential. Bulletin of Canadian Petroleum Geology, vol 56, p. 300–324.

Zhang, S. 2010. Upper Ordovician Stratigraphy and Oil Shales on Southampton Island - Field Trip Guidebook. Geological Survey of Canada, Open File 6668, 42p.

Zhang, S. 2011a. Late Ordovician conodont biostratigraphy and redefinition of the age of oil shale intervals on Southampton Island. Canadian Journal of Earth Sciences, vol. 48, p. 619–643.

Zhang, S. 2011b. Geochemistry data from three oil shale intervals in unit 1, Red Head Rapids Formation (Upper Ordovician) on Southampton Island. Geological Survey of Canada, Open File 6681, 20p.

Zhang, S. 2012. Ordovician stratigraphy and oil shale, southern Baffin Island, Nunavut — preliminary field and post-field data; Geological Survey of Canada, Open File 7199, 26 p.

Zhang, S. 2013. Ordovician conodont biostratigraphy and redefinition of the age of lithostratigraphic units on northeastern Melville Peninsula, Nunavut. Canadian Journal of Earth Sciences, vol. 50, p. 808-825

Zhang, S., and Barnes, C.R. 2007. Late Ordovician–Early Silurian Conodont Biostratigraphy and Thermal Maturity, Hudson Bay Basin. Bulletin of Canadian Petroleum Geology, vol. 55, p. 179–216.

Zhang, S. and Dewing, K. 2008. Rock-Eval data for four hydrocarbon exploration wells in Hudson Bay and Foxe basins, Geological Survey of Canada, Open File 5872, 23p.

Zhang, S., and Hefter, J., 2009. Sea Level and Paleoenvironment Control on Late Ordovician Source Rocks, Hudson Bay Basin, Canada. Eos Trans. AGU, 90(22), Jt. Assem. Suppl., Abstract CG73B-03.

Zhang, S. and Hu, K., 2013. Recognition of Devonian hydrocarbon source rocks in Beluga O-23 well, Hudson Bay Basin; Geological Survey of Canada, Open File 7433, 15 p.

Zhang, S. and Lavoie, D. 2013. Studies of Paleozoic stratigraphy and petroleum potential in the Hudson Bay and Foxe basins, Nunavut. In: Summary of Activities 2012, Canada-Nunavut Geoscience Office, p. 121–130.

Zhang, S. and Pell, J. 2013. Study of sedimentary rock xenoliths from kimberlites on Hall Peninsula, Baffin Island, Nunavut. In: Summary of Activities 2012, Canada-Nunavut Geoscience Office, p. 107–112.

ANNEXES

Annex 1.1: Rock-Eval6/TOC data for three shale intervals samples collected near Cape Donovan, Southampton Island. Shaded lines indicate S2 values > 0.35 mg HC/g TOC

Sample	Latitude	Longitude	S1	S2	PI	S3	Tmax	Tpeak	TOC	RC%	HI	OI
Lower Shale												
07CYA-Z49-01	64° 02' 12.5"N	83°39'47.9"W	0,27	12,90	0,02	0,80	414	455	2,17	1,03	594	37
07CYA-Z49-02	64° 02' 12.5"N	83°39'47.9"W	3,06	106,54	0,03	4,33	414	455	17,31	7,96	615	25
07CYA-Z49-02	64° 02' 12.5"N	83°39'47.9"W	3,37	109,17	0,03	4,26	412	453	17,04	7,45	641	25
07CYA-Z49-03	64° 02' 12.5"N	83°39'47.9"W	0,91	47,03	0,02	1,99	415	456	7,88	3,78	597	25
07CYA-Z49-04	64° 02' 12.5"N	83°39'47.9"W	1,74	54,81	0,03	0,89	416	457	7,85	3,09	698	11
07CYA-Z49-05	64° 02' 12.5"N	83°39'47.9"W	1,96	73,83	0,03	3,12	415	456	12,08	5,60	611	26
07CYA-Z49-06	64° 02' 12.5"N	83°39'47.9"W	1,62	78,62	0,02	2,92	417	458	12,66	5,82	621	23
07CYA-Z49-06	64° 02' 12.5"N	83°39'47.9"W	1,74	78,91	0,02	2,98	413	454	12,55	5,67	629	24
07CYA-Z49-07	64° 02' 12.5"N	83°39'47.9"W	1,63	72,70	0,02	3,29	415	456	12,25	5,88	593	27
07CYA-Z49-08	64° 02' 12.5"N	83°39'47.9"W	0,96	35,57	0,03	0,84	414	455	5,56	2,47	640	15
07CYA-Z49-09	64° 02' 12.5"N	83°39'47.9"W	1,40	58,43	0,02	2,10	414	455	9,56	4,47	611	22
07CYA-Z49-10	64° 02' 12.5"N	83°39'47.9"W	1,67	49,11	0,03	2,22	410	451	8,50	4,16	578	26
07CYA-Z49-11	64° 02' 12.5"N	83°39'47.9"W	0,73	55,74	0,01	2,87	411	452	10,53	5,67	529	27
07CYA-Z49-12	64° 02' 12.5"N	83°39'47.9"W	1,38	62,27	0,02	2,63	412	453	12,01	6,56	518	22
07CYA-Z49-12	64° 02' 12.5"N	83°39'47.9"W	1,47	63,40	0,02	2,75	407	448	11,02	5,47	575	25
07CYA-Z49-13	64° 02' 12.5"N	83°39'47.9"W	1,22	45,64	0,03	2,19	410	451	8,44	4,41	541	26
07CYA-Z49-13	64° 02' 12.5"N	83°39'47.9"W	1,20	44,77	0,03	2,47	409	450	8,06	4,10	555	31
07CYA-Z49-14	64° 02' 12.5"N	83°39'47.9"W	1,09	42,11	0,03	2,94	410	451	9,18	5,42	459	32
07CYA-Z49-15	64° 02' 12.5"N	83°39'47.9"W	1,57	60,49	0,03	1,95	413	454	10,52	5,22	575	19
07CYA-Z49-15	64° 02' 12.5"N	83°39'47.9"W	1,93	64,30	0,03	1,92	411	452	10,13	4,51	635	19
07CYA-Z49-16	64° 02' 12.5"N	83°39'47.9"W	1,29	55,02	0,02	3,06	410	451	9,92	5,07	555	31
07CYA-Z49-17	64° 02' 12.5"N	83°39'47.9"W	0,80	35,75	0,02	2,07	411	452	6,72	3,56	532	31
07CYA-Z49-18	64° 02' 12.5"N	83°39'47.9"W	0,04	1,88	0,02	0,40	421	462	0,55	0,37	342	73
07CYA-Z49-19	64° 02' 12.5"N	83°39'47.9"W	0,92	41,83	0,02	2,20	411	452	7,96	4,29	526	28
07CYA-Z49-20	64° 02' 12.5"N	83°39'47.9"W	2,13	92,06	0,02	5,36	414	455	16,74	8,63	550	32
07CYA-Z49-20	64° 02' 12.5"N	83°39'47.9"W	2,56	96,58	0,03	5,40	410	451	15,90	7,37	607	34

07CYA-Z49-21	64° 02' 12.5"N	83°39'47.9"W	0,03	1,56	0,02	0,30	417	458	0,43	0,28	363	70
07CYA-Z43-03B	64° 45' 29.8"N	82°22'06.7"W	1,49	61,78	0,02	2,16	415	454	10,51	5,12	588	21
07CYA-Z43-04A	64° 45' 29.8"N	82°22'06.7"W	1,46	52,16	0,03	1,73	412	451	9,25	4,68	564	19
Average									**9,77**		**567**	**28**
Middle Shale												
07CYA-Z52-01	64° 02' 12.5"N	83°39'47.9"W	0,08	6,02	0,01	0,27	422	463	0,82	0,30	734	33
07CYA-Z52-02	64° 02' 12.5"N	83°39'47.9"W	3,91	167,94	0,02	5,09	417	458	24,80	10,26	677	21
07CYA-Z52-02	64° 02' 12.5"N	83°39'47.9"W	4,12	180,99	0,02	5,57	416	457	25,56	9,89	708	22
07CYA-Z52-03	64° 02' 12.5"N	83°39'47.9"W	5,11	155,67	0,03	8,24	418	459	24,53	10,76	635	34
07CYA-Z52-03	64° 02' 12.5"N	83°39'47.9"W	6,05	163,21	0,04	8,34	416	457	24,46	9,98	667	34
07CYA-Z52-04	64° 02' 12.5"N	83°39'47.9"W	6,72	195,14	0,03	9,81	415	456	32,11	14,84	608	31
07CYA-Z52-04	64° 02' 12.5"N	83°39'47.9"W	7,18	208,92	0,03	9,94	416	457	34,10	15,62	613	29
07CYA-Z52-05	64° 02' 12.5"N	83°39'47.9"W	5,60	173,26	0,03	8,97	413	454	30,41	15,08	570	29
07CYA-Z52-05	64° 02' 12.5"N	83°39'47.9"W	6,28	191,62	0,03	9,48	412	453	31,37	14,43	611	30
07CYA-Z52-06	64° 02' 12.5"N	83°39'47.9"W	5,31	185,02	0,03	10,96	417	458	32,23	15,86	574	34
07CYA-Z52-06	64° 02' 12.5"N	83°39'47.9"W	6,01	200,50	0,03	11,31	413	454	32,01	14,29	626	35
07CYA-Z52-07	64° 02' 12.5"N	83°39'47.9"W	0,01	0,68	0,02	0,35	426	467	0,19	0,12	358	184
07CYA-Z52-08	64° 02' 12.5"N	83°39'47.9"W	1,80	74,82	0,02	3,50	420	461	10,37	3,83	722	34
07CYA-Z52-08	64° 02' 12.5"N	83°39'47.9"W	2,05	78,80	0,03	3,22	420	461	10,38	3,47	759	31
07CYA-Z40-08	64° 45' 32.8"N	82°22'10.0"W	4,23	139,21	0,03	4,96	417	456	21,62	9,42	644	23
07CYA-Z40-10	64° 45' 32.8"N	82°22'10.0"W	6,21	168,79	0,04	7,71	415	454	29,65	14,67	569	26
Average									**22,79**		**630**	**39**
Upper Shale												
07CYA-Z53-01	64° 02' 12.5"N	83°39'47.9"W	0,07	7,14	0,01	0,38	421	462	1,05	0,43	680	36
07CYA-Z53-02	64° 02' 12.5"N	83°39'47.9"W	2,02	111,07	0,02	3,81	420	461	15,52	5,93	716	25
07CYA-Z53-02	64° 02' 12.5"N	83°39'47.9"W	2,11	111,50	0,02	3,71	418	459	15,36	5,72	726	24
07CYA-Z53-03	64° 02' 12.5"N	83°39'47.9"W	4,87	178,91	0,03	6,44	417	458	26,68	11,13	671	24
07CYA-Z53-03	64° 02' 12.5"N	83°39'47.9"W	5,37	187,85	0,03	5,61	416	457	26,37	10,00	712	21
07CYA-Z53-04	64° 02' 12.5"N	83°39'47.9"W	1,68	63,76	0,03	1,72	415	456	8,58	3,06	743	20
07CYA-Z53-05	64° 02' 12.5"N	83°39'47.9"W	5,50	203,77	0,03	6,61	418	459	30,44	12,71	669	22

07CYA-Z53-05	64° 02' 12.5"N	83°39'47.9"W	6,69	223,62	0,03	6,71	416	457	30,96	11,49	722	22
07CYA-Z53-06	64° 02' 12.5"N	83°39'47.9"W	1,14	36,01	0,03	0,95	417	458	4,86	1,73	741	20
07CYA-Z53-07	64° 02' 12.5"N	83°39'47.9"W	2,67	76,67	0,03	2,16	418	459	10,47	3,77	732	21
07CYA-Z53-08	64° 02' 12.5"N	83°39'47.9"W	4,76	143,39	0,03	6,56	416	457	22,97	10,33	624	29
07CYA-Z53-08	64° 02' 12.5"N	83°39'47.9"W	5,63	151,99	0,04	6,67	415	456	22,93	9,49	663	29
07CYA-Z53-09	64° 02' 12.5"N	83°39'47.9"W	3,91	159,10	0,02	6,57	414	455	27,36	13,47	582	24
07CYA-Z53-09	64° 02' 12.5"N	83°39'47.9"W	4,53	172,13	0,03	6,96	410	451	27,32	12,28	630	25
07CYA-Z53-11	64° 02' 12.5"N	83°39'47.9"W	2,70	149,46	0,02	3,59	425	466	19,89	7,05	751	18
07CYA-Z53-11	64° 02' 12.5"N	83°39'47.9"W	2,88	154,37	0,02	3,31	423	464	19,42	6,16	795	17
07CYA-Z44-10	64° 45' 36.3"N	82°22'25.5"W	6,12	210,29	0,03	5,48	418	457	31,97	13,68	658	17
07CYA-Z44-12	64° 45' 36.3"N	82°22'25.5"W	5,52	159,83	0,03	5,24	415	454	26,61	12,57	601	20
Average									**20,49**		**690**	**23**

Annex 1.2: Rock-Eval6/TOC data for samples collected on South Baffin Island. Shaded lines indicate S2 values > 0.35 mg HC/g TOC

Sample	Latitude	Longitude	Unit	S1	S2	PI	S3	Tmax	Tpeak	TOC	RC%	HI	OI
11SZ-03-01	64°06'37.4"N	69°25'44.3"W	Amadjuak Fm	2,07	68,27	0,03	5,12	418	457	13,95	7,83	489	37
11SZ-03-02	64°06'34.1"N	69°25'38.1"W	Amadjuak Fm	1,85	61,60	0,03	3,16	420	459	11,35	5,91	543	28
11SZ-03-03	64°06'35.9"N	69°25'37.4"W	Amadjuak Fm	1,97	63,18	0,03	4,13	421	460	12,16	6,53	520	34
11SZ-03-04	64°06'35.9"N	69°25'37.4"W	Amadjuak Fm	2,29	70,89	0,03	2,91	422	461	12,51	6,26	567	23
11SZ-03-05	64°06'36.4"N	69°25'37.5"W	Amadjuak Fm	1,21	47,14	0,02	2,95	422	461	8,83	4,64	534	33
11SZ-04-01	63°58'01.0"N	69°09'54.0"W	Amadjuak Fm	1,10	55,35	0,02	5,93	423	462	12,45	7,46	445	48
11SZ-04-02	63°58'01.0"N	69°09'54.0"W	Amadjuak Fm	1,94	71,25	0,03	6,93	422	461	14,91	8,48	478	46
11SZ-04-04	63°58'01.0"N	69°09'54.0"W	Amadjuak Fm	1,39	60,19	0,02	5,85	423	462	12,36	6,95	487	47
11SZ-04-05	63°58'01.0"N	69°09'54.0"W	Amadjuak Fm	1,31	58,82	0,02	5,53	421	460	12,08	6,79	487	46
11SZ-04-07	63°58'03.2"N	69°09'54.8"W	Amadjuak Fm	1,35	60,69	0,02	5,88	424	463	12,71	7,25	477	46
11SZ-04-08	63°58'03.2"N	69°09'54.8"W	Amadjuak Fm	1,27	56,05	0,02	5,44	423	462	11,73	6,69	478	46
11SZ-04-09	63°58'03.2"N	69°09'54.8"W	Amadjuak Fm	1,86	71,42	0,03	6,43	422	461	14,78	8,35	483	44
11SZ-04-10	63°58'03.2"N	69°09'54.8"W	Amadjuak Fm	1,32	64,47	0,02	6,11	425	464	13,02	7,24	495	47
11SZ-04-11	63°58'03.2"N	69°09'54.8"W	Amadjuak Fm	1,04	49,29	0,02	4,34	423	462	9,85	5,45	500	44
11SZ-04-12	63°58'03.7"N	69°09'54.3"W	Amadjuak Fm	2,04	69,51	0,03	5,05	422	461	13,48	7,27	516	37
11SZ-04-13	63°58'03.7"N	69°09'54.3"W	Amadjuak Fm	2,67	73,74	0,03	3,69	421	460	13,61	7,06	542	27
11SZ-04-14	63°58'03.7"N	69°09'54.3"W	Amadjuak Fm	2,20	71,24	0,03	5,10	420	459	14,22	7,84	501	36
11SZ-08-03B	66°14'16.0"N	71°41'52.4"W	Amadjuak Fm	0,01	0,90	0,01	0,35	432	471	0,33	0,24	273	106
11SZ-08-04B	66°14'16.0"N	71°41'52.4"W	Amadjuak Fm	0,03	2,27	0,01	0,30	431	470	0,68	0,47	334	44
11SZ-08-05B	66°14'16.0"N	71°41'52.4"W	Amadjuak Fm	0,03	2,25	0,01	0,33	430	469	0,76	0,55	296	43
11SZ-08-06B	66°14'16.0"N	71°41'52.4"W	Amadjuak Fm	0,03	1,90	0,02	0,35	430	469	0,72	0,55	264	49
11SZ-08-07B	66°14'16.0"N	71°41'52.4"W	Amadjuak Fm	0,01	0,75	0,02	0,32	431	470	0,42	0,34	179	76
11SZ-08-08B	66°14'16.0"N	71°41'52.4"W	Amadjuak Fm	0,01	0,79	0,02	0,32	431	470	0,43	0,34	184	74
11SZ-08-09B	66°14'16.0"N	71°41'52.4"W	Amadjuak Fm	0,01	0,48	0,02	0,28	428	467	0,28	0,23	171	100
11SZ-08-11B	66°14'16.0"N	71°41'52.4"W	Amadjuak Fm	0,01	0,41	0,02	0,23	427	466	0,31	0,25	132	74
11SZ-08-13B	66°14'16.0"N	71°41'52.4"W	Amadjuak Fm	0,01	0,31	0,03	0,28	428	467	0,32	0,28	97	88

11SZ-10-17B	63°59'08.6"N	69°10'40.7"W	Amadjuak Fm	1,32	55,57	0,02	1,30	422	461	9,15	4,34	607	14
11SZ-10-17B/B	63°59'08.6"N	69°10'40.7"W	Amadjuak Fm	2,81	82,37	0,03	1,02	424	463	12,97	5,81	635	8
11SZ-10-18B	63°59'08.6"N	69°10'40.7"W	Amadjuak Fm	2,14	61,87	0,03	0,97	423	462	9,66	4,28	640	10
11SZ-10-18B/B	63°59'08.6"N	69°10'40.7"W	Amadjuak Fm	2,16	62,73	0,03	1,37	421	460	10,61	5,13	591	13
11SZ-10-19B	63°59'08.6"N	69°10'40.7"W	Amadjuak Fm	2,30	67,03	0,03	1,66	423	462	11,05	5,19	607	15
11SZ-10-19B/B	63°59'08.6"N	69°10'40.7"W	Amadjuak Fm	0,87	35,27	0,02	1,45	422	461	5,95	2,86	593	24
11SZ-10-20B	63°59'08.6"N	69°10'40.7"W	Amadjuak Fm	1,14	45,50	0,02	0,86	424	463	7,25	3,32	628	12
11SZ-10-21B	63°59'08.6"N	69°10'40.7"W	Amadjuak Fm	0,95	41,75	0,02	2,09	422	461	7,58	3,91	551	28
11SZ-10-22B	63°59'08.6"N	69°10'40.7"W	Amadjuak Fm	0,82	35,01	0,02	1,80	422	461	6,26	3,19	559	29
11SZ-10-23B	63°59'08.6"N	69°10'40.7"W	Amadjuak Fm	0,32	20,25	0,02	0,62	423	462	3,56	1,81	569	17
11SZ-10-24B	63°59'08.6"N	69°10'40.7"W	Amadjuak Fm	0,10	8,24	0,01	0,46	425	464	1,68	0,95	490	27
11SZ-10-25B	63°59'08.6"N	69°10'40.7"W	Amadjuak Fm	0,03	2,26	0,01	0,37	427	466	0,63	0,42	359	59
11SZ-10-26B	63°59'08.6"N	69°10'40.7"W	Amadjuak Fm	0,02	1,55	0,01	0,40	430	469	0,53	0,38	292	75
11SZ-10-31B	63°59'08.3"N	69°10'44.5"W	Amadjuak Fm	0,01	0,87	0,02	0,45	430	469	0,48	0,38	181	94
11SZ-10-36B	63°59'10.4"N	69°10'58.1"W	Amadjuak Fm	3,08	81,14	0,04	3,32	422	461	14,20	7,01	571	23
11SZ-16-01	65°48'55.8"N	71°58'32.1"W	Amadjuak Fm	0,01	0,20	0,03	0,34	430	469	0,18	0,15	111	189
Average										**7,62**		**439**	**47**
11SZ-11-06B	65°01'20.6"N	72°30'28.9"W	Forster Bay Fm	0,23	11,37	0,02	1,54	420	459	2,82	1,78	403	55
11SZ-12A-01	64°57'40.0"N	72°16'02.4"W	Forster Bay Fm	0,59	25,68	0,02	1,83	416	455	4,79	2,52	536	38
11SZ-13-01	64°49'33.7"N	72°29'26.2"W	Forster Bay Fm	0,32	18,39	0,02	2,09	422	461	4,10	2,43	449	51
11SZ-14-01	64°49'38.5"N	72°27'15.9"W	Forster Bay Fm	0,38	23,81	0,02	2,46	422	461	5,13	3,00	464	48
Average										**4,21**		**463**	**48**

Annex 1.3: Rock-Eval6/TOC data for the Akpatok samples. Shaded lines indicate S2 values > 0.35 mg HC/g TOC

Sample	Unit	Latitude	Longitude	S1	S2	PI	S3	Tmax	TOC	HI	OI
AK-1	unnamed	68°20'30'' W	60°25'40'' N	**0.6**	**2.07**	**0.3**	**0.91**	**431**	**0.51**	**405**	**178**
AK-1	unnamed	68°20'30'' W	60°25'40'' N	**0.9**	**2.19**	**0.3**	**0.42**	**433**	**0.61**	**339**	**68**
AK-2	unnamed	68°20'30'' W	60°25'40'' N	**0.21**	**5,55**	**0.4**	**1.52**	**429**	**1.23**	**451**	**123**
AK-2	unnamed	68°20'30'' W	60°25'40'' N	**0.25**	**6.18**	**0.4**	**1.06**	**429**	**1.41**	**438**	**75**
AK-3	unnamed	68°20'30'' W	60°25'40'' N	**0.34**	**9.64**	**0.4**	**1.42**	**427**	**1.82**	**529**	**78**
AK-3	unnamed	68°20'30'' W	60°25'40'' N	**0.39**	**10.85**	**0.3**	**1.11**	**424**	**2.11**	**514**	**52**

Annex 1.4: Rock-Eval6/TOC data for the Inco-Winisk wells. Shaded lines indicate S2 values > 0.35 mg HC/g TOC

Sample	Strat unit	Latittude	Longitude	Depth (m)	S1	S2	PI	S3	Tmax	Tpeak	TOC	RC%	HI	OI
INCO 49212														
10DKA001DW	Churchill	54.30833	-87,01	56,40	0,06	0,46	0,12	0,50	434	473	0,44	0,37	105	114
10DKA001DS	Churchill	54.30833	-87,01	96,34	0,03	0,36	0,08	0,58	433	472	0,24	0,19	150	242
10DKA001a	Boas River	54.30833	-87,01	103,20	0,46	12,11	0,04	0,96	423	460	2,61	1,51	464	37
10DKA001b	Boas River	54.30833	-87,01	105,31	2,14	51,97	0,04	1,60	425	462	8,71	4,11	597	18
10DKA001c	Boas River	54.30833	-87,01	107,07	1,69	44,03	0,04	1,30	422	459	7,60	3,70	579	17
10DKA001d	Boas River	54.30833	-87,01	108,22	2,25	53,67	0,04	1,91	423	460	9,05	4,28	593	21
10DKA001e	Boas River	54.30833	-87,01	109,80	3,06	71,67	0,04	2,92	422	459	12,84	6,46	558	23
10DKA001e	Boas River	54.30833	-87,01	109,8	2,78	70,99	0,04	3,09	420	457	12,37	6,05	574	25
10DKA001f	Boas River	54.30833	-87,01	111,34	1,96	42,35	0,04	2,04	420	457	7,92	4,10	535	26
10DKA001g	Boas River	54.30833	-87,01	112,44	1,72	36,61	0,04	1,51	424	461	6,29	3,00	582	24
10DKA001h	Boas River	54.30833	-87,01	113,76	1,59	37,59	0,04	1,37	426	463	5,93	2,60	634	23
10DKA001i	Boas River	54.30833	-87,01	114,81	0,91	30,41	0,03	1,13	426	463	4,98	2,30	611	23
!0DKA001j	Boas River	54.30833	-87,01	116,20	1,11	26,02	0,04	1,48	423	460	4,71	2,37	552	31
!0DKA001k	Bad Cache	54.30833	-87,01	117,72	0,15	2,42	0,06	0,37	428	465	0,58	0,35	417	64
INCO 49204														
!0DKA002a	Tertiary	54,31	-87,04	62,02	0,10	0,70	0,13	1,71	430	467	1,01	0,87	69	169
!0DKA002b	Tertiary	54,31	-87,04	64,66	0,10	0,67	0,13	1,77	432	469	0,93	0,79	72	190
!0DKA002c	Tertiary	54,31	-87,04	67,31	0,08	0,73	0,10	6,61	427	464	1,02	0,74	72	648
!0DKA002d	Tertiary	54,31	-87,04	69,95	0,09	0,67	0,12	2,68	431	468	0,90	0,74	74	298
!0DKA002e	Tertiary	54,31	-87,04	72,59	0,08	0,58	0,12	2,88	430	467	0,87	0,71	67	331
!0DKA002f	Tertiary	54,31	-87,04	75,22	0,12	0,90	0,12	4,39	428	465	0,94	0,71	96	467
!0DKA002g	Tertiary	54,31	-87,04	77,86	0,10	0,61	0,14	2,45	430	467	0,89	0,74	69	275
!0DKA002h	Tertiary	54,31	-87,04	79,19	0,06	0,47	0,11	1,76	435	472	0,82	0,70	57	215
!0DKA002i	Churchill	54,31	-87,04	81,03	0,32	4,41	0,07	3,49	433	470	2,29	1,74	193	152
10DKA002j	Churchill	54,31	-87,04	81,82	0,02	0,16	0,12	0,71	430	467	0,31	0,26	52	229
10DKA002k	Boas River	54,31	-87,04	83,14	2,56	50,06	0,05	1,69	422	459	7,90	3,43	634	21
10DKA002l	Boas River	54,31	-87,04	84,46	3,11	55,09	0,05	1,83	421	458	9,28	4,32	594	20
10DKA002m	Boas River	54,31	-87,04	85,79	1,34	23,31	0,05	1,16	423	460	4,19	2,06	556	28

10DKA002n	Boas River	54,31	-87,04	87,10	1,66	31,39	0,05	1,29	426	463	5,06	2,24	620	25
10DKA002o	Boas River	54,31	-87,04	88,42	2,15	37,76	0,05	1,77	422	459	6,51	3,08	580	27
10DKA002p	Boas River	54,31	-87,04	89,74	1,35	19,56	0,06	1,06	425	462	3,28	1,47	596	32
10DKA002q	Bad Cache	54,31	-87,04	91,06	0,14	0,73	0,16	0,48	426	463	0,38	0,28	192	126

Annex 1.5: Rock-Eval6/TOC data for the Ontario wells (except the Inco-Winisk wells). Shaded lines indicate S2 values > 0.35 mg HC/g TOC

Sample	Well	Latitude	Longitude	Unit	Depth (m)	S1	S2	PI	S3	Tmax	Tpeak	TOC	RC%	HI	OI
10DKA004RC	Penn #1	56,75195	-88,75351	Kenogami River	417,88	0,08	0,61	0,12	0,4	441	481	0,32	0,24	191	125
10DKA004RB	Penn #1	56,75195	-88,75351	Ekwan River	507,39	0,44	1,38	0,24	0,55	429	469	0,92	0,74	150	60
10DKA004RA	Penn #1	56,75195	-88,75351	Red Head Rapids	846,63	0,14	1,91	0,07	0,8	428	468	1,2	0,99	159	67
10DKA004CW	Penn #1	56,75195	-88,75351	Churchill River	940,28	0,14	2,28	0,06	0,69	431	470	1,2	0,97	190	58
10DKA004DA1	Penn #1	56,75195	-88,75351	Bad Cache Rapids	949,05	0,03	0,49	0,06	0,46	434	473	0,55	0,48	89	84
10DKA004EE	Penn #1	56,75195	-88,75351	Bad Cache Rapids	1012,55	0,02	0,29	0,06	0,48	436	475	0,18	0,13	161	267
10DKA004EG	Penn #1	56,75195	-88,75351	Bad Cache Rapids	1013,89	0,02	0,16	0,09	0,41	437	476	0,09	0,06	178	456
11DKA002E303	Mantle DDH-08-012	581730,82	5822252,96	Bad Cache Rapids	60,9	0,04	12,6	0	0,27	427	466	1,65	0,58	761	16
11DKA004I06	Mantle DDH-08-002	579881	5938265	Boas River	56,67	0,01	0,04	0,14	0,47	427	466	0,19	0,17	21	247
11DKA026Q12	Wallbridge WB-01-001	403922,7	6104891,82	Bad Cache Rapids	217,45	1,47	66,4	0,02	1,22	426	465	9,79	4,06	679	12
11DKA037R06	DDH 01-1530-01	689854,83	5933623,96	Severn River	110,74	0,03	0,75	0,04	0,41	428	467	0,41	0,33	183	100
11DKA037R04	DDH 01-1530-01	689854,83	5933623,96	Severn River	112,16	0,03	1,32	0,02	0,41	427	466	0,54	0,41	244	76
11DKA037G06	DDH 01-1530-01	689854,83	5933623,96	Red Head Rapids	190,5	0,01	0,03	0,21	0,36	481	520	0,11	0,09	27	327
11DKA037E03	DDH 01-1530-01	689854,83	5933623,96	Red Head Rapids	205,7	0,01	0,06	0,19	0,39	432	471	0,09	0,07	67	433
10DKA024F-02	Victor core V03-270AH	306247	5854737	Severn River	159,1	0,07	3,46	0,02	0,36	429	468	0,71	0,4	487	51
10DKA024G-01	Victor core V03-270AH	306247	5854737	Severn River	189,56	0,09	1,69	0,05	0,38	429	468	0,59	0,42	286	64

10DKA001I-03	KWG-94-09	608446	5813808	Churchill River	86,87	0,02	0,19	0,08	0,48	500	539	0,14	0,1	136	343
10DKA005K-02	KWG-94-24	591024	5833437	Churchill River	49,65	0,03	2,09	0,01	0,28	428	467	0,65	0,45	322	43
10DKA005M-04	KWG-94-24	591024	5833437	Churchill River	66,16	0,01	0,15	0,06	0,56	440	479	0,39	0,36	38	144
10DKA006I-02	KWG-95-37	604494	5919557	Bad Cache Rapids	75,96	0,03	3,63	0,01	0,81	431	470	1,02	0,68	356	79
10DKA006I-05	KWG-95-37	604494	5919557	Bad Cache Rapids	81,3	0,04	5,02	0,01	1,28	433	472	1,2	0,71	418	107

Annex 1.6: Rock-Eval6/TOC data for samples collected on the Asheweig River outcrops. Shaded lines indicate S2 values > 0.35 mg HC/g TOC.

Sample	Unit	Easting	Northing	Section	S1	S2	PI	S3	Tmax	Tpeak	TOC	RC%	HI	OI
11DKA024A01	Boas River	469184.71	5985217.61	0,05	0,85	27,66	0,03	1,16	419	459	5,35	2,91	517	22
11DKA024A06	Boas River	469184.71	5985217.61	0,2	1,37	41,09	0,03	1,20	422	462	7,36	3,75	558	16
11DKA024A09	Boas River	469184.71	5985217.61	0,24	1,77	46,52	0,04	1,06	423	463	7,77	3,69	599	14
11DKA024B02	Boas River	469184.71	5985217.61	0,28	1,23	33,02	0,04	0,78	423	463	5,38	2,47	614	14
11DKA024B05	Boas River	469184.71	5985217.61	0,325	0,74	21,77	0,03	0,89	422	462	3,92	1,98	555	23
11DKA024B11	Boas River	469184.71	5985217.61	0,42	0,97	27,59	0,03	0,68	423	463	4,48	2,07	616	15
11DKA024B17	Boas River	469184.71	5985217.61	0,505	0,18	8,49	0,02	0,67	423	463	1,64	0,88	518	41
11DKA024C01	Boas River	469184.71	5985217.61	2,4	0,04	3,47	0,01	0,69	425	465	0,87	0,55	399	79
11DKA024C07	Boas River	469184.71	5985217.61	3,28	0,01	0,74	0,02	0,49	432	472	0,41	0,33	180	120
11DKA024C10	Boas River	469184.71	5985217.61	3,55	0,07	8,00	0,01	1,25	422	462	2,00	1,27	400	63
11DKA024D04	Boas River	469184.71	5985217.61	3,95	0,04	4,60	0,01	0,87	426	466	1,09	0,66	422	80
11NST001A-01	Boas River	469184.71	5985217.61	0	1,22	34,62	0,03	0,89	422	462	5,81	2,77	596	15
11NST001A-03	Boas River	469184.71	5985217.61	0	1,43	40,98	0,03	1,13	421	461	7,28	3,69	563	16
11NST001B-01	Boas River	469184.71	5985217.61	0,1	1,91	49,67	0,04	1,01	423	463	8,41	4,04	591	12
11NST001B-02	Boas River	469184.71	5985217.61	0,2	1,22	35,79	0,03	0,79	425	465	5,83	2,70	614	14
11NST001J-01	Boas River	469184.71	5985217.61	2,45	0,70	23,24	0,03	1,49	421	461	4,51	2,42	515	33
Average											**4,51**		**516**	**36**

Annex 1.7: Rock-Eval6/TOC data for samples collected in Manitoba wells. Shaded lines indicate S2 values > 0.35 mg HC/g TOC.

Sample	Well	Stratigraphic unit	Easting	Northing	Depth_ft	S1	S2	PI	S3	T_{max}	TOC	HI	OI
106-11-HBL-WB-14	Whitebear Creek	Attawapiska	532063	6360180	108,50	0,26	0,66	0,28	0,91	408	0,66	100	138
106-11-HBL-WB-12	Whitebear Creek	Severn River			546,50	0,49	5,98	0,08	0,67	413	1,79	334	37
106-11-HBL-WB-11	Whitebear Creek	Severn River			554,88	0,33	4,68	0,07	0,58	416	1,34	349	43
106-11-HBL-WB-10	Whitebear Creek	Severn River			590,50	0,06	1,93	0,03	0,39	423	0,68	284	57
106-11-HBL-WB-13	Whitebear Creek	Severn River			706,00	0,05	1,15	0,04	0,51	427	0,55	209	93
106-11-HBL-WB-9	Whitebear Creek	Red Head Rapids			725,00	0,11	0,98	0,10	0,48	428	0,65	151	74
106-11-HBL-WB-8	Whitebear Creek	Red Head Rapids			725,30	0,20	2,12	0,09	0,50	427	1,17	181	43
106-11-HBL-WB-7	Whitebear Creek	Red Head Rapids			726,00	3,08	29,98	0,09	1,61	420	8,44	355	19
106-10-HBL WB-13	Whitebear Creek	Red Head Rapids			731,98	0,05	0,12	0,30	0,31	328	0,28	43	111
106-11-HBL-WB-6	Whitebear Creek	Red Head Rapids			755,00	0,06	0,69	0,08	0,42	427	0,82	84	51
106-11-HBL-WB-5	Whitebear Creek	Red Head Rapids			755,50	0,12	0,93	0,12	0,43	429	0,41	227	105
106-11-HBL-WB-4	Whitebear Creek	Red Head Rapids			763,50	0,04	1,54	0,03	0,39	429	0,44	350	89
106-11-HBL-WB-3	Whitebear Creek	Red Head Rapids			769,00	0,11	2,62	0,04	0,40	425	0,73	359	55
106-11-HBL-WB-2	Whitebear Creek	Red Head Rapids			769,58	0,09	1,70	0,05	0,46	429	0,67	254	69
106-11-HBL-WB-1	Whitebear Creek	Red Head Rapids			789,67	0,06	0,69	0,08	0,43	425	0,39	177	110
106-10-HBL WB-12	Whitebear Creek	Red Head Rapids			798,97	0,06	0,21	0,22	0,31	411	0,36	58	86
Zhang and Dewing 2008	Comeault No. 1	Attawapiskat	627674	6282230	225,50	0,02	0,04	0,31	0,54	323	0,10	40	540
Zhang and Dewing 2008	Comeault No. 1	Ekwan River			449,33	0,02	0,03	0,32	0,26	436	0,07	43	371
Zhang and Dewing 2008	Comeault No. 1	Ekwan River			580,42	0,05	0,91	0,05	0,28	429	0,34	268	82
Zhang and Dewing 2008	Comeault No. 1	Severn River			449,33	0,02	0,03	0,32	0,26	436	0,07	43	371
Zhang and Dewing 2008	Comeault No. 1	Severn River			580,42	0,05	0,91	0,05	0,28	429	0,34	268	82
Zhang and Dewing 2008	Comeault No. 1	Severn River			674,33	0,16	0,79	0,17	0,16	433	0,28	282	57
Zhang and Dewing 2008	Comeault No. 1	Severn River			684,00	0,24	0,89	0,21	0,20	433	0,31	287	65

Zhang and Dewing 2008	Comeault No. 1	Severn River			685,50	0,17	0,69	0,20	0,24	431	0,22	314	109
Zhang and Dewing 2008	Comeault No. 1	Severn River			704,75	0,38	2,46	0,13	0,63	423	0,86	286	73
Zhang and Dewing 2008	Comeault No. 1	Severn River			725,00	0,58	3,18	0,15	0,42	428	0,83	383	51
Zhang and Dewing 2008	Comeault No. 1	Severn River			769,33	0,92	7,10	0,11	0,63	416	1,80	394	35
Zhang and Dewing 2008	Comeault No. 1	Severn River			773,00	0,21	1,42	0,13	0,23	427	0,44	323	52
Zhang and Dewing 2008	Comeault No. 1	Severn River			796,33	0,71	11,84	0,06	0,67	425	3,10	382	22
Zhang and Dewing 2008	Comeault No. 1	Severn River			822,17	0,38	3,11	0,11	0,34	423	0,82	379	41
Zhang and Dewing 2008	Comeault No. 1	Severn River			834,58	1,06	13,30	0,07	0,56	421	3,05	436	18
Zhang and Dewing 2008	Comeault No. 1	Severn River			852,00	0,10	0,53	0,16	0,22	426	0,25	212	88
Zhang and Dewing 2008	Comeault No. 1	Severn River			909,50	0,36	4,22	0,08	0,29	422	0,93	454	31
Zhang and Dewing 2008	Comeault No. 1	Severn River			1024,00	0,09	0,49	0,15	0,35	428	0,40	122	88
Zhang and Dewing 2008	Comeault No. 1	Severn River			1029,67	0,20	3,10	0,06	0,31	425	0,75	413	41
Zhang and Dewing 2008	Comeault No. 1	Severn River			1112,00	2,50	26,83	0,09	1,66	418	6,38	421	26
Zhang and Dewing 2008	Comeault No. 1	Severn River			1144,50	1,35	11,33	0,11	0,59	416	2,46	461	24
Zhang and Dewing 2008	Comeault No. 1	Severn River			1153,25	0,47	10,33	0,04	0,49	422	1,87	552	26
Zhang and Dewing 2008	Comeault No. 1	Severn River			1219,00	0,25	1,63	0,13	0,45	425	0,73	223	62
Zhang and Dewing 2008	Comeault No. 1	Severn River			1222,00	0,63	6,57	0,09	0,34	423	1,36	483	25
Zhang and Dewing 2008	Comeault No. 1	Severn River			1303,50	0,06	0,85	0,07	0,29	431	0,25	340	116
Zhang and Dewing 2008	Comeault. No. 1	Severn River			1354,00	0,06	0,14	0,31	0,28	407	0,20	70	140
Zhang and Dewing 2008	Comeault No. 1	Severn River			1358,00	0,06	0,62	0,08	0,25	432	0,46	135	54
106-10-HBL-Com-3	Comeault No. 1	Severn River			1363,00	0,04	0,48	0,07	0,26	433	0,27	178	96
106-10-HBL-Comeault-5	Comeault. No. 1	Red Head Rapids			1389,00	0,07	0,19	0,27	0,39	415	0,42	45	93
C-1418.3	Comeault. No. 1	Red Head Rapids			1418,30	0,06	0,24	0,19	0,44	431	0,37	65	119
Zhang and Dewing 2008	Comeault. No. 1	Red Head Rapids			1420,00	0,14	0,28	0,33	0,65	426	0,43	65	151
106-10-HBL-Com-6	Comeault. No. 1	Red Head Rapids			1469,40	0,06	0,11	0,36	0,51	423	0,46	24	111
Zhang and Dewing 2008	Comeault. No. 1	Red Head Rapids			1472,00	0,03	0,12	0,23	0,32	428	0,26	46	123
Zhang and Dewing 2008	Comeault No. 1	Churchill River			1568,00	0,03	0,63	0,04	0,32	434	0,47	134	68

Zhang and Dewing 2008	Comeault. No. 1	Churchill River			1570,00	0,03	0,25	0,10	0,26	429	0,21	119	124
Zhang and Dewing 2008	Comeault No. 1	Churchill River			1698,33	0,13	0,97	0,12	0,29	435	0,25	388	116
Zhang and Dewing 2008	Comeault No. 1	Churchill River			1723,17	0,29	6,42	0,04	0,70	430	1,67	384	42
Zhang and Dewing 2008	Comeault No. 1	Churchill River			1743,00	0,37	32,56	0,01	1,76	430	4,46	730	39
Zhang and Dewing 2008	Comeault No. 1	Churchill River			1755,58	0,40	3,74	0,10	0,99	429	1,55	241	64
Zhang and Dewing 2008	Comeault No. 1	Churchill River			1764,00	0,17	3,37	0,05	0,96	432	1,06	318	91
106-10-HBL-Comeault-4	Comeault. No. 1	Churchill River			1780,00	0,09	0,20	0,30	0,58	416	0,50	40	116
Zhang and Dewing 2008	Comeault. No. 1	Churchill River			1782,50	0,02	0,10	0,19	0,31	438	0,48	21	65
Zhang and Dewing 2008	Comeault No. 1	Churchill River			1800,50	0,03	0,56	0,06	0,51	434	0,43	130	119
Zhang and Dewing 2008	Comeault No. 1	Red Head Rapid			1811,50	0,06	0,83	0,07	0,33	440	0,40	208	83
Zhang and Dewing 2008	Comeault No. 1	Bad Cache Rapids			1832,50	0,05	3,87	0,01	0,38	436	0,94	412	40
Zhang and Dewing 2008	Comeault No. 1	Bad Cache Rapids			1835,33	0,08	3,90	0,02	0,44	434	0,85	459	52
Zhang and Dewing 2008	Comeault No. 1	Bad Cache Rapids			1907,17	0,06	1,55	0,04	0,48	435	0,39	397	123
Zhang and Dewing 2008	Comeault No. 1	Bad Cache Rapids			2020,00	0,10	1,31	0,07	0,31	429	0,47	279	66
106-10-HBL-Comeault-1	Comeault No. 1	Bad Cache Rapids			2020,00	0,19	1,75	0,10	0,24	430	0,54	324	44
106-10-HBL Kask-2	Kaskattama No.1	Severn River	671277	6328360	2185,00	0,05	0,46	0,10	0,46	428	0,19	242	242
K-2195.8	Kaskattama No.1	Red Head Rapids			2195,80	0,10	0,81	0,11	0,29	440	0,34	238	85
106-10-HBL Kask-1	Kaskattama No.1	Red Head Rapids			2200,60	0,32	1,89	0,15	0,44	439	0,55	344	80
106-10-HBL Kask-3	Kaskattama No.1	Bad Cache Rapids			2626,60	0,08	0,60	0,11	0,44	427	0,74	81	59
106-10-HBL Kask-4	Kaskattama No.1	Bad Cache Rapid			2628,00	0,12	0,54	0,19	0,78	428	1,05	51	74
106-10-HBL Kask-5	Kaskattama No.1	Bad Cache Rapids			2665,00	0,07	0,20	0,27	0,65	421	0,82	24	79
106-10-HBL Kask-6	Kaskattama No.1	Bad Cache Rapids			2905,00	0,10	0,76	0,12	0,53	421	0,37	205	143
106-10-HBL Kask-7	Kaskattama No.1	Bad Cache Rapids			2907,60	0,11	0,82	0,12	0,30	422	0,37	222	81
106-10-HBL HB2-1	Pennycutaway No.2	Bad Cache Rapids	517758	6284030	336,00	0,04	0,09	0,29	0,56	363	0,39	23	144
106-10-HBL HB2-2	Pennycutaway	Bad Cache Rapids			380,00	0,27	2,81	0,09	0,44	428	1,35	208	33

	No.2												
106-10-HBL HB2-3	Pennycutaway No.2	Bad Cache Rapids			394,50	0,03	0,58	0,05	0,33	432	0,29	200	114
106-11-HBI-KK1-1	Kaskattama Kimberlite No1	Severn River	630684	6236761	900,50	0,51	5,74	0,08	0,45	418	1,53	375	29
106-10-HBL- M-1-03-1	M-1-03l	Red Head Rapids	532063	6360180	55,94	0,05	0,09	0,36	1,02	312	0,28	32	364
106-11-HBL-ADD5-1	ADD-05-01	Bad Cache Rapids	627674	6282230	250,98	0,03	0,56	0,05	0,42	427	0,23	243	183
106-10-HBL Kennco 5-1	Kennco No.5	Bad Cache Rapids	485898	6338560	846,45	0,03	0,33	0,07	0,44	425	0,26	127	169

Annex 1.8: Rock-Eval6/TOC data for samples collected in the Narwhal South O-58 well. Shaded lines indicate S2 values > 0.35 mg HC/g TOC.

Sample ID	Well	Strat. Unit	Depth ft	S1	S2	PI	S3	Tmax	TOC(%)	HI	OI
Zhang and Dewing 2008	Narwhal South	Kenogami River	1550	0,05	0,08	0,35	0,34	429	0,21	38	162
Zhang and Dewing 2008	Narwhal South	Kenogami River	1630	0,03	0,11	0,21	0,44	427	0,30	37	147
Zhang and Dewing 2008	Narwhal South	Kenogami River	1730	0,04	0,09	0,31	0,76	444	0,16	56	475
Zhang and Dewing 2008	Narwhal South	Kenogami River	1790	0,01	0,07	0,14	0,23	444	0,08	88	288
Zhang and Dewing 2008	Narwhal South	Kenogami River	1840	0,07	0,24	0,22	1,64	422	0,18	133	911
Zhang and Dewing 2008	Narwhal South	Kenogami River	1880	0,03	0,14	0,16	0,42	430	0,13	108	323
Zhang and Dewing 2008	Narwhal South	Attawapiskat	2460	0,01	0,05	0,14	0,15	442	0,06	83	250
Zhang and Dewing 2008	Narwhal South	Severn River	2550	0,01	0,04	0,17	0,28	431	0,06	67	467
Zhang and Dewing 2008	Narwhal South	Severn River	2570	0,03	0,85	0,04	0,45	432	0,27	315	167
Zhang and Dewing 2008	Narwhal South	Severn River	2600	0,12	3,34	0,03	0,68	424	0,81	412	84
Zhang and Dewing 2008	Narwhal South	Severn River	2620	0,02	0,72	0,03	0,28	435	0,20	360	140
Zhang and Dewing 2008	Narwhal South	Severn River	2640	0,01	0,31	0,04	0,24	437	0,14	221	171
Zhang and Dewing 2008	Narwhal South	Severn River	2680	0,01	0,27	0,04	0,27	433	0,14	193	193
Zhang and Dewing 2008	Narwhal South	Severn River	2750	0,02	0,25	0,07	0,48	426	0,19	132	253
Zhang and Dewing 2008	Narwhal South	Severn River	2760	0,01	0,12	0,10	0,36	423	0,16	75	225
Zhang and Dewing 2008	Narwhal South	Severn River	2870	0,01	0,23	0,06	0,27	428	0,16	144	169
Zhang and Dewing 2008	Narwhal South	Severn River	2900	0,03	0,61	0,05	0,29	429	0,20	305	145
Zhang and Dewing 2008	Narwhal South	Severn River	2920	0,02	0,18	0,08	0,18	431	0,11	164	164
Zhang and Dewing 2008	Narwhal South	Severn River	3010	0,02	0,32	0,05	0,25	430	0,14	229	179
Zhang and Dewing 2008	Narwhal South	Severn River	3090	0,02	0,29	0,07	0,34	426	0,17	171	200
Zhang and Dewing 2008	Narwhal South	Severn River	3180	0,01	0,24	0,06	0,26	430	0,14	171	186
Zhang and Dewing 2008	Narwhal South	Severn River	3210	0,02	0,27	0,07	0,30	432	0,15	180	200
Zhang and Dewing 2008	Narwhal South	Severn River	3240	0,02	0,26	0,07	0,27	436	0,09	289	300
Zhang and Dewing 2008	Narwhal South	Severn River	3260	0,02	0,20	0,07	0,25	433	0,09	222	278
Zhang and Dewing 2008	Narwhal South	Red Head Rapids	3290	0,01	0,06	0,12	0,29	430	0,13	46	223
Zhang and Dewing 2008	Narwhal South	Red Head Rapids	3320	0,01	0,16	0,08	0,26	432	0,13	123	200
Zhang and Dewing 2008	Narwhal South	Red Head Rapids	3360	0,08	0,76	0,09	0,32	436	0,48	158	67
Zhang and Dewing 2008	Narwhal South	Red Head Rapids	3440	0,02	0,11	0,13	0,80	430	0,25	44	320
Zhang and Dewing 2008	Narwhal South	Red Head Rapids	3500	0,01	0,14	0,09	0,73	427	0,26	54	281
Zhang and Dewing 2008	Narwhal South	Red Head Rapids	3510	0,02	0,17	0,10	0,42	430	0,16	106	263

Zhang and Dewing 2008	Narwhal South	Red Head Rapids	3520	0,01	0,16	0,08	0,24	432	0,10	160	240
Zhang and Dewing 2008	Narwhal South	Red Head Rapids	3560	0,01	0,17	0,08	0,35	430	0,14	121	250
Zhang and Dewing 2008	Narwhal South	Red Head Rapids	3580	0,01	0,16	0,08	0,22	431	0,14	114	157
Zhang and Dewing 2008	Narwhal South	Churchill River	3610	0,02	0,23	0,06	0,18	433	0,16	144	113
Zhang and Dewing 2008	Narwhal South	Churchill River	3620	0,01	0,18	0,07	0,21	433	0,12	150	175
Zhang and Dewing 2008	Narwhal South	Churchill River	3640	0,02	0,23	0,06	0,21	432	0,21	110	100
Zhang and Dewing 2008	Narwhal South	Churchill River	3690	0,01	0,16	0,06	0,16	433	0,18	89	89
Zhang and Dewing 2008	Narwhal South	Churchill River	3740	0,01	0,14	0,08	0,19	435	0,17	82	112
Zhang and Dewing 2008	Narwhal South	Churchill River	3770	0,01	0,12	0,06	0,26	436	0,10	120	260
Zhang and Dewing 2008	Narwhal South	Churchill River	3810	0,01	0,16	0,07	0,32	433	0,11	145	291
Zhang and Dewing 2008	Narwhal South	Churchill River	3840	0,01	0,13	0,07	0,46	434	0,11	118	418
Zhang and Dewing 2008	Narwhal South	Churchill River	3860	0,01	0,14	0,08	0,28	434	0,08	175	350
Zhang and Dewing 2008	Narwhal South	Churchill River	3910	0,02	0,19	0,09	0,33	435	0,19	100	174
Zhang and Dewing 2008	Narwhal South	Churchill River	3940	0,03	0,22	0,10	0,36	437	0,16	138	225
Zhang and Dewing 2008	Narwhal South	Churchill River	3960	0,02	0,30	0,06	0,38	435	0,18	167	211
Zhang and Dewing 2008	Narwhal South	Churchill River	3950	0,01	0,18	0,07	0,30	438	0,12	150	250
Zhang and Dewing 2008	Narwhal South	Churchill River	3970	0,01	0,19	0,07	0,31	436	0,16	119	194
Zhang and Dewing 2008	Narwhal South	Churchill River	3975	0,01	0,20	0,07	0,24	436	0,15	133	160
Zhang and Dewing 2008	Narwhal South	Bad Cache Rapids	3980	0,02	0,16	0,09	0,27	433	0,19	84	142
Zhang and Dewing 2008	Narwhal South	Bad Cache Rapids	3985	0,02	0,19	0,08	0,49	432	0,16	119	306
Zhang and Dewing 2008	Narwhal South	Bad Cache Rapids	3990	0,01	0,07	0,09	0,21	438	0,08	88	263
Zhang and Dewing 2008	Narwhal South	Bad Cache Rapids	4000	0,02	1,15	0,02	0,31	433	0,28	411	111
Zhang and Dewing 2008	Narwhal South	Bad Cache Rapids	4010	0,02	0,61	0,03	0,22	435	0,22	277	100
Zhang and Dewing 2008	Narwhal South	Bad Cache Rapids	4015	0,02	0,69	0,02	0,23	436	0,19	363	121
Zhang and Dewing 2008	Narwhal South	Bad Cache Rapids	4020	0,02	0,33	0,05	0,50	431	0,26	127	192
Zhang and Dewing 2008	Narwhal South	Bad Cache Rapids	4030	0,02	1,31	0,02	0,38	434	0,28	468	136
Zhang and Dewing 2008	Narwhal South	Bad Cache Rapids	4040	0,03	0,80	0,03	0,28	432	0,22	364	127
Zhang and Dewing 2008	Narwhal South	Bad Cache Rapids	4050	0,03	0,76	0,03	0,28	434	0,24	317	117
Zhang and Dewing 2008	Narwhal South	Bad Cache Rapids	4060	0,02	0,70	0,03	0,30	432	0,23	304	130
Zhang and Dewing 2008	Narwhal South	Bad Cache Rapids	4070	0,02	0,54	0,04	0,27	431	0,21	257	129
Zhang and Dewing 2008	Narwhal South	Bad Cache Rapids	4080	0,02	0,45	0,04	0,24	433	0,20	225	120
Zhang and Dewing 2008	Narwhal South	Bad Cache Rapids	4090	0,02	0,39	0,05	0,16	434	0,19	205	84
Zhang and Dewing 2008	Narwhal South	Bad Cache Rapids	4100	1,40	0,68	0,67	0,31	431	0,35	194	89

Zhang and Dewing 2008	Narwhal South	Bad Cache Rapids	4110	0,02	0,34	0,05	0,22	435	0,10	340	220
Zhang and Dewing 2008	Narwhal South	Bad Cache Rapids	4120	0,02	0,45	0,04	0,22	435	0,13	346	169
Zhang and Dewing 2008	Narwhal South	Bad Cache Rapids	4130	0,02	0,42	0,04	0,23	433	0,16	262	144
Zhang and Dewing 2008	Narwhal South	Bad Cache Rapids	4140	0,02	0,52	0,03	0,24	433	0,12	433	200
Zhang and Dewing 2008	Narwhal South	Bad Cache Rapids	4150	0,02	0,43	0,04	0,46	436	0,17	253	271
Zhang and Dewing 2008	Narwhal South	Bad Cache Rapids	4160	0,02	0,45	0,04	0,29	431	0,16	281	181
Zhang and Dewing 2008	Narwhal South	Bad Cache Rapids	4165	0,02	0,50	0,04	0,34	434	0,15	333	227
Zhang and Dewing 2008	Narwhal South	Bad Cache Rapids	4170	0,02	0,30	0,06	0,40	436	0,08	375	500
Zhang and Dewing 2008	Narwhal South	Bad Cache Rapids	4180	0,03	0,39	0,07	0,23	436	0,12	325	192
Zhang and Dewing 2008	Narwhal South	Bad Cache Rapids	4190	0,01	0,40	0,03	0,32	431	0,16	250	200
Zhang and Dewing 2008	Narwhal South	Bad Cache Rapids	4200	0,09	0,39	0,19	0,30	431	0,17	229	176
Zhang and Dewing 2008	Narwhal South	Bad Cache Rapids	4210	0,01	0,21	0,06	0,19	438	0,11	191	173
Zhang and Dewing 2008	Narwhal South	Bad Cache Rapids	4220	0,01	0,15	0,06	0,16	436	0,10	150	160
Zhang and Dewing 2008	Narwhal South	Bad Cache Rapids	4230	0,01	0,22	0,05	0,24	435	0,11	200	218
Zhang and Dewing 2008	Narwhal South	Bad Cache Rapids	4240	0,01	0,20	0,06	0,21	435	0,12	167	175
Zhang and Dewing 2008	Narwhal South	Bad Cache Rapids	4250	0,01	0,18	0,06	0,19	437	0,10	180	190
Zhang and Dewing 2008	Narwhal South	Bad Cache Rapids	4260	0,01	0,22	0,05	0,19	436	0,14	157	136
Zhang and Dewing 2008	Narwhal South	Bad Cache Rapids	4280	0,01	0,29	0,04	0,25	445	0,15	193	167

Annex 1.9: Rock-Eval6/TOC data for samples collected in the Polar Bear C-11 well. Shaded lines indicate S2 values > 0.35 mg HC/g TOC.

Sample ID	Well	Strat. Unit	Depth ft	S1	S2	PI	S3	Tmax	TOC(%)	HI	OI
Zhang and Dewing 2008	Polar Bear	Kenogami River	2660	0,15	1,72	0,08	0,38	427	0,50	344	76
Zhang and Dewing 2008	Polar Bear	Kenogami River	2670	0,19	2,28	0,08	0,40	425	0,56	407	71
Zhang and Dewing 2008	Polar Bear	Kenogami River	2680	0,11	1,71	0,06	0,32	427	0,48	356	67
Zhang and Dewing 2008	Polar Bear	Kenogami River	2690	0,11	1,10	0,09	0,39	431	0,36	306	108
Zhang and Dewing 2008	Polar Bear	Ekwan River	3120	0,02	0,06	0,29	4,00	413	0,29	21	1379
Zhang and Dewing 2008	Polar Bear	Ekwan River	3130	0,15	0,39	0,27	2,79	326	0,31	126	900
Zhang and Dewing 2008	Polar Bear	Ekwan River	3140	0,09	0,33	0,21	2,21	339	0,27	122	819
Zhang and Dewing 2008	Polar Bear	Ekwan River	3150	0,06	0,19	0,23	1,96	432	0,20	95	980
Zhang and Dewing 2008	Polar Bear	Severn River	3660	0,02	0,06	0,26	0,18	464	0,05	120	360
Zhang and Dewing 2008	Polar Bear	Severn River	3700	0,02	0,05	0,27	0,18	470	0,06	83	300
Zhang and Dewing 2008	Polar Bear	Severn River	3750	0,01	0,07	0,14	0,25	448	0,05	140	500
Zhang and Dewing 2008	Polar Bear	Severn River	3760	0,01	0,07	0,15	0,15	442	0,06	117	250
Zhang and Dewing 2008	Polar Bear	Severn River	3785	1,14	0,75	0,60	0,28	425	0,32	234	88
Zhang and Dewing 2008	Polar Bear	Severn River	3790	0,18	0,37	0,33	0,41	338	0,17	218	241
Zhang and Dewing 2008	Polar Bear	Severn River	3800	0,04	0,19	0,17	0,30	422	0,12	158	250
Zhang and Dewing 2008	Polar Bear	Severn River	3805	0,02	0,06	0,24	0,20	438	0,09	67	222
Zhang and Dewing 2008	Polar Bear	Severn River	3810	0,02	0,05	0,33	0,23	440	0,09	56	256
Zhang and Dewing 2008	Polar Bear	Severn River	3815	0,01	0,05	0,22	0,20	435	0,10	50	200
Zhang and Dewing 2008	Polar Bear	Severn River	3820	0,02	0,12	0,17	0,15	433	0,12	100	125
Zhang and Dewing 2008	Polar Bear	Severn River	3825	0,02	0,12	0,16	0,17	440	0,09	133	189
Zhang and Dewing 2008	Polar Bear	Severn River	3830	0,02	0,09	0,15	0,20	437	0,10	90	200
Zhang and Dewing 2008	Polar Bear	Severn River	3835	0,03	0,11	0,19	0,15	438	0,10	110	150
Zhang and Dewing 2008	Polar Bear	Severn River	3850	0,03	0,18	0,15	0,18	436	0,16	112	113
Zhang and Dewing 2008	Polar Bear	Severn River	3870	0,03	0,22	0,12	0,19	436	0,14	157	136
Zhang and Dewing 2008	Polar Bear	Severn River	3910	0,05	0,40	0,11	0,19	432	0,12	333	158
Zhang and Dewing 2008	Polar Bear	Severn River	3930	0,02	0,20	0,11	0,17	432	0,16	125	106
Zhang and Dewing 2008	Polar Bear	Severn River	3960	0,04	0,30	0,13	0,16	428	0,14	214	114
Zhang and Dewing 2008	Polar Bear	Severn River	4020	0,05	0,38	0,12	0,21	433	0,17	224	124
Zhang and Dewing 2008	Polar Bear	Severn River	4070	0,05	0,48	0,09	0,21	430	0,18	267	117

Zhang and Dewing 2008	Polar Bear	Severn River	4110	0,07	0,59	0,10	0,19	430	0,20	295	95
Zhang and Dewing 2008	Polar Bear	Severn River	4120	0,05	0,63	0,08	0,19	431	0,21	300	90
Zhang and Dewing 2008	Polar Bear	Severn River	4150	0,05	0,33	0,13	0,25	434	0,17	194	147
Zhang and Dewing 2008	Polar Bear	Severn River	4190	0,04	0,29	0,13	0,17	433	0,15	193	113
Zhang and Dewing 2008	Polar Bear	Severn River	4210	0,08	0,44	0,15	0,16	430	0,19	232	84
Zhang and Dewing 2008	Polar Bear	Severn River	4250	0,02	0,20	0,09	0,23	435	0,10	200	230
Zhang and Dewing 2008	Polar Bear	Severn River	4270	0,02	0,18	0,09	0,19	435	0,14	129	136
Zhang and Dewing 2008	Polar Bear	Severn River	4300	0,01	0,17	0,07	0,19	436	0,14	121	136
Zhang and Dewing 2008	Polar Bear	Red Head Rapids	4320	0,02	0,29	0,08	0,50	435	0,18	161	278
Zhang and Dewing 2008	Polar Bear	Red Head Rapids	4360	0,08	0,54	0,12	0,36	434	0,27	200	133
C-457654	Polar Bear	Red Head Rapids	4360	0,20	1,43	0,12	2,59	433	0,94	152	276
Zhang and Dewing 2008	Polar Bear	Red Head Rapids	4365	0,10	1,00	0,09	0,23	435	0,33	303	70
C-457655	Polar Bear	Red Head Rapids	4365	0,17	2,08	0,08	0,45	434	0,70	297	64
Zhang and Dewing 2008	Polar Bear	Red Head Rapids	4370	0,11	1,07	0,09	0,23	432	0,36	297	64
C-457656	Polar Bear	Red Head Rapids	4370	0,40	3,49	0,10	0,20	427	0,75	465	27
Zhang and Dewing 2008	Polar Bear	Red Head Rapids	4380	0,06	0,82	0,06	0,26	431	0,30	273	87
C-457657	Polar Bear	Red Head Rapids	4380	0,90	3,67	0,20	1,42	419	1,23	298	115
Zhang and Dewing 2008	Polar Bear	Red Head Rapids	4385	0,02	0,34	0,05	0,36	436	0,16	212	225
C-457659	Polar Bear	Red Head Rapids	4390	0,19	1,57	0,11	1,32	427	0,89	176	148
C-457663	Polar Bear	Red Head Rapids	4410	0,10	0,58	0,15	1,70	439	0,53	109	321
C-457664	Polar Bear	Red Head Rapids	4420	0,10	1,11	0,08	0,76	448	0,54	206	141
C-457670	Polar Bear	Red Head Rapids	4445	0,23	5,42	0,04	3,66	423	2,29	237	160
C-457672	Polar Bear	Red Head Rapids	4455	0,11	1,13	0,09	0,32	429	0,29	390	110
Zhang and Dewing 2008	Polar Bear	Red Head Rapids	4460	0,02	0,24	0,07	0,22	435	0,16	150	138
C-457673	Polar Bear	Red Head Rapids	4460	0,09	1,01	0,08	0,41	428	0,43	235	95
C-457674	Polar Bear	Red Head Rapids	4465	0,18	3,33	0,05	0,41	428	0,77	432	53
Zhang and Dewing 2008	Polar Bear	Red Head Rapids	4475	0,02	0,16	0,09	0,27	436	0,13	123	208
Zhang and Dewing 2008	Polar Bear	Red Head Rapids	4480	0,04	0,17	0,18	0,27	431	0,17	100	159
C-457677	Polar Bear	Red Head Rapids	4480	0,57	1,17	0,33	0,37	428	0,50	234	74
Zhang and Dewing 2008	Polar Bear	Red Head Rapids	4485	0,02	0,18	0,10	0,21	431	0,15	120	140
C-457678	Polar Bear	Red Head Rapids	4485	1,15	3,52	0,25	0,45	422	1,07	329	42
C-457680	Polar Bear	Red Head Rapids	4495	0,42	2,42	0,15	2,50	425	2,23	109	112

C-457683	Polar Bear	Red Head Rapids	4510	0,55	5,29	0,09	2,19	418	1,74	304	126
C-457684	Polar Bear	Red Head Rapids	4515	0,20	2,26	0,08	0,52	422	0,86	263	60
Zhang and Dewing 2008	Polar Bear	Red Head Rapids	4525	0,01	0,13	0,08	0,20	437	0,13	100	154
Zhang and Dewing 2008	Polar Bear	Red Head Rapids	4530	0,01	0,10	0,08	0,21	438	0,11	91	191
Zhang and Dewing 2008	Polar Bear	Red Head Rapids	4535	0,01	0,09	0,09	0,14	437	0,07	129	200
C-457687	Polar Bear	Red Head Rapids	4535	0,04	0,60	0,07	0,28	426	0,35	171	80
C-457691	Polar Bear	Churchill River	4560	0,64	5,43	0,11	0,71	420	1,38	393	51
C-457695	Polar Bear	Churchill River	4580	0,70	6,51	0,10	0,75	426	1,21	538	62
C-457696	Polar Bear	Churchill River	4585	0,35	3,88	0,08	0,76	424	0,98	396	78
Zhang and Dewing 2008	Polar Bear	Churchill River	4590	0,03	0,22	0,10	0,28	435	0,17	129	165
C-457699	Polar Bear	Churchill River	4600	9,98	28,42	0,26	2,70	417	5,61	507	48
C-457700	Polar Bear	Churchill River	4605	17,50	8,48	0,67	1,93	260	3,96	214	49
Zhang and Dewing 2008	Polar Bear	Churchill River	4610	0,02	0,17	0,11	0,20	436	0,10	170	200
C-457702	Polar Bear	Churchill River	4615	10,76	26,27	0,29	4,16	414	5,73	458	73
Zhang and Dewing 2008	Polar Bear	Churchill River	4630	0,05	0,45	0,10	0,25	431	0,15	300	167
Zhang and Dewing 2008	Polar Bear	Churchill River	4670	0,02	0,17	0,13	0,24	438	0,11	155	218
Zhang and Dewing 2008	Polar Bear	Churchill River	4690	0,08	0,43	0,15	0,50	431	0,20	215	250
Zhang and Dewing 2008	Polar Bear	Churchill River	4720	0,02	0,22	0,09	0,28	435	0,14	157	200
Zhang and Dewing 2008	Polar Bear	Churchill River	4750	0,25	1,30	0,16	1,31	333	0,60	217	218
Zhang and Dewing 2008	Polar Bear	Churchill River	4770	0,03	0,23	0,13	0,29	438	0,12	192	242
Zhang and Dewing 2008	Polar Bear	Churchill River	4790	0,49	1,04	0,32	0,63	428	0,32	325	197
Zhang and Dewing 2008	Polar Bear	Churchill River	4810	0,07	0,22	0,23	0,29	432	0,15	147	193
Zhang and Dewing 2008	Polar Bear	Churchill River	4830	0,01	0,18	0,07	0,25	438	0,12	150	208
Zhang and Dewing 2008	Polar Bear	Churchill River	4840	0,02	0,27	0,08	0,24	432	0,16	169	150
Zhang and Dewing 2008	Polar Bear	Churchill River	4850	0,02	0,26	0,08	0,24	432	0,16	162	150
Zhang and Dewing 2008	Polar Bear	Churchill River	4870	0,03	0,26	0,10	0,19	434	0,16	162	119
Zhang and Dewing 2008	Polar Bear	Churchill River	4875	0,03	0,32	0,08	0,28	434	0,19	168	147
Zhang and Dewing 2008	Polar Bear	Churchill River	4880	0,02	0,26	0,08	0,31	434	0,18	144	172
Zhang and Dewing 2008	Polar Bear	Churchill River	4885	0,02	0,21	0,09	0,36	435	0,20	105	180
Zhang and Dewing 2008	Polar Bear	Churchill River	4890	0,02	0,23	0,08	0,32	435	0,18	128	178
Zhang and Dewing 2008	Polar Bear	Bad Cache Rapids	4895	0,02	0,19	0,09	0,43	437	0,19	100	226
Zhang and Dewing 2008	Polar Bear	Bad Cache Rapids	4900	0,02	0,19	0,09	0,33	434	0,17	112	194

Zhang and Dewing 2008	Polar Bear	Bad Cache Rapids	4905	0,02	0,21	0,09	0,41	435	0,21	100	195
Zhang and Dewing 2008	Polar Bear	Bad Cache Rapids	4910	0,02	0,17	0,09	0,43	431	0,20	85	215
Zhang and Dewing 2008	Polar Bear	Bad Cache Rapids	4920	0,02	0,20	0,08	0,33	436	0,16	125	206
Zhang and Dewing 2008	Polar Bear	Bad Cache Rapids	4930	0,02	0,28	0,06	0,23	438	0,15	187	153
Zhang and Dewing 2008	Polar Bear	Bad Cache Rapids	4940	0,02	0,32	0,05	0,18	437	0,12	267	150
Zhang and Dewing 2008	Polar Bear	Bad Cache Rapids	4950	0,02	0,31	0,05	0,17	439	0,12	258	142
Zhang and Dewing 2008	Polar Bear	Bad Cache Rapids	4960	0,02	0,31	0,05	0,23	438	0,15	207	153
Zhang and Dewing 2008	Polar Bear	Bad Cache Rapids	4970	0,02	0,30	0,06	0,16	437	0,15	200	107
Zhang and Dewing 2008	Polar Bear	Bad Cache Rapids	4980	0,01	0,23	0,05	0,19	439	0,14	164	136
Zhang and Dewing 2008	Polar Bear	Bad Cache Rapids	4990	0,02	0,35	0,05	0,18	438	0,16	219	113
Zhang and Dewing 2008	Polar Bear	Bad Cache Rapids	5000	0,02	0,44	0,05	0,17	434	0,17	259	100
Zhang and Dewing 2008	Polar Bear	Bad Cache Rapids	5010	0,02	0,50	0,04	0,21	435	0,22	227	95
Zhang and Dewing 2008	Polar Bear	Bad Cache Rapids	5020	0,02	0,46	0,04	0,19	434	0,14	329	136
Zhang and Dewing 2008	Polar Bear	Bad Cache Rapids	5030	0,01	0,30	0,05	0,19	437	0,10	300	190
Zhang and Dewing 2008	Polar Bear	Bad Cache Rapids	5040	0,01	0,34	0,04	0,17	436	0,14	243	121
Zhang and Dewing 2008	Polar Bear	Bad Cache Rapids	5050	0,01	0,34	0,04	0,18	437	0,14	243	129
Zhang and Dewing 2008	Polar Bear	Bad Cache Rapids	5060	0,02	0,31	0,05	0,23	435	0,13	238	177
Zhang and Dewing 2008	Polar Bear	Bad Cache Rapids	5070	0,02	0,28	0,06	0,28	436	0,10	280	280
Zhang and Dewing 2008	Polar Bear	Bad Cache Rapids	5080	0,01	0,20	0,07	0,18	436	0,10	200	180
Zhang and Dewing 2008	Polar Bear	Bad Cache Rapids	5090	0,01	0,18	0,06	0,22	438	0,09	200	244
Zhang and Dewing 2008	Polar Bear	Bad Cache Rapids	5100	0,01	0,19	0,06	0,22	437	0,12	158	183
Zhang and Dewing 2008	Polar Bear	Bad Cache Rapids	5110	0,01	0,15	0,05	0,14	438	0,12	125	117

Annex 1.10: Rock-Eval6/TOC data for samples collected in the Beluga O-23 well. Shaded lines indicate S2 values > 0.35 mg HC/g TOC. Samples 12SZ-01-xx are from Zhang and Hu (2013).

Sample ID	Well	Strat. unit	Depth (m)	S1	S2	PI	S3	Tmax	TOC(%)	HI	OI
12SZ-01-01	Beluga	Williams Island	630	4,22	52,73	0,07	3,53	416	12,10	436	29
12SZ-01-02	Beluga	Murray Island	635	4,63	49,17	0,09	3,32	414	11,60	424	29
12SZ-01-03	Beluga	Moose River	640	2,63	32,75	0,07	2,58	416	7,49	437	34
12SZ-01-04	Beluga	Moose River	645	4,01	48,00	0,08	3,30	416	10,86	442	30
12SZ-01-06	Beluga	Moose River	650	3,29	39,14	0,08	2,86	413	9,29	421	31
12SZ-01-06	Beluga	Moose River	655	0,31	5,21	0,06	3,10	423	2,40	217	129
12SZ-01-07	Beluga	Moose River	660	4,17	45,72	0,08	3,24	414	10,68	428	30
12SZ-01-08	Beluga	Moose River	665	1,15	15,27	0,07	1,22	416	3,57	428	34
12SZ-01-09	Beluga	Moose River	675	3,19	36,27	0,08	2,58	415	8,09	448	32
12SZ-01-10	Beluga	Moose River	680	2,03	24,36	0,08	1,77	416	5,61	434	32
12SZ-01-11	Beluga	Moose River	685	4,43	47,57	0,09	2,95	413	10,97	434	27
12SZ-01-12	Beluga	Moose River	690	5,07	48,68	0,09	3,04	415	10,83	449	28
12SZ-01-13	Beluga	Moose River	695	3,45	40,18	0,08	2,73	416	9,08	443	30
12SZ-01-14	Beluga	Moose River	700	7,19	74,61	0,09	4,89	414	17,64	423	28
12SZ-01-15	Beluga	Moose River	710	5,05	58,45	0,08	3,99	418	13,17	444	30
12SZ-01-16	Beluga	Moose River	715	1,99	25,30	0,07	2,08	416	5,96	424	35
12SZ-01-17	Beluga	Moose River	720	2,57	29,02	0,08	2,25	415	6,48	448	35
12SZ-01-18	Beluga	Kwataboahegan	730	0,53	5,89	0,08	0,86	416	1,60	368	54
12SZ-01-19	Beluga	Kwataboahegan	760	3,03	40,12	0,07	2,52	423	8,11	495	31
12SZ-01-20	Beluga	Kwataboahegan	765	3,73	37,98	0,09	2,66	416	8,71	436	31
12SZ-01-21	Beluga	Kwataboahegan	770	0,67	6,55	0,09	2,75	420	2,57	255	107
12SZ-01-22	Beluga	Kwataboahegan	775	4,78	51,63	0,08	4,39	413	12,97	398	34
12SZ-01-23	Beluga	Kwataboahegan	780	3,85	45,76	0,08	4,45	412	11,74	390	38
12SZ-01-24	Beluga	Stooping River	785	8,53	78,14	0,10	4,91	412	18,74	417	26
12SZ-01-25	Beluga	Stooping River	810	0,55	6,64	0,08	6,34	426	4,68	142	135
12SZ-01-26	Beluga	Stooping River	835	1,72	23,36	0,07	4,93	417	8,79	266	56

12SZ-01-27	Beluga	Stooping River	850	1,00	9,53	0,10	6,12	420	5,45	175	112
12SZ-01-28	Beluga	Stooping River	875	6,58	59,92	0,10	4,42	413	14,82	404	30
	Beluga	Kenogami River	1580	0,02	0	1	0,01	0	0,01	0	100
	Beluga	Kenogami River	1590	0	0,01	0	0,01	0	0,01	100	100
	Beluga	Kenogami River	1600	0	0,01	0	0,01	0	0,01	100	100
	Beluga	Kenogami River	1610	0,01	0,02	0,33	0,01	371	0,11	18	9
	Beluga	Ekwan River	1620	0,06	0,09	0,4	0,01	423	0,4	22	2
	Beluga	Ekwan River	1630	0,02	0,09	0,18	0,01	431	0,14	64	7
	Beluga	Ekwan River	1640	0,01	0,09	0,1	0,01	435	0,09	99	11
	Beluga	Ekwan River	1650	0,05	0,05	0,5	0,01	429	0,01	500	100
	Beluga	Ekwan River	1660	0,03	0,03	0,5	0,01	431	0,04	74	25
	Beluga	Ekwan River	1680	0,09	0,11	0,45	0,01	429	0,05	220	20
	Beluga	Ekwan River	1690	0,08	0,19	0,3	0,01	431	0,04	475	25
	Beluga	Severn River	1700	0,15	0,34	0,31	0,01	433	0,05	680	20
	Beluga	Severn River	1720	0,09	0,25	0,26	0,01	431	0,03	833	33
	Beluga	Severn River	1730	0,06	0,15	0,29	0,01	430	0,08	187	12
	Beluga	Severn River	1740	0,09	0,24	0,27	0,01	433	0,1	239	10
	Beluga	Severn River	1750	0,28	0,37	0,43	0,01	433	0,14	264	7
	Beluga	Severn River	1760	0,08	0,12	0,4	0,01	431	0,02	599	50
	Beluga	Severn River	1770	0,07	0,21	0,25	0,01	431	0,03	699	33
	Beluga	Severn River	1780	0,03	0,16	0,16	0,01	434	0,03	533	33
	Beluga	Severn River	1790	0,48	0,36	0,57	1,02	432	0,11	327	927
	Beluga	Severn River	1800	0,05	0,2	0,2	0,45	433	0,04	500	1125
	Beluga	Severn River	1810	0,04	0,19	0,17	1,97	431	0,02	950	9849
	Beluga	Severn River	1820	0,03	0,25	0,11	0,72	434	0,07	357	1028
	Beluga	Severn River	1830	0,02	0,11	0,15	0,54	432	0,08	137	675
	Beluga	Severn River	1840	0,05	0,25	0,17	0,68	434	0,14	178	485
	Beluga	Severn River	1850	0,05	0,32	0,14	0,51	430	0,09	355	566
	Beluga	Severn River	1860	0,04	0,28	0,13	0,52	434	0,08	349	650
	Beluga	Severn River	1870	0,49	0,58	0,46	0,94	429	0,24	241	391
	Beluga	Severn River	1880	0	0,01	0	0,01	0	0,01	100	100
	Beluga	Severn River	1890	0,64	0,6	0,52	0,81	431	0,13	461	623
	Beluga	Severn River	1900	0,01	0,18	0,05	0,6	432	0,07	257	857

Beluga	Severn River	1910	0,04	0,27	0,13	1,05	432	0,08	337	1312
Beluga	Severn River	1910	0,05	0,19	0,21	1,11	431	0,07	271	1585
Beluga	Severn River	1920	0,05	0,23	0,18	0,45	434	0,06	383	750
Beluga	Severn River	1920	0,05	0,27	0,16	0,45	432	0,06	450	750
Beluga	Severn River	1930	0,01	0,15	0,06	0,34	435	0,03	500	1133
Beluga	Severn River	1930	0,01	0,08	0,11	0,41	434	0,03	266	1366
Beluga	Severn River	1940	0,01	0,09	0,1	0,59	431	0,08	112	737
Beluga	Red Head Rapids	1950	0,02	0,06	0,25	0,54	431	0,07	85	771
Beluga	Red Head Rapids	1950	0,03	0,26	0,1	0,5	432	0,12	216	416
Beluga	Red Head Rapids	1960	0,01	0,04	0,2	0,43	433	0,01	400	4299
Beluga	Red Head Rapids	1960	0	0,08	0	0,41	433	0,01	800	4100
Beluga	Red Head Rapids	1970	0,01	0,1	0,09	0,51	432	0,07	142	728
Beluga	Red Head Rapids	1970	0,01	0,17	0,06	0,49	432	0,05	340	979
Beluga	Red Head Rapids	1980	0,01	0,09	0,1	0,48	432	0,01	899	4799
Beluga	Red Head Rapids	1980	0,01	0,1	0,09	0,48	434	0,01	1000	4799
Beluga	Red Head Rapids	1990	0,18	0,29	0,38	1,98	425	0,09	322	2200
Beluga	Red Head Rapids	1990	0,15	0,21	0,42	1,88	430	0,12	174	1566
Beluga	Red Head Rapids	2000	0,91	0,4	0,69	1,97	428	0,32	125	615
Beluga	Red Head Rapids	2000	0,39	0,59	0,4	1,12	434	0,21	280	533
Beluga	Red Head Rapids	2010	0,27	0,21	0,56	1	432	0,12	174	833
Beluga	Red Head Rapids	2010	0,29	0,19	0,6	1,16	429	0,13	146	892
Beluga	Red Head Rapids	2020	0,57	0,45	0,56	1,01	426	0,24	187	420
Beluga	Churchill River	2030	0,15	0,12	0,56	1,05	430	0,14	85	750
Beluga	Churchill River	2040	0,2	0,17	0,54	0,81	435	0,15	113	540
Beluga	Churchill River	2040	0,25	0,15	0,63	0,94	433	0,17	88	552
Beluga	Churchill River	2050	0,21	0,06	0,78	0,79	436	0,08	74	987
Beluga	Churchill River	2050	0,23	0,17	0,58	0,78	436	0,14	121	557
Beluga	Churchill River	2060	0,05	0,12	0,29	0,52	432	0,03	400	1733
Beluga	Churchill River	2070	0,13	0,13	0,5	0,54	427	0,04	325	1350
Beluga	Churchill River	2080	0,06	0,12	0,33	0,62	430	0,04	299	1549
Beluga	Churchill River	2090	0,02	0,04	0,33	0,64	428	0,01	400	6400
Beluga	Churchill River	2100	0,11	0,19	0,37	1,49	435	0,1	190	1489
Beluga	Churchill River	2110	0,29	0,12	0,71	1,18	437	0,12	100	983

Beluga	Churchill River	2120	0,17	0,27	0,39	1,83	434	0,13	207	1407
Beluga	Bad Cache Rapids	2130	0,12	0,24	0,33	1,02	431	0,07	342	1457
Beluga	Bad Cache Rapids	2130	0,17	0,1	0,63	0,91	433	0,09	111	1011
Beluga	Bad Cache Rapids	2140	0,06	0,3	0,17	0,44	441	0,08	374	550
Beluga	Bad Cache Rapids	2140	0,06	0,2	0,23	0,47	439	0,06	333	783
Beluga	Bad Cache Rapids	2150	0,01	0,26	0,04	0,38	435	0,03	866	1266
Beluga	Bad Cache Rapids	2160	0,04	0,28	0,13	0,56	434	0,05	560	1120
Beluga	Bad Cache Rapids	2170	1,45	0,95	0,6	1,15	436	0,27	351	425
Beluga	Bad Cache Rapids	2180	0,06	0,21	0,22	0,71	433	0,04	524	1774
Beluga	Bad Cache Rapids	2190	0,03	0,15	0,17	0,6	432	0,02	749	2999
Beluga	Bad Cache Rapids	2200	0,2	0,17	0,54	0,71	417	0,1	170	709
Beluga	Bad Cache Rapids	2210	0,42	0,29	0,59	0,68	409	0,06	483	1133

Annex 1.11: Rock-Eval6/TOC data for samples collected in the Rowley well. Shaded lines indicate S2 values > 0.35 mg HC/g TOC.

Well	Unit	Depth (ft)	S1	S2	PI	S3	Tmax	TOC(%)	HI	OI
Rowley N-14	Map-Unit Ols	608	0,04	0,15	0,21	0,25	421	0,2	75	125
Rowley N-14	Map-Unit Ols	670,7	0,05	0,29	0,14	0,34	428	0,23	126	148
Rowley N-14	Map-Unit Ols	680	0,06	0,24	0,2	0,23	419	0,23	104	100
Rowley N-14	Map-Unit Ols	684,4	0,03	0,11	0,22	0,17	418	0,17	65	100
Rowley N-14	Map-Unit Ols	964	0,01	0,09	0,15	0,25	428	0,16	56	156
Rowley N-14	Map-Unit Ols	1016	0,03	0,1	0,21	0,16	436	0,12	83	133
Rowley N-14	Map-Unit Ols	1049	0,04	0,3	0,12	0,18	428	0,23	130	78
Rowley N-14	Map-Unit Ols	1050,5	0,12	1,02	0,11	0,5	433	0,63	162	79
Rowley N-14	Map-Unit Ols	1055,8	0,13	1,09	0,11	0,27	433	0,51	214	53
Rowley N-14	Map-Unit Ols	1079	0,03	0,17	0,15	0,17	423	0,18	94	94
Rowley N-14	Map-Unit Ols	1090,3	0,03	0,21	0,14	0,26	428	0,16	131	163
Rowley N-14	Map-Unit Ols	1093	0,04	1,2	0,03	0,2	432	0,36	333	56
Rowley N-14	Map-Unit Ols	1094,7	0,08	0,54	0,13	0,3	428	0,43	126	70
Rowley N-14	Map-Unit Ols	1124	0,12	2,47	0,04	0,32	435	0,6	412	53

Rowley N-14	Ship Point	1127,6	0,21	2,89	0,07	0,33	432	0,73	396	45
Rowley N-14	Ship Point	1145,6	0,04	0,4	0,1	0,19	427	0,31	129	61
Rowley N-14	Ship Point	1147	0,03	0,21	0,13	0,16	426	0,21	100	76
Rowley N-14	Ship Point	1151	0,04	0,32	0,1	0,18	423	0,23	139	78
Rowley N-14	Ship Point	1157	0,04	0,22	0,16	0,26	425	0,32	69	81
Rowley N-14	Ship Point	1159,4	0,27	4,76	0,05	0,58	432	1,67	285	35
Rowley N-14	Ship Point	1162,5	0,18	4,66	0,04	0,38	431	1,5	311	25
Rowley N-14	Ship Point	1165,2	0,04	0,16	0,2	0,23	420	0,31	52	74
Rowley N-14	Ship Point	1184,2	0,91	13,7	0,06	1,61	418	7,26	189	22
Rowley N-14	Ship Point	1202,5	0,01	0,07	0,1	0,32	415	0,35	20	91
Rowley N-14	Ship Point	1288,2	0,14	1,41	0,09	0,46	424	0,63	224	73
Rowley N-14	Ship Point	1292	0,08	0,56	0,12	0,43	418	0,39	144	110
Rowley N-14	Ship Point	1321,5	0,08	0,33	0,2	0,28	426	0,39	85	72
Rowley N-14	Ship Point	1339	0,13	1,66	0,07	0,31	415	1,04	160	30
Rowley N-14	Ship Point	1434,2	0,03	0,07	0,28	0,24	323	0,1	70	240
Rowley N-14	Ship Point	1456,5	0,02	0,04	0,32	0,24	399	0,21	19	114

Annex 1.12: Rock-Eval6/TOC data for samples collected in the Moose River Basin. Shaded lines indicate S2 values > 0.35 mg HC/g TOC.

Sample	Well	Unit	Easting	Northing	Latitude	Longitude	S1	S2	PI	S3	Tmax	TOC	HI	OI
94DKA-001B	Onakawana "B"	Long Rapid			50o 35' 24"N	81o 29' 10"W	0,15	5,32	0,03	1,21	424	2,42	220	50
94DKA-001E	Onakawana "B"	Long Rapid			50o 35' 24"N	81o 29' 10"W	0,28	10,84	0,03	4,18	415	6,21	175	67
94DKA-001F	Onakawana "B"	Long Rapid			50o 35' 24"N	81o 29' 10"W	0,39	20,42	0,02	3,58	418	6,86	298	52
94DKA-001I	Onakawana "B"	Long Rapid			50o 35' 24"N	81o 29' 10"W	1,37	58,16	0,02	3,42	419	11,21	519	31
94DKA-005F		Kwataboahegan	452571	5565793			0,34	0,74	0,31	0,70	431	0,45	164	156
94DKA-005H		Kwataboahegan	452571	5565793			0,04	0,39	0,08	0,79	424	0,43	91	184

ANNEX 2: LOW-TEMPERATURE GEOCHRONOLOGY

COMPLEMENTARY MATERIAL

Apatite fission track and U-Th/He methodology

All rock samples were broken into small pieces using a hydraulic splitter and jaw crusher, then ground in a disc mill and sieved to fragments <500 μm. The sieved material was then run over a Wilfley mineral separation table to produce an initial heavy mineral concentrate, which was then treated with conventional magnetic and heavy liquid techniques to produce an apatite-bearing fraction.

Apatite fission track – Apatite grains were mounted in epoxy resin on glass slides, ground and polished to an optical finish using diamond paste to expose internal grain surfaces. Polished mounts were etched in 5M HNO_3 for 20 seconds at 21°C to reveal the fossil tracks. Using a vacuum unit, an aluminum coating with a 5-7 nm thickness was applied to the etched mounts so as to enhance the reflectivity of the polished surface, and minimize internal reflections (Gleadow et al, 2009). Apatite grains with polished surfaces parallel to prismatic crystal faces and relatively homogeneous track distributions were selected for analysis using recent developments in digital microscopy, image analysis and computer software (designed for capturing high resolution images) which provide opportunities for a new automated counting approach for apatite fission-track analysis.

For this work, software (*TrackWorks*© and *FastTracks*©) recently developed by the Thermochronology Group at the University of Melbourne and AutoScan Systems was used. This software suite controls a Zeiss M1 digital microscope fitted with a high-resolution camera and an AutoScan© stage and is used at a total magnification of x1000 under both transmitted and reflected light for capturing a *z*-stack of images of the apatite crystals for determining the spontaneous track density on the crystals. The advantage of this procedure is that a permanent digital record of analysed crystals is stored and is available for later inspection, even after grains have been partly destroyed by laser ablation at a later stage. Further, this protocol offers improved accuracy for measuring the areas over which spontaneous tracks are counted as well as the visualization of crystals on a computer monitor.

Uranium content of the grains on which spontaneous track counts had been made was determined using an Agilent 7700x Series ICP-MS (Inductively Coupled Plasma Mass Spectrometry) system coupled with a pulsed (Q-switched) New Wave Nd:YAG laser with a wavelength of 213 nm. Laser ablation analyses were carried out under consistent conditions

(25 μm diameter beam size, ~ 2.5J/cm^2 energy, 10 Hz repetition rate, 25 seconds) on selected grains using NIST-612 glass and an in-house apatite for standardisation.

Fully etched confined track length and etch pit diameters (Dpar) of grains, were also measured from digital images after the *c*-axis had been determined using *FastTracks*© on polished surfaces parallel to prismatic crystal faces. Digital magnification that can be generated from the high-resolution images the measuring tools in this software enables the user to determine the confined fission track lengths and Dpars with improved accuracy.

Where possible, fission tracks in up to 30 suitable apatite grains were counted and 100 confined track lengths were measured per sample, in addition several Dpar measurements were carried out on each grain on which fission track counts were made.

Employing a combination of automated track counting with LA-ICP-MS (replacing conventional U determination via neutron irradiations) for this study as outlined above is a new methodology for fission-track analysis.

Apatite (U-Th-Sm)/He – Analytical protocols followed an established laboratory routine for laser He extraction from single grains (House et al, 2000). For this study, aliquots for (U-Th-Sm)/He analysis comprised single apatite crystals. Wherever possible, only clear euhedral and non-fractured grains with average grain radii in a close size range within each aliquot, between aliquots and similar to comparable samples were handpicked under an Olympus SZX12 binocular microscope. Grains were subsequently immersed in ethanol and checked under polarised light to detect possible mineral inclusions and grains with visible inclusions were discarded. However, many grains were not 100% transparent thereby hampering identification of fine inclusions, we cannot therefore rule out the possibility of small inclusions in our samples. After grain geometry had been imaged, measured and recorded for applying the α-ejection correction, samples were loaded into small, acid-treated platinum capsules. These were then outgassed under vacuum at ~900˚C for 5 minutes, using a fibre-optically coupled diode laser with an 820nm wavelength (to provide optimal coupling with samples and heating without melting, ablation or fusion), spiked with ^{3}He and gas volumes determined using a Balzers quadrupole mass spectrometer. A hot blank was run after each sample to verify complete outgassing of the apatite grains. Most samples yielded negligible amounts of gas even after the first re-extract, for all samples, the second re-extract contributed less than 0.5% of the total measured ^{4}He.

U, Th, and Sm analytical data were acquired via total dissolution of outgassed apatite in HNO_3 and analysis using an Agilent 7700x ICP-MS. Analyses were calibrated using the reference material BIVO-1, and Mud Tank apatite and international rock standard BCR-2. (U-Th-Sm)/He ages were calculated and corrected for α-emission following the approach of Farley et al. (1996). Analytical uncertainties for the University of Melbourne (U-Th)/He

facility are conservatively assessed to be ~6.2% (±1σ), which incorporates the α-correction-related constituent and takes into account an estimated 5 μm uncertainty in grain size measurements, gas analysis and ICP-MS uncertainties, but not those related to possible U and Th zonation. Accuracy and precision of U, Th and Sm content ranges up to 2% (at ±2σ), but is typically better than 1%. Durango apatite age standard (31.02 ± 1.01 Ma - McDowell et al, 2005) was routinely analysed with each batch of samples and served as further check on analytical accuracy and precision.

Sample No.	Lithology	Age	Location (Bold = well)	Easting	Northing	Latitude	Longitude	Apatite yield
Sedimentary rocks								
09SZ-21-01L	Paleozoic Sandstone	Ord	Southampton			64.2846944	-83.1066111	excellent
09SZ-21-02L	Paleozoic Sandstone	Ord	Southampton			64.2846944	-83.1066111	rare
09SZ-21-03L	Paleozoic Sandstone	Ord	Southampton			64.2846944	-83.1066111	rare
09SZ-25-01	Paleozoic Sandstone	Ord	Melville			69.4956	-82.843	rare
09SZ-27-01	Paleozoic Sandstone	Ord	Melville			69.4936	-82.8406	rare
2009-LKA-18 +19	Paleozoic Sandstone	Camb-Ord	**Akpatok F-26**			60.424606	-68.33575	minor
2009-LKA-20+21	Paleozoic Sandstone	Camb-Ord	**Akpatok F-26**			60.424606	-68.33575	rare
2009-LKA-37	Paleozoic Sandstone	Ord	**Narwhal South O-58**			58.133442	-84.134053	not detected
2009-LKA-39	Paleozoic Sandstone	Ord	**Polar Bear C-11**			58.501358	-86.788311	not detected
2009-LKA-41	Paleozoic Sandstone	Dev	**Polar Bear C-11**			58.501358	-86.788311	rare
2009-LKA-43+44	Paleozoic Sandstone	Ord	**Netsiq N-01**			59.846878	-87.516533	rare
2009-LKA-MB-01	Paleozoic Sandstone	Ord	**M-5-03**	433794	6514432			not detected
2009-LKA-MB-03	Paleozoic Sandstone	Ord	**M-2-03**	438338	6514122			not detected
2009-LKA-MB-05	Paleozoic Sandstone	Ord	**M-2-03**	438338	6514122			not detected
2009-LKA-52	Mesozoic Sandstone	Juras.	Victor Mine	305987	5856166			good
03 GRS 0022A	Core: quartz rich arenite grit with clay and silt; Ordovician	Ord	**Attawapiskat River,**			52.80801	-83.8757	possibly enough

03 GRS 26A	quartz rich, coarse grit at PC/Paleozoic contact, Ordovician	Ord	**S of Severn River, drill hole WB-001**			55.08152	-88.505	None
Crystalline rocks								
09SZ-23-01	Granite	Pc	Melville			69.4966	-82.8422	Excellent
09SZ-24-01	Granite	Pc	Melville			69.4958	-82.8435	Rare
2009-LKA-15+16+17	Gneiss	Pc	**Akpatok F-26**			60.424606	-68.33575	Excellent
2009-LKA-38	Gneiss	Pc	**Narwhal South O-58**			58.133442	-84.134053	Good
2009-LKA-40	Gneiss	Pc	**Polar Bear C-11**			58.501358	-86.788311	not detected
2009-LKA-42	Gneiss	Pc	**Beluga O-23**			59.215175	-88.557453	Good
2009-LKA-MB-02	Gneiss	Pc	**M-5-03**	433794	6514432			not detected
2009-LKA-MB-06	Gneiss	Pc	**M-2-03**	438338	6514122			not detected
2009-LKA-MB-07	Gneiss	Pc	**M-1-03**	437922	6513918			not detected
2009-LKA-MB-18	Gneiss	Pc	**M-4-03**	452492	6510505			not detected
2009-LKA-MB-20	Gneiss	Pc	**M-3-03**	437586	6514208			not detected
2009-LKA-MB-22	Gneiss	Pc	**ADD-9-1**	470286	6241708			not detected
03-PL-2614-B	Mafic	Pc	Northern Quebec	409808	6589749			not detected
03-JY-7117-B2	Mafic	Pc	Northern Quebec	479576	6326424			Good
03-JV-9017-A1 and A2	Mafic	Pc	Northern Quebec	452281	6383083			Rare
03-MB-3178-D	Mafic	Pc	Northern Quebec	409135	6410778			not detected
02-JY-9002-A2	Basalts	Pc	Northern Quebec	430696	6252313			very rare
02-JY-9024-A2+9025-A2	Basalts	Pc	Northern Quebec	429407	6254059			not detected
02-JY-9034-A3	Basalts	Pc	Northern Quebec	419919	6219550			not detected
02-JY-9035-A6	Basalts	Pc	Northern Quebec	421723	6218328			not detected
96-08-43-1	Rhyolite	Pc	South of Seal River			58.78936	-95.75658	sparse, small
96-08-40	Tonalite gneiss + amphibolite	Pc	Seal River			58.83282	-96.10948	sparse, small
07 CYA-M499	Blue-Qtz tonalite, granodiorite	Pc	Southampton Island			63.83916	-85.01008	sparse, small
96-08-15	Quartz arenite + argillite	Pc	North Knife River			58.59587	-95.07453	None

96-08-16	Quartzite, +pebble cgl	Pc	North Knife River			58.58216	-95.1526	None
BLC79 77 / BLC79 83	Pillow mafic flow - coarse grained	Pc	Ottawa_lls	545653	6617582			none detected
BLP81 126 / BLP 125	Massive coarse grained mafic flow	Pc	Ottawa_lls	539625	6615670			none detected
BL81 197	Massive coarse grained mafic flow	Pc	Smith Island	645649,3	6742181			none detected
BL82 588	Massive coarse grained mafic flow	Pc	Smith Island	633072,8	6739485			none detected
BL82 589	Massive coarse grained mafic flow	Pc	Smith Island	633087,8	6739422			none detected
BL82 711	Massive coarse grained mafic flow	Pc	Smith Island	636118,6	6742102			none detected
BL82 818	Massive coarse grained mafic breccia	Pc	Smith Island	659947,7	6753610			none detected
BL81 279	Massive mafic - coarse grained dolerite	Pc	Smith Island	658287,8	6746088			none detected
BL82 586A	apatite????	Pc	Smith Island	633054,8	6739556			none detected
2010 BTA-82	Diabase gabbro	Pc	Sutton Inlier	651053	6031858			none detected
10 RM111	Gabbro core	Pc	**Drill hole BT_09_56**	554265	5848857			Rare
97-10-395	K-spar porphyritic hblde-bi-granite	Pc	Manitoba	396670	6575164			Excellent
97-10-393	K-spar porphyritic hblde-bi-granite	Pc	Manitoba	383712	6580690			Excellent

Samples for apatite geochronology. Samples in orange had enough apatite for AFT and U-Th/He. Samples in blue had enough apatite for U-Th/He only

ANNEX 3: MAGNESIUM ISOTOPE DATA

Unit	Age	δ^{26}Mg l	2σ	δ^{25}Mg l	2σ
Dolomites					
Black River	U. Ordovician	−0.71	0.08	−0.33	0.06
Trenton	U. Ordovician	−0.97	0.12	−0.50	0.03
Red Head Rapids	U. Ordovician	−0.79	0.20	−0.43	0.13
Red Head Rapids	U. Ordovician	−1.1	0.30	−0.70	0.15
Red Head Rapids	U. Ordovician	−1.26	0.06	−0.84	0.04
Sayabec	L. Silurian (W)	−2.09	0.09	−1.06	0.08
Sayabec	L. Silurian (W)	−1.91	0.02	−0.95	0.08
Sayabec	L. Silurian (C)	−1.41	0.01	−0.73	0.04
Sayabec	L. Silurian (C)	−1.29	0.22	−0.71	0.13
Sayabec	L. Silurian (C)	−1.13	0.30	−0.59	0.18
La Vieille	L. Silurian	−3.25	0.11	−1.71	0.05
La Vieille	L. Silurian	−2.18	0.08	−1.12	0.06
West Point	L. Devonian	−0.91	0.06	−0.42	0.06
West Point	L. Devonian	−0.99	0.09	−0.59	0.05
West Point	L. Devonian	−0.78	0.17	−0.38	0.13
West Point	L. Devonian	−1.29	0.12	−0.71	0.09